2012

INVESTIGATING THE ROLE OF PRION PROTEIN POLYMORPHISMS ON PRION PATHOGENESIS

Eri Saijo
University of Kentucky, valensiae@gmail.com

STUDENT AGREEMENT:

I represent that my thesis or dissertation and abstract are my original work. Proper attribution has been given to all outside sources. I understand that I am solely responsible for obtaining any needed copyright permissions. I have obtained and attached hereto needed written permission statements(s) from the owner(s) of each third-party copyrighted matter to be included in my work, allowing electronic distribution (if such use is not permitted by the fair use doctrine).

I hereby grant to The University of Kentucky and its agents the non-exclusive license to archive and make accessible my work in whole or in part in all forms of media, now or hereafter known. I agree that the document mentioned above may be made available immediately for worldwide access unless a preapproved embargo applies.

I retain all other ownership rights to the copyright of my work. I also retain the right to use in future works (such as articles or books) all or part of my work. I understand that I am free to register the copyright to my work.

REVIEW, APPROVAL AND ACCEPTANCE

The document mentioned above has been reviewed and accepted by the student's advisor, on behalf of the advisory committee, and by the Director of Graduate Studies (DGS), on behalf of the program; we verify that this is the final, approved version of the student's dissertation including all changes required by the advisory committee. The undersigned agree to abide by the statements above.

Eri Saijo, Student

Dr. Glenn Telling, Major Professor

Dr. Joseph McGillis, Director of Graduate Studies

INVESTIGATING THE ROLE OF PRION PROTEIN POLYMORPHISMS ON PRION PATHOGENESIS

DISSERTATION

A dissertation submitted in partial fulfillment of the requirements for the degree of Doctor of Philosophy in the College of Medicine at the University of Kentucky

By

Eri Saijo

Lexington, Kentucky

Director: Dr. Glenn Telling,

Professor of Microbiology, Immunology, and Molecular Genetics

Lexington, Kentucky

2012

ABSTRACT OF DISSERTATION

INVESTIGATING THE ROLE OF PRION PROTEIN POLYMORPHISMS ON PRION PATHOGENESIS

Transmissible spongiform encephalopathies (TSEs), also known as prion diseases, are lethal and infectious neurodegenerative diseases of humans and animals. The misfolding of the normal, or cellular isoform of the prion protein (PrP^{C}) into the abnormal disease-associated isoform of PrP (PrP^{Sc}) could change the properties of PrP, consequently, PrP^{Sc} has lethal infectivity to transmit diseases. The proteinaceous infectious particle consisting mainly of PrP^{Sc} is called prion. Transmissibility of prions is strongly influenced by multiple factors including PrP polymorphisms, species barriers (PrP sequence specificity) and prion strains (conformational specificity) by unknown mechanisms. Even though the ability of prions to cross a species barrier has been recognized, the precise mechanisms of interspecies prion transmission remain unclear.

This dissertation research was conducted in order to learn more about the molecular mechanisms of conversion, propagation and transmission of PrP^{Sc}; about determinants of genetic susceptibility to infection in prion diseases; and about understanding those mechanisms, which might govern the zoonotic potential of prion diseases.

First, we investigated the transmissibility risk of multiple strains of Chronic Wasting Disease, which is a cervid TSE, with humanized transgenic mice and showed that the transmission barriers between cervid and the humanized mice are high. Next, the structural factors underlying the species barrier of prion diseases were studied using cell culture systems by systematically introducing amino acid substitutions in the regions of PrP, where the most divergences of different PrP species are recognized. Thirdly, we investigated the effects of the genetic susceptibility to prions as well as conversion kinetics and properties of PrP^{Sc} using Tg mice expressing ovine PrP polymorphism (OvPrP) at codon 136 either alanine (A) or valine (V). The templating characteristics of $OvPrP^{Sc}$-V136 were dominant over $OvPrP^{Sc}$-A136 under co-expressions of $OvPrP^{C}$-A136 and

OvPrP^{C}-V136. Finally, the function of PrP was studied in relation to the pathogenesis of Alzheimer's disease.

These studies demonstrated that the conformational compatibility between PrP^{C} and PrP^{Sc} contributed to the conversion kinetics and species barrier. We concluded that the conformational compatibility of PrP^{C} to PrP^{Sc} is controlled not only by the PrP sequence specificity but also by the tertiary structure of PrP^{C}.

KEYWORDS: Prion Protein, Species Barrier, Prion Strain,
PrP Polymorphisms, Zoonotic Potential

ERI SAIJO

Student's Signature

August 16, 2012

Date

INVESTIGATING THE ROLE OF PRION PROTEIN POLYMORPHISMS ON PRION PATHOGENESIS

By

Eri Saijo

Dr. GLENN TELLING

Director of Dissertation

Dr. JOSEPH MCGILLIS

Director of Graduate Studies

August 16, 2012

TABLE OF CONTANTS

Abbreviations

AD	Alzheimer's Disease
ADAM	Alpha Disintegrin and Metalloproteinase
aMCI	Amnestic Mild Cognitive Impairment
APP	Amyloid Precursor Protein
Aβ	Amyloid Beta
BSE	Bovine Spongiform Encephalopathy
bp	Base Pair(s)
CDR	Clinical Dementia Rating
CJD	Creutzfeldt-Jakob Disease
CERAD	Consortium to establish a registry for Alzheimer's Disease
CWD	Chronic Wasting Disease
dpi	Days Post Inoculation
ELISA	Enzyme-Linked Immunosorbent Assay
FFI	Fatal Familial Insomnia
GSS	Gerstmann-Sträussler-Scheinker
kDa	Kilodalton
KO	Knock-Out
mAb	Monoclonal Antibody
mAD	Mild Alzheimer's Disease
MBM	Meat and Bone Meal
MMSE	Mini-Mental State Examination
NCI	No Cognitive Impairment
NMR	Nuclear Magnetic Resonance

PBS	Phosphate Buffered Saline
PCR	Polymerase Chain Reaction
PK	Proteinase K
PMCA	Protein Misfolding Cyclic Amplification
PMI	Post-Mortem Interval
PRNP	Gene encoding human Prion Protein
Prnp	Gene encoding mammalian except human Prion Protein
PrP	Prion Protein
PrP^{C}	Normal Cellular isoform of Prion Protein
PrP^{Sc}	Abnormal Disease-Causing isoform of Prion Protein
PrP*	Intermediate form of Prion Protein
RFLP	Restriction Fragment Length Polymorphism
RML	Rocky Mountain Laboratories mouse adapted scrapie
sCJD	Sporadic Creutzfeldt-Jakob Disease
SEM	Standard Errors of the Mean
SD	Standard Deviation
SDS	Sodium Dodecyl Sulfate
SSBP/1	Scrapie Sheep Brain Pool number 1
TACE	Tumor Necrosis Factor alpha-Converting Enzyme
TBS	Tris-Buffered Saline
TBST	Tris-Buffered Saline with Tween 20
TME	Transmissible Mink Encephalopathy
TSE	Transmissible Spongiform Encephalopathy
Tg	Transgenic

vCJD	Variant Creutzfeldt-Jakob Disease
WT	Wild-Type

Chapter 1

Introduction to prion biology

Transmissible spongiform encephalopathies (TSEs), or prion diseases, are a group of fatal and transmissible neurodegenerative diseases affecting the central nervous system (CNS) of humans and animals (Prusiner, 1998). Currently, no cure is known for any prion disease. A typical clinical sign of patients with prion disease is a progressive dementia, while sheep, cattle and cervid generally present ataxic illness (Parry, 1962; Wells *et al.*, 1987; Williams & Young, 1980). In about the last decade, the view has acquired wide acceptance that TSEs are caused by the misfolding of the normal, or cellular, form of the prion protein (commonly designated PrP^{C}) into infectious di**s**ease-**c**ausing PrP (PrP^{Sc}) in the brain (Prusiner, 1998). Prions are infectious protein consisting of pathogenic PrP^{Sc} and defined as a "**pro**teinaceous **in**fectious particle that lacks nucleic acid" (Prusiner, 1982). The underlying mechanisms of conversion and propagation of PrP^{Sc} as well as transmission of prions are still under investigation.

TSEs in humans

Human prion diseases occur in various forms, including genetic, sporadic and infectious disorders. Inherited forms of human prion diseases are Gerstmann-Sträussler-Scheinker (GSS), Fatal Familial Insomnia (FFI) and familial Creutzfeldt-Jakob disease (CJD). Germ-line mutations in the PrP gene (*PRNP*) are the cause of all of the inheritable prion diseases (Colby & Prusiner, 2011). In

contrast, somatic mutations in *PRNP,* or spontaneous conformation conversion of PrP^{C} to PrP^{Sc}, are the most likely cause of such prion diseases as, sporadic CJD and sporadic Fatal Insomnia (Colby & Prusiner, 2011). Sporadic CJD is the most common form of human prion diseases accounting for approximately 85% of prion disease patients (Colby & Prusiner, 2011). Infectious prion disease forms include Kuru and variant or iatrogenic CJDs. Kuru was found in a Fore linguistic group residing in the highlands of Papua, New Guinea, and person-to-person transmission occurred through the tribe practice of ritual cannibalism (Klitzman *et al.*, 1984). Variant CJD (vCJD) is that form of human prion disease best known among the general public. Epidemiological and experimental studies have provided good evidence that vCJD might be caused by the consumption of bovine spongiform encephalopathy (BSE)-contaminated products (Asante *et al.*, 2002; Bruce *et al.*, 1997; Collinge *et al.*, 1996; Scott *et al.*, 1999; Will *et al.*, 1996). Iatrogenic CJD is most likely induced by the accidental use of prion-contaminated surgical tools (Davanipour *et al.*, 1984; Kondo & Kuroiwa, 1982; Masters & Richardson, 1978; Will & Matthews, 1982), as well as by transmission from human growth hormone and gonadotropin, dura matter grafts, and transplants of corneas harvested from individuals who died from CJD (Duffy *et al.*, 1974; Koch *et al.*, 1985).

TSEs in animals

TSEs in animals include chronic wasting disease (CWD) of deer, elk and moose, scrapie of sheep, goat and moufflon, transmissible mink encephalopathy, BSE,

feline spongiform encephalopathy (FSE) and exotic ungulate encephalopathy (EUE). FSEs affect domestic cats (Leggett *et al.*, 1990; Wyatt *et al.*, 1991) and captive wild members of the cat family (Eiden *et al.*, 2010; Lezmi *et al.*, 2003). EUEs are found in exotic zoo ruminants of the cattle family (Kirkwood & Cunningham, 1994). CWD, scrapie, TME and BSE are described below in more detail.

Chronic wasting disease (CWD), a TSE of free-ranging and captive deer, elk and moose, is highly contagious (Baeten *et al.*, 2007; Miller *et al.*, 2000; Williams, 2005; Williams & Young, 1980, 1982, 1992). Since it was first recognized in a wildlife facility in Northern Colorado in 1967 (Williams & Young, 1980), cases of CWD have increasingly been reported from this and additional states, while other cases have shown up abroad. As of 2012, CWD has been identified in 18 states: Colorado, Wyoming, South Dakota, Nebraska, Wisconsin, New Mexico, Minnesota, Oklahoma, Illinois, Utah, New York State, West Virginia, Kansas, Michigan, Virginia, Missouri, North Dakota and Maryland (Chronic Wasting Disease Alliance, 2012). It has also appeared in two provinces (Alberta and Saskatchewan) in Canada (Chronic Wasting Disease Alliance, 2012). In South Korea, deer imported from Canada are found to be CWD positive in 2005 (Kim *et al.*, 2005). Since then, CWD has been recognized in South Korea (Sohn, 2011). It is difficult to determine how CWD has spread throughout North America, inasmuch as CWD is not always found in states adjoining the affected states. Plausible explanations include the simple fact of increased awareness of CWD,

inadvertent interstate transfer of asymptomatic infected animals, or the possibility that CWD is a sporadic disease. Thus, CWD's origins in North America are unclear.

It has been debated whether endemic levels of CWD are maintained due to high efficiency of horizontal transmission of CWD in North America. One possible explanation is that decomposing carcasses of CWD-affected animals, feces, urine or saliva remain as highly contagious prion sources in an environment to continue spreading disease in animals. Some studies report that prions could bind to metal and mineral deposits in the soil and be maintained in the soil over decades (Johnson *et al.*, 2006; Miller *et al.*, 2004; Seidel *et al.*, 2007). Prions have been identified in bedding, food and water shared by CWD-affected animals (Mathiason *et al.*, 2009), in saliva (Haley *et al.*, 2009; Mathiason *et al.*, 2006), in urine (Haley *et al.*, 2009), in feces (Tamguney *et al.*, 2009b) and in antler velvet (Angers *et al.*, 2009), all of which are potential sources for infectious transmission. When prions are shed to the environment, whether soil or aquatic, prions remain in the environment over period of time. When animals have any contacts with prions remained in the environment, prions could invade the animals. Even though the levels of prions might be low in the environment, animals could develop disease by repeated exposures.

Could new CWD strains arise and acquire new host-range properties during horizontal transmission? It has been questioned whether intraspecies transmission of CWD increase chances of propagating new strains, which might have lower cervid to human species barriers (Barria *et al.*, 2011). There is so far

strong evidence that at least two distinct strains of CWD propagate in deer and elk (Angers *et al.*, 2010). Since efficient horizontal transmission of CWD has been evidenced, natural CWD agents are most likely going through serial passages among cervid in wild or captive environments. Intraspecies transmissions *in vivo* and *in vitro* increased the propagation of human PrP^{Sc} *in vitro* (Barria *et al.*, 2011), suggesting that there is potential for the spread of CWD to humans by intraspecies transmissions. In addition, it has been reported that other forms of prions are able to change transmission properties during interspecies passages, with resultant change of the host range (Bartz *et al.*, 1998) and the production of multiple strains (Bessen & Marsh, 1992b). There thus remains a meaningful potential for the adaptation of CWD prions, so that they acquire the property of infecting multiple new species, including humans. It would therefore be important to understand how strains arise in the environment that CWD is constantly disposed.

Scrapie is a TSE of sheep, goats and moufflon (Dickinson, 1976; Wood *et al.*, 1992). The first recognized cases of scrapie were documented in England in 1732, with further cases in Germany in 1759 (reviewed in (Prusiner, 2004)). Thus, scrapie has been recognized for around 300 years and has been spread across the world, especially in the northern hemisphere, by importing and exporting domestic sheep. Curiously, Australia and New Zealand are recognized as scrapie free countries (Hunter & Cairns, 1998). When scrapie turned up in those countries, entire flocks were terminated to prevent its spread to other

flocks. Moreover, Australia and New Zealand use more stringent surveillance systems to maintain a scrapie-free environment.

The transmissibility of TSEs was first demonstrated in sheep using brain homogenates from scrapie-affected sheep (Cuillé & Chelle, 1936, 1938). Subsequent sheep studies reported that different scrapie sources produced different transmission characteristics. In early studies of sheep scrapie, classical scrapie sheep brain pool number 1 (SSBP/1)-inoculated sheep was classified positive or negative, developing upon the incubation time after inoculation (Dickinson, 1976). The gene involved in the incubation period was called *Sip* (for scrapie incubation period) and later identified as a PrP gene (Basler *et al.*, 1986) and two alleles were indicated as sA and pA (partially dominant) (Dickinson & Outram, 1988). The negative group of sheep survived from subcutaneous (s.c.) inoculation of scrapie, and the associated gene was characterized as Sip^{pApA} (Foster & Hunter, 1991). In contrast, sheep from the positive group developed disease within 150-400 days after inoculation; here, the genes were identified as either Sip^{sAsA} or Sip^{sApA} (Foster & Hunter, 1991). The results indicated that sheep carrying Sip^{sA} developed disease with a shorter incubation time than sheep with Sip^{pApA}. Interestingly, the negative group sheep developed diseases with a shorter incubation time with a different classical scrapie isolate, referred to as CH1641, and BSE prions than the positive group sheep (Foster & Dickinson, 1988b; Foster *et al.*, 1993), indicating that the gene Sip^{pApA}, which is associated with a long incubation time with SSBP/1 prion, behaves differently with other prion isolates. These studies presented indications that interactions between

genetic variations in the ovine PrP gene and prion strains were not straightforward, and that disease outcomes/incubation times depended upon the combinations between genetic variations of PrP^{C} and strain variations of PrP^{Sc}.

The genetic susceptibility of sheep to scrapie has been studied using mouse models after the discovery of the PrP gene (*Prnp* in mice or *PRNP* in higher eukaryotes). Since then, the genetic linkage between *Prnp* and the length of scrapie incubation time was established in mice (Carlson *et al.*, 1986). Furthermore, two distinct alleles in *Prnp* were identified, and the biological property of short or long scrapie prion incubation times was associated with these two alleles (Westaway *et al.*, 1987). Later studies demonstrated that one allele was converted to PrP^{Sc} more efficiently over the other; in addition, the copy number of *Prnp* in Tg mice controlled the incubation time (Carlson *et al.*, 1994; Westaway *et al.*, 1987). Interestingly, these findings do not apply for some prion strains.

Three major scrapie susceptibility-linked polymorphisms were identified in the ovine PrP gene including amino acid residues at 136 (alanine [A] or valine [V]), 154 (arginine [R] or histidine [H]) and 171 (glutamine [Q], R or H) (Goldmann *et al.*, 1991; Goldmann *et al.*, 1994). Transmission studies in Cheviot sheep showed that homozygosity for V at codon 136 was associated with short incubation times after inoculation with SSBP/1, while heterozygosity was linked to longer incubation times (Goldmann *et al.*, 1994). Sheep homozygous for A at codon 136 were resistant to SSBP/1 inoculation (Goldmann *et al.*, 1994). The same findings were also reported in studies with US sheep (Maciulis *et al.*,

1992), suggesting that the scrapie susceptibility-linked polymorphism at codon 136 was not limited to Cheviot sheep. It has been reported that the polymorphism of Q or R at residue 171 is also correlated with susceptibility to scrapie (Goldmann *et al.*, 1994; Westaway *et al.*, 1994a). Q171 is linked to susceptibility to scrapie, while R171 is correlated with resistant to scrapie. Sheep homozygous for R at codon 171 did not develop disease upon inoculation of SSBP/1, and sheep heterozygous for Q/R at codon 171 were relatively resistant. Limited studies in Cheviot and Icelandic sheep showed that H at residue 154 conferred resistance to scrapie (Baylis *et al.*, 2004; Hunter *et al.*, 1996; Laplanche *et al.*, 1993; Thorgeirsdottir *et al.*, 1999). Thus, the H154Q polymorphism is linked to a small extent to a sheep's susceptibility.

In contrast, CH1641 isolate has a completely different propensity for those three polymorphisms. Unlike SSBP/1, A136 and V136 are most susceptible and resistant to CH1641, respectively (Goldmann *et al.*, 1994). In addition, it has been reported that homozygosity for Q at codon 171 was linked to short incubation times, and sheep heterozygous for Q/R at codon 171 presented much longer incubation time with CH1641 (Goldmann *et al.*, 1994). In conclusion, the combined effects of genetic polymorphism of the ovine PrP gene and agent strain variation act to present a complex picture of scrapie susceptibility in sheep.

Taken together, three major sheep PrP polymorphisms participate in determining susceptibility and resistance to scrapie; however, the participation of each polymorphism in susceptibility involves in different levels. Since two dimorphisms and one trimorphism play roles here, 12 combinations of these

polymorphisms are possible. Nonetheless, only 5 out of 12 combinations have been reported from the sheep flocks, the frequency of appearance of any of the other combinations is extremely low (Belt *et al.*, 1995; Ikeda *et al.*, 1995). The five combinations are A at codon 136, R at codon 154 and R at codon 171 (ARR), ARQ, AHQ, ARH and VRQ, and homozygous for ARR and VRQ are most resistant and susceptible to scrapie, respectively. Even though two additional combinations of AHR and VRR were later reported (Kutzer *et al.*, 2002), the five genotypes appear with higher frequencies. Subsequent studies by multiple investigators have reported the same polymorphic effects on the susceptibility of scrapie *in vivo* and *in vitro* studies. However, the underlying mechanisms of how the polymorphisms regulate the susceptibility and resistance to scrapie are still not clear.

Transmissible mink encephalopathy (TME) is a sporadic form of TSEs found in farmed mink (Hartsough & Burger, 1965). TME was first reported in 1947 in a farm in Brown County, Wisconsin, then again later in 1961 in several farms in Sheboygan, Calumet and Manitowoc Counties, Wisconsin, with a third outbreak in 1963 in Sawyer County, Wisconsin. The affected farms in Wisconsin all fed mink with a ready-mix feed supplied and manufactured by the same feed plant, which suggests that the disease was caused by the consumption of prion-contaminated food (Liberski *et al.*, 2009). The last outbreak was found in 1985 in Stetsonville, Wisconsin, where it was later found that TME-affected mink had been fed contaminated cattle meat from downer dairy cows. In order to examine

whether the contaminated cattle were the cause of TME, infected cattle tissue was experimentally inoculated into groups of mink, resulting in the development of fatal diseases (Marsh & Bessen, 1993). Additional TME cases were reported in Idaho (Hartsough & Burger, 1965), Canada (Hadlow & Karstad, 1968), Finland and the former East Germany (Hartung *et al.*, 1970; Johannsen & Hartung, 1970) and the former Soviet Union (Danilov *et al.*, 1974; Dukur *et al.*, 1986).

The interspecies transmission studies of TME-affected mink agents from the last outbreak in Stetsonville were performed using Syrian golden hamsters, and TME-infected hamsters showed two distinct clinical presentations including hyper (HY) and drowsy (DY) after third passages (Bessen & Marsh, 1992b). The characteristics of the HY and DY differed in incubation time, brain titer, lesion profiles in the brain, pathogenicity as well as biochemical properties (Bessen & Marsh, 1992a, b). The HY has a shorter incubation time and high brain titer, whereas the DY has a longer incubation time and low brain titer. Interestingly, when the HY and DY agents were inoculated back to mink, only the DY agent could produce disease in mink (Bessen & Marsh, 1992b). The DY agent was able to produce disease in hamsters after long incubation time thus still retained the transmissibility property. These studies suggested that TME from the Stetsonville contained the mixed strains of both HY and DY, moreover, the DY was the major pathogen. The studies in TME were the first study to identify the different biochemical properties of multiple strains present in prions.

Bovine spongiform encephalopathy (BSE) is a TSE of cattle, and first found in 1986, in Weybridge, United Kingdom (Wells *et al.*, 1987). Since 1986, the numbers of BSE cases in United Kingdom rapidly increased in the following six years, and the peak of BSE cases was reported during 1992 and 1993. Subsequently, the numbers of BSE were gradually declined over the next decade. BSE incidence was found to coincide with feeding of meat and bone meal (MBM) as a dietary protein supplement in dairy herds (Wilesmith *et al.*, 1991). MBM was produced from rendered animal parts, and was generally fed to cattle from one-week-old of age until the time of slaughter. The identification of the source of outbreak and vigorous actions were able to control the epidemic of BSE in Great Britain by 2002. In the course of the epidemiological studies, one hypothesis was raised that sheep scrapie-contaminated materials were mixed into the MBM at the slaughterhouse plants and fed to cattle, which developed disease because scrapie materials were present all the time at the slaughterhouse (Taylor, 1989; Taylor, 1996; Wilesmith *et al.*, 1991; Wilesmith *et al.*, 1988). In addition, scrapie is endemic in sheep populations in Great Britain. However, the hypothesis BSE was derived form a scrapie strain has not been established.

In 1994, few years after the peak of BSE, the first cases of vCJD were diagnosed in teenagers and young adults in Great Britain (Will *et al.*, 1996). In the following years, more vCJD cases were reported in Great Britain as well as in other countries, and more than 200 individuals with vCJD have been reported (World Health Organization, 2012). The epidemiological studies of vCJD

concluded that those individuals with vCJD developed disease because of the consumption of BSE-contaminated cattle products (Prusiner, 2004). BSE is the first established case of interspecies transmission of TSE to humans. Since then, the zoonotic potential of TSEs became more concerns when we thought about the animals in TSEs.

Prion protein and its isoforms

The PrP gene is well-conserved protein among mammalian species and is ubiquitously expressed, particularly in the CNS, and especially in neurons, in both diseased and non-diseased brains (Prusiner, 1998). PrP is a glycoprotein that is attached to the cell membrane through a glycosylphosphatidylinositol (GPI) anchor (Stahl *et al.*, 1990; Stahl *et al.*, 1987). PrP transits in the secretory pathway of endoplasmic reticulum (ER). Posttranslational modification of PrP starts after entering the ER, which is mediated by an amino (N)-terminal signal peptide of 22 amino acids (Hope *et al.*, 1986; Turk *et al.*, 1988) and carboxyl (C)-terminal signal peptide of 23 amino acids (Heske *et al.*, 2004; Stahl *et al.*, 1990) (Figure 1.1.) (Holscher *et al.*, 2001). When entered ER, the N-terminal signal peptide is cleaved by a signal peptidase. During passage through ER, two N-linked carbohydrate chains are attached to asparagines at residues 180 and 196 (mouse numbers) (Haraguchi *et al.*, 1989), and a disulfide bond is formed between residues 178 and 213 (mouse numbers) (Turk *et al.*, 1988). Finally, in order to bring about attachment to the cell membrane, a GPI-anchor is added following cleavage of the C-terminal signal peptide (Endo *et al.*, 1989; Oesch *et*

al., 1985). During the secretory pathway, an ER-based quality control removes misfolded PrP to the cytosol for proteasomal degradation (Drisaldi *et al.*, 2003). The whole process of maturation to transportation is accomplished within one hour (Borchelt *et al.*, 1990; Caughey *et al.*, 1989). The half-life PrP^{C} in chronically infected cells was found to be approximately 5 hours, while that of PrP^{Sc} was approximately 15 hours (Table 1.1.) (Borchelt *et al.*, 1990).

The 'natural' or 'normal' functions of PrP have not been clearly identified, although PrP appears to be involved in signal transduction (reviewed in (Taylor & Hooper, 2006; Tsui-Pierchala *et al.*, 2002)), synaptic transmission (Collinge *et al.*, 1994), neuroprotection (reviewed in (Roucou & LeBlanc, 2005; Roucou *et al.*, 2004)), immunoregulation (reviewed in (Isaacs *et al.*, 2006)), copper binding (reviewed in (Millhauser, 2007; Vassallo & Herms, 2003), induction of apoptosis (Kim *et al.*, 2004; Kuwahara *et al.*, 1999), circadian rhythm and sleep (Medori *et al.*, 1992), adaptation to stress (Nico *et al.*, 2005), and memory processing (Coitinho *et al.*, 2007; Coitinho *et al.*, 2006). Even though PrP is ubiquitously expressed in the adult brain, the expression of PrP during early stages of development is tightly regulated (Mobley *et al.*, 1988), suggesting a possible important function of PrP during development. However, *Prnp* deficient ($Prnp^{0/0}$) mice develop normally and have a normal lifespan (Bueler *et al.*, 1992), raising the possibility that loss of PrP might be compensated by unknown functionally related proteins.

Both PrP^{C} and PrP^{Sc} consist of the same primary structure and appear to possess invariant posttranslational modifications (Stahl *et al.*, 1993). However,

Fourier-transform infrared (FTIR) and circular dichroism (CD) studies showed that PrP^{C} consisted mainly of α-helices (40%) and small percent of β-sheets, while PrP^{Sc} contained more β-sheets (45%) and a lesser quantity of α-helices (30%) (Pan *et al.*, 1993; Pergami *et al.*, 1996). Further, structural studies of recombinant PrP using solution phase nuclear magnetic resonance (NMR spectroscopy) identified three α-helices and two regions of β-sheet structures (Riek *et al.*, 1996; Zahn *et al.*, 2000).

The differing biochemical properties of PrP^{C} and PrP^{Sc} are summarized in Table 1.1. Sensitivity to protease digestion has been used to distinguish PrP^{C} and some forms of PrP^{Sc} (Prusiner, 2004). After protease digestion of PrP^{Sc}, it produces protease-resistant molecules of approximately 142 amino acids with a molecular mass of 27-30 kDa, referred to as PrP 27-30 (Figure 1.1.) (Bolton *et al.*, 1982; Prusiner *et al.*, 1982). However, PrP^{C} and some other forms of PrP^{Sc}, referred to as protease-sensitive PrP^{Sc} (Gambetti *et al.*, 2008) are completely digested under the same conditions of protease digestion. It is important to note the existence of protease-sensitive PrP^{Sc}, which has been reported to be involved in specific types of human prion diseases (Colucci *et al.*, 2006; Gambetti *et al.*, 2011; Gambetti *et al.*, 2008). Furthermore, PrP^{Sc} tends to form oligomers and/or aggregates including amyloid plaques and fibrils. In contrast, PrP^{C} remains monomeric. The solubilities of the two isoforms are different: PrP^{C} is soluble, PrP^{Sc} is not. Therefore, after ultracentrifugation at 100,000 *x g*, PrP^{Sc} can be collected into pellets. As mentioned above, the half-life of PrP^{C} is known to be approximately 5 hours, whereupon PrP^{C} will be recycled by cells. However,

PrP^{Sc} is known to not merely to survive for long periods, but also to accumulate to the point of causing disease. PrP^{C} is not infectious. However, when PrP^{C} undergoes the conformational changes to unfold α-helices and refold into β-sheets to convert into PrP^{Sc}, it gains a lethal infectivity (Prusiner, 1998). Furthermore, prions consisting of solely PrP^{Sc} are resistant to heat, harsh chemicals and denaturants (Gordon, 1946) as well as UV irradiation (Alper *et al.*, 1967).

PrP^{C} → PrP^{Sc} conversion models

It is widely accepted that PrP^{C} undergoes a profound conformational structural change to become the pathogenic PrP^{Sc} isoform, and the conformational change requires PrP^{C} and PrP^{Sc} (Prusiner, 1998). The conversion of PrP^{Sc} does not require nucleic acids; however, RNA facilitates conformational conversion *in vitro* conversion assays (Deleault *et al.*, 2003; Wang *et al.*, 2010). This “protein only hypothesis” has been supported by extensive prion researches, even though the exact PrP^{C} to PrP^{Sc} conversion mechanisms have not been yet established. However, the two important models of PrP^{Sc} conversion and propagation have been proposed: namely the heterodimer template-associated and nucleated-polymerization models. The template-associated model was proposed to explain the replication of PrP^{Sc} (Cohen *et al.*, 1994). Although the nucleated-polymerization model was originally offered to explain polymerization of proteins (Oosawa & Asakura, 1975), it has been employed to explain the amyloid

formation in the protein misfolding diseases including prion diseases (Gajdusek, 1994a, b; Harper & Lansbury, 1997).

The heterodimer template-associated model suggests that monomeric PrP^{Sc} becomes a template to convert PrP^{C} to PrP^{Sc} (Figure 1.2.A) (Cohen *et al.*, 1994). In this model, PrP^{C} is in equilibrium with an intermediate form, referred to as PrP*, and PrP* can form a heterodimer complex with PrP^{Sc}, which becomes a template to alter the conformation of PrP* into infectious isoform PrP^{Sc}, resulting in the formation of a homodimer complex. The homodimer complex can dissociate into two monomers, which can become additional templates to produce more PrP^{Sc}. A hypothetical protein X is thought to play roles in the conversion of PrP^{C} to PrP^{Sc} and also catalyze the PrP^{Sc} conversion (Kaneko *et al.*, 1997; Telling *et al.*, 1995; Telling *et al.*, 1994). In this model, PrP^{Sc} is thermodynamically stable compared to PrP^{C}; furthermore, the conversion of PrP^{Sc} from PrP* is less likely to happen without a catalyst.

Several series of experiments demonstrated the exponential growth of PrP^{Sc} (Kocisko *et al.*, 1995; Kocisko *et al.*, 1994); however, the template-associated model alone does not accommodate the explanation of rapid formation of PrP^{Sc} fibrils or aggregates. To yield a plausible explanation of this exponential polymerization event and subsequent rapid accumulation of PrP^{Sc}, two hypotheses were proposed based on the nucleated-polymerization theory (Masel *et al.*, 1999). One theory is called the *autocatalytic nucleated-polymerization model* (Figure 1.2.B.) (Cohen *et al.*, 1994). In this model, PrP^{C} directly interacts with PrP^{Sc} seed in fibril or aggregate forms, and the conversion

reaction is the rate-limiting step. The PrP^{Sc} conversion step might be catalyzed by protein X. Another scenario is the *non-catalytic nucleated-polymerization model* (Figure 1.2.C.) (Caughey *et al.*, 1995). Unlike the autocatalytic model, PrP* rather than PrP^{C} interacts with the seed to form stable polymers, and the PrP^{Sc} conversion step occurs "non-catalytically". The rate-limiting step is the reversible reaction between PrP^{C} and PrP^{*}, and the reaction might be facilitated by protein X. The rest of the steps to form PrP^{Sc} fibrils and aggregates are irreversible. In the nucleation-associated models, the initial formation of PrP^{Sc} seeds might require a longer time. However, once stable PrP^{Sc} seeds are assembled, the addition of PrP^{Sc} to the seeds can be accelerated. In addition, fragmentation of the fibrils can fabricate more seeds for more nucleation reactions.

Even though there are three kinetic models of the PrP^{Sc} conversion to help clarify matters, no one model alone can explain every case of the PrP^{Sc} propagation. The heterodimer template-associated model explains an initial formation of PrP^{Sc}. When the accumulation of PrP^{Sc} reaches a threshold that cells cannot clear, PrP^{Sc} might form oligomeric fibrils, following which nucleated-polymerization would ensue to propagate additional PrP^{Sc}. Therefore, it might be more practical to imagine that combinations of these models provide better insight into the precise mechanisms of the PrP^{Sc} conversion.

In vitro conversion of PrP^{Sc}: cell-free conversion vs. protein misfolding cyclic amplification (PMCA)

The molecular mechanisms underlying the conversion of PrP^{C} to PrP^{Sc} have long been of concern in prion research. One investigative approach was developed using an *in vitro* system called *cell-fee conversion*, which involves mixing labeled recombinant PrP with a 50-fold molar excess semi-purified PrP^{Sc} and incubating for 2-45 hours at 37°C (Caughey *et al.*, 1995; Kocisko *et al.*, 1994). PrP^{Sc} conversion can be monitored and quantified by monitoring accumulation of newly converted labeled protease-resistant PrP^{Sc}, and it was reported that approximately 20% of PrP^{C} was converted to PrP^{Sc} in this cell-free conversion system (Caughey *et al.*, 1995; Horiuchi & Caughey, 1999). The conversion process involves two kinetic steps of interaction and conformational change (DebBurman *et al.*, 1997; Horiuchi & Caughey, 1999). The first step is for PrP^{C} to interact with PrP^{Sc}, where the interaction depends on the compatibility of their primary structures. The second step is the conversion of PrP^{C} to PrP^{Sc} by undergoing structural change to become a protease-resistant PrP^{Sc} (Callahan *et al.*, 2001; DebBurman *et al.*, 1997; Horiuchi & Caughey, 1999; Rigter & Bossers, 2005).

Soto and his colleagues developed another *in vitro* system to propagate PrP^{Sc} called *protein misfolding cyclic amplification* (PMCA), which is accomplished by mixing approximately 30-fold molar excess of either recombinant PrP or brain homogenates as PrP^{C} source into PrP^{Sc} as a template, then incubating in repeated cycles of sonication and incubation at 37°C (Saborio *et al.*, 2001). PMCA involves two alternative steps of sonication and incubation. The first step, sonication, breaks PrP^{Sc} fibrils or aggregates into fragments, which

allows them to become a template or to grow into larger fibrils or aggregates again, by adding newly synthesized PrP^{Sc} onto the nucleation sites. During the second step, incubation, PrP^{C} is recruited by the PrP^{Sc} templates and undergoes structural change to become PrP^{Sc}, whereby it can become a new template or be added onto the existing PrP^{Sc}.

The cell-free conversion system has provided strong evidences, in addition to numerous animal studies, that PrP^{Sc} contains all information necessary to convert PrP^{C} into PrP^{Sc}, and that the conversion process is independent of nucleic acids. Moreover, the above two *in vitro* systems gave proof that PrP^{Sc} becomes a template to convert PrP^{C} into PrP^{Sc}. More efficient conversion of PrP^{Sc} in PMCA using brain homogenates suggests that other molecules also facilitate the PrP^{Sc} conversion, and it supports the speculation that conversion of PrP^{Sc} requires the presence of protein X. Together, the *in vitro* conversion systems can be a powerful tool to understand the kinetics of conversion of PrP^{Sc}.

Zoonotic potential of TSEs from species barriers to prion strains

TSEs are diseases of animals and humans. Transmissions of TSEs are constrained by a species barrier, which can be described in difficulty or impossibility of prion propagation from one species to another (Wickner *et al.*, 2009). The higher the species barrier between a host and donor is, the longer the incubation time requires. The species barrier is generally difficult to overcome in the transmission of prions. However, the diseases are unique in a way that the

pathogen prions, which consist with only proteins, could overcome the species barrier by propagating new prion strains.

The presence of different strains in scrapie has been recognized since 1960s (Pattison & Millson, 1961). The classical definition of prion strains is defined by incubation time and neuronal vacuolation profiling (Dickinson *et al.*, 1968; Fraser & Dickinson, 1973), moreover, the biochemical properties including PrP^{Sc} profiling, deposition, glycosylation and migration patterns are taken into account for additional characterization of prion strains (Prusiner, 2004). The unique properties of prion strains can be maintained during propagation and subsequently passaged onto next hosts. Although the primary structure of PrP is an important determinant of prion species barriers (Telling *et al.*, 1995; Telling *et al.*, 1994), prion strains are also involve in the susceptibility to infection of prions between species. Since prion strains are subject to apparent mutations and selective amplification (Li *et al.*, 2010), the selection process of prion strains might allow adapting a new host range and overcoming a species barrier. Therefore, understanding the molecular mechanisms responsible for interspecies transmission of prions are essential for controlling the transmissions of prions horizontally as well as vertically.

Transgenics in prion research

Prion research has benefited from the development of Tg mice, which are produced by integrating a target gene at random sites using homologous recombination. The use of Tg mice makes it possible to control the genetic

background compared to other animal studies, such as, sheep, cervid and bovine. Tg mouse models not only are cost-effective but also accelerate understanding of prion diseases and development of new therapeutic approaches.

The first PrP gene knockout (*Prnp*$^{0/0}$) mouse was generated in 1992 (Bueler *et al.*, 1992). Importantly, the *Prnp*$^{0/0}$ mice were resistant to prions (Bueler *et al.*, 1993). The *Prnp*$^{0/0}$ mice did not have any developmental issues and have a normal lifespan (Bueler *et al.*, 1992) even though some studies showed that altered synaptic behavior, such as, synaptic inhibition in the hippocampal brain slices of the *Prnp*$^{0/0}$ mice (Collinge *et al.*, 1994; Whittington *et al.*, 1995). However, other groups reported the absence of the synaptic inhibition in the brains of the *Prnp*$^{0/0}$ mice (Herms *et al.*, 1995; Lledo *et al.*, 1996). Other line of *Prnp*$^{0/0}$ mice generated by other group showed ataxia around 70 weeks of age, and the loss of Purkinje cells were observed in the brain (Sakaguchi *et al.*, 1996). However, the ataxia and loss of Purkinje cells were rescued by crossing to Tg mice overexpressing mouse PrP (Nishida *et al.*, 1999), suggesting that PrP might play roles in the Purkinje cells mediated atrophy, which presents in ataxia.

Mice expressing different expression levels of PrP revealed that the incubation time after inoculation was inversely proportional to the expression levels of PrP in Tg mice (Prusiner *et al.*, 1990). In addition, Tg mice overexpressing Syrian hamster or sheep PrP spontaneously developed disease at older age (Westaway *et al.*, 1994b). However, overexpression of PrP does not always produce spontaneous disease. For example, Tg mice expressing human

PrP with a mutation from glutamic acid (E) to lysine (K) at codon 200, which are found in FFI patients, did not develop spontaneous disease (Asante *et al.*, 2009). Gene-targeted knockin (targeted gene insertion to a *Prnp* specific locus) mice expressing human PrP encoding a mutation from aspartic acid to asparagine at codon 177 developed spontaneous disease at older age (Jackson *et al.*, 2009). Even though locations of the mutations involved in FFI were not exactly same between the overexpressed (Asante *et al.*, 2009) and knockin (Jackson *et al.*, 2009) mice, these results suggest that a knockin mouse model is the better system to study FFI. The knockin mouse model allows determining the functions of PrP under the endogenous environment since a mouse PrP gene is replaced with a target gene at the specific locus.

Another advantage of Tg mice is to be able to study the functions of PrP using chimeric proteins. Tg mice expressing a chimeric PrP between mouse and human was generated previously, and the study showed that the specific part of mouse PrP was required for the efficient propagation of PrP^{Sc} (Telling *et al.*, 1995; Telling *et al.*, 1996), suggesting a hypothesis that PrP^{Sc} conversion requires interactions between PrP at the mouse specific site and mouse specific cofactors or chaperons.

Roles of PrP concerning the pathogenesis of Alzheimer's disease

Alzheimer's disease (AD) is a progressive neurologic disease resulting in dementia and loss of cognitive function (Reitz *et al.*, 2012). Oligomeric and fibrillar forms of the amyloid β (Aβ) peptide, derived from the amyloid precursor

protein (APP), are thought to drive the pathogenesis of AD. The formation of oligomeric Aβ or amyloid fibrils results in reduced neuronal activity and synaptic plasticity, leading to neuronal cell death in the CNS by unclear mechanisms. There are similarities between the pathologies of AD and prion diseases.

Both AD and prion disease share common features, such as, amyloid plaques, significant neuronal loss, abnormal activities of synapses and gliosis around amyloid plaques (Garcao *et al.*, 2006; Hardy & Gwinn-Hardy, 1998). The main components of amyloid plaques in AD are Aβ42 and 40 peptides (Debatin *et al.*, 2008). Interestingly, it has been reported that punctate PrP^{C} was immunohistochemically detected in Aβ plaques in AD brains (Ferrer *et al.*, 2001). In prion diseases, the amyloid plaques mainly consist of PrP^{Sc} (Garcao *et al.*, 2006). In both diseases, the mechanisms of neuronal cell death caused by Aβ42 and PrP^{Sc} are still unclear.

Recent studies indicated a direct link between prion and AD, and suggested that PrP^{C} is a receptor for mediating the toxic effects of oligomeric Aβ (Gimbel *et al.*, 2010; Lauren *et al.*, 2009). Strittmatter and his colleagues demonstrated that oligomeric Aβ42, but not the monomer, bound to PrP^{C} with nanomolar affinity and disrupted synaptic plasticity in hippocampal slices from PrP wild-type mice (Lauren *et al.*, 2009). They further showed that the disruption by oligomeric Aβ42 was prevented in the absence of PrP^{C} and was blocked by anti-PrP antibody treatments. They suggested that the binding of oligomeric Aβ42 to PrP^{C} caused synaptic dysfunction. However, other groups failed to replicate the same effects of PrP^{C} using the *Prnp* knockout or mouse PrP

overexpressing Tg mice (Balducci *et al.*, 2010; Calella *et al.*, 2010). Strittmatter group demonstrated in the subsequent study that PrP^C required for axonal degradation, loss of synaptic markers, early death and learning and memory deficits in AD Tg mice (Gimbel *et al.*, 2010).

It has been considered that prion diseases are caused by not only a gain of neurotoxic function by converting to PrP^{Sc} from PrP^C but also a loss of protective function of PrP^C (Winklhofer *et al.*, 2008). As explained in the earlier section, PrP^C is involved in signal transduction, synaptic transmission, neuroprotection and many others; however, a clear picture of the physiological function of PrP^C is still under investigation. Thus, understanding the roles of PrP^C in the pathogenesis of AD will greatly help to identify the function of PrP^C.

Dissertation research

This dissertation consists of 6 chapters. In this dissertation, I am addressing the fundamental question: what are the molecular mechanisms of PrP^{Sc} conversion and genetic susceptibility to infection in prion diseases? I will address the underlying mechanisms of the transmission/species barrier of prion infection by investigating the transmission of prions between different species and within the same species. I will utilize Tg mouse and *in vitro* PrP^{Sc} conversion models to answer the above question. I will examine the transmission/species barrier of prions by directly testing the transmission risks of CWD into humans using Tg mouse models in Chapter 2. Next, I will examine the structural factors underlying the species barrier and susceptibility to prion infection using cell culture models

in Chapter 3. I will also discuss the transmission barriers within the same species in Chapter 4. Finally, I will investigate the function of PrP^C in the pathogenesis of AD in Chapter 5.

Chapter 2 will explore the transmission risks of CWD into humans using Tg mice expressing human PrP. I will address the impacts of the human PrP polymorphism at codon 129 coding either methionine or valine on the interspecies transmission of multiple strains of CWD.

Chapter 3 will discuss the structural factors involve in susceptibility to prion infection. I will utilize cell culture models to test the hypothesis that the loop region between the β2-sheet and α2-helix and its interaction site at the C-terminal region of PrP determines the susceptibility to prions. First, I will explain whether the structural definitions of the β2-α2 loop would change susceptibility to prions. Then, I will explain whether interrupting the interaction between the β2-α2 loop and C-terminal of PrP would alter susceptibility to prion infection. Finally, I will explain whether introducing the substitutions of horse specific amino acid residues in the β2-α2 loop and its interaction region at the C-terminal of mouse PrP would change susceptibility to prions. The series of cell culture studies were aimed to understand the roles of the PrP structures in the susceptibility to infection in prion pathogenesis by systematically introducing substitutions of amino acids in specific regions of PrP.

Chapter 4 will discuss how the transmission barrier of prions within the same species is determined by a PrP polymorphism. I will address how the ovine polymorphism at codon 136 expressing either alanine or valine determines

susceptibility to infection of classical sheep scrapie isolates using Tg mouse models and a unique antibody to distinguish the ovine 136 polymorphism. I will ask the following three questions regarding the effects of co-expressing A136 and V136 alleles on the replication of scrapie.

(1) Are OvPrP-A136 and OvPrP-V136 independently converted to PrP^{Sc}, and their properties also independently maintained?

(2) Does conversion of $OvPrP^{C}$-V136 dominate that of $OvPrP^{C}$-A136?

(3) Does expression of either allele inhibit conversion of the other?

In addition, I will apply computational modeling approaches to explain potential structural differences between the ovine PrP polymorphisms at codon 136, which might elucidate the effects of genetic susceptibility on prion pathogenesis.

Chapter 5 will explore the role of PrP in the pathogenesis of Alzheimer's disease by quantifying the expressed levels of PrP in the brains from individuals with different stages of AD. I will detail unaltered PrP expression in the rostrocaudal regions of individuals with different stages of AD. I will also address whether there is a correlation between the human PrP polymorphism and the levels of PrP expression, and whether there is a correlation between the human PrP polymorphism at codon 129 and onset of AD.

In Chapter 6, I will discuss how the findings in the previous chapters are tied together into the conformational selection model, which explains the selective conformations between PrP^{C} and PrP^{Sc} are determined for conversion of PrP^{C} to occur. Furthermore, I will propose future studies to further expand the understanding of the molecular mechanisms of conversion of PrP^{Sc}.

Table 1.1. Biochemical properties of PrP. The cellular isoform of prion protein (PrP^{C}) retains normal structural conformation and is expressed in healthy and diseased individuals. The disease-associated pathogenic isoform PrP^{Sc} is a misfolded form of PrP and can polymerize into fibrils and/or aggregates resulting in highly infectious PK-resistant protein.

PrP^{C}	**PrP^{Sc}**
Normal, cellular	Disease-causing
α-helix rich	β-sheet rich
PK sensitive	Partially PK resistant
Monomer	Polymer/fibril/aggregate
Soluble	Insoluble
Short (5 hours half life)	Long (years to decades)
Not infectious	Infectious

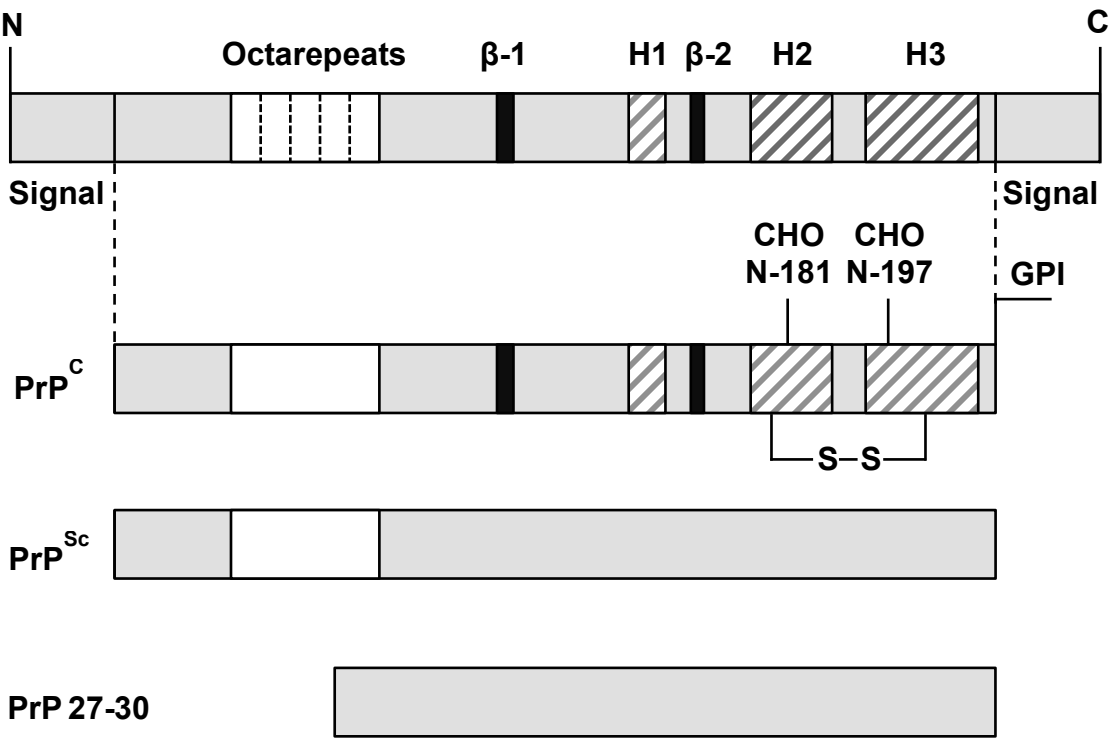

Figure 1.1. Structural features of mouse PrP that encodes a protein of 254 amino acids. The top bar diagram indicates that PrP contains five octarepeats (PHGGGWGQ), three α-helices and two β-sheets. Two secretory signal peptides reside at the amino (N)-terminal (residues 1-22) and carboxyl (C)-terminal (residues 232-254) of PrP. Both of the signal peptides mediate to enter the secretory pathway of endoplasmic reticulum (ER). Posttranslational modification of PrP starts after entering the ER. The N-terminal signal peptide is cleaved by a signal peptidase when entered ER. Then, two N-linked carbohydrate chains (CHO) are attached to asparagines at codon 180 and 196, and a disulfide bond (S-S) is formed between codons 178 and 213. Finally, in order to bring about attachment to the cell membrane, a glycosylphosphatidylinositol (GPI)-anchor is attached to the C-terminal of PrP at residue 231 following cleavage of the C-terminal signal peptide. The mature PrP^{C} (the second bar diagram) is 209 amino acids in length (residues 23-231). In the secretory pathway, an ER-based quality control removes misfolded PrP to the cytosol for proteasomal degradation. The whole process of maturation to transportation is accomplished within one hour. The third bar diagram indicates PrP^{Sc} has the octarepeats, one disulfide bond and two glycosylations; however, the secondary structure of PrP^{Sc} has not been well characterized except a β-sheet rich structure. After limited protease digestion of PrP^{Sc}, the C-terminal of PrP^{Sc} is remained to form a protease-resistant molecule of approximately 142 amino acids with a molecular mass of 27-30 kDa, referred to as PrP 27-30 (the bottom diagram).

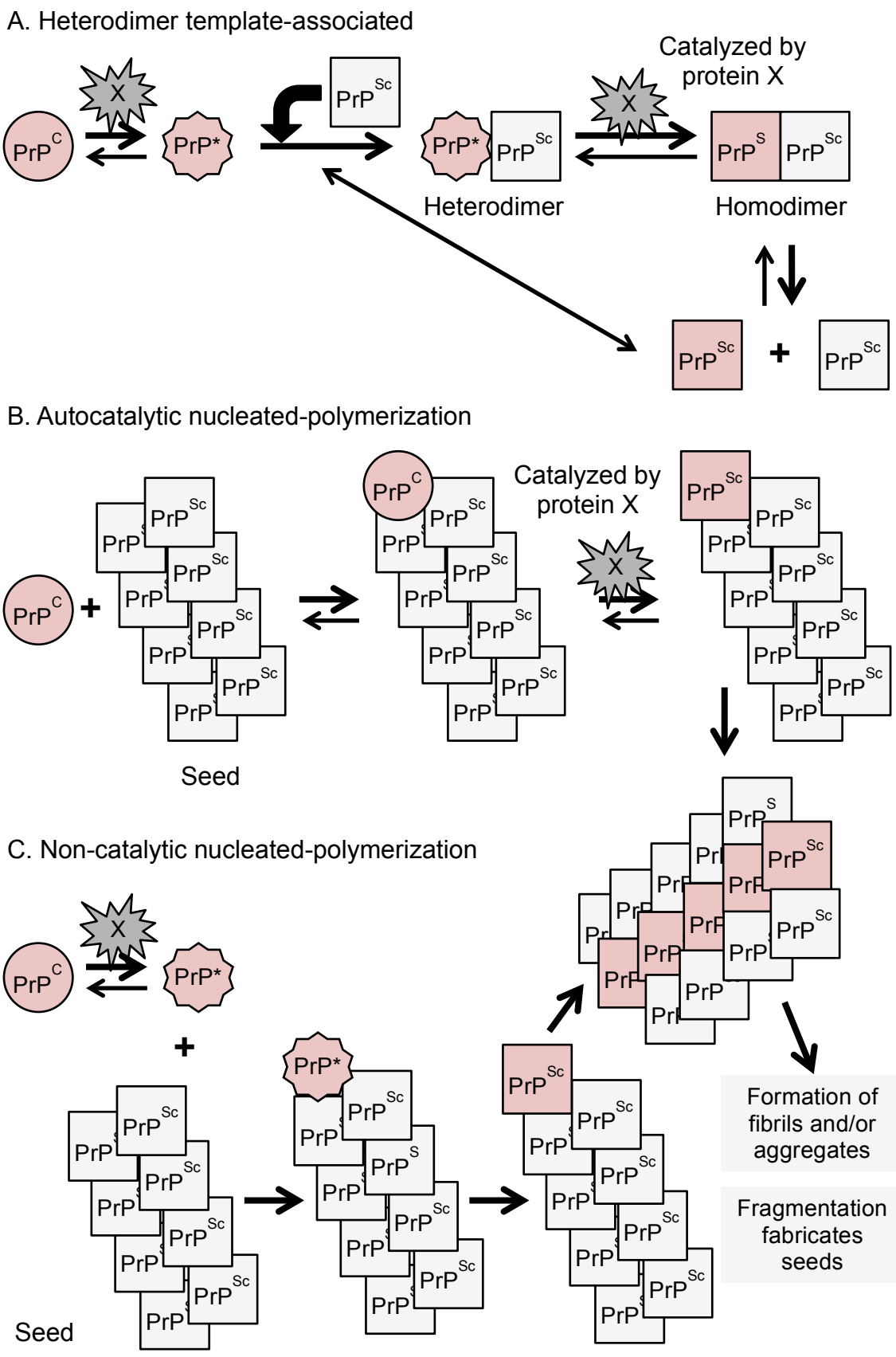
A. Heterodimer template-associated
Catalyzed by protein X
PrP^C
X
PrP*
PrP^Sc
Heterodimer
PrP^S
Homodimer
B. Autocatalytic nucleated-polymerization
Catalyzed by protein X
Seed
C. Non-catalytic nucleated-polymerization
Seed
Formation of fibrils and/or aggregates
Fragmentation fabricates seeds

Figure 1.2. Template-associated and nucleated-polymerization models of prion conversion. A. PrP^{C} is in equilibrium with an intermediate form, referred to as PrP*, and PrP* can form a heterodimer complex with PrP^{Sc}, which becomes a template to alter the conformation of PrP* into infectious isoform PrP^{Sc}, resulting in the formation of a homodimer complex. The homodimer complex can dissociate into two monomers, which can become additional templates to produce more PrP^{Sc}. A hypothetical protein X is thought to play roles in the conversion of PrP^{C} to PrP^{Sc} and also catalyze the PrP^{Sc} conversion. PrP^{Sc} is thermodynamically stable compared to PrP^{C}; furthermore, the conversion of PrP^{Sc} from PrP* is less likely to happen without a catalyst. B. The autocatalytic nucleated-polymerization model offers an additional explanation of the exponential growth of PrP^{Sc}. In this model, PrP^{C} directly interacts with PrP^{Sc} seed in fibril or aggregate forms, and the conversion reaction is the rate-limiting step. The PrP^{Sc} conversion step might be catalyzed by protein X. Since the seed is thermodynamically stable, the addition of new PrP^{Sc} can accelerate the formation of longer fibrils or larger aggregates. C. The non-catalytic nucleated-polymerization model explains that PrP* rather than PrP^{C} interacts with the seed to form stable polymers, and the PrP^{Sc} conversion step occurs non-catalytically. The rate-limiting step is the reversible reaction between PrP^{C} and PrP^{*}, and the reaction might be facilitated by protein X. The rest of the steps to form PrP^{Sc} fibrils and aggregates are irreversible.

Chapter 2

Transgenetic modeling of the CWD species barrier to humans

Introduction

Chronic wasting disease (CWD) is a transmissible spongiform encephalopathy (TSE) affecting free-ranging and captive deer, elk, and moose, and is highly contagious (Baeten *et al.*, 2007; Miller *et al.*, 2000; Williams, 2005; Williams & Young, 1980, 1982, 1992). Since 1967, when the first case of CWD was reported in Colorado, the endemic area in North America has steadily spread, with other cases reported abroad (Williams & Young, 1980). In fact, by 2005, CWD was reported from 12 states in the United States and 2 provinces in Canada with an additional case in South Korea (Chronic Wasting Disease Alliance, 2012; Kim *et al.*, 2005; Prusiner, 2004). Moreover, by 2012, new CWD cases had been identified in those 12 states and in 7 other states as well as in South Korea (Chronic Wasting Disease Alliance, 2012; Sohn, 2011). The increasing incidence of CWD in wild and captive-farm animals in North America raises doubts about the safety of consuming potentially CWD-contaminated cervid meat or products. The transmissibility risk of CWD into humans remains unclear at the present time.

The transmission of bovine spongiform encephalopathy (BSE) into humans has been reported worldwide, and more than 200 people have developed and died from variant Creutzfeldt-Jakob disease (vCJD) through

exposure to BSE-contaminated products (Prusiner, 2004; World Health Organization, 2012). Given that wild game animals, especially deer and elk, are extensively hunted and consumed throughout North America, and the zoonotic potential of BSE is now recognized (Bruce *et al.*, 1997; Scott *et al.*, 1999), these facts arouse related epidemiological concerns as to whether CWD from deer and elk is transmissible to humans, likewise whether a CWD epidemic in deer and elk populations might increase transmission risks for humans.

In recent years, numerous approaches have been employed to address these issues. In one approach, transmissibility of CWD has been tested through the use of transgenic (Tg) mouse models. To date, studies of this nature report no evidence of the transmission of CWD into the transgenic mice expressing human PrP (Kong *et al.*, 2005; Sandberg *et al.*, 2010; Tamguney *et al.*, 2006; Wilson *et al.*, 2012). Another approach used two nonhuman primate species, squirrel monkeys and cynomolgus macaques, as a model of CWD transmission to humans. Two studies reported that squirrel monkeys inoculated orally and intracerebrally with CWD from deer and elk developed disease, and the accumulation of PrP^{Sc} was detected in their brains (Marsh *et al.*, 2005; Race *et al.*, 2009b). However, cynomolgus macaques, which are evolutionally closer to humans (Hayasaka *et al.*, 1988), did not develop any signs of disease following either oral or intracerebral transmission of deer and elk CWD isolates (Marsh *et al.*, 2005; Race *et al.*, 2009b). A third approach involves possible links between the high prevalence of CWD in deer and elk and the incidence of CJD in Colorado, where CWD is endemic. In this approach, epidemiological surveillance

studies were conducted. Thus far, no positive associations have been found (Belay *et al.*, 2004; Mawhinney *et al.*, 2006). Other studies, focusing on the conversion of human PrP^{Sc}, used an *in vitro* model. These likewise reported that CWD PrP^{Sc} failed to convert human PrP^{C} into PrP^{Sc} (Barria *et al.*, 2011; Kurt *et al.*, 2009). In addition, the extremely inefficient conversion of recombinant human PrP^{Sc} using CWD PrP^{Sc} in comparison with the species matched (cervid) recombinant PrP^{Sc} conversion was reported (Raymond *et al.*, 2000). Together, the above-mentioned studies suggest that there is a high species barrier between cervid and human.

Although the previously mentioned studies suggest that CWD presents a low risk of the zoonotic potential, other recent studies remind us that there still are significant questions about the transmissibility of CWD into humans. One of those concerns the tissues consumed by humans which are derived from deer or elk with CWD, including skeletal muscle (Angers *et al.*, 2006), antler velvet (Angers *et al.*, 2009), blood (Mathiason *et al.*, 2006) and fat (Race *et al.*, 2009a), particularly when such tissues harbor infectious prions. Another study found that at least two distinct strains of CWD (referred to as CWD1 and CWD2) propagate in deer and elk (Angers *et al.*, 2010); however, the host-range properties of CWD1 and CWD2 are still unknown. A further complication is the fact that prion strains can mutate to adapt not only within the same species with different genetic backgrounds, such as animals of same species expressing *Prnp* polymorphisms, but also following transmission to a new host (Asante *et al.*, 2002; Lloyd *et al.*, 2004; Mead *et al.*, 2009; Wadsworth *et al.*, 2004). Such

mutational events can result in the formation of new prion strains with unpredictable biological properties, including the acquisition of a new host-range. Consequently, it is difficult to predict the number of CWD strains that may exist and propagate in a given population of animals. In this connection, it is extremely important to assess the transmissibility of new CWD strains into humans when such strains are identified.

Codon 129, and the corresponding 132 residue in elk, significantly influenced the transmission of BSE and CWD prions respectively in Tg mouse models (Green *et al.*, 2008). It would follow from this that, the genetic susceptibility of humans to CWD should also be determined. Moreover, cervid PrP^{Sc} converted human PrP^{C} after CWD prions were stabilized by successive passages *in vivo* and *in vitro* (Barria *et al.*, 2011), suggesting the potential adaptation of cervid PrP^{Sc} in humans to develop disease. In spite of all these many and varied concerns, it does seem that the species barrier of prion transmission species barrier between human and cervid is certainly not easy to overcome. There remains significant potential that new CWD strains can arise and acquire new host-range during horizontal transmission.

The studies detailed below aim to test whether CWD1 and CWD2 strains are transmissible to Tg(HuPrP) mice, and to address the impact of the human PrP methionine (M) or valine (V) residue 129 polymorphism on the CWD-to-human species barrier. To address the hypotheses, Tg(HuPrP) mice encoding either M or V129 human PrP polymorphism referred to as Tg(HuPrP-M129) and Tg(HuPrP-V129) mice were intracerebrally inoculated with previously

characterized CWD1 and CWD2 strains. The Soto group demonstrated the amplification of human PrP^{Sc} with the successive stabilized CWD *in vitro*, Tg(HuPrP) mice were intracerebrally inoculated with CWD prions that had been passaged multiple times in Tg mice expressing deer PrP to determine whether the propagation of human PrP^{Sc} could occur with the stabilized CWD isolate in the animal system.

Materials and Methods

Transgenic mice expressing human PrP. Hemizygous Tg mice expressing human PrP encoding either M or V at residue 129 (referred to as Tg(HuPrP-M129)$6816^{+/-}$ and Tg(HuPrP-V129)$7826^{+/-}$, respectively) were previously generated (Kurt *et al.*, 2009). Tg mouse lines were maintained by breeding with *Prnp* knockout (*Prnp*$^{0/0}$) FVB mice on an FVB background, referred to as FVB/*Prnp*$^{0/0}$ mice. Tg offspring were identified by tail biopsy and extraction of genomic DNA followed by polymerase chain reaction (PCR) screening for the presence of the transgene using a standard protocol. Briefly, approximately 1 cm of tail tissue was digested overnight at 55°C with proteinase K (PK) at a final concentration of 0.5 mg/ml in 50 mM Tris pH 8.0, 100 mM ethylenediaminetetraacetic acid (EDTA), 0.5% sodium dodecyl sulfate (SDS), the DNA extracted with phenol and chloroform and concentrated by ethanol precipitation. Tg(HuPrP-M129)$6816^{+/-}$ and Tg(HuPrP-V129)$7826^{+/-}$ were used in the following studies. The expression levels of PrP in the brains of Tg(HuPrP-M129)$6816^{+/-}$ and Tg(HuPrP-V129)$7826^{+/-}$ mice are 16-fold and 2-fold

overexpressed comparing to PrP expressed in the brains of wild-type FVB mice, respectively (Figure 2.1.).

Transmission studies and CWD inocula. Pertinent information on the CWD inocula used in the following studies is summarized in Tables 2.1. and 2.3. Elk CWD isolate (99W12389) was obtained from a CWD affected elk from the Wyoming State Veterinary Laboratory. Elk Bala05 CWD isolate was obtained from an elk, which was naturally affected with CWD, from the Canadian Food Inspection Agency, Ottawa, Ontario Canada. Deer CWD isolate (9179) was obtained from a deer, which was naturally affected with CWD, from Wyoming (Angers *et al.*, 2010). Deer H92 CWD isolate was obtained from a mule deer, which was naturally affected with CWD, from Colorado State University, Fort Collins, Colorado. The CWD isolates 99W12389, Bala05 and 9179 previously produced disease in Tg(Deer PrP)$1536^{+/-}$ mice expressing deer PrP, previously referred to as Tg(CerPrP)$1536^{+/-}$ mice. These isolates were selected because their biological properties upon transmission reflected phenotypes that were consistent with CWD1, CWD2 and mixtures of the two CWD types (CWD mix) (Angers *et al.*, 2010).

In separate studies, H92 isolate was serially passaged three times in Tg(Deer PrP)$1536^{+/-}$ mice and characterized as CWD mix (Angers *et al.*, 2010). In the tertiary passage, one Tg(Deer PrP)$1536^{+/-}$ mouse inoculated with the serially passaged H92 CWD developed disease at 193 days post inoculation (dpi), which will be referred as a short incubation time; and another Tg(Deer

PrP)1536$^{+/-}$ mouse with the serially passaged H92 CWD developed disease at 299 dpi, referred as a long incubation time. In this study, two diseased Tg(Deer PrP)1536$^{+/-}$ mouse brains from the short and long incubation time groups were used to inoculate Tg(HuPrP-M129)6816$^{+/-}$ and Tg(HuPrP-V129)7826$^{+/-}$ mice (Table 2.4.).

Blocks of the CWD-positive brains were prepared as 10% (w/v) in sterile phosphate buffered saline (PBS) lacking Ca^{2+} and Mg^{2+} ions by repeated extrusion through a series of needles of decreasing diameter from 18 gauge to 22 gauge. Ten-percent brain homogenate was diluted to 1% (v/v) in PBS and thoroughly homogenized using a 26 gauge needle syringe. Groups of 5-week-old Tg(HuPrP-M129)6816$^{+/-}$ and Tg(HuPrP-V129)7826$^{+/-}$ mice were anesthetized with halothane and injected with 30 µl of 1 % (w/v) brain homogenate intracerebrally into the right parietal lobe using a 26 gauge needle syringe.

Determination of incubation time. Animals were monitored for general health on a daily basis as well as for manifestations of progressive neurological dysfunction normally associated with prion diseases. The clinical manifestation of disease was determined by the presence of at least three of the following clinical signs: truncal ataxia, kyphotic posture, hind-limb paresis, loss of extensor reflex, difficulty righting from a supine position, flattened gait and tail stiffening. Animals were diagnosed when at least two investigators agree with the clinical manifestation of disease. Severity of clinical signs were scored for 13 clinical signs using 0 = absence, 1 = mild, 2 = moderate and 3= severe. In addition, all

animals were recorded on video at the time of diagnosis and/or right before termination. The incubation time was defined as a period of the time between the day the prion was inoculated and the first day the diagnosis was given; therefore, the incubation time was indicated in 'days post inoculation' (dpi).

Detection of PrP^{Sc} by western blotting analysis. The right hemisphere of each brain was collected for western blot analysis. Ten-percent (w/v) brain homogenates were prepared in sterile PBS by repeated extrusions through a series of needles of decreasing diameter from 18 to 22 gauge.

The concentration of total protein in each sample was determined by bicinchoninic acid assay and standardized for each lane (40 μg per lane). Proteins were resolved by sodium dodecyl sulfate-polyacrylamide gel electrophoresis and transferred to polyvinylidene difluoride Immobilon-FL (PVDF) membranes (Millipore). The transferred membrane was blocked with 5% (w/v) non-fat milk in 0.5% (v/v) Tween-20 in Tris-buffered saline (TBST) and immunoprobed with mouse monoclonal antibody anti-PrP PRC5 followed by horseradish peroxidase-conjugated anti-mouse secondary antibody. Proteins were visualized using ECL Plus (GE Healthcare) in an FLA-5000 scanner (Fujifilm Life Science). The expression levels of PrP^{C} in Tg(HuPrP) mice were determined by reading each histogram of PrP^{C} signals on the western blot using MultiGauge (Fujifilm Life Science).

All brain samples from the CWD-inoculated Tg(HuPrP-M129)$6816^{+/-}$ and Tg(HuPrP-V129)$7826^{+/-}$ mice with and without manifestation of neurological

dysfunction were analyzed for the presence of PrP^{Sc} by western blotting. Four µl of 10% brain homogenate mixed in PBS with 2% sarkosyl was treated with PK with a final concentration of 100 µg/ml for 1 hour at 37°C and ultracentrifuged at 100,000 × *g* for 1 hour at 4°C to concentrate PrP^{Sc}. Digested and undigested samples were assessed by western blotting with appropriate controls. An FVB/$Prnp^{0/0}$ (KO) was used as a negative control for the anti-PrP antibody. An uninfected Tg(HuPrP) was used as a negative control for the presence of PK resistant PrP^{Sc}. The deer CWD (99W12389) was used as a positive control for the presence of PK resistant PrP^{Sc}. Electrophoresis, transfer of proteins to a PVDF membrane and western blotting using PRC5 were performed as described above.

Evaluation of spongiform degeneration. Spongiosis development is a neuropathological feature of prion diseases including CWD, and representative animals displaying signs of neurological dysfunction were determined for vacuolation (spongiform change) in the brain. The left hemisphere of each brain was collected for neuropathological analyses. The half-brains were fixed in 4% formaldehyde for 24 hours, transferred to sterile PBS and paraffin wax embedded. Brain sections of 8 µm thickness were coronally cut to areas corresponding to the four levels of the brain containing the nine brain regions including the medulla, cerebellum, midbrain, hypothalamus, thalamus, hippocampus, paraterminal body and cerebral cortex at the levels of the septum and hippocampus (Figure 2.4.). The brain sections were collected on positively

charged slides. Harris haematoxylin and eosin (H & E) staining was performed by a standard method at the Veterinary Diagnosis Laboratory Colorado State University. Appropriate positive (RML diseased wild-type FVB mouse brains) and negative controls (uninfected Tg(HuPrP-M129)6816$^{+/-}$ and Tg(HuPrP-V129)7826$^{+/-}$ mouse brains) were also performed with experiments. The H & E staining provides nuclear staining and counterstaining to provide guidance to observe the vacuolation development on brain sections. The criteria for spongiosis development in prion diseases are: (1) region specific (Figure 2.4.), (2) appearing between nerve cell bodies and (3) the formation of vacuolation, which can be diffuse but intensive or appearing in the groups which often look to be a floral form (Figure 2.5.10.) (Prusiner, 2004). In addition to the positive control explained above, another positive control, CWD-inoculated Tg(Deer PrP)1536$^{+/-}$ mouse brain, on which the H & E staining was performed previously, was used (Figure 2.5.10.). The images were taken on a BX60 microscope equipped with a DP-71 charge-coupled diode (CCD) camera (Olympus) and composed with Adobe Photoshop.

Statistical analysis. Statistical analysis of impacts of the human PrP polymorphism at codon 129 on the manifestation of clinical signs in CWD-inoculated Tg(HuPrP-M129)6816$^{+/-}$ and Tg(HuPrP-V129)7826$^{+/-}$ mice was performed using a Fisher's exact test for each CWD prion strain separately. Statistical analysis of the severity of clinical signs was determined using a Kruskal-Wallis one-way analysis of variance (ANOVA) to compare six groups

(CWD1, CWD2 or CWD mix inoculated Tg(HuPrP-M129)6816$^{+/-}$ and Tg(HuPrP-V129)7826$^{+/-}$ mice) for each clinical sign. All data were analyzed with GraphPad Prism 5. Differences with $p < 0.05$ was considered to be a significant.

Results

Manifestation of clinical signs in CWD-inoculated Tg(HuPrP) mice. Tg(HuPrP-M129)6816$^{+/-}$ and Tg(HuPrP-V129)7826$^{+/-}$ mice expressing PrP in the central nervous system (CNS) at levels 16-fold and 2-fold higher than an FVB mouse were used in the following studies, respectively (Figure 2.1.) Three of eight Tg(HuPrP-M129)6816$^{+/-}$ mice inoculated with CWD1 (99W12389 elk isolate from Wyoming) developed truncal ataxia, hind-limb paresis and difficulty righting from a supine posture. The mean incubation time for mice to manifest clinical signs was 442 ± 90 dpi (± standard error of the mean, SEM) (range, 263–532 dpi) (Table 2.1. Table 2.2. and Figure 2.2.). Additional neurological dysfunctions including kyphotic posture, tail stiffening, loss of extensor reflex, flattened gait, head bobbing, aggressive behavior, slowed movement and rough coat, were also observed in three of the CWD1-inoculated Tg(HuPrP-M129)6816$^{+/-}$ mice. Four of eight Tg(HuPrP-M129)6816$^{+/-}$ mice inoculated with CWD2 (Bala05 elk-isolate from Ontario Canada) developed tail stiffening, hind-lib paresis and loss of weight or condition after an average of 425 ± 60 dpi (range, 284–551 dpi) (Table 2.1. Table 2.2. and Figure 2.2.). These mice also exhibited some of the following neurological dysfunctions: truncal ataxia, kyphotic posture, loss of extensor reflex, difficulty righting, flattened gait, head bobbing, aggressive behavior,

slowed movement and rough coat. Two of eight Tg(HuPrP-M129)6816$^{+/-}$ mice inoculated with CWD mix (9179 deer isolate from Wyoming) developed kyphotic posture, tail stiffening, slowed movement and rough coat after an average of 354 ± 70 dpi (range, 315–393 dpi) (Table 2.1. Table 2.2. and Figure 2.2.). These two mice also exhibited some of the following neurological dysfunctions: truncal ataxia, loss of extensor reflex, circling and loss of weight or condition.

One of eight Tg(HuPrP-V129)7826$^{+/-}$ mice inoculated with CWD1 developed tail stiffening, head bobbing and rough coat after 543 dpi (Table 2.1. Table 2.2. and Figure 2.2.). None of eight Tg(HuPrP-V129)7826$^{+/-}$ mice inoculated with CWD2 presented clinical signs after 657 dpi (Table 2.1. Table 2.2. and Figure 2.2.). One of seven Tg(HuPrP-V129)7826$^{+/-}$ mice inoculated with CWD mix developed truncal ataxia, kyphotic posture, tail stiffening, loss of extensor reflex, flattened gait, slowed movement, dull or rough coat and loss of weight or condition after 488 dpi (Table 2.1. Table 2.2. and Figure 2.2.). Other study animals did not present with clinical signs associated with prion disease and died from unrelated medical issues, such as, skin irritation, development of abdominal mass or pulmonary issues (open circles in Figure 2.2.). The remaining animals in these studies were terminated at 657 dpi due to aging (triangles in Figure 2.2.).

Severity of clinical signs manifested by CWD-inoculated Tg(HuPrP-M129)6816$^{+/-}$ and Tg(HuPrP-V129)7826$^{+/-}$ mice was scored and summarized in Table 2.2. Scores were determined by each clinical sign in each animal, and a sum of scores given for each animal was indicated under each clinical sign

(Table 2.2). A total score of severity of clinical signs in CWD1-inouclated Tg(HuPrP-M129)6816$^{+/-}$ mice was 42 consisting of scores of 11 clinical signs: truncal ataxia (a score was 6, scores will be indicated in parenthesis for the following clinical signs), kyphotic posture (1), tail stiffening (5), hind-limb paresis (6), loss of extensor reflex (4), difficulty righting from a supine position (5), flattened gait (4), head bobbing (2), aggressive behavior (1), slowed movement (3) and dull or rough coat (5) (Table 2.2.). A total score of severity of clinical signs in CWD2-inouclated Tg(HuPrP-M129)6816$^{+/-}$ mice was 56 consisting of scores of 12 clinical signs: truncal ataxia (2), kyphotic posture (4), tail stiffening (8), hind-limb paresis (4), loss of extensor reflex (4), difficulty righting from a supine position (4), flattened gait (6), head bobbing (1), aggressive behavior (6), slowed movement (4), dull or rough coat (6) and loss of weight or condition (7) (Table 2.2.). A total score of severity of clinical signs in CWD mix-inoculated Tg(HuPrP-M129)6816$^{+/-}$ mice was 14 consisting of scores of 8 clinical signs: truncal ataxia (1), kyphotic posture (2), tail stiffening (2), loss of extensor reflex (1), slowed movement (2), circling (1), dull or rough coat (4) and loss of weight or condition (1) (Table 2.2.). A total score of severity of clinical signs in CWD1-inouclated Tg(HuPrP-V129)7826$^{+/-}$ mice was 3 consisting of scores of 3 clinical signs: tail stiffening (1), head bobbing (1), and dull or rough coat (1) (Table 2.2.). A total score of severity of clinical signs in CWD mix-inoculated Tg(HuPrP-V129)7826$^{+/-}$ mice was 11 consisting of scores of 8 clinical signs: truncal ataxia (1), kyphotic posture (2), tail stiffening (1), loss of extensor reflex (1), flattened gait (1), slowed movement (1), dull or rough coat (2) and loss of weight or

condition (2) (Table 2.2.). Statistical analysis of the severity of the clinical signs was performed using a Kruskal-Wallis one-way ANOVA between groups. The total scores of severity of clinical signs between different CWD prions and between Tg(HuPrP-M129)6816$^{+/-}$ and Tg(HuPrP-V129)7826$^{+/-}$ mice were not statistically significant; however, one clinical sign, difficulty righting from a supine position was turned out to be statistically significant ($p<0.043$) (Table 2.2.). Two other clinical signs including hind-limb paresis and loss of weight or condition were borderline significant ($p<0.055$ and $p<0.061$, respectively) (Table 2.2.).

CWD1 and CWD2 inoculated Tg(HuPrP-M129)6816$^{+/-}$ mice exhibited multiple clinical signs, which were rapidly progressed. On the other hand, CWD mix inoculated Tg(HuPrP-M129)6816$^{+/-}$ mice developed fewer neurological signs compared to CWD1 and CWD2 inoculated Tg(HuPrP-M129)6816$^{+/-}$ mice. CWD1 and CWD mix inoculated Tg(HuPrP-V129)7826$^{+/-}$ mice also exhibited fewer neurological signs than CWD-inoculated Tg(HuPrP-M129)6816$^{+/-}$ mice. A Fisher's exact test was performed to determine whether the human PrP 129 polymorphism impacted on the manifestation of clinical signs in CWD-inoculated Tg(HuPrP-M129)6816$^{+/-}$ and Tg(HuPrP-V129)7826$^{+/-}$ mice; however, no statistically significant difference ($p<0.05$) between M and V at the 129 polymorphism was found in each CWD-inoculated animal group. The p-value of a Fisher's exact test in CWD2-inoculated Tg(HuPrP-M129)6816$^{+/-}$ and Tg(HuPrP-V129)7826$^{+/-}$ mice turned out to be a borderline significance ($p>0.077$) (Table 2.1.). Overall, Tg mice expressing the HuPrP polymorphism M129 mice tended to develop more overt clinical signs compared to Tg(HuPrP-V129)7826$^{+/-}$ mice.

No evidence of PrP^{Sc} in the CWD inoculated Tg mouse brains. The right half-brains of all the animals in the studies were analyzed for the presence of PK resistant PrP^{Sc} in western blotting analyses. Even though the samples were enriched for the presence of aggregated PrP, by ultracentrifugation in the presence of non-denaturing detergents, which is a property of disease-associated PrP, PrP^{Sc} was not detected by western blotting in any of the study animals. Two representative samples from each group of the CWD1, CWD2 and CWD mix inoculated Tg(HuPrP) mice are shown along with PK-digested and -undigested samples, as well as with appropriate positive and negative controls, in Figure 2.3. As negative control, uninfected Tg(HuPrP) mouse brains were used and showed the presence of PrP^{C} but not PrP^{Sc}. As positive control, deer CWD (99W12389) isolate was used and revealed PrP^{Sc} in the sample, demonstrating our ability to distinguish disease-associated PrP in this assay.

Absence of spongiform degeneration in the brains of clinically affected CWD inoculated Tg(HuPrP) mice. Selected brains from animals manifesting clinical signs were further analyzed for the development of spongiosis. Nine brain regions, including the medulla, cerebellum, midbrain, hypothalamus, thalamus, hippocampus, paraterminal body, cerebral cortex at the levels of the septum and hippocampus, were assessed for the development of disease-related vacuolation in CWD inoculated Tg(HuPrP) mice, which manifested clinical signs (Table 2.4.). Even though the CWD inoculated Tg(HuPrP) mice presented prion disease-

associated clinical signs, disease-associated spongiosis was not observed in any of the analyzed mice (Figure 2.5.). Some spongiosis observed in the brains was not region specific and did not appear to be the result of neuronal vacuolation those observations were inconsistent with the types of prion disease-associated spongiosis (Figure 2.5.10.). Since many of the study animals were aged (some were close to 600 days old), the spongiosis observed in those animal brains were more likely associated with aging.

No signs of disease in Tg(HuPrP) mice inoculated with CWD prions passaged multiple times in Tg(Deer PrP)1536$^{+/-}$ mice. In separate studies, Tg(HuPrP-M129)6816$^{+/-}$ and Tg(HuPrP-V129)7826$^{+/-}$ mice were intracerebrally inoculated with CWD isolates that had been passaged multiple times in Tg(Deer PrP)1536$^{+/-}$ mice (Table 2.4.). None of the mice developed neurological dysfunctions, and all died from unrelated medical issues (range, 162-646 dpi) (Table 2.4. and Figure 2.6.). Ten Tg(HuPrP-V129)7826$^{+/-}$ mice, which did not develop any clinical signs, were terminated at 560 dpi, while eight Tg(HuPrP-M129)6816$^{+/-}$ mice, which did exhibit clinical signs, were further observed for the progression of neurological dysfunction. Four Tg(HuPrP-M129)6816$^{+/-}$ mice inoculated with serially passaged CWD from a short incubation time group, and another four Tg(HuPrP-M129)6816$^{+/-}$ mice inoculated with serially passaged CWD from a long incubation time group, did not progress the clinical signs in the next 100 days. Thus, all remaining mice were terminated at 646 dpi.

Discussion

To model the species barrier between humans and CWD prions, Tg(HuPrP-M129)6816$^{+/-}$ and Tg(HuPrP-V129)7826$^{+/-}$ mice were tested for their susceptibility to CWD1 and CWD2 strains as well as isolates containing a mixture of both. A subset of CWD-inoculated animals developed the progressive clinical signs; however, the examination of brain material from these diseased mice failed to confirm the presence of protease-resistant human PrP^{Sc} or neuropathological signs associated with prion disease (Table 2.2. and Figure 2.3.). These results are consistent with a significant species barrier in humans to these CWD strains. The additional assessment of the susceptibility to the serially passaged CWD isolates was also performed using Tg(HuPrP-M129)6816$^{+/-}$ and Tg(HuPrP-V129)7826$^{+/-}$ mice. None of the serially passaged CWD inoculated animals developed disease with the absence of clinical signs and PrP^{Sc} in the brains. Because of the lack of disease, the impact of human PrP 129 polymorphism on the susceptibility of CWD was inconclusive in the above studies.

In these studies, the species barrier between the CWDs and Tg(HuPrP) mice was not overcome in the primary transmission. PrP^{Sc} deposition and spongiform development were not identified in the 16-fold and 2-fold overexpressing Tg(HuPrP-M129)6816$^{+/-}$ and Tg(HuPrP-V129)7826$^{+/-}$ mouse brains, respectively. However, the presence of progressive signs of neurological dysfunction in the CWD-inoculated Tg(HuPrP) mice cannot be ignored. This suggests that the conversion of human PrP^{Sc} might occur, but slowly, when

cervid PrP^{Sc} is intracerebrally inoculated into Tg(HuPrP) mice. Race and colleagues demonstrated that gradual adaptation of hamster PrP^{Sc} to mouse PrP^{C} occurred slowly in two distinct phases, including an abnormal protease-resistant PrP (PrP-res)-negative phase followed by a replication phase during serial passages (Race *et al.*, 2002). In addition, protease-resistant PrP^{Sc} was not always detectable in both of the phases (Race *et al.*, 2002). In the present study, the PK-resistant PrP^{Sc} and spongiform change were undetectable in the brains from the CWD-inoculated Tg(HuPrP) mice; however, the propagation of PK-sensitive PrP^{Sc} might occur in the brains causing the clinical signs. Moreover, the formations of PK-sensitive PrP^{Sc} plaques and spongiform degenerative have been identified in diseased human brains (Gambetti *et al.*, 2008; Zou *et al.*, 2010b). Another group also reported that sheep scrapie diseased brains in some cases contained far more PK-sensitive PrP^{Sc} than PK-resistant PrP^{Sc}, and the PK-sensitive PrP^{Sc} had an ability to produce PK-resistant PrP^{Sc} *in vitro* (Thackray et al., 2007; Tzaban et al., 2002). These studies raise a question whether PK-sensitive PrP^{Sc} is present in the CWD-inoculated Tg(HuPrP) mice. If so, the manifestation of clinical signs in those Tg(HuPrP) mice might be a result of accumulation of PK-sensitive PrP^{Sc} in the brain.

If true prion transmission has occurred, the CWD-inoculated Tg(HuPrP) mice in the studies might be in either PrP-res-negative or replication phases. Therefore, a subset of the CWD-inoculated Tg(HuPrP) mice manifested the neurological dysfunction, which might be caused by the accumulation of human PrP^{Sc}, in the absence of a detectable amount of proteinase-resistant PrP^{Sc} in the

brains. To fully address this issue in the near future, one might find it useful to serially passage the brain materials from the CWD-inoculated Tg(HuPrP) mice displaying clinical signs into the genotype matched Tg(HuPrP) mice.

Prion disease incubation times in humans are known to extend for decades. In fact, Kuru, a human prion disease found in Papua New Guinea, has a report incubation time of over 50 years (Collinge *et al.*, 2006; Collinge *et al.*, 2008). This shows that quite lengthy periods are required for replication of PrP^{Sc} in humans, before disease development without a species barrier. In the present study, most of the CWD inoculated Tg(HuPrP) mice remained without signs of prion disease for >600 dpi even though a subset of the animals are clinical (Figure 2.2.). Four other studies also reported the negative transmissions of CWD into Tg mice expressing human PrP encoding either M or V at residue 129 (Kong *et al.*, 2005; Sandberg *et al.*, 2010; Tamguney *et al.*, 2006; Wilson *et al.*, 2012). The Gambetti group reported that three out of 29 CWD-inoculated Tg mice expressing human PrP M 129 polymorphism (Tg40) presented mild ataxia without accumulation of either PK-resistant and PK-sensitive PrP^{Sc} after >756 dpi, and another group of CWD-inoculated humanized mice expressing the M 129 polymorphism (Tg1) did not present any clinical signs after >657 dpi. Based on the absence of PrP^{Sc} and lack of such key neuropathological features as, spongiform change, gliosis and PrP^{Sc} plaques in the brain, it was concluded that the mild ataxia in three Tg40 mice was not associated with prion disease. The Prusiner group inoculated 8 different CWD isolates from elk and deer into Tg(HuPrP-M129)440 hemizygous mice and reported no clinical signs in CWD-

inoculated Tg440 mice after >500 dpi. The Collinge group also reported no clinical signs in CWD-inoculated Tg(HuPrP-M129)45, Tg(HuPrP-M129)35 and Tg(HuPrP-V129)152 homozygous mice after >700 dpi. The histology of CWD-inoculated Tg(HuPrP) mouse brains was not different from age-matched non-inoculated Tg(HuPrP) mouse brains. The Barron's group reported no clinical signs in CWD-inoculated Tg(HuPrP-M129) and Tg(HuPrP-V129) homozygous mice, or in Tg(HuPrP-M/V129) hemizygous mice after >680 dpi, >722 dpi, >730 dpi, respectively. Considering the long incubation times in human for prion diseases, one has reason to think the incubation time of 500-700 days might be insufficient for accumulation of detectable amounts of PrP^{Sc} in the brain, or to cause CWD disease in Tg(HuPrP) mice.

Furthermore, the hamster-to-mouse species barrier of prion was overcome after three serial passages of a total of 1200 to >1550 days (Race *et al.*, 2002). PK-resistant PrP^{Sc} started appearing in the brains of asymptomatic mice inoculated with brain homogenates from the mouse passaged hamster prions from the secondary transmission; and in the next transmission with brain homogenates from the secondary transmission, disease was produced in mice. The study demonstrated that the gradual adaptation of hamster prion required a substantial amount of time even between the rodents. Therefore, serial passages of the materials from the CWD-inoculated Tg(HuPrP) mice need to be evaluated for clearly establishing lack of transmission of CWD into humans.

It was essential to further analyze the CWD-inoculated Tg(HuPrP) mice with clinical signs for the development of prion diseases due to the inconclusive

results of the presence of the clinical signs without PrP^{Sc} deposition in the Tg mice. Spongiosis development, which is a neuropathological feature of prion diseases including CWD, was also examined in the clinical Tg(HuPrP) mice with CWD. The features for spongiosis development in prion diseases are: (1) region specific (Figure 2.4.), (2) appearing between nerve cell bodies and (3) the formation of vacuolation, which can be diffuse but intensive or appearing in the groups which often look to be a floral form (Figure 2.5.) (Prusiner, 2004). The analyzed CWD-infected Tg(HuPrP) mouse brains with clinical signs presented fewer vacuolations between or on cells; in those which did show, vacuoles appeared only randomly in their brains. Therefore, vacuolation found in these animals was not associated with prion diseases. More precise evaluation of the disease associated spongiosis development in the CWD inoculated Tg(HuPrP) mouse brains could be done if a PBS inoculated age matched Tg(HuPrP) mouse brain was available for a prion disease negative control. The age matched control from the genotype matched Tg mice would be a great help in evaluating whether vacuolation in the brain is due to aging or to prion diseases. As an additional positive control, Tg(HuPrP) mice with human prion diseases would be useful. Other groups have been utilizing the Tg(HuPrP) mouse model to study the interspecies transmission of prions as well as the biochemical properties of PrP^{Sc} (Asante *et al.*, 2002; Wadsworth *et al.*, 2004). Information based on the Tg mouse model has advanced our understanding of the species barrier of prions to humans including BSE (Asante *et al.*, 2002; Wadsworth *et al.*, 2004). In future studies, the named positive and negative controls would be extremely helpful in

assessing any associations among the intensity of vacuolation in specific regions, clinical signs and presence or absence of PrP^{Sc} deposition or plaques in CWD-inoculated Tg(HuPrP) mice.

Codon 129 polymorphism of the human PrP has an impact on the susceptibility to prion diseases including BSE, and the M 129 polymorphism was reported to be more susceptible to BSE and variant CJD (Lloyd *et al.*, 2004; Wadsworth *et al.*, 2004). In the present studies, we expected that the CWD-inoculated Tg(HuPrP-M129)$6816^{+/-}$ mice were more likely to develop multiple clinical signs than were Tg(HuPrP-V129)$7826^{+/-}$ mice (Table 2.2.). However, it was not clear whether the PrP 129 polymorphism impacted on the development of the multiple clinical sings in Tg(HuPrP-M129)$6816^{+/-}$ mice. The higher number of Tg(HuPrP-M129)$6816^{+/-}$ mice which manifested the multiple clinical signs might be due to the overexpression of PrP because Tg(HuPrP-M129)$6816^{+/-}$ mice express 8-fold higher levels of PrP than do Tg(HuPrP-V129)$7826^{+/-}$ mice. It has been reported that there is a reciprocal relationship between the expression level of PrP and onset of disease (Prusiner *et al.*, 1990). The higher the level of PrP expressed in Tg mice, the shorter the incubation time after inoculation with prions. Since protease-resistant PrP^{Sc} could not be detected in either the CWD-inoculated Tg(HuPrP-M129)$6816^{+/-}$ or the Tg(HuPrP-V129)$7826^{+/-}$ mice, there is perhaps reason to support that the human 129 polymorphism might not have an impact on the conversion efficiency of PK-resistant PrP^{Sc} during the primary transmission.

The present study showed that a significantly high species barrier between cervid and humans exists. CWD transmission studies in Tg(HuPrP) mice were performed by the intracerebral inoculation, which is considerably more efficient in transmitting prions than oral consumption (Prusiner *et al.*, 1985; Race *et al.*, 2009b). If CWD is transmitted to humans, consumption of CWD-contaminated products is the most likely route into humans. The present studies and others show that none of the CWD-inoculated Tg(HuPrP) mice accumulated PK-resistant PrP^{Sc} in their brains, suggesting a lower risk of transmission of CWD into humans. In view of the substantial incubation times for humans prion diseases, as well as the remarkable persistence of prions in adapting within both the same and in different species, it is important to continue evaluating the transmission of CWD in serial passages, as well as to test new strains of CWD as identified for verifying the transmission of CWD into humans.

Mindful of existing data on the successful amplification of human PrP^{Sc} with serially stabilized CWD isolates *in vivo* and *in vitro*, Tg(HuPrP) mice were also inoculated with the CWD isolates which had been passaged multiple times in Tg(Deer PrP)$1536^{+/-}$ mice. The intent was to test whether the selected CWD PrP^{Sc} increased its pathogenicity to humans during adaptation through the multiple passages in Tg(Deer PrP)$1536^{+/-}$ mice. Unlike in the *in vitro* study, evidence of PrP^{Sc} propagation was not observed in the CWD-inoculated Tg(HuPrP) mice; none of the mice developed any clinical signs after >646 dpi. The different results might be due to the use of two different systems. The present study used an animal model, and the previous study used a cell free

amplification system *in vitro*. In addition, as discussed above, the length of the incubation time even up to 646 dpi might not be long enough to see disease development in those study animals.

Even though the present studies did not prove the CWD transmission into Tg(HuPrP) during the primary passage, the zoonotic potential of CWD has not been eliminated. As there is always the possibility of preclinical and subclinical carriers of BSE in humans, it is important to take into consideration that a similar situation might occur with CWD. The modified hypothesis is that PK-sensitive PrP^{Sc} is first propagated in CWD-inoculated Tg(HuPrP) mouse brain with or without the presentation of clinical signs; later PK-resistant PrP^{Sc} becomes detectable. To address this hypothesis, brain materials from the CWD-inoculated Tg(HuPrP) mice with clinical signs in these studies will be passaged to genotype matched Tg(HuPrP) mice. When the mice manifest clinical signs, the presence of both PK-sensitive and resistant PrP^{Sc} needs to be determined in addition to the neuropathological features.

Table 2.1. Transmission of CWD isolates into Tg(HuPrP-M129)6816$^{+/-}$ and Tg(HuPrP-V129)7826$^{+/-}$ mice. Incubation time indicates days post inoculation (dpi) in mean ± SEM (standard error of the mean). The PrP expression was determined by comparing to a wild-type FVB mouse. A Fisher's exact test was performed to determine whether the human PrP 129 polymorphism impacted on the manifestation of clinical signs in CWD-inoculated Tg(HuPrP-M129)6816$^{+/-}$ and Tg(HuPrP-V129)7826$^{+/-}$ mice; however, no statistically significant difference (p<0.05) between M and V at the 129 polymorphism was found in each CWD-inoculated animal group. The p-value of a Fisher's exact test in CWD2-inoculated Tg(HuPrP-M129)6816$^{+/-}$ and Tg(HuPrP-V129)7826$^{+/-}$ mice turned out to be a borderline significance (p>0.077).

Prion	**CWD1**		**CWD2**		**CWD mix**	
Isolate	99W12389		Bala05		9179	
Location	Wyoming		Ontario Canada		Wyoming	
Origin	Elk		Elk		Deer	
Recipient Tg	HuPrP M129	HuPrP V129	HuPrP M129	HuPrP V129	HuPrP M129	HuPrP V129
PrP expression (n-fold)	16	2	16	2	16	2
Incubation time (dpi)	442 ± 90	543	425 ± 60	-	354 ± 70	488
No. of animals with clinical signs/ a total No. of animals inoculated	3/8	1/8	4/8	0/8	2/8	1/7

Table 2.2. Summary of neurological dysfunctions manifested in the CWD inoculated Tg(HuPrP-M129)6816$^{+/-}$ and Tg(HuPrP-V129)7826$^{+/-}$ mice. The number of CWD-inoculated Tg(HuPrP) mice with clinical signs is indicated in parentheses in each section of clinical signs. Severity of clinical signs were scored for 13 clinical signs using 0 = absence, 1 = mild, 2 = moderate and 3= severe. A total score of clinical signs manifested in animals were indicated in each section of clinical signs. A total score of all clinical signs were shown in the last row under each CWD-inoculated animal group. Statistical analysis of severity of clinical signs was determined using a Kruskal-Wallis one-way analysis of variance. A p-value is reported only when the value is significant (p<0.05) or borderline significant. 'No' indicates p>0.1.

Recipient Tg	***p*<0.1**	**HuPrP-M129**			**HuPrP-V129**	
Inoculum		**CWD1**	**CWD2**	**CWD mix**	**CWD1**	**CWD mix**
No. of animals with clinical signs/ a total No. of animals inoculated		**3/8**	**4/8**	**2/8**	**1/8**	**1/7**
Truncal ataxia	No	6 (3)	2 (2)	1 (1)		1 (1)
Kyphotic posture	No	1 (1)	4 (3)	2 (2)		2 (1)
Tail stiffening	No	5 (2)	8 (4)	2 (2)	1 (1)	1 (1)
Hind-limb paresis	0.055	6 (3)	4 (3)			
Loss of extensor reflex	No	4 (2)	4 (3)	1 (1)		1 (1)
Difficulty righting from a supine position	0.043	5 (3)	4 (2)			
Flattened gait	No	4 (2)	6 (3)			1 (1)
Head bobbing	No	2 (1)	1 (1)		1 (1)	
Aggressive behavior	No	1 (1)	6 (2)			
Slowed movement	No	3 (2)	4 (3)	2 (2)		1 (1)
Circling	No			1 (1)		
Dull or rough coat	No	5 (3)	6 (3)	4 (2)	1 (1)	2 (1)
Loss of weight or condition	0.061		7 (4)	1 (1)		2 (1)
Total score	No	**42**	**56**	**14**	**3**	**11**

Table 2.3. Origin of CWD isolate used in serial transmission studies.

Prion	CWD mix
Original isolate	H92
Location	Colorado
Origin	Mule deer

Table 2.4. Transmission of serially passaged CWD isolates into Tg(HuPrP-M129)6816$^{+/-}$ and Tg(HuPrP-V129)7826$^{+/-}$ mice. Elk CWD H92 isolate was passaged three times in Tg(Deer PrP)1536$^{+/-}$ mice prior to testing the transmission of CWD in Tg(HuPrP) mice in this study. Two individual samples were chosen from a pool of short incubation time group (200 dpi) and a pool of long incubation time group (300 dpi) to inoculate groups of Tg(HuPrP-M129)6816$^{+/-}$ and Tg(HuPrP-V129)7826$^{+/-}$ mice. Incubation time or time of death indicates days post inoculation (dpi). Time of death shows a period of time from the day that a first animal was terminated to the day that a last animal was terminated. The PrP expression was determined by comparing to a wild-type FVB mouse.

Inoculum	H92 CWD passaged multiple times in Tg(Deer PrP) mice			
	Short incubation time (193 dpi)		Long incubation time (299 dpi)	
Recipient Tg	HuPrP M129	HuPrP V129	HuPrP M129	HuPrP V129
PrP expression (n-fold)	16	2	16	2
Time of death (dpi)	543 – 646	171 – 560	162 – 646	451 - 560
No. of animals ill/ No. of animals inoculated	0/6	0/7	0/6	0/7

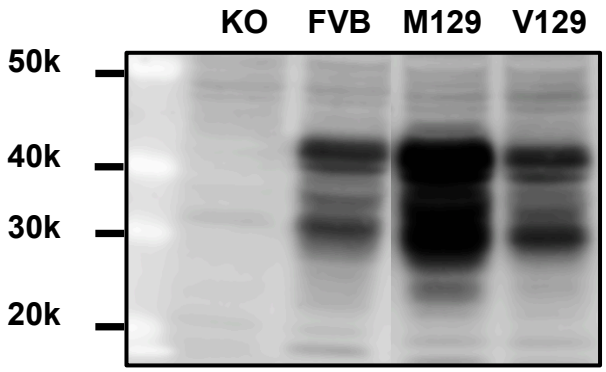

Figure 2.1. The expression levels of PrP in the transgenic mouse brains compared to a wild-type FVB mouse brain. The PrP^{C} expression levels in Tg(HuPrP-M129)6816$^{+/-}$ and Tg(HuPrP-V129)7826$^{+/-}$ mouse brains were determined by comparing to a wild-type FVB mouse brain in western blot using anti-PrP PRC5 monoclonal antibody. The PrP^{C} levels in Tg(HuPrP-M129)6816$^{+/-}$ and Tg(HuPrP-V129)7826$^{+/-}$ overexpressed 16-fold and 2-fold more than the FVB, respectively. A total amount of protein was standardized to 40µg per lane. An FVB/*Prnp*$^{0/0}$ (KO) is used as a negative control. Molecular markers indicate 50, 40, 30 and 20 kDa from top to bottom. Two cropped images are from the same exposure of the same blot.

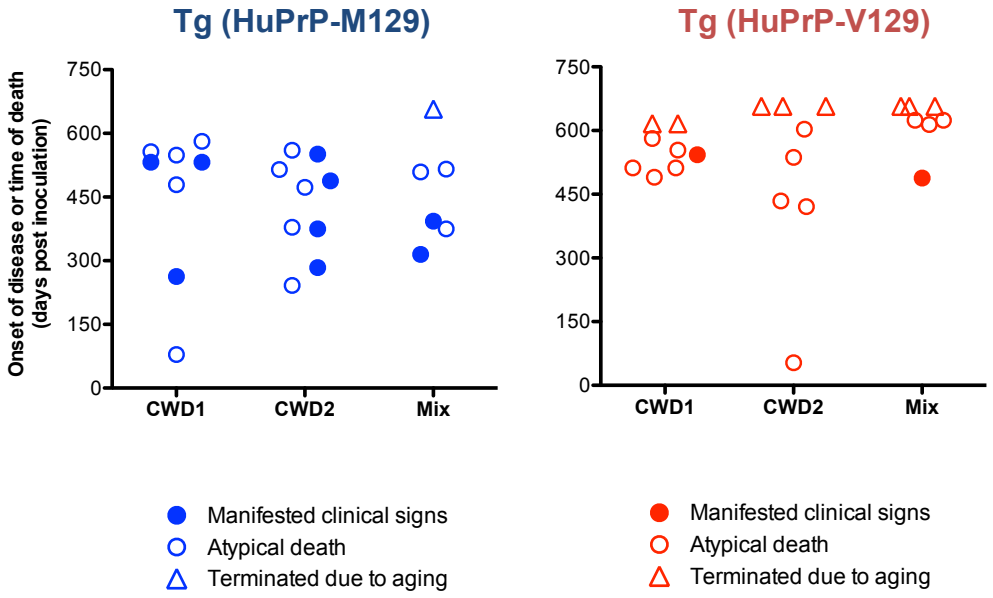

	Incubation time, days ± SEM (manifestation of clinical signs, n/n_0)		
Recipient	CWD 1	CWD 2	CWD mix
Tg (HuPrP-M129)	442 ± 90 (3/8)	425 ± 60 (4/8)	354 ± 70 (2/7)
Tg (HuPrP-V129)	543 (1/8)	(0/8)	488 (1/7)

Figure 2.2. Summary of incubation times of CWD-inoculated Tg(HuPrP) mice. Some inoculated animals manifested clinical signs associated with prion disease that were rapidly progressive (filled circles). Atypical death indicates that animals die from unrelated causes (open circles). Animals not developing prion disease were sacrificed 650 days after inoculation (triangles). The incubation times of CWD-inoculated Tg(HuPrP-M129)$6816^{+/-}$ and Tg(HuPrP-V129)$7826^{+/-}$ mice with clinical signs were summarized in the table. Incubation time indicates days post inoculation (dpi) in mean ± SEM (standard error of the mean).

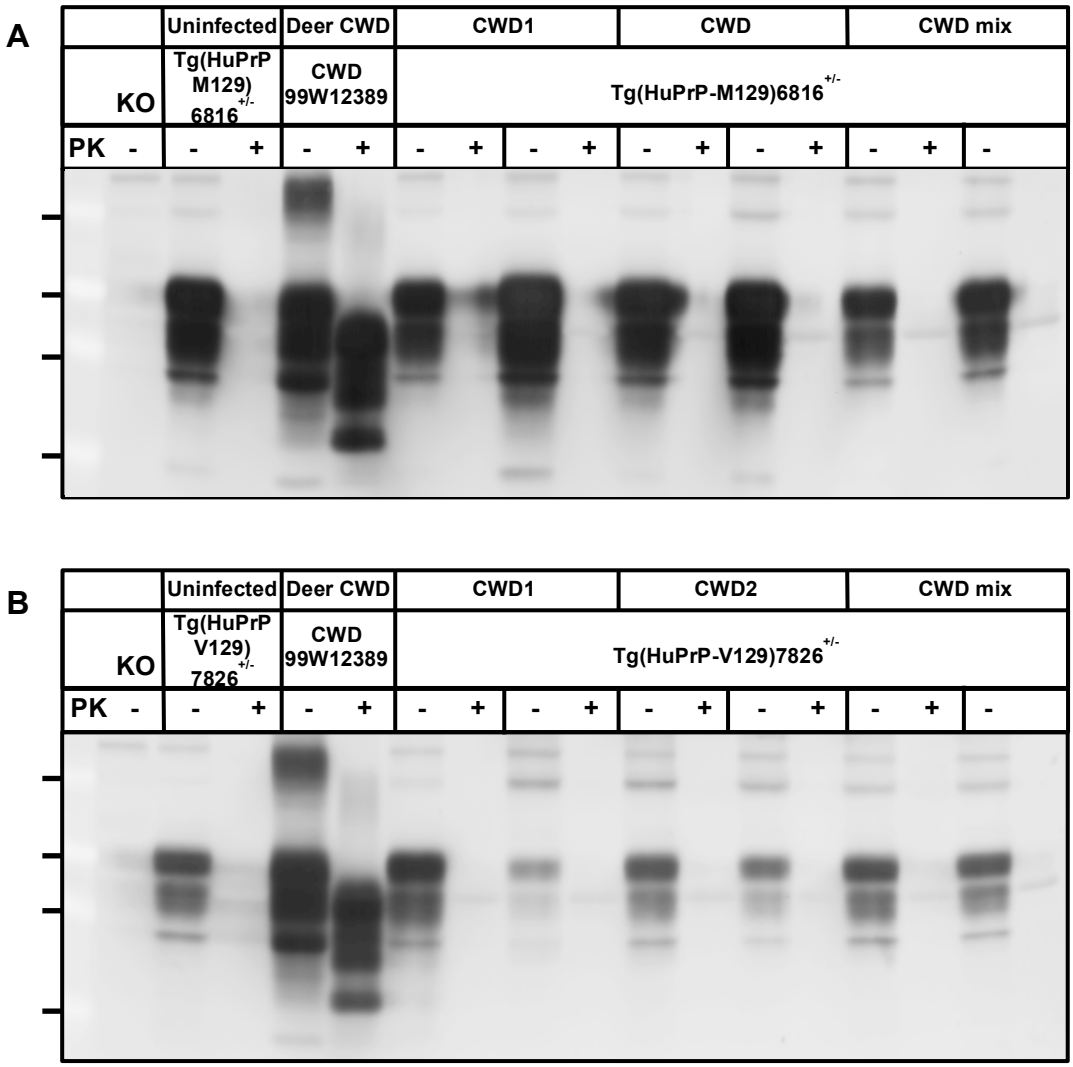

Figure 2.3. Western blot analysis showed that there is no evidence of protease-resistant PrP^{Sc} deposition in the brains from CWD-inoculated Tg(HuPrP-M129)6816$^{+/-}$ and Tg(HuPrP-V129)7826$^{+/-}$ mice. Representative samples from each group of the CWD1, CWD2 and CWD mix inoculated Tg(HuPrP-M129)6816$^{+/-}$ and Tg(HuPrP-V129)7826$^{+/-}$ mice were shown in A and B, respectively. Blots were probed with anti-PrP PRC5 monoclonal antibody. An FVB/*Prnp*$^{0/0}$ (KO) is used as a negative control for the anti-PrP antibody. An uninfected Tg(HuPrP) was used as a negative control for the presence of proteinase K (PK) resistant PrP^{Sc}. The deer CWD (99W12389) was used as a positive control for the presence of PK resistant PrP^{Sc}. Samples, which were treated with PK, indicate (+). Samples without PK digestion indicate (-). Molecular markers indicate 53, 36, 28 and 19 kDa from top to bottom.

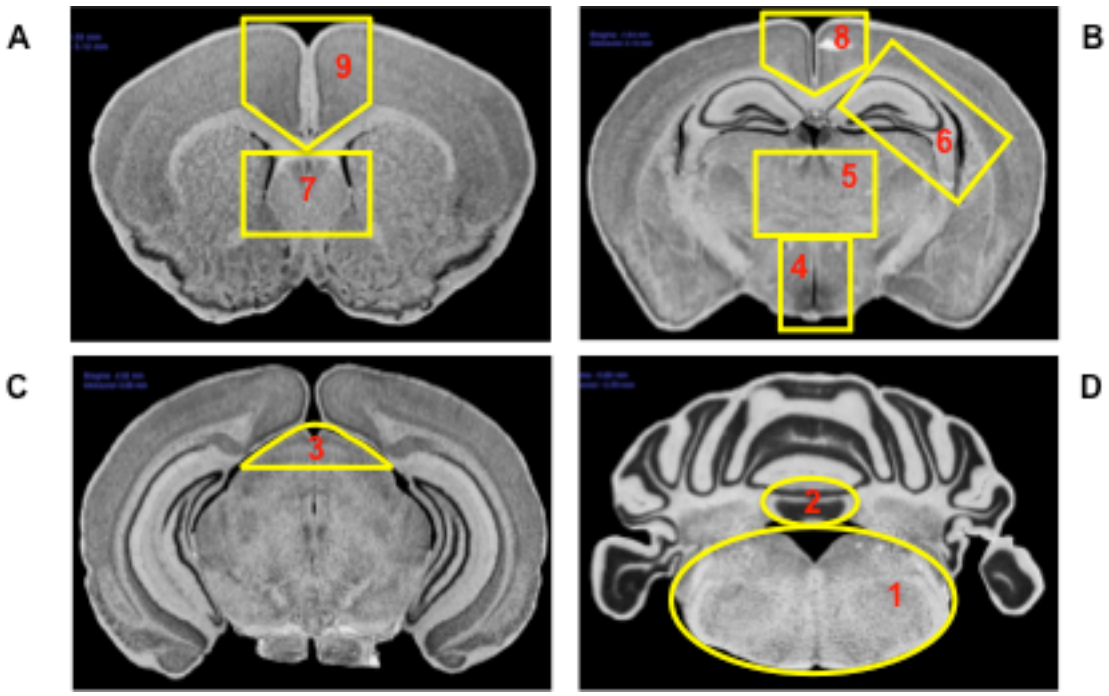

Figure 2.4. Evaluation of spongiosis degeneration in the mouse brain with prion disease. Nine brain regions were assessed for the development of spongiosis in diseased animals. A. paraterminal body (7) and cerebral cortex (9) at the level of the septum. B. hypothalamus (4), thalamus (5), hippocampus (6) and cerebral cortex (8). C. midbrain (3). D. medulla (1) and cerebellum (2).

1. Medulla

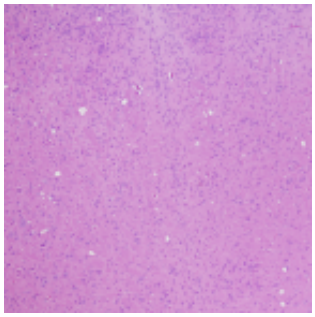

2. Cerebellum

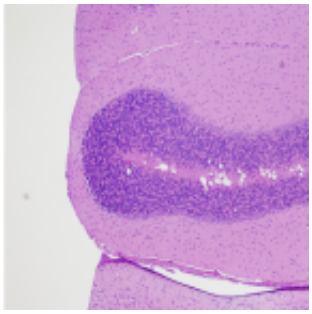

3. Midbrain

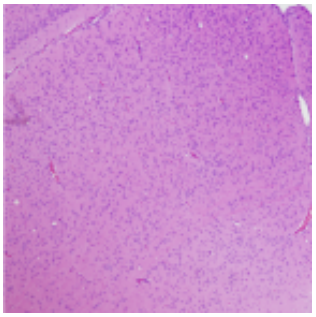

4. Hypothalamus

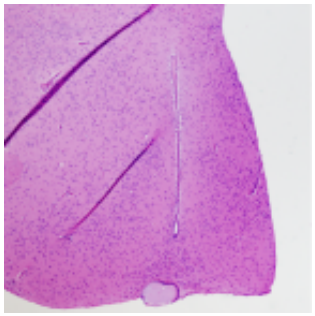

5. Thalamus

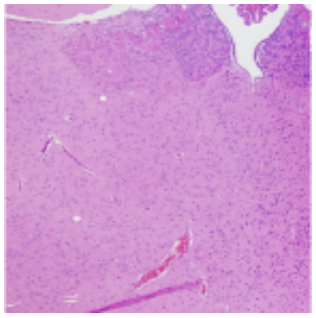

6. Hippocampus

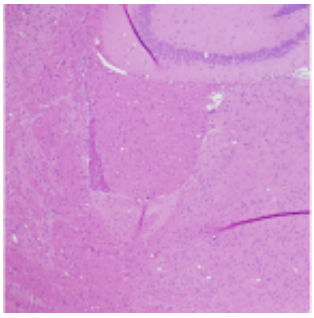

7. Paraterminal body

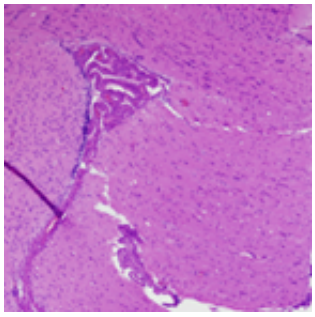

8. Cerebral

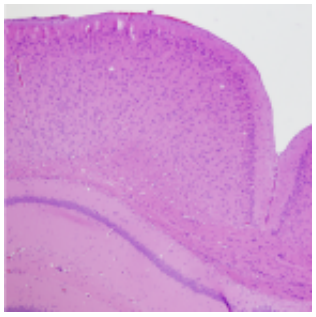

9. Cerebral cortex

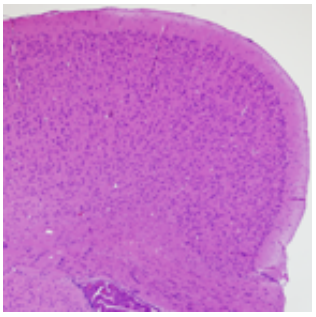

10. Positive control Hippocampus

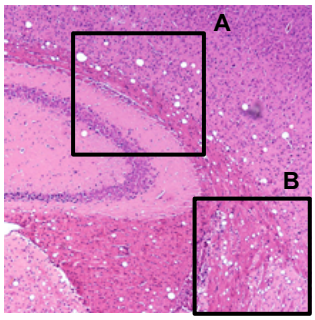

10-A. Enlarged image from positive control

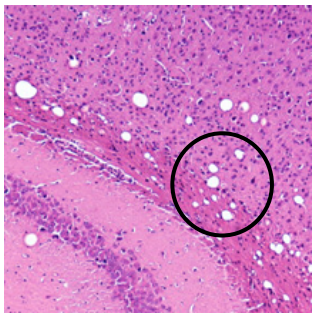

10-B. Enlarged image from positive control

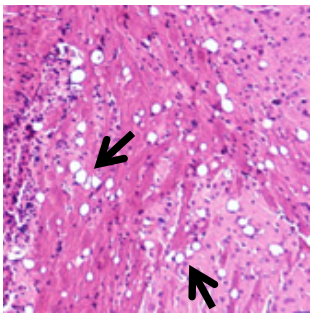

Figure 2.5. No spongiosis degeneration in the brains of CWD-inoculated Tg(HuPrP) mice was observed. Nine brain regions were assessed for the development of disease related vacuolations in CWD-inoculated Tg(HuPrP) mice, which manifested clinical signs. Nine brain regions are (1) medulla, (2) cerebellum, (3) midbrain, (4) hypothalamus, (5) thalamus, (6) hippocampus, (7) paraterminal body, (8 and 9) cerebral cortex. A positive control of spongiosis degeneration from a CWD1-inoculated Tg(Deer PrP)1536$^{+/-}$ mouse brain (hippocampus) (10). Two enlarged image of the positive control (10) are shown in 10-A and 10-B. The circle in 10-A indicates a size of vacuoles varies in the brain, and vacuoles appear between dark purple spots (cell nuclei), showing that spongiform changes appear between cells. Arrows in 10-B indicates vacuolations are diffuse but intensive in the specific brain regions and appear in the groups. The magnification of the images (1-10) is 100X.

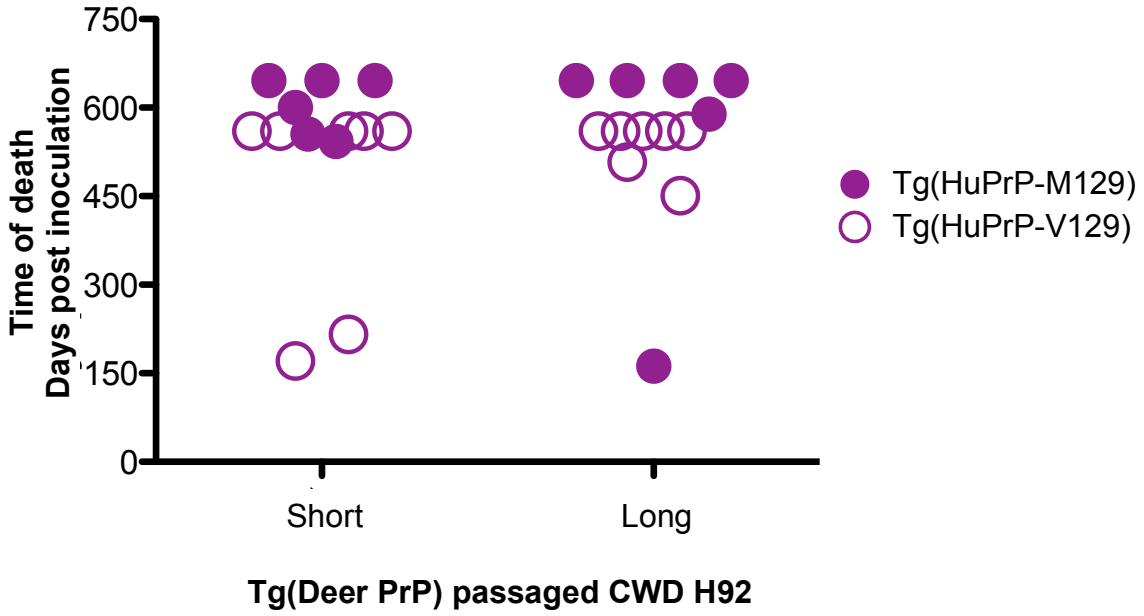

Figure 2.6. No Tg(HuPrP) mice developed prion disease after 500 days post inoculation of serially passaged deer CWD isolates. Tg(HuPrP-M129)6816$^{+/-}$ and Tg(HuPrP-V129)7826$^{+/-}$ mice inoculated with the mule deer CWD H92 isolates that had been passaged multiple times in Tg(Deer PrP)1536$^{+/-}$ mice, did not develop signs of prion disease. Filled circles indicate CWD inoculated Tg(HuPrP-M129)6816$^{+/-}$ mice. Open circles indicate CWD inoculated Tg(HuPrP-V129)7826$^{+/-}$ mice.

Chapter 3

Investigating the role of the β2-α2 loop and its interaction site of the C-terminal region of mouse prion protein in prion propagation using cell culture models

Introduction

Transmissibility of prion diseases within the same species is highly efficient; however, prions are not always transmittable from one species to another. This phenomenon is referred to as a species barrier or transmission barrier. The ability of prions to cross a species barrier has been recognized, for example, the interspecies transmission of bovine spongiform encephalopathy (BSE) into humans (Bruce *et al.*, 1997; Scott *et al.*, 1999). Since then, the zoonotic potential of prions is particularly important in understanding the interspecies transmission of prions.

The primary structure of prion protein (PrP) is well conserved among mammalian species (Prusiner, 1998). A small difference in the primary structures of mammalian PrPs is concentrated in the loop region between the β2-sheet and α2-helix, therefore, it has been proposed that the β2-α2 loop of PrP governs a species barrier (Billeter *et al.*, 1997; Schatzl *et al.*, 1995). Further, mouse-human chimeric transgenic (Tg) studies suggest that the species barrier between human and mouse is mediated by a hypothetical ‘protein X’ (Telling *et al.*, 1995), while

an NMR structural study postulated that a potential binding site of protein X in PrP is located within the loop region between the β2-sheet and α2-helix (Billeter *et al.*, 1997). Since the C-terminal domain of PrP with residue 121-231 among mammalian species has a 90% identity, the three-dimensional structure of PrP(121-231) was anticipated to be identical among species (Billeter *et al.*, 1997). However, numerous NMR studies revealed fine differences in the tertiary structures of mammalian PrPs, especially in the β2-α2 loop region, suggesting that the subtle differences in the tertiary structure of PrP plays a role in a species barrier (Christen *et al.*, 2008; Christen *et al.*, 2009; Fernandez-Funez *et al.*, 2011; Gossert *et al.*, 2005; Perez *et al.*, 2010; Zhang, 2011). Sigurdson and her colleagues generated Tg mice expressing the altered β2-α2 loop and challenged the Tg mice with prions, resulting in changes in incubation times (Sigurdson *et al.*, 2010; Sigurdson *et al.*, 2011).

The loop linking the β2-sheet and α2-helix in PrP resides in amino acid residues between 164 and 174 (mouse numbers), and its structure in mammals is highly diverged among mammals (Gossert *et al.*, 2005). NMR structural studies reported that, in mice, humans and bovines, the β2-α2 loop of PrP was highly disordered, meaning that the loop was flexible (Gossert *et al.*, 2005), whereas in elk, bank voles, wallabies, horses, dogs, cats, pigs, rabbits and sheep carrying a polymorphism at residue 168 expressing either histidine or arginine, PrP have distinctly well-defined structure, meaning that the loop is rigid (Christen *et al.*, 2009; Gossert *et al.*, 2005; Lysek *et al.*, 2005; Perez *et al.*, 2010; Zhang, 2011). The Prusiner and Wüthrich groups resolved the structure of Syrian

hamster PrP, and later the Wüthrich group reported that the structure of the β2-α2 loop in Syrian hamster PrP was partially defined and shown to be similar to elk PrP (Gossert *et al.*, 2005). A comparison of primary structures of mouse PrP with a flexible loop, and elk PrP with a rigid loop reveals that two amino acid residues are different at 169 and 173. Focusing on those two residues, the Wüthrich group performed a NMR structural study and showed that the double substitutions S169N and N173T in recombinant mouse PrP could produce a rigid loop, while the single substitution N173T was not sufficient to produce a rigid loop (Gossert *et al.*, 2005). The following molecular dynamics simulation study demonstrated that amino acid at residue 169 in the β2-α2 loop of PrP controlled the structure of the loop (Gorfe & Caflisch, 2007). The single substitution S169N in mouse PrP changed the β2-α2 loop to rigid, therefore, it would seem that residue 169 has more impact on conferring rigidity on the loop structure than does residue 173 (Gorfe & Caflisch, 2007).

Intrigued by the afore-mentioned series of NMR structural studies, the Aguzzi group generated Tg mice overexpressing mouse PrP with the double substitutions S169N and N173T in the β2-α2 loop on a *Prnp* knockout background, referred to as *tg*1020 mice, and reported that *tg*1020 mice spontaneously developed disease at 145 to 637 days of age (Sigurdson *et al.*, 2009). The brains of diseased mice accumulated PK-resistant PrP^{Sc}, and disease was shown to be transmissible (Sigurdson *et al.*, 2009). Subsequently, Tg mice expressing mouse PrP with the single substitution D166S in the β2-α2 loop on a *Prnp* knockout background (TgMoPrP^{166}) were generated, and these mice

spontaneously developed disease around 500 days of age (Sigurdson *et al.*, 2011). In contrast to *tg*1020, these diseased mice accumulated PK-sensitive PrP^{Sc} in the brain (Sigurdson *et al.*, 2011). Moreover, mouse-adapted RML scrapie prions and CWD prions produced disease in *tg*1020 mice at 323 ± 92 days post inoculation (dpi) and 279 ± 48 dpi, respectively, demonstrating that, in comparison with wild-type mice, disease onset with RML is delayed, but with CWD is accelerated (Sigurdson *et al.*, 2010). Interestingly, both *tg*1020 and $TgMoPrP^{166}$ mice had the rigid β2-α2 loop based on the previous NMR structural studies (Gossert *et al.*, 2005; Perez *et al.*, 2010), respectively.

The Sigurdson group further demonstrated that the species barrier could be lowered by presenting the identical amino acid residue at 169 between donor and host PrP (Bett *et al.*, 2012). Similarly, when $TgMoPrP^{166}$ mice were inoculated with RML and CWD, only RML-infected $TgMoPrP^{166}$ mice developed disease, indicating the substitution D166S had little impact on the susceptibility of these mice to mouse prions (Bett *et al.*, 2012). Additionally, the single substitutions D166A, D166G, D166S and D166E were introduced in mouse PrP and generated in a catecholaminergic differentiated (CAD) neuronal cell culture system, and all of the variant mouse PrPs were susceptible to RML infection (Bett *et al.*, 2012). These findings resulted in the hypothesis that the primary structural elements within the β2-α2 loop of PrP are what determine the species barrier, rather than the structure of the loop, whether flexible or rigid.

However, there could be additional regions determining the susceptibility to prions. The C-terminal region of PrP cannot be ignored since codon 225

polymorphism of cervid PrP either serine (S) or phenylalanine (F), strongly influences susceptibility to CWD (Jewell *et al.*, 2005). The frequency of SF (heterozygous) or FF (homozygous) genotypes in CWD-positive free-ranging deer was significantly lower than cervid homozygous for SS, suggesting that deer PrP with either genotype heterozygous for SF or homozygous for FF is less likely to develop CWD prion disease (Jewell *et al.*, 2005). Another finding of the NMR structural study is that a long-range interaction between the β2-α2 loop and C-terminal region of PrP in tammar wallaby exists (Christen *et al.*, 2009). It was reported that residue 165 (mouse number) in the β2-α2 loop and residue 224 (mouse number) interacted closely, suggesting that the interaction of two regions rather than the β2-α2 loop alone determines susceptibility to prions (Christen *et al.*, 2009). Therefore, it becomes essential to study whether long-range interaction between the β2-α2 loop and C-terminal region of PrP does indeed control the susceptibility of prions.

Which residues in the β2-α2 loop and C-terminal region of PrP do in fact control the susceptibility of prions? In attempt to answer this question, the primary structures of horse and mouse PrP were aligned. As a result, three amino acid residues in the β2-α2 loop and two amino acid residues in the C-terminal region were mismatched. Interestingly, no TSEs have thus far been reported in horses. Studying the effects of introducing horse-specific substitutions into mouse PrP could help to clarify more precisely which specific amino acid residues determine the transmission efficiency.

In the present study, it is hypothesized that the β2-α2 loop and C-terminal region as a whole determines the susceptibility of prions. To study the hypothesis, various substitutions were introduced to mouse and horse PrP to see whether the substitutions altered the susceptibility to RML, CWD or horse prions in cell culture. The study consists of three parts; the susceptibility of prions was determined in association with 1) the structural definition of the β2-α2 loop of PrP with either flexible or rigid, 2) the interaction between the β2-α2 loop and C-terminal region of PrP, and 3) unique amino acid residues in the β2-α2 loop and C-terminal region of horse PrP.

Materials and Methods

Cell cultures. Rabbit epithelial kidney (RK13) cells (ATCC, CCL-37, Manassas, VA) were maintained in Dulbecco's Modified Eagle's Medium (DMEM) (Sigma, St. Louis, MO) supplemented with 10% fetal bovine serum (FBS) and 1% penicillin/streptomycin (Pen/Strep) at 37°C in a humidified 5% CO_2 incubator. RK13 cells were observed daily and split at 1:10 dilution every 5 days.

Plasmid constructions. The mouse PrP encoding sequence with a point or double mutation(s) were designed between two restriction endonuclease enzyme sites *AflII* at the 5' and *EcoRI* at the 3' end. Mutated expression cassettes were synthesized and cloned into pUC57 by GenScript (Piscataway, NJ). Digested expression cassettes were cloned into the *AflII* and *EcoRI* restriction sites of the mammalian expression vector pIRESpuro3 (Clontech, Mountain View, CA). The

presence of the inserts was verified by colony polymerase chain reaction (PCR). Table 3.1. summarizes the information about the 15 constructs generated in the study. Six expression vectors carrying a point mutation in the β2-α2 loop of mouse PrP are referred to in the following way: mouse PrP with the substitution of serine (S) with asparagine (N) at codon 169 (mPrP[S169N] for short), mouse PrP with the substitution of N with threonine (T) at codon 173 (mPrP[N173T]), mouse PrP with the substitution of valine (V) with alanine (A) at codon 165 (mPrP[V165A]), mouse PrP with the substitution aspartic acid (D) with S at codon 166 (mPrP[D166S]), mouse PrP with the substitution of glutamine (Q) with glutamic acid (E) at codon 167 (mPrP[Q167E]) and mouse PrP with the substitution of N with lysine (K) at codon 173 (mPrP[N173K]). Three expression vectors containing double mutations in the β2-α2 loop of mouse PrP are referred to as mPrP[S169N, N173T], mPrP[D166S, Q167E] and mPrP[D166S, N172K]. Four expression vectors carrying a point mutation in the C-terminal interaction site of mouse PrP with the substitution of tyrosine (Y) with A at codon 224 (mPrP[Y224A]), the substitution of Y with A at codon 225 (mPrP[Y225A]), the substitution of Y with phenylalanine (F) at codon 224 (mPrP[Y224F]) and the substitution of Y with Q at codon 225 (mPrP[Y225Q]). One expression vector carrying a double mutation in the C-terminal interaction site of mouse PrP is referred to as mPrP[Y224A, Y225A]. One expression vector harboring a point mutation in the β2-α2 loop of horse PrP is referred to as HorsePrP[S167D].

Generation of stably transfected RK13 cells expressing mutant mouse or horse PrP. RK13 cells were plated in 6-well plates with DMEM/FBS lacking antibiotics one day prior to transfection. Transfection was performed using Lipofectamine 2000 (Invitrogen, Carlsbad, CA). DNA-Lipofectamine complexes were prepared by mixing 4 µg of DNA with 10 µl of lipofectamine in Opti-MEM I Reduced Serum Medium (Invitrogen, Carlsbad, CA) without serum. RK13 cells were rinsed with Opti-MEM to remove residual serum, then 200 µl of the DNA-Lipofectamine complexes were gently added onto the monolayer of cells. After 5 hours incubation, the complexes were removed from cell cultures, and DMEM with FBS and Pen/Strep was added onto the transfected RK13 cells. After 48 hours, the medium was replaced with DMEM/10% containing 1 µg/ml of puromycin. Selective medium was changed every 3 days until resistant cells were obtained. Expression levels of PrP were determined by western blotting comparing expression levels to that of RK13 cells expressing a wild-type mouse PrP (RKM). RK13 cells were also transfected with empty pIRESpuro3 vectors. As negative controls for transfection, additional RK13 cells were transfected with DNA alone without lipofectamine and with lipofectamine alone without DNA.

Prion inocula. A pool of wild-type FVB mouse brains, which died following infection with mouse-adapted Rocky Mountain Laboratories (RML) scrapie prions, was used as mouse prion inoculum. A brain from a transgenic (Tg) mouse expressing elk PrP, referred to as Tg(ElkPrP)5037, which had succumbed to disease following infection with a pool of CWD-affected elk brains, referred to

05-0306 obtained from our collaborators at the Canadian Food Inspection Agency, Ottawa, Ontario Canada was used as the CWD inoculum. These prion-infected brains were prepared at 10% (w/v) in Opti-MEM by repeated extraction through successively decreasing needle diameter from 18 to 22 gauge. Further, 10% brain homogenates from RML and CWD prions were diluted, respectively, to 0.2 and 1% (w/v) in Opti-MEM and thoroughly homogenized using a 26 gauge needle syringe.

Hemizygous Tg mice expressing horse PrP encoding K at residue 175 were previously generated on a *Prnp* knockout FVB background, and referred to as Tg(EqPrP)$5525^{+/-}$. Groups of Tg(EqPrP)$5525^{+/-}$ mice were infected with sheep scrapie SSBP/1 prions, as a result, 2 out of 6 Tg(EqPrP)$5525^{+/-}$ mice developed disease (unpublished data). It is important to note that the brain materials from two diseased Tg(EqPrP)$5525^{+/-}$ mice were inoculated into another groups of Tg(EqPrP)$5525^{+/-}$ mice; however, none of the mice developed disease (unpublished data). A brain homogenate from a diseased Tg(EqPrP)$5525^{+/-}$ mouse, referred to as horse prion, was used for cell infections in this study. The brain homogenate was diluted to 0.8% (w/v) in Opti-MEM as described above.

Cell infections. For cell infection, 10^6 cells/ml were plated in 6-well plates one day prior to infection. Cells were rinsed with cold PBS twice, then either RML or CWD prions in a total volume of 1 ml per well was added to cell monolayers. After 5 hours, 2 ml of Opti-MEM medium containing 10% FBS was added. Next day, cells were transferred at 1:1 dilution to 10 cm plates and split at 1:10 dilution

every 5 days up to 5 passages. Cells were lysed in cold lysis buffer (0.5% sodium deoxycholate, 0.5% Igepal CA-630, 150 mM NaCl, and 50 mM Tris, pH 7.5) for 5 minutes in ice. Cell lysates were analyzed for PrP^{C} or PrP^{Sc} in western blotting.

Analysis of PrP^{C} and PrP^{Sc}. Cell lysates from each cell line including both infected and uninfected samples were collected at passage 3 and 5 after infection. The concentration of total protein in each sample was determined by bicinchoninic acid assay. For undigested samples, the total amount of proteins was standardized at 30 µg per lane when anti-PrP 6H4 or PRC5 antibodies were used for analysis. The total amount of proteins was standardized at 90 µg per lane when anti-PrP PRC9 antibody was used for analysis. For proteinase K (PK) digestion, total protein in cell lysates was normalized to 2 mg/ml in cold lysis buffer with PK added at a final concentration of 50 µg/ml. PK-digested cell lysates were ultracentrifuged at 100,000 *x g* for 1 hour at 4°C. The pellet was resuspended in sodium dodecyl sulfate-polyacrylamide (SDS)-page loading buffer, boiled at 100°C for 5 minutes and examined by western blotting. Proteins were resolved by SDS gel electrophoresis and transferred to polyvinylidene difluoride Immobilon-FL (PVDF-FL) membranes (Millipore). The membrane was blocked with 5% non-fat milk in 0.5% Tween-20 in Tris-buffered saline (TBST) and immunoprobed with anti-PrP mouse monoclonal antibody (mAb) 6H4 (Prionics AG, Schlieren-Zurich), PRC5, or PRC9 followed by horseradish peroxidase-conjugated anti-mouse secondary antibody. Proteins were visualized

using ECL Plus (GE Healthcare) using an FLA-5000 scanner (Fujifilm Life Science). The expression levels of PrP^C in cell lines were determined by densitometric analysis of PrP^C signals on the western blot using MultiGauge (Fujifilm Life Science).

Cell blotting. Cells were plated onto plastic coverslips in 12-well plates five passages after infection. Cells were grown to confluence, medium removed and washed twice with cold PBS. The side of the coverslips on which cells were grown was placed face down onto a PVDF membrane pre-soaked with cold lysis buffer and pressed firmly for 1 minute to transfer all cells onto the membrane. Coverslips were carefully removed. Membranes were air-dried for 2 hours and stored at -20°C. Membranes were re-wetted with cold lysis buffer and treated with PK at a final concentration of 5 μg/ml in cold lysis buffer for 90 minutes at 37°C with constant shaking. Protease digestion was terminated by the addition of phenylmethylsulfonyl fluoride (PMSF) at a final concentration of 2 mM for 20 min. Membranes were rinsed four times with distilled water and immersed in 3 M guanidine isothiocyanate/10 mM Tris-HCl, pH 8.0 for 10 minutes then rinsed four times with distilled water. Membranes were immunoprobed with 6H4 in the same way as with western blots described above.

Results

In this study, rabbit epithelial kidney (RK13) cells were used to assess the correlations between the β2-α2 loop and prion susceptibility. RK13 cells have

been used to study the propagation of PrP^{Sc} *in vitro* since the Vilette group established that RK13 cells expressing rodent, ovine and cattle PrP were permissive to multiple prion infections (Courageot *et al.*, 2008; Vilette *et al.*, 2001). The use of a RK13 cell culture model accelerates studies in the pathogenesis of prions by as a quicker and cost-effective model in addition to animal models. No detectable amount of endogenous PrP is expressed in RK13 cells, even though RK13 cells have a *Prnp* gene. Thus, RK13 cells are effectively natural PrP knockout cells. In contrast to animal models, the use of cell culture systems in general allow us to control more variables in experiments, making them an ideal *in vitro* cell model to study the propagation of prions.

Levels of PrP in RK13 cells expressing mutant PrP. All of the newly generated 15 cell lines showed detectable levels of PrP on western blots using 6H4 or PRC5 (Figure 3.1. and 3.2.). Most of the mutant cell lines expressed 1.6-fold to 1.9-fold higher PrP levels than RKM on the western blot probed with 6H4 except for 1.2-fold in RKM[V165A], 3.5-fold in RKM[Y225A], 2.2-fold in RKM[Q167E] and 2.5-fold in RKM[D166S, Q167E] (Figure 3.2.). The blot probed with PRC5 showed 1.2-fold to 1.6-fold higher PrP levels compared to RML in most of the cell lines except 0.8-fold in RKM[V165A] and 2-fold in RKM[Y225A] (Figure 3.2.). Both results showed that RKM[V165A] expressed relatively lower levels of PrP and RKM[Y225A] expressed relatively higher levels of PrP compared to RKM. The rest of the cell lines expressed a similar range of PrP levels. In addition, it is important to point out that PrP was not detected in RK13

cells with an empty pIRESpuro3 vector (RKV), confirming that RK13 cells did not express detectable levels of PrP (Figure 3.1.).

Both 6H4 and PRC5 antibodies equally recognized the mutant mouse PrP in cell culture; however, reactivity with PRC9 antibody was dependent on mutations within PrP. PRC9 could not recognize the mutant mouse PrP when amino acid residue at 224 was mutated from tyrosine (Y) to either alanine (A) or phenylalanine (F) (Table 3.2. and Figure 3.2.). Moreover, PRC9 lost reactivity when Y at residue 225 in mouse PrP was mutated to glutamine (Q) but not F (Table 3.2.). In addition, mouse PrP with the substitution V165A was not recognized by PRC9. For this reason, in the following experiments, only 6H4 and PRC5 were used for immunoblotting since PRC9 varies in reactivity with the mutant mouse PrP's.

Changing the β2-α2 loop structure of mouse PrP altered susceptibility to RML but not CWD. Two amino acids are different between mouse and elk PrP within the β2-α2 loop. Mouse PrP contains serine (S) at residue 169 and asparagine (N) at residue 173 and keeps the β2-α2 loop flexible, while elk PrP contains N at residue 169 (mouse number) and threonine (T) at residue 173 (mouse number) and has a rigid loop (Gossert *et al.*, 2005).

In the first experiment, the flexible β2-α2 loop of mouse PrP was changed to the rigid loop by introducing the double mutation at residue 169 from S to N and at residue 173 N to T. The western blot showed that PrP^{Sc} did not accumulate in RML-infected RKM[S169N, N173T] cells at passage 3 (Figure

3.3.A). Next, the single substitution S169N was introduced in to mouse PrP, and this substitution was sufficient to change the flexible β2-α2 loop of mouse PrP to the rigid loop (Sigurdson *et al.*, 2011). RKM[S169N] cells also lost the susceptibility to RML at passage 3 (Figure 3.3.B). RML-infected RKM[S169N] cells were maintained for up to five passages after infection to see if delayed propagation of PrP^{Sc} occurred. However, PrP^{Sc} was absent in the RML-infected cells at passage 5 on western blot, suggesting that RKM[S169N] cells were resistant to RML (Figure 3.3.C). This result indicates that changing the loop structure in mouse PrP led to loss of susceptibility to RML. In contrast, the lack of PrP^{Sc} in CWD-infected RKM[S169N, N173T] and RKM[S169N] cells showed that introducing the rigid loop in mouse PrP was not sufficient to confer susceptibility to CWD (Figure 3.4.A and B, respectively).

Subsequently, the substitution N173T was introduced into mouse PrP. Even though this single substitution was sufficient to maintain a flexible β2-α2 loop (Gossert *et al.*, 2005), the point mutation resulted in inhibition of PrP^{Sc} formation following infection with RML (Figure 3.3.D).

PrP^{Sc} was not identified in CWD-infected RKM[N173T] cells at passage 3, showing that the substitution were not sufficient to confer susceptibility to an otherwise mouse PrP primary structure to CWD prions (Figure 3.4.C).

For RML infection, both RML/FVB and RML/RKM presented PK-resistant PrP^{Sc} in each blot, indicating our ability to detect RML PrP^{Sc} on western blots (Figure 3.3.). The presence of PrP^{C} and absence of PrP^{Sc} in the uninfected cell lines were confirmed, showing that the positive signal of PrP^{Sc} was valid. Every

blot showed the absence of signals in uninfected RKV samples indicating that the antibody recognition on western blots was specific to PrP. In addition, the absence of signals in infected RKV controls indicates that no residual PrP^{Sc} from the inoculum remained at passage 3 or 5. The presence of PK-resistant PrP^{Sc} in RML-infected RKM indicated the cell infection was successful.

Likewise, for CWD infection, both CWD/Tg(ElkPrP) and CWD/RKE presented PK-resistant PrP^{Sc} in each blot, indicating our ability to detect CWD PrP^{Sc} on western blots (Figure 3.4.). The presence of PrP^{C} and absence of PrP^{Sc} in the uninfected cell lines were confirmed showing that the positive signal of PrP^{Sc} is valid. The absence of signals in CWD-infected RKM indicating that no residual PrP^{Sc} from the inoculum remained at passage 3. The presence of PK-resistant PrP^{Sc} in CWD-infected RKE indicates the cell infection was successful. Those positive and negative controls demonstrated that it was possible to infect cells and detect newly generated PrP^{Sc} in this assay.

The antibody specificity and absence of residual inocula was verified by examining the absence of PrP^{C} and PrP^{Sc} in RKV on western blots. The ability to detect RML PrP^{Sc} on western blots was verified by presenting the PK-resistant PrP^{Sc} from brain homogenates from RML-infected wild-type FVB mice (RML/FVB) and/or cell lysates from RML-infected RKM cells (RML/RKM). The presence of PrP^{C} and absence of PrP^{Sc} in the uninfected cell lines were confirmed, thus the accumulation of PrP^{Sc} was due to prion infection. The presence of PK-resistant PrP^{Sc} in RML-infected RKM indicated that the cell infection was successful.

In addition to the above controls, the detectability of CWD PrP^{Sc} on western blots was verified by presenting the PK-resistant PrP^{Sc} from brain homogenates from Bala05 CWD-infected Tg(ElkPrP) mice (CWD/Tg(ElkPrP)) and cell lysates from CWD-infected RKE cells (CWD/RKE). Successful CWD infection was demonstrated by presenting the presence of PK-resistant PrP^{Sc} in CWD-infected RKE. RKM was used as a negative control for the infection of CWD prion because mouse PrP is resistant to PrP^{Sc} propagation. The absence of signals in CWD-infected RKM indicates that no residual PrP^{Sc} from the inoculum remained at passage 3. Those positive and negative controls demonstrated that the ability to infect cells and detect newly generated PrP^{Sc} in this assay.

For dot blotting, infected and uninfected samples were determined for the accumulation of PrP^{Sc}. As negative control, uninfected samples were used for the absence of PrP^{Sc}. As positive control, cell lysates from RK13 cells expressing elk PrP (RKE) chronically infected with sheep scrapie SSBP/1 or 48x35 isolates were used. The absence and presence of PrP^{Sc} in the negative and positive controls demonstrated this technique's ability to detect PrP^{Sc}.

Interrupting the interaction between the β2-α2 loop and C-terminal region in mouse PrP changed the susceptibility to RML. Inspired by the NMR study of tammar wallaby PrP (Christen *et al.*, 2009), alanine substitutions were introduced to mouse PrP at residues 165, 224 and 225, in order to establish whether interrupting the interaction between the β2-α2 loop and C-terminal regions

altered susceptibility to RML. The alanine substitution at residue 165 in the β2-α2 loop of mouse PrP has been previously shown to make the flexible loop of mouse PrP into the rigid loop (Christen *et al.*, 2009). The western blot showed ambiguous signals of PrP^{Sc} from RML-infected RKM[V165A] cells; however, these were most likely due to leaked signals from neighboring samples (Figure 3.5.A.). In the following experiment, the dot blot confirmed that RML failed to propagate PrP^{Sc} in RKM[V165A] cells (Figure 3.7.). The absence of PrP^{Sc} accumulation in RML-infected RKM[Y224A] and RKM[Y225A] cells was verified by western and dot blotting, indicating that two residues in the C-terminal interaction site are important determinants for the susceptibility to RML (Figure 3.5.B. and 3.7.). Although RKM[Y224A] and RKM[Y225A] cells was flexible and rigid loops between the β2-sheet and α2-helix, respectively (Christen *et al.*, 2009), both of the cell lines lost susceptibility to RML, indicating that the structural definition of the β2-α2 loop did not correlate with the susceptibility of RML. In addition, the double mutation at residue 224 and 225 failed to propagate PrP^{Sc} upon RML infection (Figure 3.5.A.). Some signals were shown in PK-digested uninfected RKM[Y224A] and RKM[Y225A] cells (Figure 3.5.A). These were most likely due to either undigested PrP or leaked samples from the neighboring lanes since PK-resistant core of PrP^{Sc} at 27-30 kDa was not present in those lanes. Moreover, the dot blot, which is a sensitive assay for PrP^{Sc} detection (Scott *et al.*, 1993), confirmed RML-infected RKM[Y224A], RKM[Y225A] and RKM[Y224A, Y225A] cells could not produce PrP^{Sc} at passage 3 (Figure 3.7.). The above results indicate that secondary structural constrains,

producing rigidity or flexibility within the β2-α2 loop, do not determine susceptibility to RML prions. Rather, the results suggest that specific primary determinants at key residues within the β2-α2 loop and C-terminal regions determine susceptibility to RML.

Horse-specific substitutions within the β2-α2 loop and its interaction site of mouse PrP resulted in loss of susceptibility to RML. In order to study unique amino acid residues in the β2-α2 loop and C-terminal regions of horse PrP, horse specific substitutions at residues 166, 167,172, 224 and 225 were introduced into the mouse PrP primary structure. RK13 cells expressing those mutant mouse PrP constructs were tested for susceptibility to RML prions. It should be noted that previous work showed substitution of D166S in the β2-α2 loop of mouse PrP changed the loop from flexible to rigid, whereas other single or double substitutions except the double substitution of D166S and Q167E did not alter the structure of the β2-α2 loop (Perez *et al.*, 2010). Our western blot data showed that a weak signal of PK-resistant PrP^{Sc} around 19 and 27-25 kDa in the sample from RML-infected RKM[D166S] cells at passage 3 (Figure 3.6.A.). Moreover, the dot blot showed no accumulation of PrP^{Sc} in RML-infected RKM[D166S] cells at passage 5 (Figure 3.7.). The results of the western and dot blotting indicate that conversion of PrP^{Sc} was inefficient and unstable in RML-infected RKM[D166S] cells. Accumulation of PrP^{Sc} was not detected in RML-infected RK13 cells expressing horse PrP with a substitution of S to D at codon 167 (HorsePrP[S167D]) by both western and dot blotting. In conclusion,

changing a single residue in horse PrP at residue 167 to corresponding residue in mouse PrP was insufficient to induce susceptibility to RML prions (Figure 3.6.A. and Figure 3.7.).

Although the apparent signal in the PK-digested sample from RML-infected RKM[Q167E] cells was present, the signal was most likely due to the undigested PrP or leaked sample from the neighboring lanes (Figure 3.6.B.). Moreover, the dot blot showed no accumulation of PrP^{Sc} in RML-infected RKM[Q167E] cells (Figure 3.7.). The absence of PrP^{Sc} was shown in RKM[D166S, Q167E] cells by both western and dot blotting (Figure 3.6.B.). RKM[N172K] and RKM[D166S, N172K] cells failed to accumulate PrP^{Sc} upon RML infection (Figure 3.6.C. and Figure 3.7). Therefore, the substitutions Q167E and N172K with or without D166S in mouse PrP resulted in the loss of susceptibility to RML. Both western and dot blotting failed to detect PrP^{Sc} in RML-infected RKM[Y224A] and RKM[Y225A] cells (Figure 3.6.D. and Figure 3.7). The substitutions Y224A and Y225A in the C-terminal region, which is the interaction site of the β2-α2 loop, of mouse PrP kept the loop flexible but resulted in the loss of the susceptibility to RML.

Horse-specific substitutions in mouse PrP were not sufficient to stimulate susceptibility to horse prion. RK13 cells expressing selected mutant mouse PrP including RKM[D166S], RKM[D166S, Q167E], RKM[D166S, N172K], RKM[Y224F], RKM[Y225Q] and RK13HorsePrP[S167D] were infected with horse prions generated in Tg mice expressing horse PrP (unpublished data). The dot

blot showed that none of above horse-prion infected cells accumulated PrP^{Sc} at passage 5 (Figure 3.7.). In addition, horse prion infected RKM cells also failed to produce PrP^{Sc}, indicating the presence of species barrier between mouse and horse PrP (Figure 3.7.).

Discussion

NMR structural studies have shown that specific residues within the β2-α2 loop and the C-terminal region interact in the tertiary structure of PrP (Christen *et al.*, 2009). In order to test the hypothesis that these residues play a role in determining susceptibility to prion infection, various mutations were introduced in the β2-α2 loop and/or the C-terminal region. RK13 cells expressing those variant mouse PrP were infected with RML or CWD to determine whether these mutations altered the ability of the expressed PrP to be converted to PrP^{Sc} (Table 3.1.). Substitutions in the β2-α2 loop and C-terminal region of mouse PrP were sufficient to prevent PrP^{Sc} conversion upon RML prion infection (Figure 3.3., 3.5., 3.6. and 3.7.). Introducing the rigid loop in mouse PrP created the transmission barrier to RML (Figure 3.3.) but did not lower the transmission barrier of CWD (Figure 3.4.). Disrupting the interaction between the β2-α2 loop and C-terminal region of mouse PrP also offered protection from the RML transmission (Figure 3.3. and 3.4.). The results of detailed examination of diverged amino acid residues in the β2-α2 loop and C-terminal region of mouse PrP identified more precisely the specific amino acid residues playing critical roles in prion transmission. In other words, changing the primary structure of the β2-α2 loop

and C-terminal region modifies susceptibility to prions, suggesting that the distinctive amino acid residues in those critical regions of PrP make a significant contribution to constructing a species barrier.

The diverged primary structures of PrP in the β2-α2 loop region among mammals guided us to this investigation of the role of the loop in a species barrier. NMR structural and animal studies suggested that the structural definition of the β2-α2 loop decides the susceptibility of RML and CWD (Gorfe & Caflisch, 2007; Gossert *et al.*, 2005; Sigurdson *et al.*, 2010). In addition, the most recent study from the Sigurdson group suggested that the narrowed area of the primary structure of the β2-α2 loop determined the interspecies prion conversion (Bett *et al.*, 2012). In the present study, the series of experiments with RML transmission demonstrated that the point mutations in the β2-α2 loop and C-terminal interaction region were sufficient to create a transmission barrier in cell cultures, although some substitutions maintained the flexible loop. Even though the β2-α2 loop of PrP is involved in determining a species barrier, choosing either flexible or rigid loop between β2-sheet and α2-helix in PrP does not regulate the susceptibility to prions. Consistent with the recent report from the Sigurdson group (Bett *et al.*, 2012), the structural definition of the β2-α2 loop of PrP has little involvement in prion transmission.

To investigate whether the interaction between the β2-α2 loop and C-terminal region plays a role in prion transmission, single or double substitutions were introduced in mouse PrP at residues 165, 224 and 225. Long-range interactions were reported between residue 165 in the β2-α2 loop and residue

224 in the C-terminal region of tammar wallaby PrP (Christen *et al.*, 2009). Since the previous NMR study showed that alanine substitutions at residue 165, 224 and 225 interrupted the interaction between the loop and C-terminal region of PrP (Christen *et al.*, 2009), in the present study, it was anticipated that interrupting the interaction could change the prion transmission. To directly address this question, we infected RK13 cells expressing the variant mouse PrP lacking the interaction with RML prions. As a result, all of the variant PrP lost the susceptibility to RML, suggesting that the interaction between the β2-α2 loop and C-terminal region of PrP has a great impact on a species barrier.

The β2-α2 loop of PrP consists of eleven amino acids, and four out of eleven are conserved among mammalian species. Two amino acid residues at 166 and 172 (mouse number) are conserved among the mammalian species except horses. One amino acid at residue 170 is conserved among species but unique in tammar wallaby PrP. Another four amino acid residues at 165, 167, 169 and 173 are divergent among the species. The studies *in vivo* and *vitro* demonstrated that the amino acid residue 169 played significant roles in the conversion of PrP^{Sc} (Avbelj *et al.*, 2011; Kurt *et al.*, 2009; Sigurdson *et al.*, 2010), suggesting the residue has an important role in the prion transmission. In addition, horse-specific amino acid residue 166 had been reported to have a little influence on the prion transmission (Bett *et al.*, 2012). However, roles of the five other diverged amino acid residues have not been studied in relation to prion transmission. In order to study the roles of each amino acid in the β2-α2 loop and C-terminal region of PrP in the prion transmission, the above diverged seven

amino acid residues in the loop and its interaction site were mutated in mouse PrP. As anticipated, the substitution S169N in mouse PrP altered susceptibility to RML in cell culture consistent with the result of Tg mouse expressing mouse PrP with the S169N substitution (Sigurdson *et al.*, 2010). Even though the conversion of PrP^{Sc} was not efficient in RK13 cells expressing mouse PrP[D166S], the substitution did not completely prevent the PrP^{Sc} propagation.

The present study also supports the data that the Tg mice expressing $MoPrP^{166}$ maintained susceptibility to RML and produced PK-resistant PrP^{Sc} (Sigurdson *et al.*, 2011). An additional study might explain the reason why the substitution of D166S in mouse PrP is susceptible to RML. TgF35 mice expressing deletion mutant mouse PrP (Δ32-134) spontaneously developed disease; however, TgF35 mice were rescued by either coexpressing wild-type mouse PrP or mouse PrP[D166S], suggesting that mouse PrP[D166S] could serve similar functions to wild-type PrP (Sigurdson *et al.*, 2010).

In the present study, substitutions of other five residues at 165, 167, 170, 172 and 173 were also examined as to whether susceptibility to RML was altered in cell culture. As a result, the conversion of PrP^{Sc} prevented in the RML-infected RK13 cells expressing those five variant mouse PrP, suggesting those five residues have significant effects on the prion transmission. The present study evinces the specific six amino acid residues in the β2-α2 loop of mouse PrP that play significant roles in deciding the susceptibility of RML.

The present study showed that introducing elk PrP residues in mouse PrP (S169N and N173T) was not sufficient to lower the transmission barrier of CWD

in cell culture. Additionally, RML failed to propagate in RK13 cells expressing most of the variant mouse PrP except D166S. The results suggest that lowering the existing species barrier is challenging; however, a single amino acid substitution of mouse PrP is sufficient to inhibit the propagation of PrP^{Sc} with RML. In order to further test the transmission barrier, RK13 cells expressing variant mouse PrP with horse specific substitutions were infected with horse prion. The horse specific substitutions of D166S, Q167E, N172K, Y224F and Y225Q in mouse PrP were unable to convert PrP^{Sc} responding to horse prion infection, indicating that the single substitutions were not able to lower the transmission barrier of horse prion. Nonetheless, the limitations to the experiments with horse prion infection in cell culture need to be discussed. The horse prion has not yet proven to be transmissible because the secondary passage of the material could not produce disease in $Tg(EqPrP)^{+/-}$ mice. Because the transmissibility properties of horse prion remain unclear, a positive control for the infection assay with horse prion was unavailable. RK13 cells expressing a wild-type horse PrP (RK13HorsePrP) were not included, although the transmissibility of horse prion was uncertain in cell culture. In the present study, horse prion infection was performed along with RML infection, and the cell infection procedure was verified by presenting successful RML infection results. In future studies, it will be interesting to examine whether the same amino acid residues required for RML transmission in mouse PrP also determines the susceptibility of horse prion.

The primary structure of PrP is not the only critical determinant for the transmission barrier of prions. The primary structures of human and cattle PrP are not identical; however, BSE prions have an ability to produce disease-related PrP^{Sc} in Tg mice expressing human PrP (Lloyd *et al.*, 2004; Wadsworth *et al.*, 2004). This suggests that there are additional requirements for the transmission of prions. Another possible requirement for prion transmission is a three-dimensional compatibility between host PrP^{C} and donor PrP^{Sc}. The conformational compatibility can be obtained even when there are variations in the primary structures of host and donor PrP. In any study of the effects of compatibility between donor PrP^{Sc} and host PrP^{C} on the transmission barrier of prions, it will be extremely challenging to directly obtain the structural information of native PrP^{C} and especially PrP^{Sc} because there are still limitations to the resolution of current technologies. Instead, by way of an extension to the present study, systematic studies of introducing multiple substitutions in mammalian PrP may well be useful in gaining more insight into the transmission of prions.

Table 3.1. Summary of expression vectors for point or double mutation(s) to alter the structure of the β2-α2 loop in mouse PrP. The mammalian expression plasmid pIRESpuro3 carrying 15 different mutant PrP were constructed. Three mutants followed by an elk PrP include elk specific substitutions at residues 169 and/or 173 in mouse PrP. Four mutants followed by a wallaby PrP include alanine substitutions at residues 165, 224 and/or 225 in mouse PrP. Seven mutants followed by a horse PrP include horse specific substitutions at residues 166, 167, 172, 224 and/or 225 in mouse PrP. The last mutant in the table is a horse PrP variant with a point mutation at residue 167 (horse number which is equivalent to 166 in mouse). Bold letters indicate mutated amino acid residues in the constructs. N/D indicates that the loop structure has not been determined by NMR.

PrP	Amino acid residue (mouse number)								Structure of β2-α2 loop based on NMR
	β2-α2 loop						C-terminal		
	165	166	167	169	172	173	224	225	
Mouse PrP (mPrP)	**V**	**D**	**Q**	**S**	**N**	**N**	**Y**	**Y**	Flexible
Elk PrP	V	D	Q	N	N	T	Y	Y	Rigid
mPrP[S169N]	V	D	Q	**N**	N	N	Y	Y	Rigid
mPrP[N173T]	V	D	Q	S	**N**	**T**	Y	Y	Flexible
mPrP[S169N, N173T]	V	D	Q	**N**	**N**	**T**	Y	Y	Rigid
Wallaby PrP	I	D	Q	G	N	S	A	Q	Rigid
mPrP[V165A]	**A**	D	Q	S	N	N	Y	Y	Rigid
mPrP[Y224A]	V	D	Q	S	N	N	**A**	Y	Flexible
mPrP[Y225A]	V	D	Q	S	N	N	Y	**A**	Rigid
mPrP[Y224A, Y225A]	V	D	Q	S	N	N	**A**	**A**	Rigid
Horse PrP	V	S	E	S	K	N	F	Q	Rigid
mPrP[D166S]	V	**S**	Q	S	N	N	Y	Y	Rigid
mPrP[Q167E]	V	D	**E**	S	N	N	Y	Y	Flexible
mPrP[N172K]	V	D	Q	S	**K**	N	Y	Y	Flexible
mPrP[D166S, Q167E]	V	**S**	**E**	S	N	N	Y	Y	N/D
mPrP[D166S, N172K]	V	**S**	Q	S	**K**	N	Y	Y	Rigid
mPrP[Y224F]	V	D	Q	S	N	N	**F**	Y	Flexible
mPrP[Y225Q]	V	D	Q	S	N	N	Y	**Q**	Flexible
HorsePrP[S167D]	V	**D**	E	S	K	N	F	Q	N/D

Table 3.2. Reactivities of anti-PrP mAbs with the PrP variants carrying the altered β2-α2 loop and its interaction at the C-terminal of PrP. The expression levels of PrP in RK13 cells expressing variant mouse or horse PrP were determined using three different anti-PrP mAbs including 6H4, PRC5 and PRC9. A positive (+) indicates a mAb could recognize a variant PrP, whereas a negative (−) indicates a mAb did not recognize a variant PrP. N/D indicates the β2-α2 loop structure has not been determined by NMR or the reactivity of an antibody has not been determined.

RK13 cells expressing mutant or wild-type PrP	Structure of β2-α2 loop based on NMR	mAb		
		PRC9	**6H4**	**PRC5**
Mouse PrP (RKM)	Flexible	+	+	+
RKM[S169N]	Rigid	+	+	N/D
RKM[N173T]	Flexible	+	+	N/D
RKM[S169N, N173T]	Rigid	+	+	N/D
RKM[V165A]	Rigid	−	+	+
RKM[Y224A]	Flexible	−	+	+
RKM[Y225A]	Rigid	+	+	+
RKM[Y224A, Y225A]	Rigid	−	+	+
RKM[D166S]	Rigid	+	+	+
RKM[Q167E]	Flexible	+	+	+
RKM[N172K]	Flexible	+	+	+
RKM[D166S, Q167E]	N/D	+	+	+
RKM[D166S, N172K]	Rigid	+	+	+
RKM[Y224F]	Flexible	−	+	+
RKM[Y225Q]	Flexible	−	+	+
RK13HorsePrP[S167D]	N/D	−	+	+

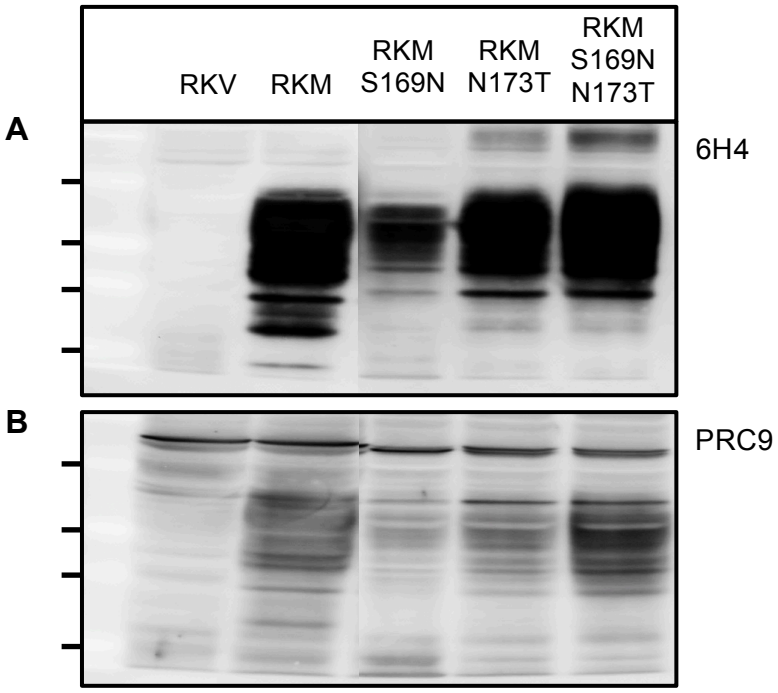

Figure 3.1. Expression of PrP in RK13 cells expressing variant mouse PrP. The expression of PrP was determined in RKM[S169N], RKM[N173T] and RKM[S169N, N173T] on western blots using mAb 6H4 (A) and PRC9 (B). The above western blots showed all of three cell lines expressed the sufficient levels of PrP. RK13 cells with an empty vector (RKV) were used as a negative control. RK13 cells expressing a wild-type mouse PrP (RKM) were used as a positive control. Molecular markers indicate 53, 36, 28 and 19 kDa from top to bottom. Cropped images are from the same exposure of the same blot.

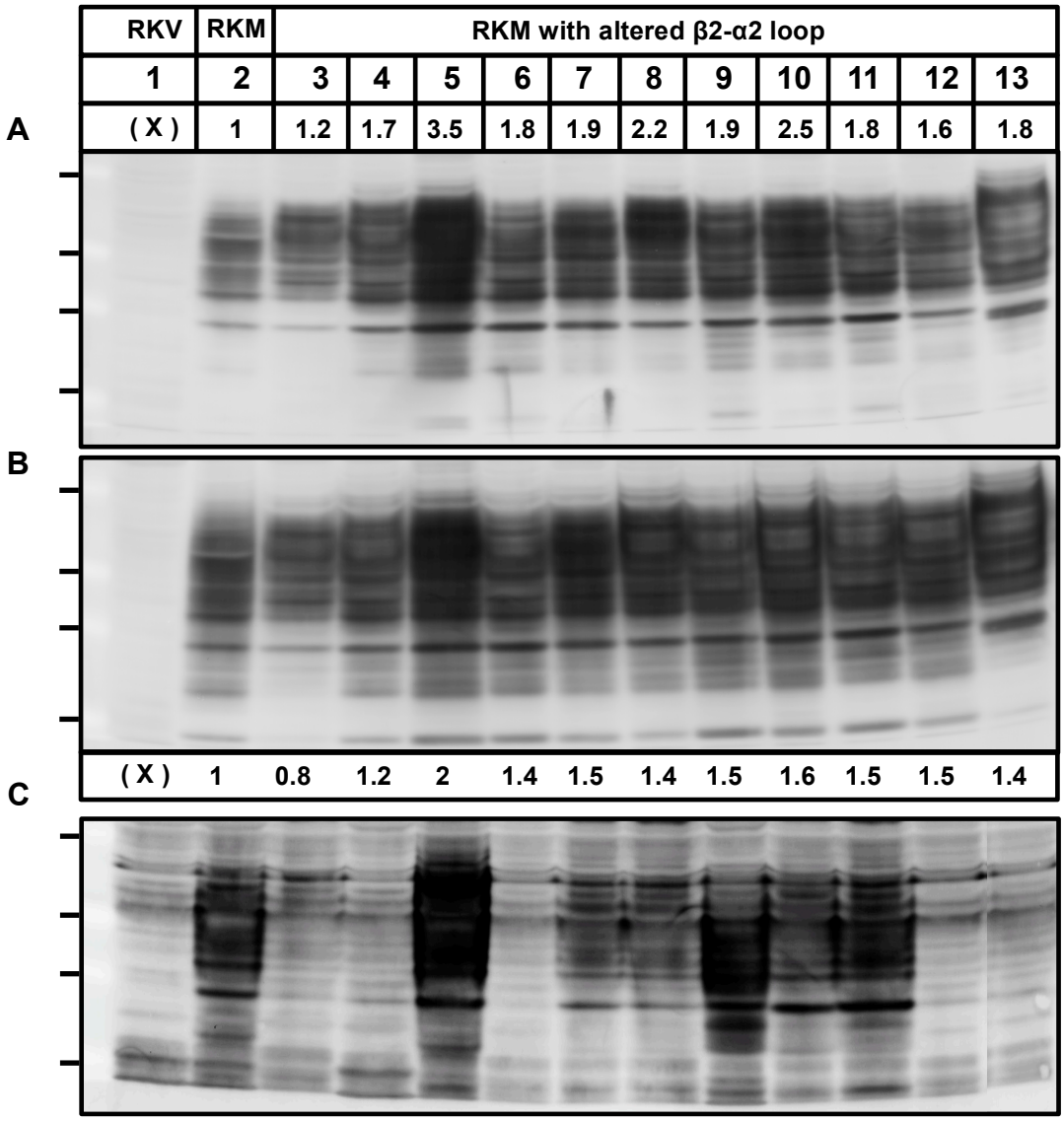

Figure 3.2. PrP expression levels in RK13 cells expressing variant mouse PrP carrying the altered β2-α2 loop. The western blots with anti-PrP mAb 6H4 (A) and PRC5 (B) showed that all of the cell lines expressed sufficient levels of PrP. The last western blot was probed with anti-PrP mAb PRC9, which is a mouse specific antibody (C). PRC9 recognizes some of the mutant cell lines but not all of the lines. Lanes 1. RK13 cells with an empty pIRESpuro vector (RKV); 2. RK13 cells expressing a wild-type mouse PrP (RKM); 3. RKM[V165A]; 4. RKM[Y224A]; 5. RKM[Y225A]; 6. RKM[Y224A, Y225A]; 7. RKM[D166S]; 8. RKM[Q167E]; 9. RKM[N172K]; 10. RKM[D166S, Q167E]; 11. RKM[D166S, N172K]; 12. RKM[Y224F]; 13. HorsePrP[S167D]. The numbers shown under the blots (A and B) indicate the levels of PrP in each cell line through comparison to RKM. Molecular markers indicate 53, 36, 28 and 19 kDa from top to bottom. Cropped images are from the same exposure of the same blot.

A

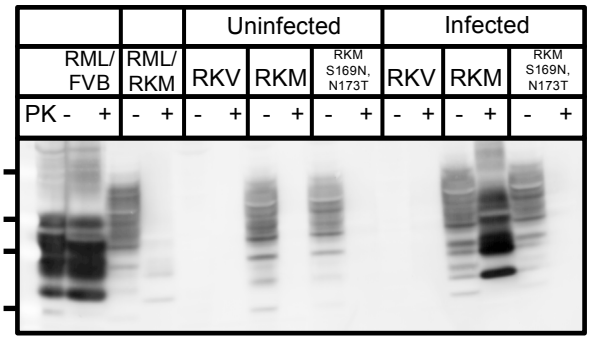
Uninfected
Infected
RML/ FVB
RML/ RKM
RKV
RKM
RKM S169N, N173T
PK - +

B

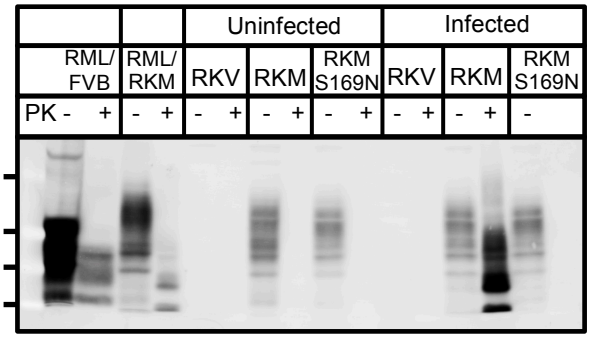
Uninfected
Infected
RML/ FVB
RML/ RKM
RKV
RKM
RKM S169N
PK - +

C

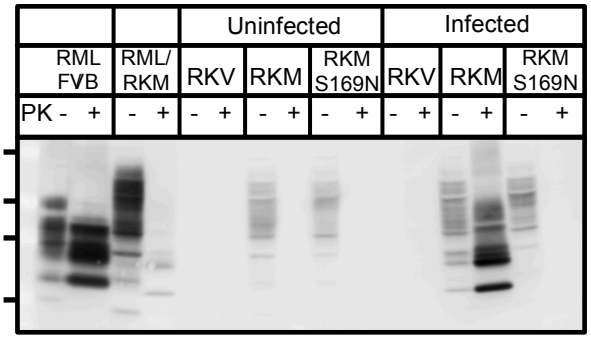
Uninfected
Infected
RML FVB
RML/ RKM
RKV
RKM
RKM S169N
PK - +

D

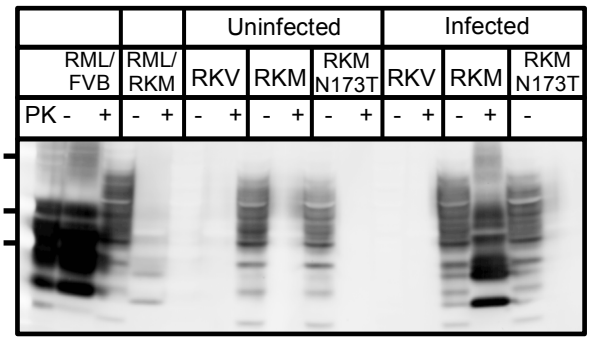
Uninfected
Infected
RML/ FVB
RML/ RKM
RKV
RKM
RKM N173T
PK - +

Figure 3.3. Altering the structure of the β2-α2 loop in mouse PrP changed the susceptibility to RML. All western blots were probed with anti-PrP 6H4 antibody. A. The western blot showed that PrP^{Sc} did not accumulate in RML-infected RKM[S169N, N173T], the flexible β2-α2 loop of mouse PrP was changed to the rigid loop, suggesting that RKM[S169N, N173T] cells lost susceptibility to RML prions at passage 3. B. RML-infected RKM[S169N] cells also did not show accumulation of PrP^{Sc} at passage 3. C. RML-infected RKM[S169N] cells were maintained for up to five passages after infection to see if delayed propagation of PrP^{Sc} occurred. However, PrP^{Sc} was absent in the RML-infected cells at passage 5 on western blot, suggesting that RKM[S169N] cells were resistant to RML. D. RML failed to produce PrP^{Sc} in RKM[N173T] cells, even though this single substitution was sufficient to maintain a flexible β2-α2. RML/FVB indicates brain homogenates from RML-infected wild-type FVB mice. RKM is RK13 cells expressing a wild-type mouse PrP. RML/RKM are RML-infected RKM. Samples treated with proteinase K (PK) indicate (+). Samples without PK digestion indicate (-). Molecular markers indicate 53, 36, 28 and 19 kDa from top to bottom.

A

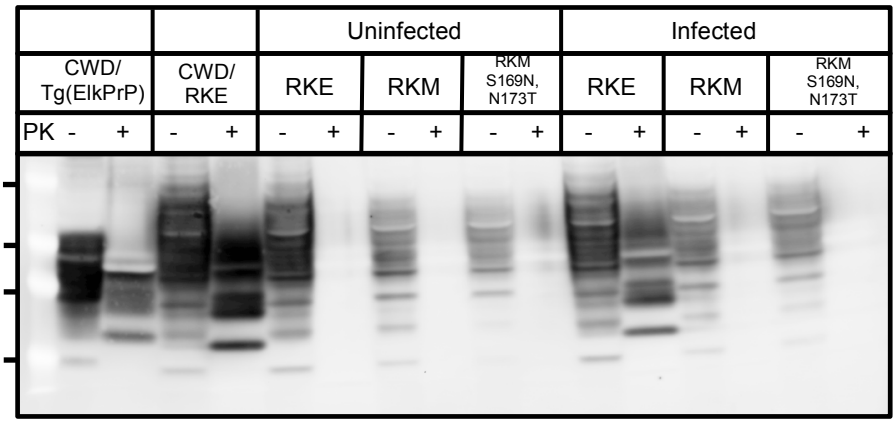
Uninfected
Infected
CWD/ Tg(ElkPrP)
CWD/ RKE
RKE
RKM
RKM S169N, N173T
RKE
RKM
RKM S169N, N173T
PK - + - + - + - + - + - + - + - +

B

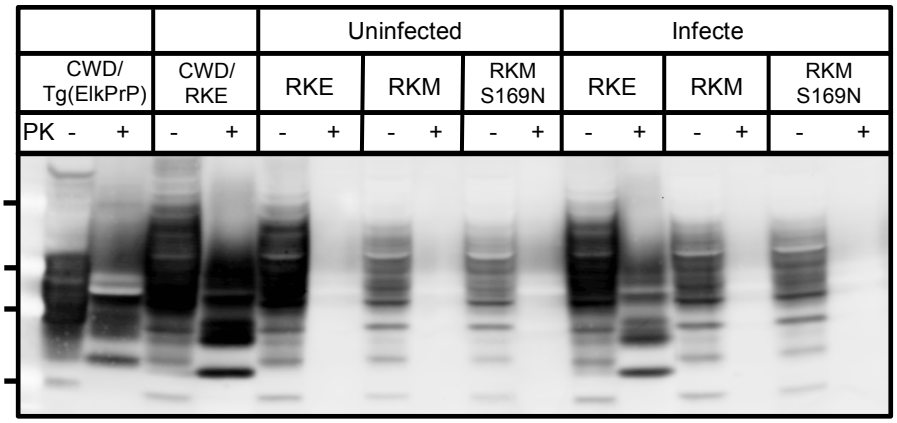
Uninfected
Infecte
CWD/ Tg(ElkPrP)
CWD/ RKE
RKE
RKM
RKM S169N
RKE
RKM
RKM S169N
PK - + - + - + - + - + - + - + - +

C

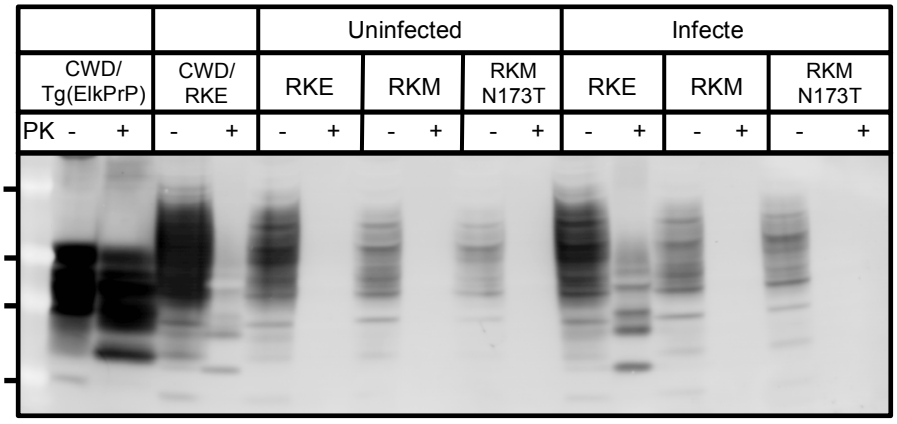
Uninfected
Infecte
CWD/ Tg(ElkPrP)
CWD/ RKE
RKE
RKM
RKM N173T
RKE
RKM
RKM N173T
PK - + - + - + - + - + - + - + - +

Figure 3.4. Introducing the rigid loop in mouse PrP was not sufficient to gain susceptibility to CWD. CWD infected mutant cells were examined for the conversion of PrP^{Sc} at passage 3. All western blots were probed with anti-PrP 6H4 antibody. A. CWD-infected RKM[S169N, N173T] cells failed to produce PrP^{Sc}. B. CWD-infected RKM[S169N] also did not accumulate PrP^{Sc}. The lack of PrP^{Sc} in CWD-infected RKM[S169N, N173T] and RKM[S169N] cells showed that introducing the rigid loop in mouse PrP was not sufficient to confer susceptibility to CWD. C. PrP^{Sc} was not identified in CWD-infected RKM[N173T] cells at passage 3, showing that the substitution were not sufficient to confer susceptibility to an otherwise mouse PrP primary structure to CWD prions. CWD/Tg(ElkPrP) indicates brain homogenates from CWD (Bala05)-infected Tg(ElkPrP) mice. RKE is RK13 cells expressing elk PrP. CWD/RKE is RKE cells were chronically infected with CWD. RKM is RK13 cells expressing a wild-type mouse PrP. Samples treated with proteinase K (PK) indicate (+). Samples without PK digestion indicate (-). Molecular markers indicate 53, 36, 28 and 19 kDa from top to bottom.

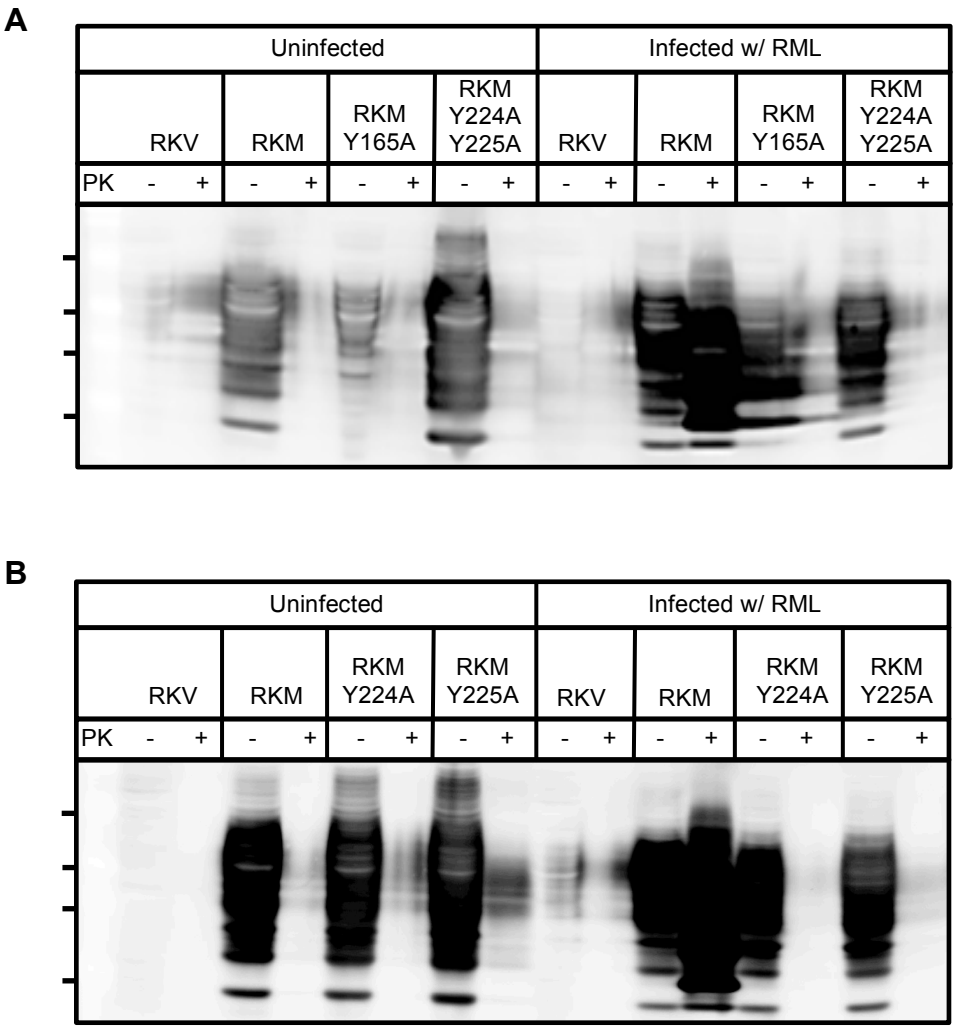

Figure 3.5. Interrupting the interaction between the β2-α2 loop and C-terminal of mouse PrP changed susceptibility to RML prions. Infected and uninfected samples were determined for the propagation of PrP^{Sc} followed by the infection of RML prions at passage 3. All western blots were probed with anti-PrP mAb PRC5. Introducing substitution Y165A in the β2-α2 loop of mouse PrP changes the interaction between the β2-α2 loop and C-terminal region, and the substitution resulted in loss of susceptibility to RML (A). Additionally, the point or double substitutions at Y224A and/or Y225A at the C-terminal of mouse PrP were introduced. PrP^{Sc} did not accumulate in RK13 cells expressing RKM[Y224A, Y225A] (A). Further, both RML prions failed to accumulate PrP^{Sc} in RKM[Y224A] and RKM[Y225A] cells. Interrupting the interaction between the β2-α2 loop and C-terminal of mouse PrP was sufficient to lose susceptibility to RML prions. RKV is RK13 cells with an empty vector. RKM is RK13 cells expressing a wild-type mouse PrP. Samples treated with proteinase K (PK) indicate (+). Undigested samples indicate (-). Molecular markers indicate 53, 36, 28 and 19 kDa from top to bottom.

A

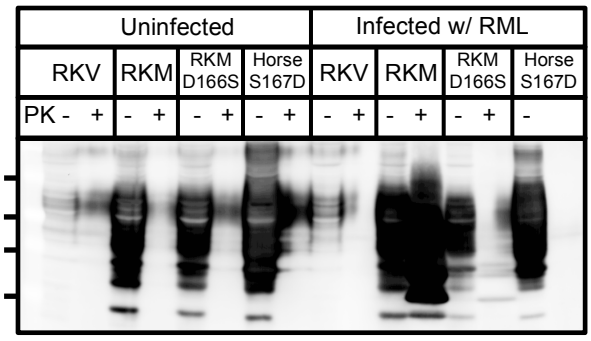
Uninfected
Infected w/ RML
RKV
RKM
RKM D166S
Horse S167D
RKV
RKM
RKM D166S
Horse S167D
PK - + - + - + - + - + - + - + -

B

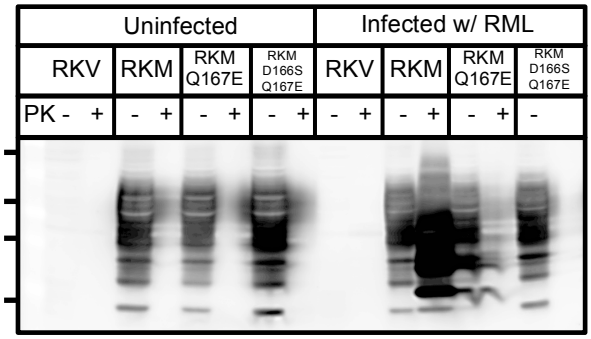
Uninfected
Infected w/ RML
RKV
RKM
RKM Q167E
RKM D166S Q167E
RKV
RKM
RKM Q167E
RKM D166S Q167E
PK - + - + - + - + - + - + - + -

C

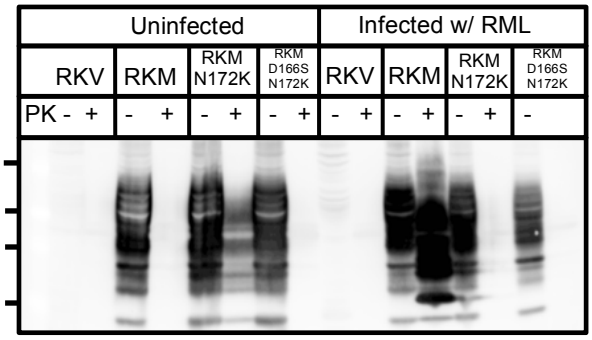
Uninfected
Infected w/ RML
RKV
RKM
RKM N172K
RKM D166S N172K
RKV
RKM
RKM N172K
RKM D166S N172K
PK - + - + - + - + - + - + - + -

D

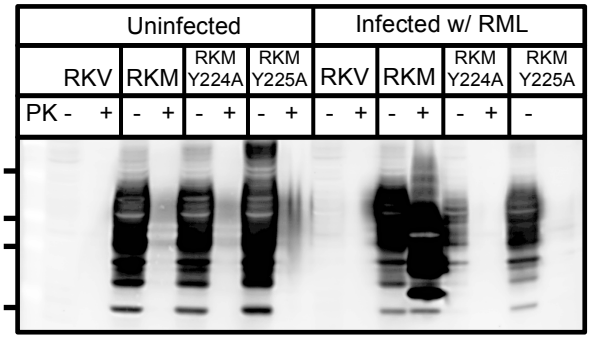
Uninfected
Infected w/ RML
RKV
RKM
RKM Y224A
RKM Y225A
RKV
RKM
RKM Y224A
RKM Y225A
PK - + - + - + - + - + - + - + -

Figure 3.6. Horse-specific substitutions within the β2-α2 loop and its interaction site of mouse PrP resulted in loss of susceptibility to RML. In order to study unique amino acid residues in the β2-α2 loop and C-terminal regions of horse PrP, horse specific substitutions at residues 166, 167, 172, 224 and 225 were introduced into the mouse PrP primary structure. RK13 cells expressing those mutant mouse PrP constructs were tested for susceptibility to RML prions. Infected and uninfected samples were determined for the conversion of PrP^{Sc} followed by the infection of RML prions at passage 3. All western blots were probed with mAb PRC5. A. The western blot showed that a weak signal of proteinase K (PK)-resistant PrP^{Sc} around 19 and 27-25 kDa in RML-infected RKM[D166S] cells. However, accumulation of PrP^{Sc} was not detected in RML-infected RK13 cells expressing horse PrP with a substitution of S to D at codon 167 (HorsePrP[S167D]). B. Although the apparent signal in the PK-digested sample from RML-infected RKM[Q167E] cells was present, the signal was most likely due to the undigested PrP or leaked sample from the neighboring lanes. RML-infected RKM[Q166S, Q167E] cells did not accumulate PrP^{Sc}. C. RKM[N172K] and RKM[D166S, N172K] cells failed to accumulate PrP^{Sc} upon RML infection. D. The western blot failed to detect PrP^{Sc} in RML-infected RKM[Y224A] and RKM[Y225A] cells. RKV is RK13 cells with an empty vector. RKM is RK13 cells expressing a wild-type mouse PrP. Samples treated with proteinase K (PK) indicate (+). Samples without PK digestion indicate (-). Molecular markers indicate 53, 36, 28 and 19 kDa from top to bottom.

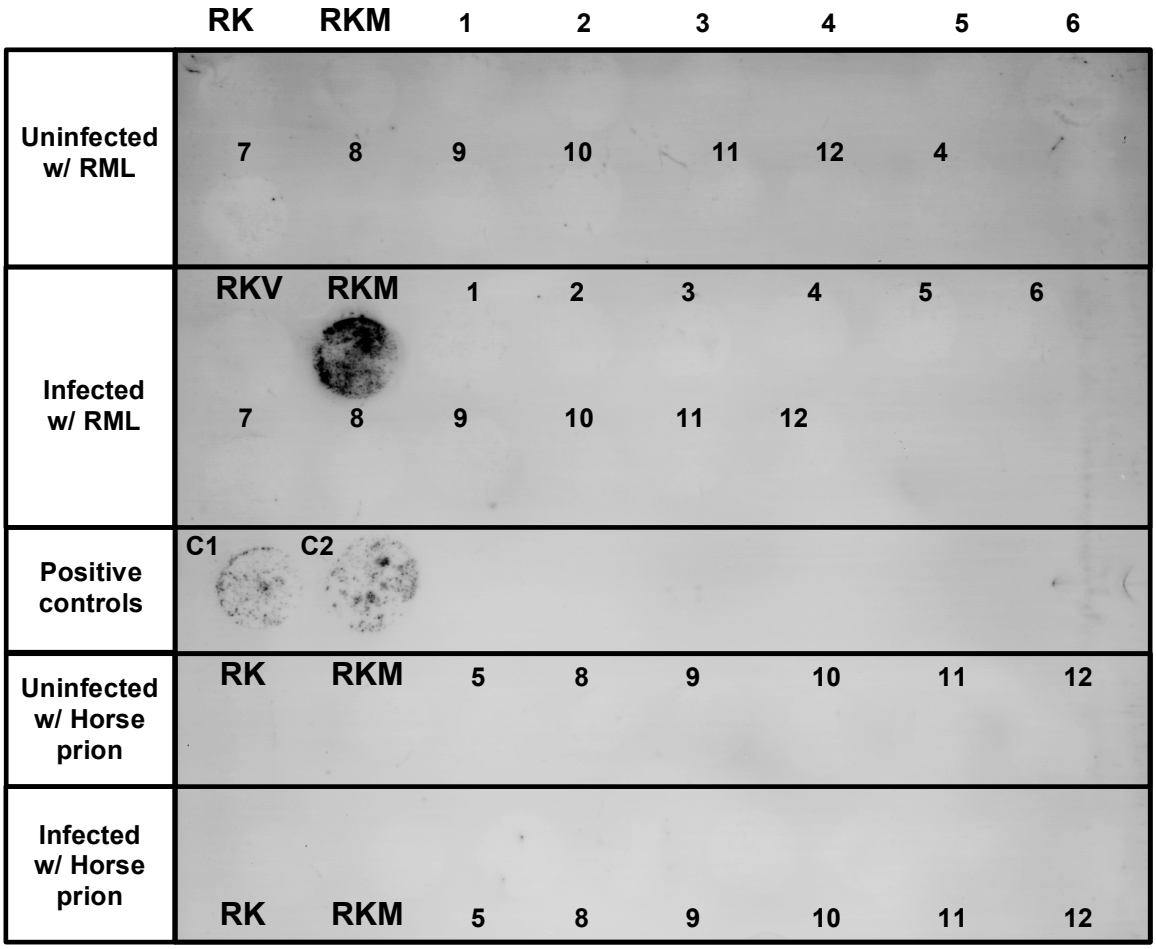

Figure 3.7. Absence of PrP^{Sc} in RML or horse prion infected RK13 cells expressing mutant mouse PrP on cell blotting analysis at passage 5. Prion infected and uninfected samples were determined for the accumulation of PrP^{Sc} using a cell blotting technique, and the analyses confirmed the absence of PrP^{Sc} in the mutant RK13 cells followed by the infection of RML or horse prions. Selected variant mouse PrP including the hore-specific substitutions at residues 166, 167, 172, 224 and/or 225 (mouse numbers), were tested for susceptibility of horse prion. Additionally, the variant horse PrP (HorsePrP[S167D]) was also tested for susceptibility to horse prion. However, horse prion-infected RK13HorsePrP[S167D] cells failed to convert PrP^{Sc}. As positive controls, RK13 cells expressing elk PrP, which were chronically infected with sheep scrapie 48x35 (C1) or SSBP/1 (C2) were used for the presence of PrP^{Sc} signals. RKV is RK13 cells with an empty vector. RKM is RK13 cells expressing a wild-type mouse PrP. 1. RKM[V165A]; 2. RKM[Y224A]; 3. RKM[Y225A]; 4. RKM[Y224A, Y225A]; 5. RKM[D166S]; 6. RKM[Q167E]; 7.RKM[N172K]; 8. RKM[D166S, Q167E]; 9. RKM[D166S, N172K]; 10. RKM[Y224F]; 11. RKM[Y225Q] 12. RK13 HorsePrP[S167D].

Chapter 4

A 'dominant' OvPrP^{Sc}-V136 conformation leads to forced templating of OvPrP^{C}-A136

Introduction

Classical scrapie, long documented as a lethal infectious neurological disease in sheep, goat and moufflon, is by now classified as a transmissible spongiform encephalopathy (TSE)- a prion disease (Dickinson, 1976; Wood *et al.*, 1992). Though its causative agent is now known, scrapie remains a serious problem with growing numbers of cases reported from many countries, necessitating vigilant monitoring and surveillance worldwide in sheep industries. As one result, the European Union and the United States have begun selective breeding of scrapie resistant sheep to increase the frequency of scrapie resistant genotypes (Commission, 2003; U.S. Department of Agriculture, 2012). There is, however, some debate as to whether the reduction of genetic variability in sheep results in loss of some of rare breeds (Alvarez *et al.*, 2007; Windig *et al.*, 2007; Windig *et al.*, 2004). A further concern is that such selective breeding might make possible the emergence or adaptation of new strains of scrapie in the selected genotypes. In order to optimize the selective breeds most effectively and to prevent the worst scenario from happening, we require better understanding of how ovine polymorphisms affect both susceptibility and resistance of scrapie.

The ovine PrP (OvPrP) gene is known to be highly polymorphic; however, three major polymorphisms at codon 136 (alanine [A] or valine [V]), 154 (arginine

[R] or histidine [H]), and 171 (glutamine [Q], R or H) have been identified to have the most impact on susceptibility to classical scrapie (Goldmann *et al.*, 1991; Goldmann *et al.*, 1994). The common haplotype is A at codon 136, R at codon 154 and Q at codon 171 (ARQ), which is a less susceptible genotype to classical scrapie isolate SSBP/1 (sheep-passaged scrapie isolate 1); on the other hand, it is also the haplotype most susceptible to another scrapie isolate CH1641 (Baylis & Goldmann, 2004; Dickinson & Outram, 1988; Foster & Dickinson, 1988b; Goldmann *et al.*, 1994). Genetic susceptibility to SSBP/1 and CH1641 isolates has been characterized experimentally by passaging through different breeds of sheep (Goldmann *et al.*, 1994; Westaway *et al.*, 1994a) and transgenic (Tg) mice expressing OvPrP encoding either ARQ (Baron *et al.*, 2004) or VRQ (Tamguney *et al.*, 2009a). Studies with sheep revealed that five combinations of the above polymorphisms appeared with any degree of frequency, and they are ARR, ARQ, AHQ, ARH and VRQ (Belt *et al.*, 1995; Ikeda *et al.*, 1995). In addition, sheep homozygous for ARR and VRQ are most resistant and susceptible to scrapie, respectively (Goldmann *et al.*, 1994). In contrast, A136 and V136 are most susceptible and resistant to CH1641, respectively (Goldmann *et al.*, 1994). Taken together, numerous studies of scrapie isolates have continuously shown that scrapie susceptibility is strongly linked to polymorphisms (Hunter, 2007); however, the molecular mechanisms that link the PrP genotype to scrapie susceptibility and incubation period continued to be poorly understood.

Immunological tools that are able to distinguish polymorphic alleles especially at codon 136 and 171 are extremely useful in studying the effects of

polymorphisms on scrapie propagation. The previous studies have shown monoclonal antibodies (mAbs) to be capable of distinguishing OvPrP between Q171 and R171 alleles (Bilheude *et al.*, 2007; Jacobs *et al.*, 2011; Moudjou *et al.*, 2004), and four antibodies are available to differentiate the OvPrP 171 polymorphism. Moudjou et al. produced two mAb antibodies; mAb V5 identifies R171, mAb V61 identifies Q171. Another mAb, 2A11, was produced by a French group and had reactivities with Q and H but not R at codon 171 (Bilheude *et al.*, 2007). The Langeveld group used mAb SAF84, which recognizes Q at codon 171, to demonstrate that substantially reduced level of $OvPrP^{Sc}$ with R171 was converted under conditions of co-expression of Q171 and R171 (Jacobs *et al.*, 2011). However, the mAb known as PRC5 is the first antibody to differentiate OvPrP alleles expressing A and V at codon 136 (Kang *et al.*, 2012), and, we show here, was additionally able to provide insight into polymorphic effects on scrapie conversion.

In the present study, we employ transgenic and immunological tools to assess the mechanisms by which the OvPrP 136 polymorphism controls scrapie susceptibility. The use of mouse mAb PRC5 enabled differentiation of OvPrP-A136 from OvPrP-V136 in Tg(OvPrP) mice co-expressing A136 and V136. With those tools, we could pursue the following three questions regarding the effects of co-expressing A136 and V136 alleles on the replication of scrapie.

(1) Are OvPrP-A136 and OvPrP-V136 independently converted to PrP^{Sc}, and their properties also independently maintained?

(2) Does conversion of $OvPrP^{C}$-V136 dominate that of $OvPrP^{C}$-A136?

(3) Does expression of either allele inhibit conversion of the other? In light of the study on the Q171R polymorphism (Jacobs *et al.*, 2011) and of above questions, we hypothesized that $OvPrP^{C}$-V136 was preferentially converted to PrP^{Sc} under co-expressions of $OvPrP^{C}$-A136 and $OvPrP^{C}$-V136, and that the survival time of SSBP/1 in Tg(OvPrP-A/V136) would be relatively longer than SSBP/1-inoculated Tg(OvPrP-V136) mice.

First, heterozygous Tg(OvPrP) mice expressing the A and V at codon 136 (Tg(OvPrP-A/V136)) were generated and intracerebrally inoculated with SSBP/1 scrapie prions. When SSBP/1-inoculated animals developed disease, the properties of $OvPrP^{Sc}$-A136 and $OvPrP^{Sc}$-V136 were examined by western blotting and histoblotting analyses using mAb anti-PrP PRC5 and 6H4. Next, the kinetics of PrP^{Sc} conversion were studied in relation to the interactions of multiple allelic forms of PrP^{C} to different allelic forms of PrP^{Sc} using protein misfolding cyclic amplification (PMCA). We demonstrated for the first time that the templating characteristics including the kinetics of conversion and properties of PrP^{Sc} (deposition patterns) are independently unique to each allele. Moreover, the present study showed that the templating characteristics of $OvPrP^{Sc}$-V136 are dominant over $OvPrP^{Sc}$-A136 when both of the alleles are present.

Materials and Methods

Generation of ovine transgenic mice. Hemizygous Tg mice expressing ovine PrP encoding either A or V at residue 136 were previously generated and are referred to as Tg(OvPrP-A136)$3533^{+/-}$ and Tg(OvPrP-V136)$4166^{+/-}$, respectively

(Green, 2007). Briefly, ovine PrP (OvPrP) ARQ and VRQ open reading frame cassettes containing the mouse signal peptide instead of an ovine signal peptide were obtained from Dr. Nora Hunter. The OvPrP-ARQ and OvPrP-VRQ sequences were cloned into the cosSHa.Tet cosmid expression vector for transgene expression as described previously (Scott *et al.*, 1992). The purified OvPrP-ARQ and OvPrP-VRQ DNA were then microinjected into the pronuclei of fertilized FVB/*Prnp*$^{0/0}$ and wild-type FVB oocytes, respectively. Positive transgenic founders were identified by polymerase chain reaction (PCR) screening of the genomic DNA. Tg(OvPrP) mice were backcrossed to a *Prnp* knockout (*Prnp*$^{0/0}$) background to maintain hemizygous transgenic lines. To produce Tg(OvPrP-A/V136) heterozygous mice, homozygous lines of Tg(OvPrP-A136) and Tg(OvPrP-V136) were produced, and Tg(OvPrP-A136)$^{+/+}$ and Tg(OvPrP-V136)$^{+/+}$ homozygous mice were mated to generate a heterozygous line of Tg(OvPrP-A/V136) mice expressing OvPrP with A/V at residue 136. The relative expression levels of PrP in the brains of each Tg mouse line were determined by comparison with PrP expressed in the brains of wild-type FVB mice on western blots using anti-PrP mAb 6H4 (Prionics).

Analysis of sheep polymorphism at codon 136. Genomic DNA was extracted from brain homogenates of healthy Tg(OvPrP-A136)3533$^{+/-}$ and Tg(OvPrP-V136)4166$^{+/-}$ mice. The sense primer (5'-GGACAGGGCAGTCCTGGA-3') and antisense primer (5'-GATGAGGAGGATCACAGGAGG-3') were used to amplify the *Prnp* encoding sequence using PCR. The *Prnp* codon 136 polymorphism was

assessed by digestion of the amplicons with endonucleases *BspHI* (New England Biolabs. Inc.), and the digested products were analyzed on 1% agarose gels.

Transmission studies and scrapie isolates. Three natural sheep scrapie isolates SSBP/1, CH1641 and 48x35 and two goat scrapie isolates 76/12/14 and 76/12/22 were used for the transmission experiments to Tg mice. Classical sheep scrapie isolate SSBP/1 is a pool of six to eight natural sheep scrapie brains that were subsequently passaged through Cheviot sheep at the Neuropathogenesis Unit (NPU), Edinburgh UK. The polymorphisms of the original pooled sheep inoculum included VRQ, ARQ and possibly others (Dickinson, 1976), but the genetic makeup of sheep propagating the subsequently passaged SSBP/1 is unclear. The 48x35 sheep scrapie isolate was recovered from a natural scrapie case in a heterozygous VRQ/ARQ Cheviot sheep with L at codon 141 in the ARQ allele the NPU. CH1641 is also the result of a naturally infected Cheviot sheep from the NPU flock. SSBP/1, 48x35, and CH1641 were obtained from Dr. Nora Hunter, NPU. The US goat scrapie 76/12/14, and 76/12/14 isolates were obtained from Dr. Jason Bartz (Creighton University, Omaha NE) and were the results of experimental studies at Creighton University. In addition, two isolates of cervid adapted SSBP/1 were used. These cervid adapted SSBP/1 isolates were generated by inoculating natural sheep scrapie SSBP/1 into Tg(CerPrP)1536$^{+/-}$ and Tg(CerPrP-L132)1973$^{+/-}$, which

express wild-type deer PrP, and deer PrP genetically modified to express leucine at residue 132, respectively, at the University of Kentucky (Green *et al.*, 2008).

Natural isolates of US sheep scrapie positive and negative sheep brain samples were collected from the scrapie flock in Idaho, and sheep were exposed to scrapie either during young or adult ages. Those sheep brain samples were obtained from Dr. Jürgen Richt (Kansas State University, Manhattan KS). The genotyping of sheep PrP was performed by the laboratory at Idaho State University.

Ten-percent brain homogenates of scrapie-positive brains were prepared at 10% (w/v) in sterile phosphate buffered saline (PBS) lacking Ca^{2+} and Mg^{2+} ions by repeated extrusions through a series of needles of decreasing diameter from 18- to 22- gauge. Ten-percent brain homogenates were further diluted to 1% (w/v) in PBS and thoroughly homogenized using a 26-gauge needle syringe. Groups of 5-week-old Tg(OvPrP-A136)3533$^{+/-}$, Tg(OvPrP-V136)4166$^{+/-}$ and Tg(OvPrP-A/V136) mice were anesthetized with halothane and injected with 30 µl of 1% (w/v) brain homogenate intracerebrally into the right parietal lobe using a 26- gauge needle syringe. Hemizygous Tg(OvPrP-A136)3533$^{+/-}$ and Tg(OvPrP-V136)4166$^{+/-}$ mice were inoculated with SSBP/1, CH1641, 48x35, 76/12/22, or 76/12/14, and cervid adapted SSBP/1. Tg(OvPrP-A/V136) mice heterozygous for A/V codon 136 were inoculated with SSBP/1.

Determination of incubation time. The general health of the mice was monitored on a daily basis. The onset of prion diseases was diagnosed by

observation of the progressive development of at least three of the following clinical signs: truncal ataxia, loss of extensor reflex, difficulty righting from a supine position, plastic tail, head bobbing or tilting, kyphotic posture, circling and paresis/paralysis. Animals were diagnosed when at least two investigators agreed with the clinical manifestation of disease. In addition, selected animals were recorded on video at the time of diagnosis and/or right before termination. The incubation time of prion diseases is defined as a period of time from the day of inoculation to the first day of the diagnosis. Therefore, the incubation time was indicated in days post inoculation (dpi).

Western blot analysis. The right hemisphere of each brain was collected for western blot analysis. Ten-percent brain homogenates, prepared as described previously, were digested with 40 μg/ml of proteinase K (PK) (Roche) in the presence of 2% sarkosyl for 1 hour at 37°C. The concentration of total protein in each sample was determined by bicinchoninic acid assay. Undigested brain samples were also examined. For the study of mAb PRC5, total protein concentrations were standardized for each lane (40 μg per lane in Figure 4.1.). Natural sheep and goat scrapie isolates were standardized for 20 μg (undigested) and 150 μg (digested) of total protein per lane (Figure 4.5.). US sheep scrapie isolates were standardized for 20 μg (undigested) and 80 μg (digested) of total protein per lane (Figure 4.6.). In the transmission studies of SSBP/1 into Tg mice, undigested and digested samples were standardized for 25 and 100 μg of total protein per lane, respectively (Figure 4.8.). Unless otherwise

indicated, undigested samples were prepared by mixing 20 µl of 10% brain homogenate with 40 µl of PBS and 20 µl of 4X sodium dodecyl sulfate polyacrylamide gel electrophoresis (SDS-PAGE) sample loading buffer (200 mM Tris-HCl pH 6.8, 8% SDS, 40% glycerol, 50mM ethylenediaminetetraacetic acid (EDTA), and 0.08% bromophenol blue), and 30 µl of the mixture was loaded in each lane. For digested samples, 50 µl of 10% brain homogenate was prepared in 200 µl of PBS in the presence of 2% sarkosyl and digested with PK. The digested sample was mixed with 90 µl of 4X SDS-PAGE sample loading buffer. Each lane contained with 100 µl of the sample mixture.

Proteins were resolved by discontinuous SDS-PAGE and electrophoretically transferred to Immobilon-FL polyvinylidene difluoride (PVDF) membranes (Millipore). The transferred membrane was blocked with 5% non-fat milk in Tris-buffered saline containing 0.5% Tween-20 (TBST) and immunoprobed with anti-PrP mAbs 6H4, PRC1 or PRC5 followed by horseradish peroxidase-conjugated anti-mouse IgG secondary antibody. Proteins were visualized using enhanced chemiluminescence (ECL Plus, GE Healthcare) using an FLA-5000 scanner (Fujifilm Life Science). The expression levels of PrP^C in Tg(OvPrP) mice were determined by densitometric analysis of PrP^C signals on the western blot using MultiGauge (Fujifilm Life Science).

Histoblots. Histoblots were performed according to the protocol previously described (Taraboulos *et al.*, 1992). Briefly, 10 µm thick coronal brain sections were prepared on uncoated glass slides and transferred to nitrocellulose

membrane. The membranes were either treated or untreated with 1.8 mg/ml of PK and probed with mAb 6H4 and PRC5 followed by alkaline phosphatase-conjugated goat anti-mouse secondary antibody (Southern Biotech). Images were documented with a NikonDMX 1200F digital camera in conjunction with Metamorph software (Molecular Devices).

Protein Misfolding Cyclic Amplification (PMCA) Assay. Brains from healthy Tg(OvPrP-A136)3533$^{+/-}$, Tg(OvPrP-V136)4166$^{+/-}$ and FVB/*Prnp*$^{0/0}$ mice were perfused with 5 mM EDTA in PBS. Ten-percent brain homogenates of the perfused brains were prepared in conversion buffer (150 mmol/L NaCl, 1.0% Triton X-100 and Roche's Complete Protease Inhibitor Cocktail in PBS) and briefly centrifuged (60 seconds at 500 rpm) to spin down debris. The PrP expression level in Tg(OvPrP-A136)3533$^{+/-}$ is twice as high as in Tg(OvPrP-V136)4166$^{+/-}$ (Figure 4.7.C.). Therefore, the substrate of OvPrP-A/V136 was prepared by mixing 10% brain homogenates of Tg(OvPrP-A136)3533$^{+/-}$ and Tg(OvPrP-V136)4166$^{+/-}$ mice at 1:2 dilution. OvPrP-A136 substrate alone was prepared by mixing 10% brain homogenates of Tg(OvPrP-A136)3533$^{+/-}$ mice with an equal volume of 10% brain homogenate of FVB/*Prnp*$^{0/0}$ mice. Undiluted 10 % brain homogenate of Tg(OvPrP-V136)4166$^{+/-}$ mice was used for OvPrP-V136 substrate alone.

Ten-percent brain homogenates of SSBP/1-infected Tg(OvPrP-A136)3533$^{+/-}$ and Tg(OvPrP-V136)4166$^{+/-}$ diseased mice were used as SSBP/1-A136 and SSBP/1-V136 seeds, respectively. The PMCA with SSBP/1-A136 seed

was performed by serial dilutions of seed in substrate at 1:30, 1:90, 1:270 and 1:810 dilutions for a total of 48 cycles. The PMCA with SSBP/1-V136 seed was performed with a fixed ratio of seed in substrate at 1:180 dilution, and samples were collected every 2 hours during a total of 12 hours' reaction (24 cycles). Undiluted 10% brain homogenates of CH1641-infected Tg(OvPrP-A136)3533$^{+/-}$ diseased mice were used as CH1641-A136 seed. The PMCA with CH1641-A136 seed was performed with a fixed ratio of seed to substrate at 1:60 dilution, and samples were collected every 12 hours over the course of 48 hours (96 cycles). One cycle is 20 seconds sonication followed by 30 minutes incubation at 37°C. Controls were also prepared by incubating samples at 37°C for the duration indicated above. The SSBP/1-V136 PMCA experiments were repeated three times using three different seeds and substrates, and the CH1642-A136 PMCA experiments were performed twice with two different seeds and substrates. Amplified and control samples were digested with PK at a final concentration of 0.33 µg/µl and analyzed on western blots using mAb 6H4 and PRC5. Amplified PrP^{Sc} was quantified by densitometric analysis of PrP^{C} signals on the western blot using MultiGauge (Fujifilm Life Science), and PrP^{Sc} signals were normalized to signals of 37°C incubated controls at the same time points. The normalized PrP^{Sc} values and standard errors of the mean were prepared in graphs using GraphPad Prism 5 (GraphPad Software, Inc.).

Statistical analysis. Survival curves of SSBP/1-inoculated Tg(OvPrP-V136)4166$^{+/-}$ and Tg(OvPrP-A/V136) mice were statistically analyzed using a

Log-rank test. Statistical analysis of western blot data from the SSBP/1-V136 PMCA and CH1641-A136 PMCA was performed using a one-way analysis of variant (ANOVA) at the fixed time points separately. When appropriate, differences between groups were probed using a Newman-Keuls post hoc test. All data were analyzed with GraphPad Prism 5. Differences with $P < 0.05$ was considered to be a significant and indicated with asterisks.

Comparative computational modeling of ovine PrP. Structural differences in the A136 and V136 variants of ovine PrP (residues 114-228) were visualized in VMD (the NAMD molecular dynamics visualizer, available at http://www.ks.uiuc.edu/Research/vmd/). Each of the two structures was compared based on the 2.5-Å-resolution crystal structures of the corresponding antibody-bound PrP variant (Eghiaian *et al.*, 2004). The computational modeling was performed in corroboration with Dr. Michel Sheetz (Center for Computational Science, University of Kentucky).

Results

Distinguishing the OvPrP polymorphism between A136 and V136 using mAb PRC5. Western blot analyses show that mAb PRC5 is able to recognize PrP from a wide range of species including mouse, deer, elk, bovine, equine, and human with methionine (M) or valine (V) 129 polymorphism (Figure 4.1.B.). However, the reactivity of mAb PRC5 is limited to OvPrP-A136, and OvPrP-V136 is not recognized (Figure 4.1.B.). The expression of PrP in all species including

OvPrP-V136 was confirmed in western blots probed with mAb 6H4 (Figure 4.1.A.). The absence of signals in FVB/*Prnp*$^{0/0}$ (KO) samples show the recognition of the antibodies is specific to PrP (Figure 4.1.). The ability to distinguish OvPrP 136 polymorphism was further tested with increased numbers of Tg(OvPrP) samples, and mAb PRC5 recognized only OvPrP-A136 samples (Figure 4.2.B.). The PrP expression of Tg(OvPrP-V136)4166$^{+/-}$ and Tg(OvPrP-A136)3533$^{+/-}$ was verified by mAb 6H4 (Figure 4.2.A.).

Next, brain homogenates from multiple diseased Tg(OvPrP-A136)3533$^{+/-}$ and Tg(OvPrP-V136)4166$^{+/-}$ mice were assessed for the accumulation of PK-resistant PrP^{Sc} using mAb PRC5. Consistent with previous data (Figure 4.1. and 4.2.), mAb PRC5 recognized PrP^{C}-A136 as well as PrP^{Sc}-A136 in diseased Tg(OvPrP-A136)3533$^{+/-}$ mice (Figure 4.3.B.).

The genotype of the Tg(OvPrP) mouse brain samples used to study the characteristics of mAb PRC5 was verified by RFLP using endonuclease *BspHI,* which recognizes the DNA sequence at V136 in ovine PrP and digests into two fragments of 279 and 251 base pairs (bp). All of the OvPrP-V136 samples (V0-7) showed two digested fragments of 279 and 251 bp, indicating that the genotype of the samples matched with the expressed 136 polymorphism of PrP (Figure 4.4.). All of the OvPrP-A136 samples (A1-5) showed only undigested bands at 530 bp, confirming correspondence of PrP 136 polymorphism with the genotype. Together, all the above data demonstrated that mAb PRC5 is a uniquely appropriate tool for distinguishing the A or V OvPrP polymorphism at codon 136.

Furthermore, sheep and goat scrapie samples including three classical sheep isolates SSBP/1, CH1641 and 48x35 and two goat isolates 76/12/14, and 76/22/15 isolates were characterized using mAb 6H4 and PRC5. The western blot probed with PRC5 showed that SSBP/1 and 48x35 isolates contained a lesser amount of $OvPrP^{Sc}$-A136 (Figure 4.5.). CH1641 sheep and two goat scrapie isolates were recognized by both 6H4 and PRC5 (Figure 4.5.). The presence of PrP^{C} and absence of PrP^{Sc} in non-diseased sheep sample as well as the absence of PrP signals in KO samples demonstrated that the ability to detect disease-associated PrP^{Sc} in this assay.

Brain samples from the US sheep scrapie affected flock were examined on western blots using mAb 6H4 and PRC5. The US sheep scrapie positive samples showed PK resistant PrP^{Sc} (Figure 4.6.). However, low levels of PrP^{Sc} were detected in one out of four samples homozygous for V at codon 136 and Q at codon 171 and one sample heterozygous for A/V at codon 136, homozygous for R at codon 154 and Q at codon 171 (Figure 4.6.A.). PK-resistant PrP^{Sc} was absent in the scrapie negative samples (Figure 4.6.). The presence of $OvPrP^{Sc}$-A136 was identified in the samples heterozygous for A/V at codon 136 using mAb PRC5 (Figure 4.6.B.). Three out of four samples of heterozygous A136V polymorphism showed significantly low levels of $OvPrP^{Sc}$-A136, and only one sample presented relatively higher levels of $OvPrP^{Sc}$-A136 (Figure 4.6.B.). Interestingly, the expression of OvPrP-A136 was not identified by mAb PRC5 in one scrapie negative sample heterozygous for A136V polymorphism (Figure

4.6.B.); thus, the genotype of the sample should be validated by DNA sequencing.

Susceptibility to multiple scrapie isolates is strongly dependent on OvPrP A136V polymorphism. Transmission studies of scrapie isolates into Tg(OvPrP-A136)3533$^{+/-}$ and Tg(OvPrP-V136)4166$^{+/-}$ mice, which were previously performed in our group, are summarized in Table 4.1., and pertinent information includes the origin of scrapie inocula, mean incubation time, attack rates and number of animals inoculated with scrapie (Green, 2007). The transmission studies of multiple scrapie isolates demonstrated that Tg(OvPrP-A136)3533$^{+/-}$ and Tg(OvPrP-V136)4166$^{+/-}$ mice were vulnerable to prion infection, and the susceptibility of the scrapie isolates was tightly regulated by OvPrP A136V polymorphism. For instance, the attack rates in SSBP/1-inoculated Tg(OvPrP-A136)3533$^{+/-}$ and Tg(OvPrP-V136)4166$^{+/-}$ mice were 100%; however, the incubation times were significantly different between the Tg(OvPrP) mice (Table 4.1. and Figure 4.7.A.). SSBP/1-inoculated Tg(OvPrP-V136)4166$^{+/-}$ mice developed disease at 132 ± 2 dpi, while SSBP/1-inoculated Tg(OvPrP-A136)3533$^{+/-}$ mice required much longer times to develop disease, e.g. 412 ± 49 dpi (Table 4.1. and Figure 4.7.A.). On the other hand, CH1641 could produce disease in Tg(OvPrP-A136)3533$^{+/-}$ mice at 310 ± 21 dpi, whereas not in Tg(OvPrP-V136)4166$^{+/-}$ at >450 dpi (Table 4.1. and Figure 4.7.B.). The results of the transmission studies in Tg(OvPrP) mice are consistent with previously published sheep studies about the effects of polymorphisms on scrapie

susceptibility, and it has been reported that OvPrP-V136 is more susceptible to SSBP/1 and less susceptible to CH1641 (Goldmann *et al.*, 1994). In addition, the OvPrP-A136 is most resistant genotype for SSBP/1 but most susceptible for CH1641 (Goldmann *et al.*, 1994). Moreover, another UK sheep scrapie isolate 48x35 produced disease only in Tg(OvPrP-V136)4166$^{+/-}$ mice at 365 ± 21 dpi but not in Tg(OvPrP-A136)3533$^{+/-}$ at >575 dpi, and the genetic susceptibility or resistance of 48x35 isolate was similar to SSBP/1 (Table 4.1.). Two US goat scrapie isolates 76/12/22 and 76/12/14 could produce disease in Tg(OvPrP-A136)3533$^{+/-}$ at 313 ± 15 and 270 ± 3 dpi, respectively.

Interspecies transmission studies of SSBP/1 were previously performed by inoculating SSBP/1 into Tg(CerPrP-M132) and Tg(CerPrP-L132) mice, and both animals manifested clinical signs at 241 ± 16 and 290 ± 6 days, respectively (Green *et al.*, 2008). These cervid-adapted SSBP/1 prions were transmitted back to Tg(OvPrP-A136)3533$^{+/-}$ and Tg(OvPrP-V136)4166$^{+/-}$ mice. As a result, Tg(CerPrP-M132) mouse passaged SSBP/1 produced disease in Tg(OvPrP-V136)4166$^{+/-}$ mice at 150 ± 5 dpi and Tg(OvPrP-A136)3533$^{+/-}$ mice at 231 ± 14 dpi (Table 4.1.), and the incubation times were extended in Tg(OvPrP-V136)4166$^{+/-}$ mice and substantially shortened in Tg(OvPrP-A136)3533$^{+/-}$ mice, when compared to the transmission date with original SSBP/1 in those Tg mice. Tg(CerPrP-L132) passaged SSBP/1 produced disease in Tg(OvPrP-V136)4166$^{+/-}$ mice at 335 ± 14 dpi and Tg(OvPrP-A136)3533$^{+/-}$ mice at 248 ± 14 dpi (Table 4.1.), and the genetic susceptibility was inverted compared to the transmission data of original SSBP/1 in Tg(OvPrP) mice. Thus, modification of

the transmission properties of SSBP/1 occurred during the propagation of these prions in the Tg(CerPrP) mice.

The above Tg mouse studies confirmed that the susceptibility and resistance of SSBP/1 and CH1641 scrapie isolates were tightly regulated by the OvPrP A136V polymorphism. Moreover, it was demonstrated that Tg(OvPrP-A136)3533$^{+/-}$ and Tg(OvPrP-V136)4166$^{+/-}$ are ideal animal models to investigate the underlying mechanisms of how the OvPrP genotype acts upon scrapie susceptibility and incubation time. In addition, the use of mAb PRC5 makes it possible to distinguish the A136V polymorphism and further to study the conditions of co-expressing OvPrP-A136 and OvPrP-V136. To study the PrP^{Sc} conversion in the heterozygous state, Tg(OvPrP-A/V136) mice was generated by crossing homozygous Tg(OvPrP-A136)3533$^{+/+}$ and Tg(OvPrP-V136)4166$^{+/+}$.

The expression levels of PrP^{C} in Tg(OvPrP-A136)3533$^{+/-}$, Tg(OvPrP-V136)4166$^{+/-}$ and Tg(OvPrP-A/V136) mouse brains were determined through comparison with wild-type FVB mouse brains on western blots using mAb 6H4 and PRC5. Tg(OvPrP-A136)3533$^{+/-}$ mice express 30% higher levels of PrP, and Tg(OvPrP-V136)4166$^{+/-}$ mice express 35% lower levels of PrP (Figure 4.7.C.). The levels of PrP were 23% higher in heterozygous Tg(OvPrP-A/V136) mice compared to FVB mice (Figure 4.7.C.). The levels of PrP in all three Tg(OvPrP) mouse lines are fairly close to those of wild-type FVB mice. It is interesting to note that Tg(OvPrP-V136)4166$^{+/-}$ mice express less PrP than Tg(OvPrP-A136)3533$^{+/-}$ mice. However, SSBP/1-inoculated-Tg(OvPrP-V136)4166$^{+/-}$ mice

developed disease with much shorter incubation times than do Tg(OvPrP-A136)3533$^{+/-}$ mice (Table 4.1. and Figure 4.7.A.).

Ample replication of PrP^{Sc}-A136 was identified in SSBP/1-inoculated Tg(OvPrP-A/V136) heterozygous mice. SSBP/1-inoculated Tg(OvPrP-A/V136) mice manifested clinical signs at 105 ± 5 dpi and developed disease even faster than Tg(OvPrP-V136)4166$^{+/-}$ mice (p<0.0001, Figure 4.7.A.). The accumulation of PK-resistant PrP^{Sc} in the brains of SSBP/1-inoculated Tg(OvPrP-A/V136) mice was examined by western blotting using mAb 6H4 and PRC5 along with the control brain samples of SSBP/1-inoculatd Tg(OvPrP-A136)3533$^{+/-}$ and Tg(OvPrP-V136)4166$^{+/-}$ mice (Figure 4.8.). All diseased Tg(OvPrP) mouse brains contained PK-resistant PrP^{Sc} which could be detected on western blots with 6H4 (Figure 4.8.A.). The western blot probed with PRC5, only detects OvPrP-A136, revealed that OvPrP^{C}-A136 was already converted to PrP^{Sc} in Tg(OvPrP-A/V136) mice at 105 ± 5 dpi (Figure 4.8.B.). Considering that SSBP/1-inoculated Tg(OvPrP-A136)3533$^{+/-}$ developed disease at 412 ± 49 dpi (Table 4.1. and Figure 4.8.), the conversion of OvPrP^{Sc}-A136 in SSBP/1-inoculated Tg(OvPrP-A/V136) mice at around 110 days dpi was unexpected. Signals in brain homogenates from SSBP/1-inoculated Tg(OvPrP-V136)4166$^{+/-}$ mice were absent in the western blot with mAb PRC5, confirming PRC5 is capable to distinguish OvPrP-A136 from OvPrP-V136 (Figure 4.8.B.).

OvPrP^{Sc}-A136 acquired properties of OvPrP^{Sc}-V136 in SSBP/1-inoculated Tg(OvPrP-A/V136) mice. To determine the global deposition patterns of PrP^{Sc} in the CNS of diseased Tg mice, we analyzed coronal brain sections including the following regions: septum to hippocampus, hippocampus to thalamus, mid-brain to pons and oblongata from SSBP/1-infected Tg(OvPrP-A136)3533$^{+/-}$, Tg(OvPrP-V136)4166$^{+/-}$ and Tg(OvPrP-A/V136) mice and examined them by histoblots using either mAb 6H4 or PRC5 in the presence or absence of PK (Figure 4.9.). The use of mAb PRC5 made it possible to identify the presence of OvPrP^{Sc}-A136. Consequently, the punctate deposition pattern of OvPrP^{Sc}-A136 was revealed in SSBP/1-inoculated Tg(OvPrP-A136)3533$^{+/-}$ by mAb PRC5 (left images in Figure 4.9.) and 6H4 (data not shown). On the other hand, a diffuse deposition pattern of OvPrP^{Sc}-V136 was observed in SSBP/1-inoculated Tg(OvPrP-V136)4166$^{+/-}$ using mAb 6H4 (2nd image from right in Figure 4.8,); however, the PrP^{Sc}-V136 signals were not identified by mAb PRC5 (2nd image from left in Figure 4.8.), confirming that mAb PRC5 only identified OvPrP-A136. Interestingly, SSBP/1-inoculated Tg(OvPrP-A/V136) mice presented an accumulation of OvPrP^{Sc}-A136, and the deposition pattern was diffuse, which was indistinguishable from that of Tg(OvPrP-V136)4166$^{+/-}$ (right in Figure 4.8.), suggesting that OvPrP^{Sc}-A136 acquires the properties of OvPrP^{Sc}-V136 in SSBP/1-inoculated Tg(OvPrP-A/V136) mice. Additionally, the expression of PrP^{C} in the brains of diseased animals was confirmed by histoblotting in the absence of PK (data not shown), and brain samples of uninfected animals showed only PrP^{C} but not PrP^{Sc} (data not shown). The absence of PrP^{C} and PrP^{Sc} was

confirmed in brain samples from KO mice, indicating the ability to detect disease-associated PrP^{Sc}.

Propagation of $OvPrP^{Sc}$-A136 with SSBP/1-V136 seed was promoted by the presence of $OvPrP^{Sc}$-V136. The above immunoblotting data suggest that $OvPrP^{C}$-A136 used $OvPrP^{Sc}$-V136 as a template to convert itself to PrP^{Sc}. As a result, $OvPrP^{Sc}$-A136 would appear to have acquired the property of $OvPrP^{Sc}$-V136 in SSBP/1-inoculated Tg(OvPrP-A/V136) mice. To further investigate the interactions between PrP^{C} and PrP^{Sc} under conditions of co-existence of $OvPrP^{C}$-A136 and $OvPrP^{C}$-V136, we used PMCA to quantify the amplification of PrP^{Sc} at subsequent multiple time points or serial dilutions of seed to substrate. In addition, we examined whether either $OvPrP^{C}$-A136 or $OvPrP^{C}$-V136 was preferentially converted to PrP^{Sc} with the homogenous genotype of SSBP/1-A136 or SSBP/1-V136 seeds, and whether the presence of either inhibited conversion of the other.

In order to study the rates of PrP^{Sc} conversion, we collected samples every 2 hours for a total of 12 hours of PMCA. As predicted, the amplification of SSBP/1-V136 seed with the genotype matched substrate $OvPrP^{C}$-V136 resulted in the efficient propagation of $OvPrP^{Sc}$-V136 (Figure 4.10.B.). On the other hand, SSBP/1-V136 was not able to convert $OvPrP^{C}$-A136 to PrP^{Sc} by PMCA (Figure 4.10.A. and D.), suggesting that the interaction of $OvPrP^{Sc}$-V136 and $OvPrP^{C}$-A136 was not sufficient to produce $OvPrP^{Sc}$-A136. Interestingly, the propagation of $OvPrP^{Sc}$-A136 was identified when both of $OvPrP^{C}$-V136 and $OvPrP^{C}$-A136

substrates were mixed together (Figure 4.10.F.). The quantification of amplified PrP^{Sc} signals showed that the conversion of $OvPrP^{Sc}$-V136 was first identified after 6 hours of amplification, and the conversion of $OvPrP^{Sc}$-A136 was recognized after 8 hours of amplification under the co-existence of both alleles (Figure 4.11.), indicating that the preferential conversion of PrP^{Sc}-V136 was followed by the propagation of $OvPrP^{Sc}$-A136. Moreover, the different rates of conversion of PrP^{Sc} between OvPrP-A136 and OvPrP-V136 in the presence of both alleles suggest that $OvPrP^{Sc}$-V136 helps the propagation of $OvPrP^{Sc}$-A136.

Statistical analyses were performed at fixed time points (2, 4, 6, 8, 10 or 12 hours separately) using a one-way ANOVA, and significant difference was reported at 10 hours (p<0.0016) and 12 hours (p<0.01). A Newman-Keuls multiple comparison post-hoc test showed the following groups are statistically significant at 10 hours: A/V136-PRC5 vs. A/V136-6H4. Moreover, the Newman-Keuls reported that the following groups are also statistically significant at 12 hours: A/V136-PRC5 vs. V136-6H4.

SSBP/1-A136 produced successful conversion of PrP^{Sc} only with $OvPrP^{C}$-A136 substrate. PMCA of SSBP/1-A136 was performed in serial dilutions of seed to substrate to see whether PrP^{Sc} could be amplified for 98 cycles (48 hours). The amplification of SSBP/1-A136 seed to $OvPrP^{C}$-A136 substrate at 1:30, 1:90, 1:270 and 1:810 dilutions was able to produce PrP^{Sc} (Figure 4.12.A. and D.). However, inefficient amplification of PrP^{Sc}-V136 was observed at 1:90 and 1:270 dilutions. PrP^{Sc} signals at 1:30 dilution in Figure 4.12.B. and E were

most likely coming from the seed SSBP/1-A136. Since OvPrP^{Sc}-V136 would not be recognized by mAb PRC5, the amplified signal on the western blot probed with mAb PRC5 indicated that PrP^{Sc} signals at 1:30 dilution were from the seed. Under the co-presence of OvPrP-A136 and OvPrP-V136 alleles, the PrP^{Sc} conversion was not as efficient as the amplification with OvPrP^{C}-A136 alone. Some amplification of PrP^{Sc} was observed at 1:30 and 1:90 dilutions, but no amplification of PrP^{Sc} was detected at 1:270 and 1:810 dilutions (Figure 4.12.C. and F.). These data indicated that PMCA of SSBP/1-A136 was able to amplify PrP^{Sc} with OvPrP^{C}-A136 compared to OvPrP^{C}-V136 or the mixture of both.

Reduced amount of PrP^{Sc}-A136 was amplified with CH1641-A136 seed in PMCA when the both A136 and V136 alleles existed. PMCA of CH1641-A136 seed with OvPrP-A136, OvPrP-V136 and the mixture of both was performed independently, twice, to examine the compatibility of the seed and substrates for the conversion of PrP^{Sc}. In addition, the amplified samples were collected every 12 hours in a total of 48 hours amplification to study the rate of PrP^{Sc} conversion. As predicted on the basis of the animal studies, the genotyped matched reaction of CH1641-A136 seed and OvPrP^{C}-A136 substrate produced OvPrP^{Sc}-A136 efficiently (Figure 4.14.A. and D.). However, inefficient amplification of OvPrP^{Sc}-V136 was observed with PMCA of CH1641-A136 (Figure 4.14.B.). When two substrates were mixed, reduced amplification of OvPrP^{Sc} in PMCA of CH1641-A136 was observed (Figure 4.14.C. and F.). Interestingly, the western blot probe with mAb PRC5 showing only OvPrP^{Sc}-A136 allele displayed that the efficiency

of $OvPrP^{Sc}$-A136 conversion was reduced remarkably (Figure 4.14.F.). Statistical analyses were performed at fixed time points (12, 24, 36 or 48 hours separately) using a one-way ANOVA, and statistical significance was reported at 24 hours (**p<0.013). A Newman-Keuls multiple comparison post-hoc test showed the following groups are statistically significant at 24 hours: A/V136-PRC5 vs. A136-PRC5 and A/v136-6H4 vs. A136-PRC5. The quantification of PMCA amplified signals from each group revealed that the amplification of $OvPrP^{Sc}$-A136 was inhibited when two substrates were mixed (Figure 4.15.).

CH1641-A136 was compatible with $OvPrP^{C}$-A136 but not $OvPrP^{C}$-V136 for the conversion of PrP^{Sc}. Unlike SSBP/1-V136, the presence of another allele, in this case OvPrP-A136, did not promote the conversion of incompatible allele OvPrP-V136 in PMCA of CH1641-A136 under the co-presence of two alleles. Instead, the presence of OvPrP-V136 obstructed conversion of $OvPrP^{Sc}$-A136.

These data suggest that the rates of PrP^{Sc} conversion were efficient when the genotype of seed and substrate were identical. If the seed and substrate carry different genotypes, the amplification of PrP^{Sc} becomes inefficient. In addition, the rates of PrP^{Sc} conversion were also different among three scrapie isolates. Even though the different effects of the A136V polymorphism on the propagation of PrP^{Sc} were demonstrated by the animal and PMCA studies, it is still not clear what are the differences between OvPrP-A136 and OvPrP-V136 besides in the primary structures.

Computational modeling of structures of OvPrP-A136 and OvPrP-V136 predicted local structural differences in the α-helices and the long-range interaction between the β2-α2 loop and tyrosine at codon 228. To gain more insight into possible conformational differences, we visualized the structures of OvPrP-A136 and OvPrP-V136 corresponding to amino acid residues 114-228 in VMD (Figure 4.17.). Each of the structures includes the disordered N-terminal structure and three α-helices (H1-3) shown in red ribbons (Figure 4.17.). When the structures of OvPrPA-136 and OvPrP-V136 were superimposed, the composed image showed that the two structures were not aligned exactly the same (Figure 4.18.). The most apparent difference between two OvPrP structures was the orientation of Y at codon 228 in the C-terminal region (indicated in a yellow circle in Figure 4.18.). In OvPrP-V136, the ring structure of Y228 at the C-terminal region faced down and was positioned in close proximity to the loop between the β2-sheet and α2-helix, suggesting the long-range interaction of the Y at codon 228 and β2-α2 loop. On the other hand, the ring structure of Y228 flipped away from the β2-α2 loop in OvPrP-A136. The NMR structural study of tammar wallaby PrP reported a long-range interaction between the β2-α2 loop and C-terminal region, which appeared to work together to control the susceptibility to prions (Christen *et al.*, 2009). Additionally, a series of the cell culture studies in Chapter 3 above demonstrated that the interference of the long-range interaction by the substitutions of amino acids in the β2-α2 loop and C-terminal region altered susceptibility to prions (Figure 3.5 to 3.7.). Based on those findings, we surmised that the difference in the orientation of Y228 is a

possible explanation of differences in the susceptibility or resistance to classical scrapie isolates.

Furthermore, the subtle differences between OvPrP-A136 and OvPrP-V136 were found in the structures of three α-helices (H-1, H-2 and H-3), and most conformational changes were concentrated in H-1. The N-terminal of H-1 was relaxed and C-terminal of H-1 opened up in OvPrP-A136; therefore, the diameter of H-1 in OvPrP-V136 was relatively smaller than OvPrP-A136 (Figure 4.19.C.). In addition, the N-terminal of H-1 had less twist in OvPrP-A136. The difference in H-2 was that the C-terminus had an additional twist in OvPrP-V136 but not OvPrP-A136 (Figure 4.19.A and B.). In more detail, the conformational differences were found in the orientation of the following amino acid residues: asparagine at codon 147 and glutamic acid at codon 155 in H-1, asparagine at codon 176 and lysine at codon 188 in H-2, and glutamic acid at codon 203 in H-3 and Y at codon 228.

Discussion

Our transmission studies of classical sheep scrapie isolates in Tg(OvPrP-A136)3533$^{+/-}$ and Tg(OvPrP-V136)4166$^{+/-}$ mice demonstrated that the susceptibility and resistance to the scrapie isolates were consistent with the previously reported sheep study (Goldmann *et al.*, 1994). In contrast to the findings reported in previous sheep transmission studies that the incubation time of SSBP/1-affected sheep heterozygous for the A136V genotype rise between those of sheep homozygous for A136 and V136 (Goldmann *et al.*, 1994),

SSBP/1-inoculated Tg(OvPrP-A/V136) heterozygous mice developed disease even faster than did Tg(OvPrP-V136)4166$^{+/-}$ mice. This relatively rapid incubation time might be associated with the propagation of both PrP^{Sc}-A136 and PrP^{Sc}-V136. Western blots and histoblots demonstrated that the conversion of $OvPrP^{Sc}$-A136 occurred at around 100 dpi in SSBP/1-infected Tg(OvPrP-A/V136) mice, and the deposition patterns of $OvPrP^{Sc}$-A136 were indistinguishable from $OvPrP^{Sc}$-V136 under co-expressions of OvPrP-A136 and OvPrP-V136, suggesting that the dominant conformational selection occurred during the propagation of SSBP/1. PMCA of SSBP/1-A136, SSBP/1-V136 and CH1641-A136 demonstrated that the rates of PrP^{Sc} conversion were different between A136 and V136 polymorphisms. Furthermore, the comparative structural studies revealed differences in the orientation of amino acid molecules located in three α-helices, resulting in the conformational differences between OvPrP-A136 and OvPrP-V136. Taken together, the above data provide new models for explaining how the polymorphism participates in the propagation of PrP^{Sc} as described details in the section below.

The levels of PrP in Tg(OvPrP-A136)3533$^{+/-}$, Tg(OvPrP-V136)4166$^{+/-}$ and Tg(OvPrP-A/V136) mice are close to those found in wild-type FVB mice (Figure 4.7.). In this regard, those Tg mouse lines are unique compared to other overexpressing Tg(OvPrP) mice, such as: TgOvPrP4 (3-fold to sheep), TgOvPRC59 (3-fold to sheep), TgShp XI (4-8 fold), Tg338 (8-10 fold to sheep), and Tg301 (8-fold to sheep) (Cordier *et al.*, 2006; Kupfer *et al.*, 2007; Le Dur *et al.*, 2005; Vilotte *et al.*, 2001). Even though the levels of PrP in Tg(OvPrP-

V136)4166$^{+/-}$ mice is half of the levels expressed in Tg(OvPrP-A136)3533$^{+/-}$ mice, SSBP/1-inoculated Tg(OvPrP-V136)4166$^{+/-}$ mice developed disease much faster than Tg(OvPrP-A136)3533$^{+/-}$ mice. Therefore, we feel justified in concluding that susceptibility was primarily controlled by the A136V polymorphism instead of the expression levels of PrP.

The unique immunological tool, mAb PRC5 distinguishing OvPrP-A136 from OvPrP-V136 allowed us to study the mechanism of conversion of SSBP/1 scrapie in Tg(OvPrP) mice. Western blots probed with mAb PRC5 presented evidence that a significant amount of PrP^{Sc}-A136 was already converted in SSBP/1-inoculated Tg(OvPrP-A/V136) heterozygous mice around 110 dpi. Even though it is not certain whether the propagation of PrP^{Sc}-A136 occurred as early as 110 dpi in SSBP/1-inoculated Tg(OvPrP-A136)3533$^{+/-}$ mice, which required around 400 dpi, we unexpectedly found the ample conversion of PrP^{Sc}-A136 in SSBP/1-inoculated Tg(OvPrP-A/V136) mice. The Langeveld group reported that low levels of PK-resistant OvPrP^{Sc}-R171 in classical scrapie inoculated Tg(OvPrP-A/V136, R/R154, R/Q171) heterozygous mice were detected using mAb SAF84 which identifies OvPrP-Q171 (Jacobs *et al.*, 2011). These studies suggest that two polymorphisms at codon 136 and 171 within OvPrP serve different functions in the propagation of PrP^{Sc}.

The deposition patterns of PrP^{Sc} have been well-characterized for prion strain-typing in classical scrapie-affected sheep brains (Beck *et al.*, 2010; Jeffrey & Gonzalez, 2007; Spiropoulos *et al.*, 2007) since the development of spongiosis is not always the hallmark of prion pathogenesis in classical scrapie. This is

especially true with regard to SSBP/1 (Begara-McGorum *et al.*, 2002; Houston *et al.*, 2002) and to CH1641 (Foster & Dickinson, 1988a). In addition, the PrP^{Sc} profiling on western blotting appears to be homogenous and does not provide much information about differences in scrapie-affected brain samples (Jeffrey & Gonzalez, 2007). It was also true in the present study that the western blot profiles did not distinguish among A136, V136 and A/V136 samples (Figure 4.8.). The deposition patterns of PrP^{Sc} in brains of scrapie-affected sheep homozygous for ARQ/ARQ were described in terms of predominant "granular deposits" or "highly distinctive deposits" (Beck *et al.*, 2010; Jeffrey & Gonzalez, 2007; Spiropoulos *et al.*, 2007), all of which indicates punctate deposition patterns of a sort also shown in SSBP/1-inoculated Tg(OvPrP-A136)$3533^{+/-}$ mice in the present study (left images in Figure 4.9.). In contrast, the PrP^{Sc} profiling in scrapie-affected sheep homozygous for VRQ/VRQ was illustrated as consisting of "mild diffused" or "coalescing plaques" (Beck *et al.*, 2010; Jeffrey & Gonzalez, 2007; Spiropoulos *et al.*, 2007), consistent with the diffuse deposition pattern in SSBP/1-inoculated Tg(OvPrP-V136)$4166^{+/-}$ mice (the 2^{nd} image from right in Figure 4.9.). The distinctive PrP^{Sc} profiling differences found between OvPrP-A136 and OvPrP-V136 do correspond to the pathology of scrapie-diseased sheep brains. Moreover, scrapie-affected sheep heterozygous for ARQ/VRQ showed "coalescing plaques" or "widespread general neutrophil deposition" (Beck *et al.*, 2010; Spiropoulos *et al.*, 2007), and these observations were also in line with diffuse PrP^{Sc} deposition in SSBP/1-inoculated Tg(OvPrP-A/V136) mice (right images in Figure 4.9.). Even though the previously reported studies used

immunohistochemistry to profile the PrP^{Sc} deposition patterns, we consider that the histoblotting technique used in the present study was sensitive enough to represent the distinctive patterns of PrP^{Sc} in SSBP/1-inoculated Tg(OvPrP) mice. In addition to the previously reported findings, the use of mAb PRC5 provided the information exclusive to the $OvPrP^{Sc}$-A136 profiling, and the present study showed that $OvPrP^{Sc}$-A136 could attain the properties of $OvPrP^{Sc}$-V136 upon co-expression of both alleles.

Furthermore, PMCA of SSBP/1-V136 demonstrated that the conversion of $OvPrP^{Sc}$-A136 was assisted by the presence of OvPrP-V136 in the presence of both alleles. Accordingly, it is hypothesized that a 'dominant' $OvPrP^{Sc}$-V136 conformation leads to forced templating of $OvPrP^{C}$-A136. However, the 'dominant' conformational selection was not observed in PMCA of CH1641-A136. This suggests that the templating mechanism of $OvPrP^{Sc}$-V136 might be unique to the SSBP/1 isolate. Bossers group reported that the OvPrP Q171R polymorphism had a dominant-negative inhibition on the conversion of PrP^{C}-R171 to PrP^{Sc}, and that the inhibition was not due to the lack of binding or interaction of PrP^{C}-R171 to PrP^{Sc} (Rigter & Bossers, 2005). Hence, OvPrP-V136 has a dominant-positive templating effect, while OvPrP-R171 has a dominant-negative inhibition. Thus, the 'dominant' templating mechanism of $OvPrP^{Sc}$-V136 might be unique to the 136 polymorphism. Together, the above data indicate that the scrapie susceptibility-linked polymorphisms affect the conversion of PrP^{Sc} by modulating the properties of both PrP^{C} and PrP^{Sc}.

Based on the animal and PMCA studies, I propose the potential mechanisms of propagation of SSBP/1 as illustrated in Figure 4.13. The following proposed models are based on the heterodimer template-associated model (Cohen *et al.*, 1994). Thus, PrP^{C} is in equilibrium with an intermediate form of PrP*, and the formation of PrP* is thought to be facilitated by a hypothetical protein X (Kaneko *et al.*, 1997; Telling *et al.*, 1995; Telling *et al.*, 1994). The conversion of PrP* to PrP^{Sc} is a catalytic step, and the operative catalyst might be protein X or other molecules. It is important to note that although natural sheep scrapie isolate SSBP/1 consists of mainly a VRQ genotype, it is a pool of multiple combinations of genotypes, suggesting that different conformations of PrP^{Sc} are available in the isolate (a box on the top right corner in Figure 4.13.). The first model in Figure 4.13. indicates that the conversion of $OvPrP^{Sc}$-V136 is efficient with the genotype matched SSBP/1-V136, therefore, the survival time of SSBP/1-inoculated Tg(OvPrP-V136) mice is relatively shorter than Tg(OvPrP-A136) mice. On the other hand, the propagation of SSBP/1-A136 with $OvPrP^{C}$-A136 is not as efficient a process as the propagation of SSBP/1-V136 with $OvPrP^{C}$-V136 even though the genotypes between PrP^{Sc} and PrP^{C} are identical. Therefore, the survival time of SSBP/1-inoculated Tg(OvPrP-A136) mice is much longer due to the slow conversion rate of $OvPrP^{Sc}$-A136 (2^{nd} model in Figure 4.13.). In those proposed models, the conformations of PrP^{Sc} differ between $OvPrP^{Sc}$-V136 (pentagon) and $OvPrP^{Sc}$-A136 (triangle), inasmuch as the histoblotting data showed diffuse vs. punctate deposition patterns of PrP^{Sc} in SSBP/1-inoculated Tg(OvPrP-V136)$4166^{+/-}$ and Tg(OvPrP-A136)$3533^{+/-}$ mice,

respectively (Figure 4.9.). The last model in Figure 4.13. indicates that $OvPrP^{C}$-A136 and $OvPrP^{C}$-V136 are co-expressed, the conversion of $OvPrP^{Sc}$-V136 occurs followed by the conversion of $OvPrP^{Sc}$-A136. The intermediate forms of OvPrP*-V136 and OvPrP*-A136 interact to transform the conformation of OvPrP*-A136 into the conformation of OvPrP*-V136, and the adaptation of OvPrP*-V136 conformation in PrP*-A136 allows SSBP/1-V136 to become a template for the conversion to PrP^{Sc}. Therefore, the conformation of $OvPrP^{Sc}$-A136 is identical to $OvPrP^{Sc}$-V136. The histoblots probed with mAb PRC5, which identifies only OvPrP-A136, indicated that the diffuse deposition patterns of $OvPrP^{Sc}$-A136 in SSBP/1-inoculated Tg(OvPrP-A/V136) mice were indistinguishable from the pattern in SSBP/1-inoculated Tg(OvPrP-V136) mice (Figure 4.9.). In the final proposed model, the conversion of $OvPrP^{Sc}$-A136 is promoted by the presence of the other allele, V136, and the conversion of both alleles can promote quicker development of disease in SSBP/1-inoculated Tg(OvPrP-A/V136) mice compared to Tg(OvPrP-V136) mice.

In the final proposed model (Figure 4.13.), the intermediate form PrP* may play an important role in the conversion of SSBP/1-V136 with the co-expression of $OvPrP^{C}$-A136 and $OvPrP^{C}$-V136. PrP^{C} has been proposed to undergo a dramatic unfolding of α-helices to generate the β-sheet rich structure of PrP^{Sc} (Cobb *et al.*, 2007; Lu *et al.*, 2007). The presence of unfolded intermediates of PrP has been detected (Chen *et al.*, 2011), and these intermediate forms are proposed as a more proximal precursor of PrP^{Sc} than PrP^{C} (Roder & Colon, 1997). The kinetic unfolding study of OvPrP ARQ and ARR identified a

population of intermediates formed during unfolding and refolding candidates. ARQ resulted in a larger population of unfolded intermediates compared to ARR, suggesting that differences in the population of intermediates can govern the susceptibility to scrapie isolates (Chen *et al.*, 2011). In general, ARR is a more resistant allele for classical sheep scrapie isolates (Goldmann *et al.*, 1994). These previously published studies support the involvement of unfolded intermediate isoforms of PrP^{C} in the structural conversion of PrP^{Sc} as well as the susceptibility to scrapie.

The propagation mechanisms of SSBP/1-A136 and CH1641-A136 exhibit similarities in the effects of the A136V polymorphism with co-expressions of $OvPrP^{C}$-A136 and $OvPrP^{C}$-V136. When only $OvPrP^{C}$-A136 is available, does propagation of $OvPrP^{Sc}$-A136 occur. However, the propagation of $OvPrP^{Sc}$-A136 is interfered with when $OvPrP^{C}$-V136 is also available for the conversion of PrP^{Sc} (Figure 4.16.). Even though the inhibitory effect of OvPrP-V136 was observed in PMCA of CH1641-A136 and SSBP/1-A136, it is not clear which isoforms of PrP^{C}, PrP* or PrP^{Sc} inhibit the conversion of $OvPrP^{Sc}$-A136 in the presence of both alleles. The question arises as to whether the SSBP/1-A136 isolate becomes more similar to CH1641-A136 or whether CH1641-A136 is originated from a SSBP/1-A136 isolate.

To answer these questions, we consider that the deposition patterns of PrP^{Sc} and neuropathological examinations in either CH1641-A136 or SSBP/1-A136-inouclated animals would be informative. Serial passage of SSBP/1-A136 into Tg(OvPrP-A136) mice might answer whether SSBP/1-A136 can adapt

different strain properties, such as those of CH1641. For example, an incubation time might become similar to CH1641-inoculated mice, and/or OvPrP-V136 might become no longer susceptible to SSBP/1-A136.

Our interspecies transmission studies of cervid adapted SSBP/1 isolates in Tg(OvPrP-A136)3533$^{+/-}$ and Tg(OvPrP-V136)4166$^{+/-}$ mice demonstrated that the properties of original SSBP/1 were altered during the incubation of SSBP/1 in Tg(CerPrP-L132)1973$^{+/-}$ and Tg(OvPrP-M132) mice. The genetic susceptibility of cervid adapted SSBP/1 isolates in Tg(OvPrP-A136)3533$^{+/-}$ and Tg(OvPrP-V136)4166$^{+/-}$ mice turned out to be completely different from original SSBP/1. These studies indicated that new prion strains could arise from an existing strain, for example, SSBP/1 during the adaptation of PrP^{Sc} in new host species.

Biophysical structural studies demonstrated that the action of structural change of PrP^{C} required the unfolding of H1 to open up the globular domain between the S1-H1-S2 and H2-H3 (Adrover *et al.*, 2010; Eghiaian *et al.*, 2007). When PrP^{C} undergoes unfolding, the S1-H1-S2 and H2-H3 domains were separated while linked by the S2-H2 loop (Prigent & Rezaei, 2011). Therefore, the conformation of the S2-H2 loop plays a role in oligomerization. The unfolding process was initiated by binding hypothetical protein X to the S2-H2 loop (Kaneko *et al.*, 1997). The present computational studies comparing the structures between OvPrP-A136 and OvPrP-V136 revealed that the majority of differences were found in the H1, and the orientation of Y at codon 228 was located in closer proximity to the S2-H2 loop in OvPrP-V136 but not in OvPrP-A136. These findings suggest that the structural differences between the

polymorphic variants are associated with the susceptibility to scrapie. It might be that either protein X or PrP^{Sc} favors one conformation over the other to trigger the unfolding events of PrP^{C} to obtain the β-sheet rich structure of PrP^{Sc}, ultimately leading to oligomerization of PrP^{Sc}.

In conclusion, the templating characteristics including the kinetics of conversion and properties of PrP^{Sc} found in the propagation of SSBP/1 appeared to be unique to the scrapie isolate. Under conditions of co-expression, $OvPrP^{C}$-V136 facilitates the conversion of $OvPrP^{Sc}$-A136, and the templating characteristics of $OvPrP^{Sc}$-V136 are dominant over $OvPrP^{Sc}$-A136. On the other hand, CH1641 does not have the same templating characteristics, and the scrapie susceptibility-linked polymorphisms could control the conversion of PrP^{Sc} by modulating both PrP^{C} and PrP^{Sc}.

Table 4.1. Transgenic modeling of the OvPrP 136 polymorphism on scrapie susceptibility. Incubation times indicate days post inoculation (dpi) in mean ± SEM (standard error of the mean). ND indicates that transmission studies of the goat scrapie isolates into Tg(OvPrP-V136)4166$^{+/-}$ were not performed.

Scrapie Isolate	Origin	Mean incubation time (± SEM) days, (n/n_0)	
		Tg(OvPrP-V136)4166$^{+/-}$	Tg(OvPrP-A136)3533$^{+/-}$
SSBP/1	UK Sheep	132 ± 2 (8/8)	412 ± 49 (6/6)
48x35	UK Sheep	365 ± 21 (7/7)	>575 (0/5)
CH1641	UK Sheep	> 450 (0/5)	310 ± 21 (6/6)
76/12/22	US Goat	ND	313 ± 15 (7/7)
76/12/14	US Goat	ND	270 ± 3 (4/4)
Cer-SSBP/1	Tg(CerPrP)1536$^{+/-}$	150 ± 5 (7/7)	231 ± 14 (7/7)
Cer-SSBP/1	Tg(CerPrP-L132)1973$^{+/-}$	335 ± 14 (8/8)	248 ± 14 (4/4)

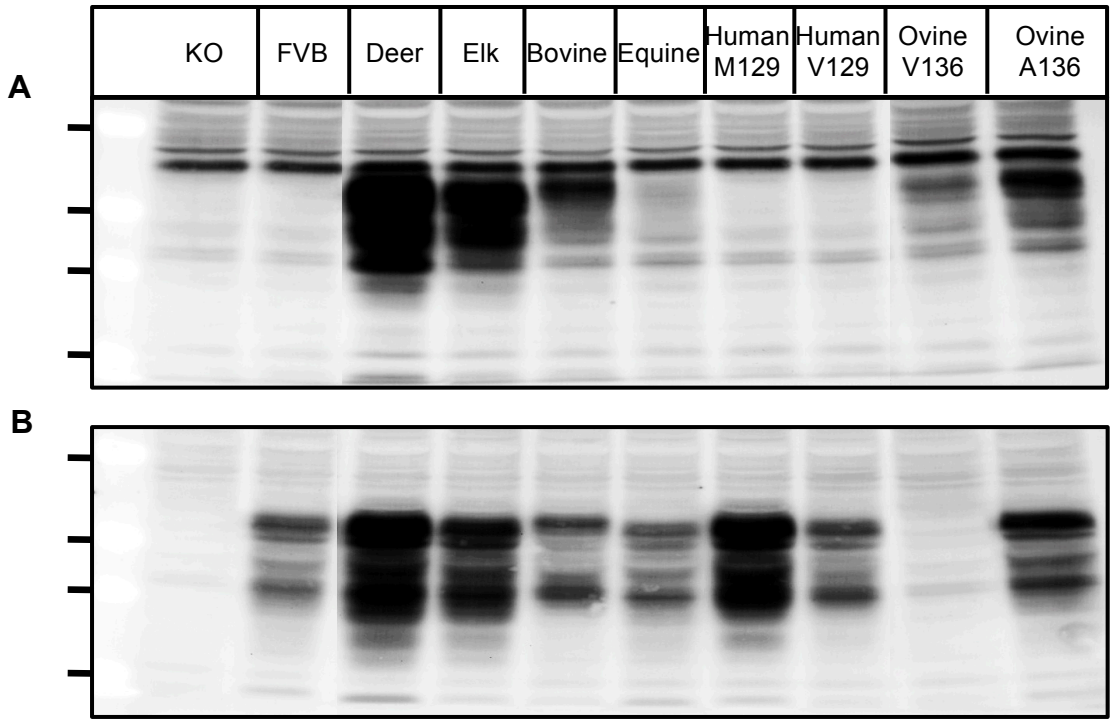

Figure 4.1. Anti-PrP mAb PRC5 is capable of distinguishing the ovine PrP polymorphism alanine from valine at codon 136. Western blot analyses of brain homogenates from Tg mice expressing multiple species of PrP shows mAb PRC5 has reactivities with a wide-range of PrP species but not OvPrP-V136. A. Western blot probed with anti-PrP mAb PRC1 shows the presence of PrP in both OvPrP-A136 and OvPrP-V136 samples. B. The western blot including the same PrP samples determined in the western blot with mAb PRC1 (A) was probed with mAb PRC5 shows that the absence of PrP signals in OvPrP-V136 but the presence of the signals in OvPrP-A136, indicating that PRC5 is an OvPrP-A136 specific antibody. FVB is a wild-type mouse. A Prnp0/0 knockout (KO) is used as a negative control. Molecular markers indicate 50, 40, 30 and 20 kDa from top to bottom.

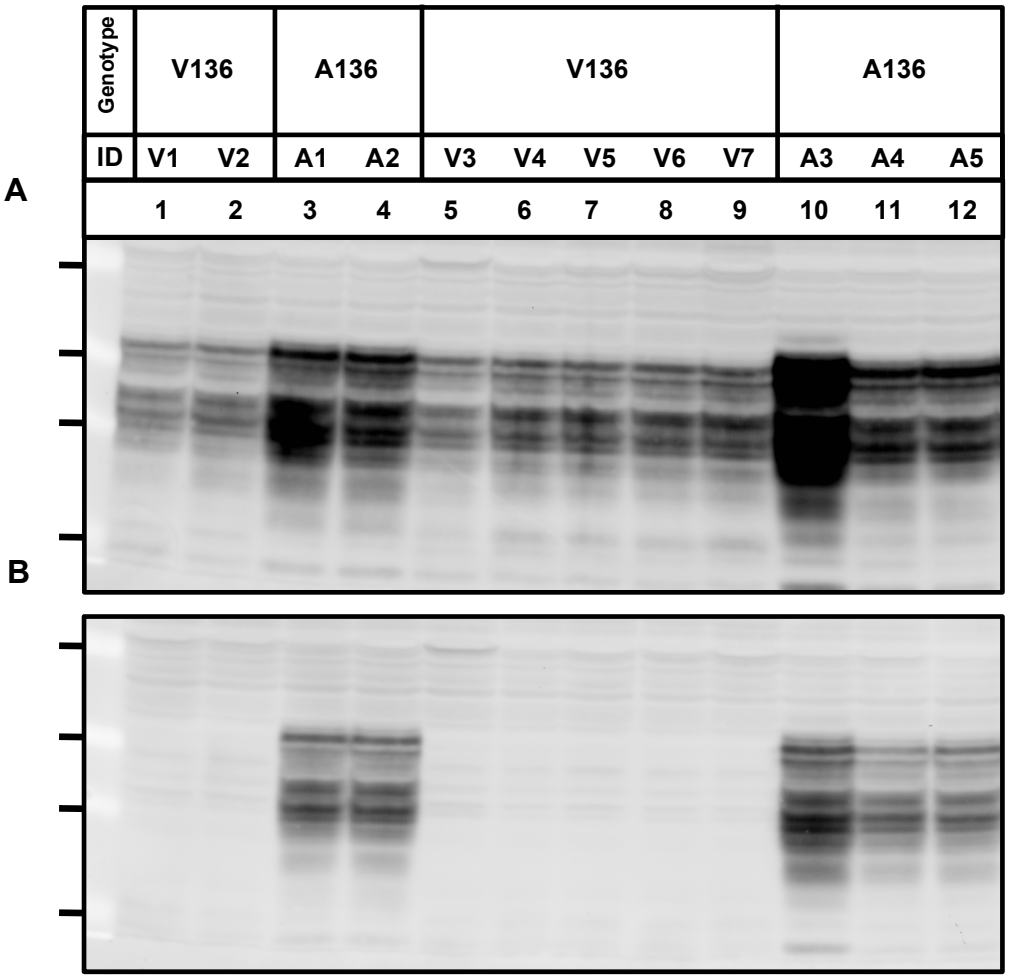

Figure 4.2. Further testing the specificity of mAb PRC5 against OvPrP-A136 polymorphism with a larger number of Tg(OvPrP) samples. Lane 1, 2 and 5 to 9 include brain homogenates from Tg(Ovine PrP-V136)4166$^{+/-}$. Lane 3, 4 and 10 to 12 contain brain homogenates from Tg(Ovine PrP-A136)3533$^{+/-}$. Animal identifications (ID) are indicated above lane numbers. A. Western blot probed with mAb 6H4 shows that all brain samples include PrP. B. Western blot including the same samples presented in A was examined with mAb PRC5. Consistent with the previous data (Figure 4.1.), PRC5 distinguishes OvPrP-A136 from OvPrP-V136. Molecular markers indicate 50, 40, 30 and 20 kDa from top to bottom.

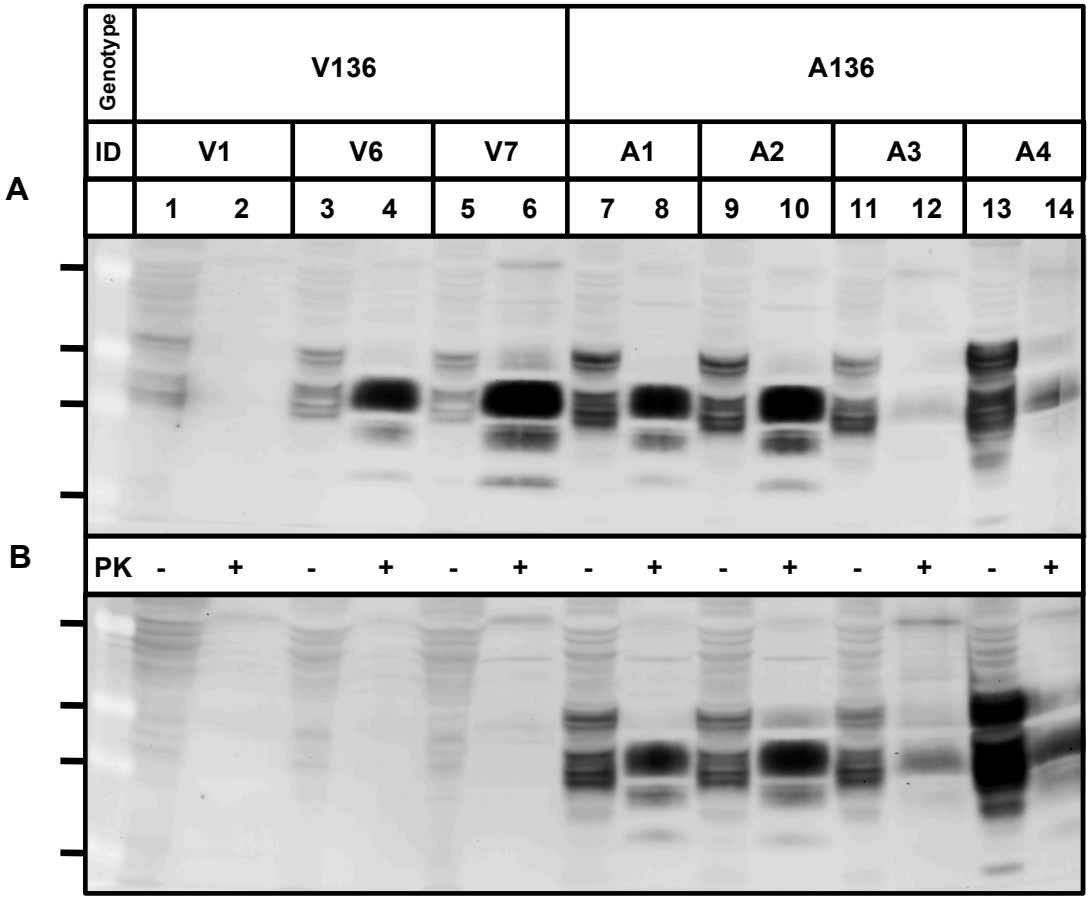

Figure 4.3. Anti-PrP mAb PRC5 can recognize both PrP^{C} and PrP^{Sc} on western blotting. Representative samples from the previous experiment (Figure 4.2.) was either digested or undigested with proteinase K (PK) and tested whether mAb PRC5 is able to recognize PrP^{Sc}. Lane 3 to 6 include brain homogenates from diseased Tg(OvPrP-V136)$4166^{+/-}$ mice. The animal with an ID number V1 was inoculated with sheep scrapie CH1641, which could not produce disease in Tg(OvPrP-V136)$4166^{+/-}$. Thus, the signal of PrP^{Sc} should be absent as shown in lane 2. Lane 7 to 14 contains brain homogenates from diseased Tg(OvPrP-A136)$3533^{+/-}$ mice. PK digested (+) and undigested (-) samples are examined in the both blots. A. The presence of PrP^{C} in all of the samples was confirmed by the western blot with mAb 6H4. B. The same samples examined in the above western blot (A) were also determined on another western blot with mAb PRC5. The western blot with PRC5 was able to recognize both PrP^{C} and PrP^{Sc} of Tg(OvPrP-A136)$3533^{+/-}$ samples. Molecular markers indicate 50, 40, 30 and 20 kDa from top to bottom.

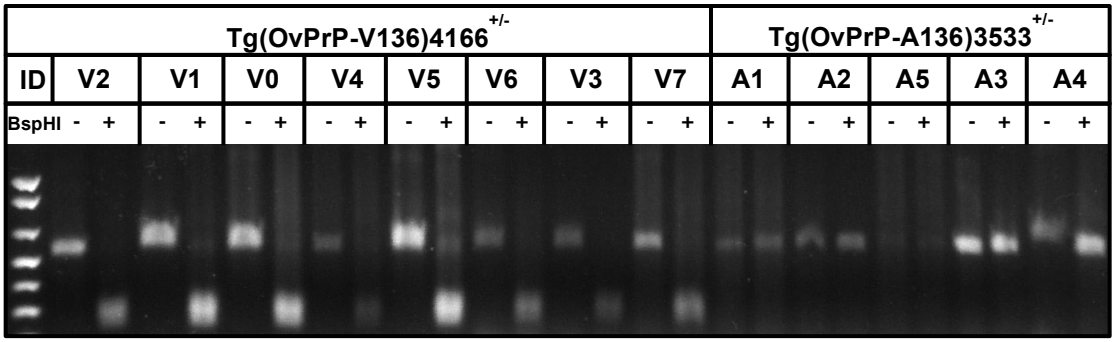

Figure 4.4. Restriction Fragmented Length Polymorphism (RFLP) validated that the genotype was corresponding to the expressed 136 polymorphism of PrP. The genotypes of the previously analyzed mouse samples including both Tg(OvPrP-A136)3533$^{+/-}$ and Tg(OvPrP-V136)4166$^{+/-}$ were validated by RFLP analysis. Restriction endonuclease enzyme *BspHI* recognizes the DNA sequence at V136 in OvPrP and digests into two fragments of 279 and 251 bp, whereas, OvPrP-A136 remains undigested (530 bp). All of eight Tg(OvPrP-V136)4166$^{+/-}$ mouse samples (ID numbers V0-V7) show digested fragments at 279 and 251 bp. Five samples from Tg(OvPrP-A136)3533$^{+/-}$ mice (ID numbers A1-A5) show only undigested bands at 530 bp. The above RFLP data confirmed that the genotype of the samples matched with the expressed 136 polymorphism of PrP (Figure 4.2. and 4.3.). Molecular markers indicate 1000, 850, 650, 500, 400 and 300 bp from top to bottom.

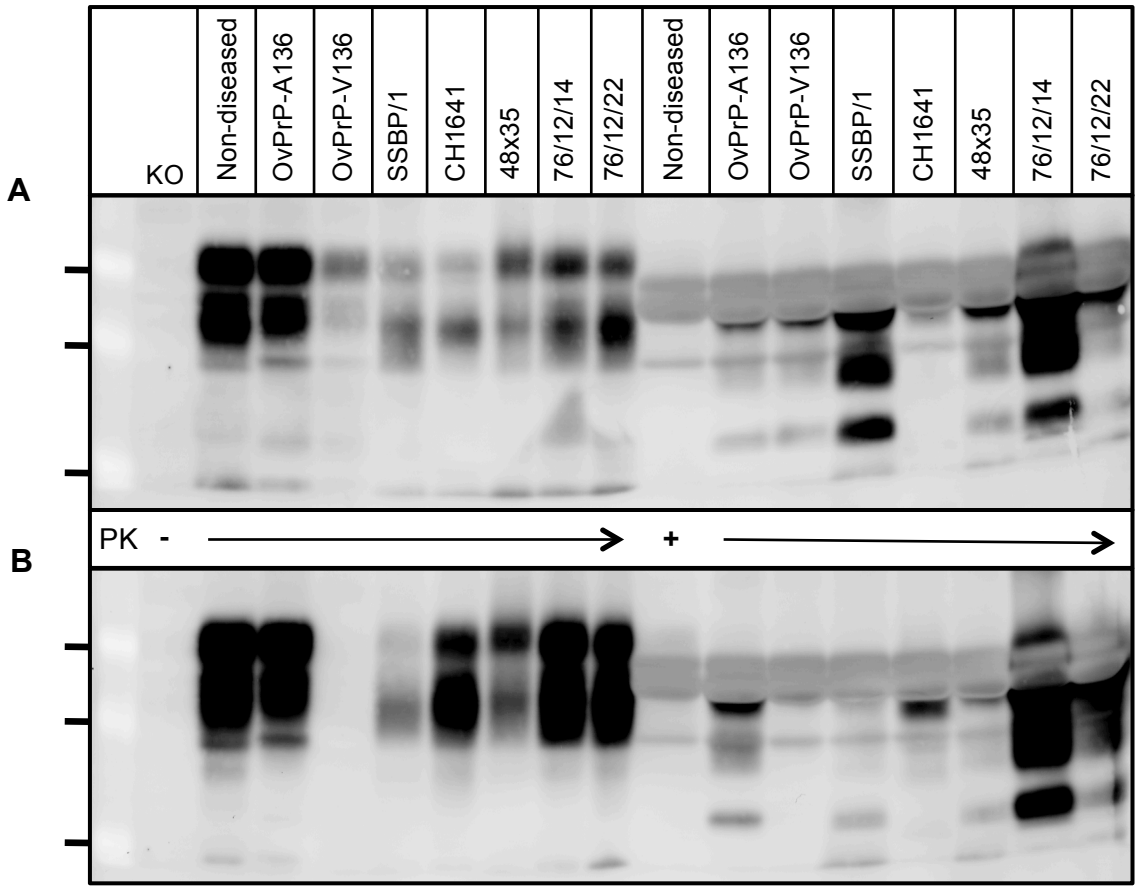

Figure 4.5. Natural sheep and goat scrapie prions were recognized by mAb PRC5. Brain homogenates of sheep brains with SSBP/1, CH1641 or 48x35 sheep scrapie prions and of goat brains with 76/12/14 or 76/12/22 goat prions were examined whether mAb PRC5 was able to recognize those sheep and goat samples on western blots. *Prnp* knockout FVB mouse brains (KO) were used as a negative control. Non-diseased indicates a brain homogenate of healthy sheep, and it was used as a non-diseased control for the absence of PrP^{Sc}. OvPrP-A136 and OvPrP-V136 includes brain homogenates from SSBP/1-inoculated Tg(OvPrP-ARQ)$3533^{+/-}$ and Tg(OvPrP-VRQ)$4166^{+/-}$ mice, respectively. Proteinase K (PK) digested (+) samples were examined along with undigested (-) samples. A. Western blot probed with mAb 6H4 presents that all brain samples contain PrP. B. The same samples presented in the above western blot (A) were also examined on another western blot probed with mAb PRC5. Molecular markers indicate 50, 40, 30 and 20 kDa from top to bottom.

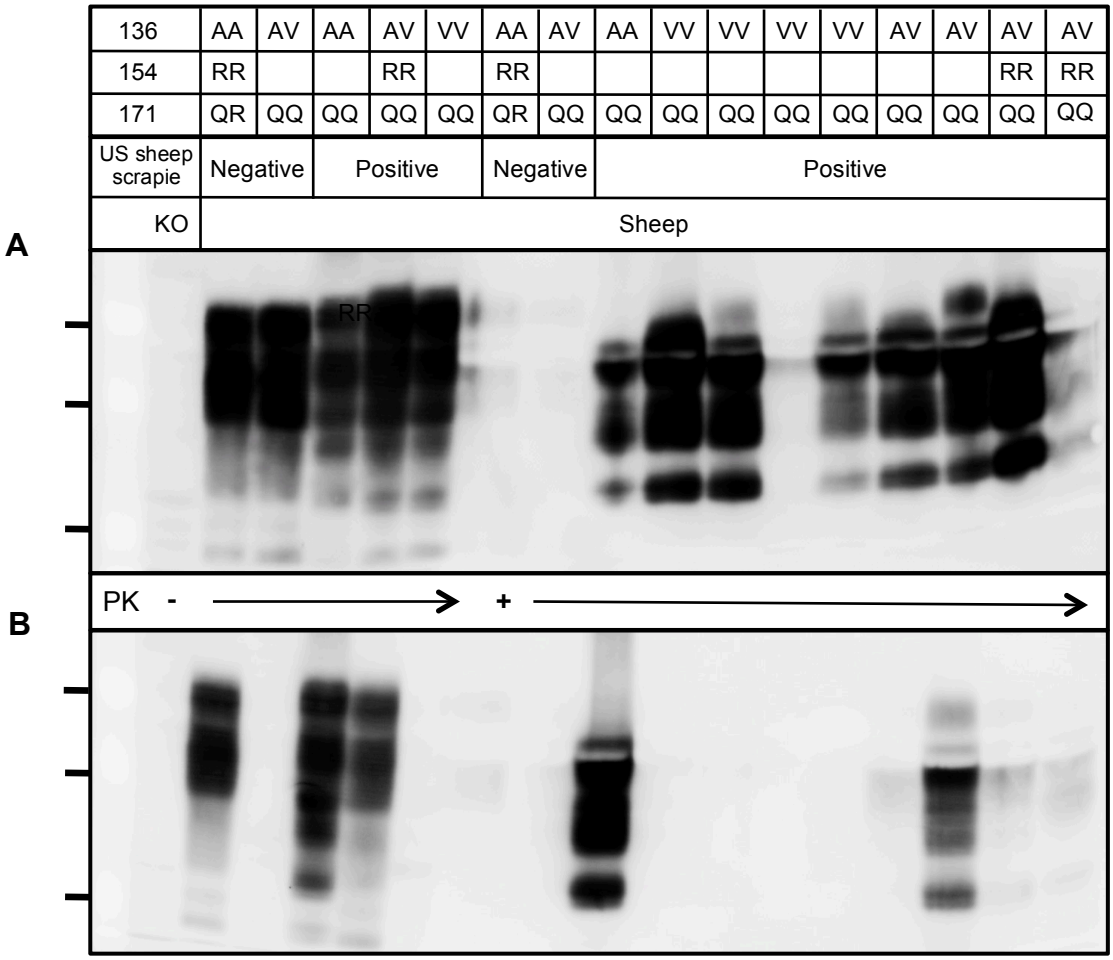

Figure 4.6. Anti-PrP mAb PRC5 was able to recognize an A136 allele in sheep brain samples with or without US sheep scrapie. Different genotypes of sheep samples from a US sheep scrapie affected flock were examined on western blots with mAb PRC5. Proteinase K (PK) digested (+) and undigested samples (-) are determined on the bots. A. The western blot probed with mAb 6H4 presents all brain samples contain PrP. B. The western blot including the same samples examined on the above blot (A) was analyzed with mAb PRC5. The blot with PRC5 recognized only an A136 allele in homozygous or heterozygous samples, corresponding to the genotype indicated above. Three OvPrP polymorphisms at codons 136, 154 and 171 are indicated, and a blank box indicates a genotype at the position was not reported. Molecular markers indicate 40, 30 and 20 kDa from top to bottom.

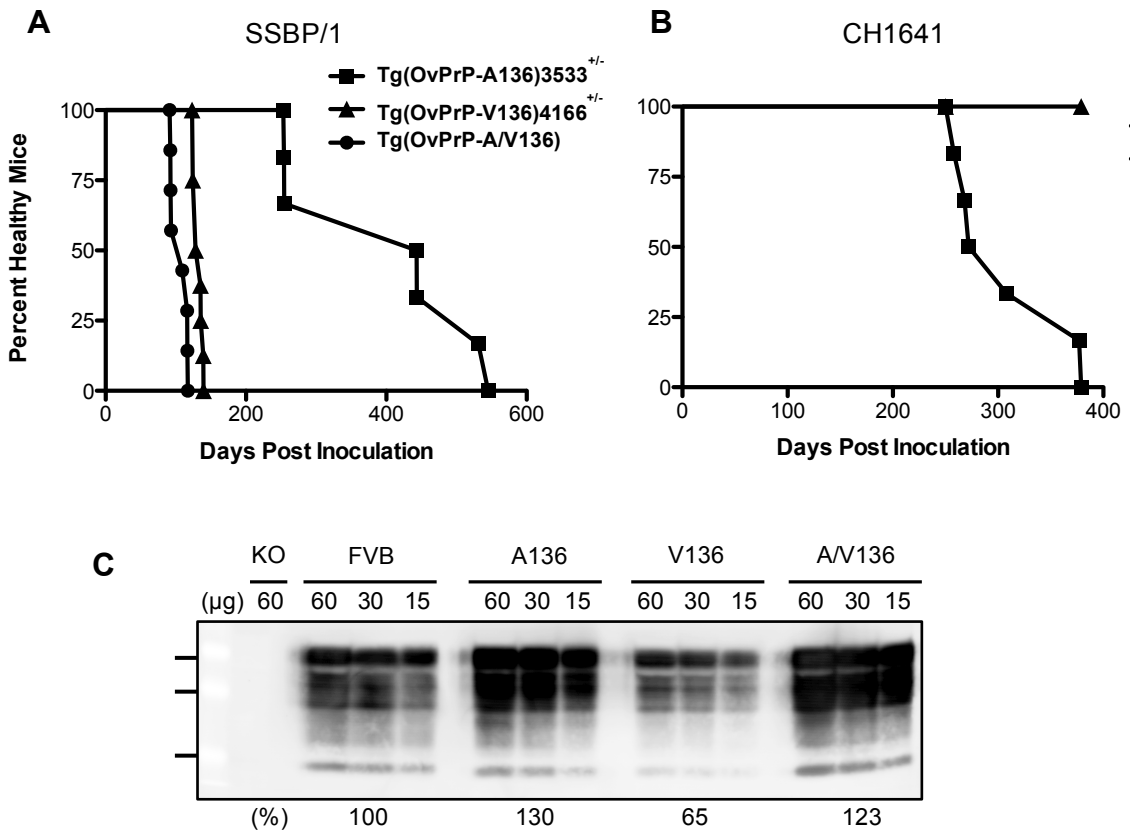
A
SSBP/1
Tg(OvPrP-A136)3533+/-
Tg(OvPrP-V136)4166+/-
Tg(OvPrP-A/V136)
Percent Healthy Mice
100
75
50
25
0
0
200
400
600
Days Post Inoculation
B
CH1641
100
75
50
25
0
0
100
200
300
400
Days Post Inoculation
C
KO
FVB
A136
V136
A/V136
(µg) 60 60 30 15 60 30 15 60 30 15 60 30 15
(%) 100 130 65 123

Figure 4.7. Tg(OvPrP) mice expressing A136, V136 or A and V136 showed different susceptibilities to SSBP/1 and CH1641. A. Survival curves of SSBP/1-inoculated Tg(OvPrP-A136)3533$^{+/-}$, Tg(OvPrP-V136)4166$^{+/-}$ and Tg(OvPrP-A/V136) mice were shown. The mean incubation time for Tg(OvPrP-A136)3533$^{+/-}$ and Tg(OvPrP-V136) 4166$^{+/-}$ are 412 ± 49 days post inoculation (dpi) (attack rate, 6/6) and 132 ± 2 dpi (attack rate, 8/8), respectively. SSBP/1-inoculated Tg(OvPrP-A/V136) mice heterozygous for A and V at codon 136 developed disease with a shorter incubation time at 105 ± 5 dpi (attack rate, 7/7). The Log-rank test analysis showed that each incubation time was statistically different (p<0.0001). B. Survival curves of CH1641-inoculated Tg(OvPrP-A136)3533$^{+/-}$and Tg(OvPrP-V136)4166$^{+/-}$ mice are presented. Unlike SSBP/1, CH1641-inoculated Tg(OvPrP-V136)4166$^{+/-}$ mice (n = 5) failed to develop disease at > 450 dpi. CH1641-inoculated Tg(OvPrP-A136)3533$^{+/-}$ mice developed disease at 310 ± 21 dpi (attack rate, 6/6). The above data shows the susceptibility of SSBP/1 and CH1641 to Tg(OvPrP) mice is associated with the 136 polymorphism. C. The expression levels of PrP in Tg(OvPrP-A136)3533$^{+/-}$, Tg(OvPrP-V136)4166$^{+/-}$ and Tg(OvPrP-A/V136) mouse brains were examined through comparison with wild-type FVB mice on western blotting using mAb 6H4. Tg(OvPrP-A136)3533$^{+/-}$ mice express 30% higher levels of PrP, and Tg(OvPrP-V136)4166$^{+/-}$ mice express 35% lower levels of PrP. The levels of PrP were 23% higher in heterozygous Tg(OvPrP-A/V136) mice compared to FVB mice. The concentrations of total protein were standardized to 60, 30 and 15 µg per lane. A FVB *Prnp*$^{0/0}$ (KO) was used as a negative control. Molecular markers indicate 36, 28 and 19 kDa from top to bottom.

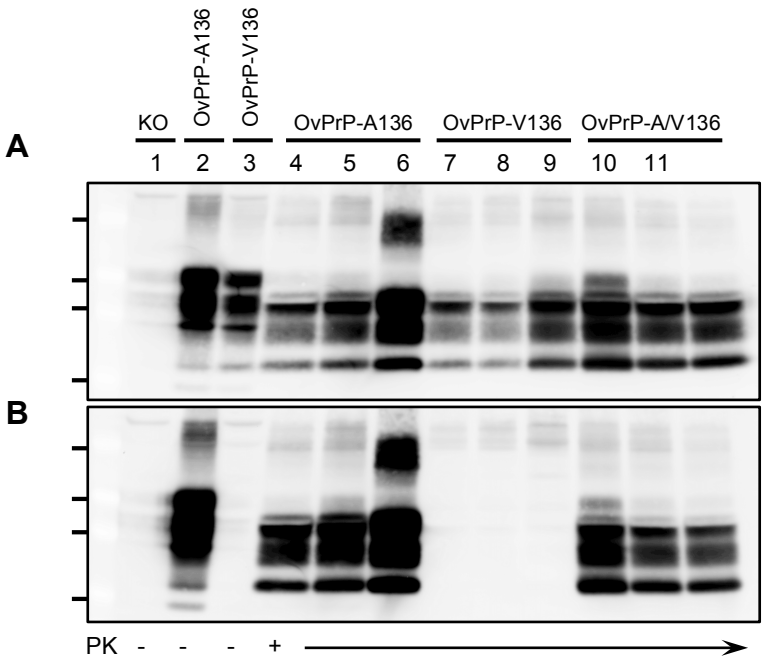

Figure 4.8. Ample signals of PrP^{Sc}-A136 were observed in SSBP/1-inoculated Tg(OvPrP-A/V136) heterozygous mouse brains. Western blotting analyses show that protease-resistant $OvPrP^{Sc}$ was accumulated in the SSBP/1-inoculated brains from Tg(OvPrP-A136)$3533^{+/-}$, Tg(OvPrP-V136)$4166^{+/-}$ and Tg(OvPrP-A/V136) mice. A. Both OvPrP-A136 and OvPrP-V136 alleles were shown on the blot with mAb 6H4. Three samples from each group are shown and all included PrP^{Sc} in the brains. B. OvPrP-A136 but not OvPrP-V136 alleles was shown on the blot with mAb PRC5. Interestingly, $OvPrP^{Sc}$-A136 was accumulated in SSBP/1-inoculated Tg(OvPrP-A/V136) mouse brains (lane 10-12), indicating that OvPrP-A136 was already converted to PrP^{Sc} at 105 ± 5 dpi. It is important to note that SSBP/1-inoculated Tg(OvPrP-A136)$3533^{+/-}$ mice required much longer incubation time to develop disease at 412 ± 49 dpi (Figure 4.7.A.). Proteinase K (PK) digested (+) and undigested (-) samples were analyzed. Lane1, PK(-) *Prnp* knockout FVB (KO); lane 2, PK(-) Tg(OvPrP-A136)$3533^{+/-}$; lane 3, PK(-) Tg(OvPrP-V136)$4166^{+/-}$; lane 4-6, PK(+) Tg(OvPrP-A136)$3533^{+/-}$; lane 7-9, PK(+) Tg(OvPrP-V136)$4166^{+/-}$; lane 10-12, PK(+) Tg(OvPrP-AV136). Molecular marker indicates 53, 36, 28 and 19 kDa from top to bottom.

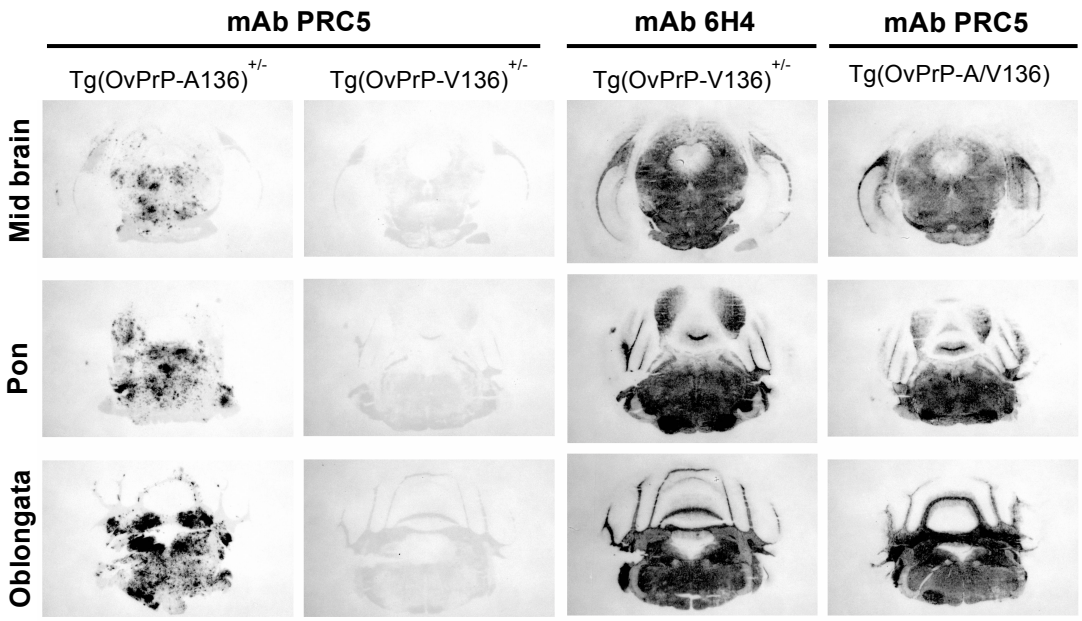

Figure 4.9. OvPrP^{Sc}-A136 acquires properties of OvPrP^{Sc}-V136 in SSBP/1 diseased Tg(OvPrP-A/V136) mice. Histoblots were treated with proteinase K (PK) and determined with either mAb 6H4 or PRC5. Punctate deposition of OvPrP^{Sc}-A136 was observed in SSBP/1-inoculated Tg(OvPrP-A136)3533$^{+/-}$ mouse brains at the levels of the mid-brain, pons and oblongata (left images). On the other hand, diffused deposition patterns were observed in SSBP/1-inoculated Tg(OvPrP-V136)4166$^{+/-}$ mouse brains (second from right images). As shown in the previous western blots (Figure 4.8.), the conversion of OvPrP^{Sc}-A136 allele in SSBP/1-inoculated Tg(OvPrP-A/V136) heterozygous mouse brains was observed in histoblots as well. The histoblot data revealed that deposition patterns of OvPrP^{Sc}-A136 were diffused and identical to OvPrP^{Sc}-V136 under the state of co-expression of A136 and V136 (right images), indicating the recruitment of PrP^{C}-A136 by PrP^{Sc}-V136.

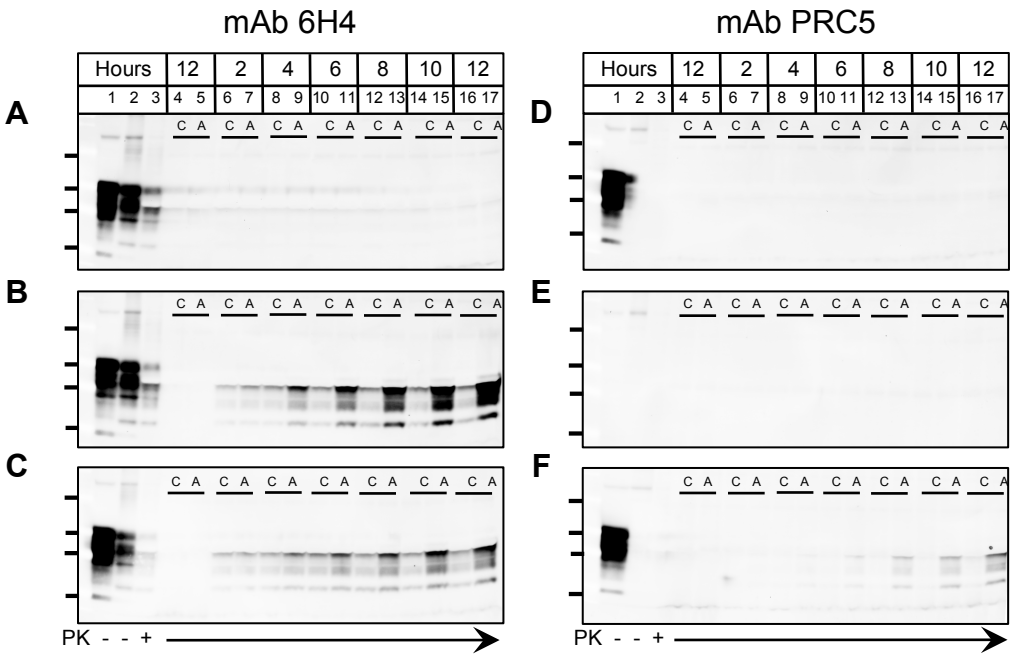

Figure 4.10. OvPrP-A136 allele was converted to PrP^{Sc} only in the presence of OvPrP-V136 allele by PMCA with SSBP/1-V136 seed. SSBP/1 diseased Tg(OvPrP-V136)4166$^{+/-}$ mouse brains were used as SSBP/1-V136 seed. Brain homogenates from healthy Tg(OvPrP-A136)3533$^{+/-}$ (A, D) and Tg(OvPrP-V136)4166$^{+/-}$ (B, E) mice were mixed with the SSBP/1-V136 seed. A mixture of brain homogenates from Tg(OvPrP-A136)3533$^{+/-}$ and Tg(OvPrP-V136)4166$^{+/-}$ mice at the ratio corresponding to equal PrP expression levels was prepared and mixed with the SSBP/1-V136 seed (C, F). Amplified (A) and 37°C incubated control (C) samples were collected every 2 hours in the total of 12 hours of PMCA (48 cycles). The samples were digested with PK and analyzed for PrP^{Sc} conversion on western blots along with controls including undigested (-) substrates (lane 1), digested (+, lane 2) and undigested (lane 3) seed. In addition to those controls, PMCA reactions without seed were also prepared, and those samples were digested with PK (lanes 4, 5). Western blots A, B and C were probed with mAb 6H4 showing a total PrP^{Sc}, and blots D, E and F were probed with mAb PRC5 presenting only $OvPrP^{Sc}$-A136. Unsuccessful amplification of $OvPrP^{Sc}$-A136 was observed in OvPrP-A136 substrate alone (A, D). On the other hand, OvPrP-V136 allele was efficiently converted to PrP^{Sc} (B). The mixture of OvPrP-A136 and OvPrP-V136 showed amplification of PrP^{Sc} (C, F). Those data showed that amplification of $OvPrP^{Sc}$-A136 was observed only in the presence of OvPrP-V136 alleles with SSBP/1-V136 (F), indicating that the recruitment of $OvPrP^{C}$-A136 by $OvPrP^{Sc}$-V136 promotes the $OvPrP^{Sc}$-A136 conversion. Molecular marker indicates 53, 36, 28 and 19 kDa from top to bottom.

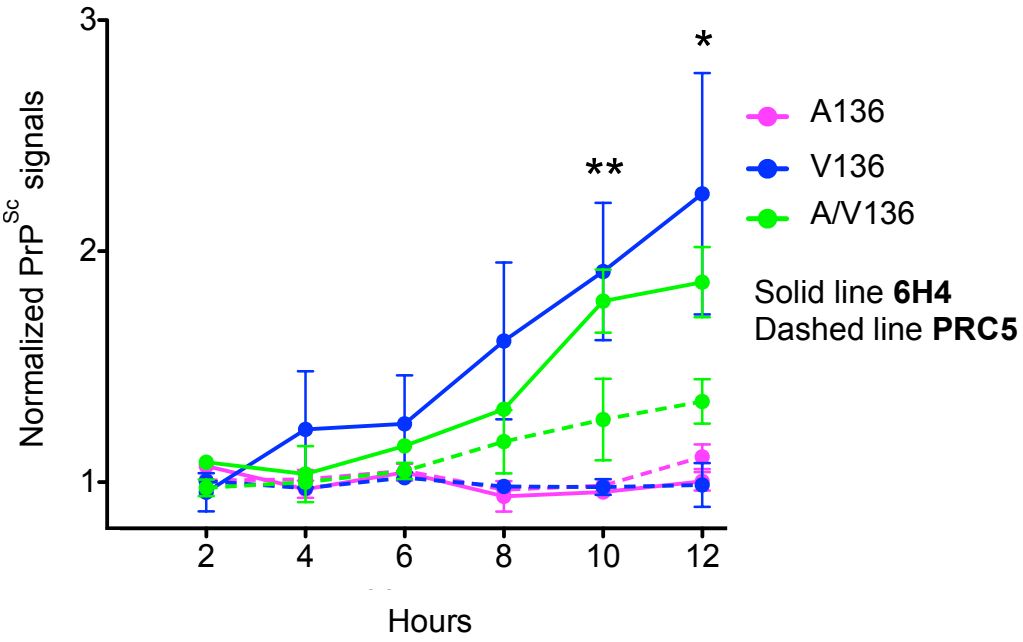

Figure 4.11. Conversion of OvPrP^{Sc}-V136 appears to take place followed by conversion of OvPrP^{Sc}-A136 in PMCA with SSBP/1-V136 seed. Three independent experiments of PMCA with SSBP/1-V136 were performed, and three experimental data were plotted in the graph. Amplified PrP^{Sc} signals were normalized to signals of 37°C incubated controls at the same time points. Normalized PrP^{Sc} signals on western blots with mAb 6H4 presenting a total PrP^{Sc} were shown in solid lines. Normalized PrP^{Sc} signals on western blots with PRC5 presenting only OvPrP-A136 are plotted in dashed lines. The gradual increase of amplified OvPrP^{Sc}-V136 is evidenced in PMCA reactions with OvPrP-V136 substrate alone (blue solid line). Unsuccessful amplification of OvPrP^{Sc}-A136 is observed in reactions with OvPrP-A136 substrate alone (pink solid and dashed lines). However, amplification of OvPrP^{Sc}-A136 was observed only when OvPrP^{Sc}-V136 was co-existed in PMCA reactions, indicating that the recruitment of OvPrP^{C}-A136 by OvPrP^{Sc}-V136 promotes the OvPrP^{Sc}-A136 conversion. Error bars indicate standard errors of the mean. Statistical analyses were performed at fixed time points (2, 4, 6, 8, 10 or 12 hours separately) using a one-way ANOVA, and asterisks at 10 hours (**p<0.0016) and 12 hours (*p<0.01) indicate significant difference. A Newman-Keuls multiple comparison post-hoc test showed the following groups are statistically significant at 10 hours: A/V136-PRC5 vs. A/V136-6H4. Moreover, the Newman-Keuls reported that the following groups are also statistically significant at 12 hours: A/V136-PRC5 vs. V136-6H4.

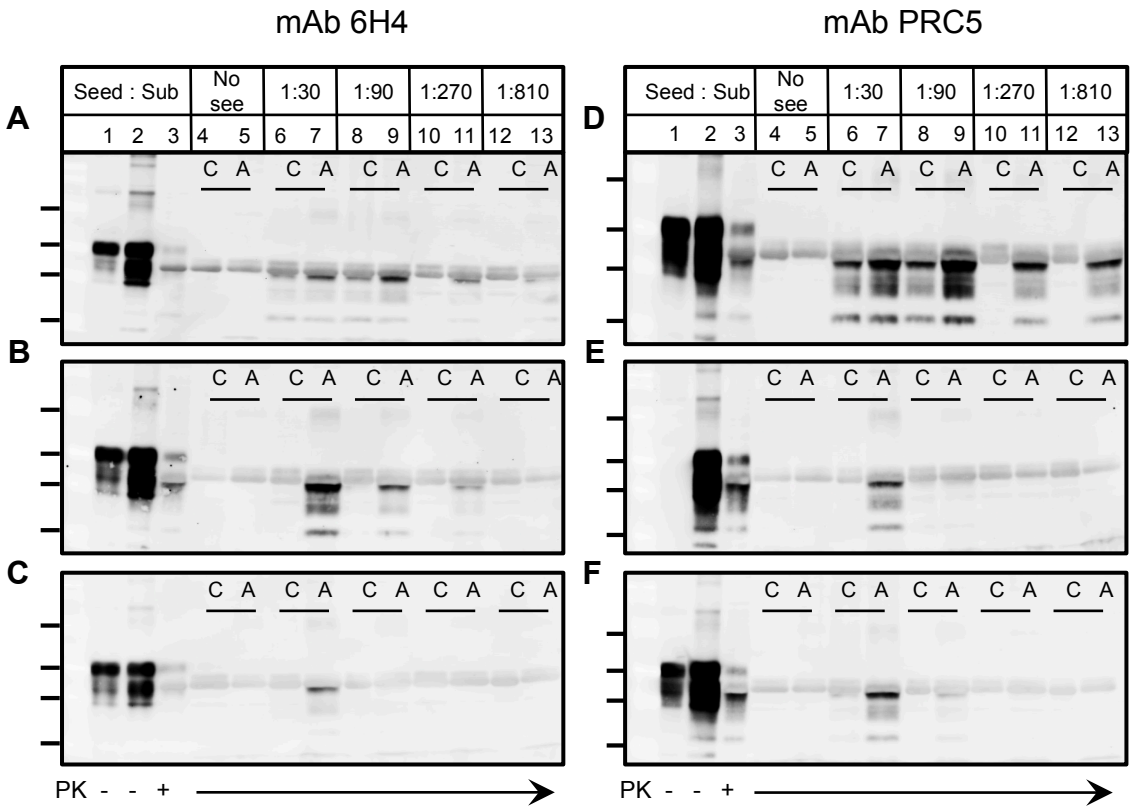

Figure 4.12. PMCA of SSBP/1-A136 produced successful conversion of PrP^{Sc} only with $OvPrP^{C}$-A136 substrate. PMCA of SSBP/1-A136 was performed in serial dilutions of seed to substrate to see whether PrP^{Sc} could be amplified after 98 cycles (48 hours). The amplification of SSBP/1-A136 seed to $OvPrP^{C}$-A136 substrate at 1:30, 1:90, 1:270 and 1:810 dilutions was able to produce PrP^{Sc} (A. and D). However, inefficient amplification of PrP^{Sc}-V136 was observed at 1:90 and 1:270 dilutions (B). PrP^{Sc} signals at 1:30 dilution (B and E) were most likely coming from the seed SSBP/1-A136. Since $OvPrP^{Sc}$-V136 would not be recognized by mAb PRC5, the amplified signal on the western blot probed with mAb PRC5 indicated that PrP^{Sc} signals at 1:30 dilution were from the seed. Under the co-presence of OvPrP-A136 and OvPrP-V136 alleles, the PrP^{Sc} conversion was not as efficient as the amplification with $OvPrP^{C}$-A136 alone. Some amplification of PrP^{Sc} was observed at 1:30 and 1:90 dilutions, but no amplification of PrP^{Sc} was detected at 1:270 and 1:810 dilutions (C and F). These data indicated that PMCA of SSBP/1-A136 was able to amplify PrP^{Sc} with $OvPrP^{C}$-A136 compared to $OvPrP^{C}$-V136 or the mixture of both. Lanes 1: undigested substrate, 2: undigested seed, 3: PK-digested seed, 4: PMCA reaction without seed (No seed) incubated at 37°C without sonication, 5: No seed incubated at 37°C with sonication, 6-13: PMCA samples at multiple dilutions. PMCA samples (lanes 4 to 13) were digested with PK. Molecular marker indicates 53, 36, 28 and 19 KDa from top to bottom.

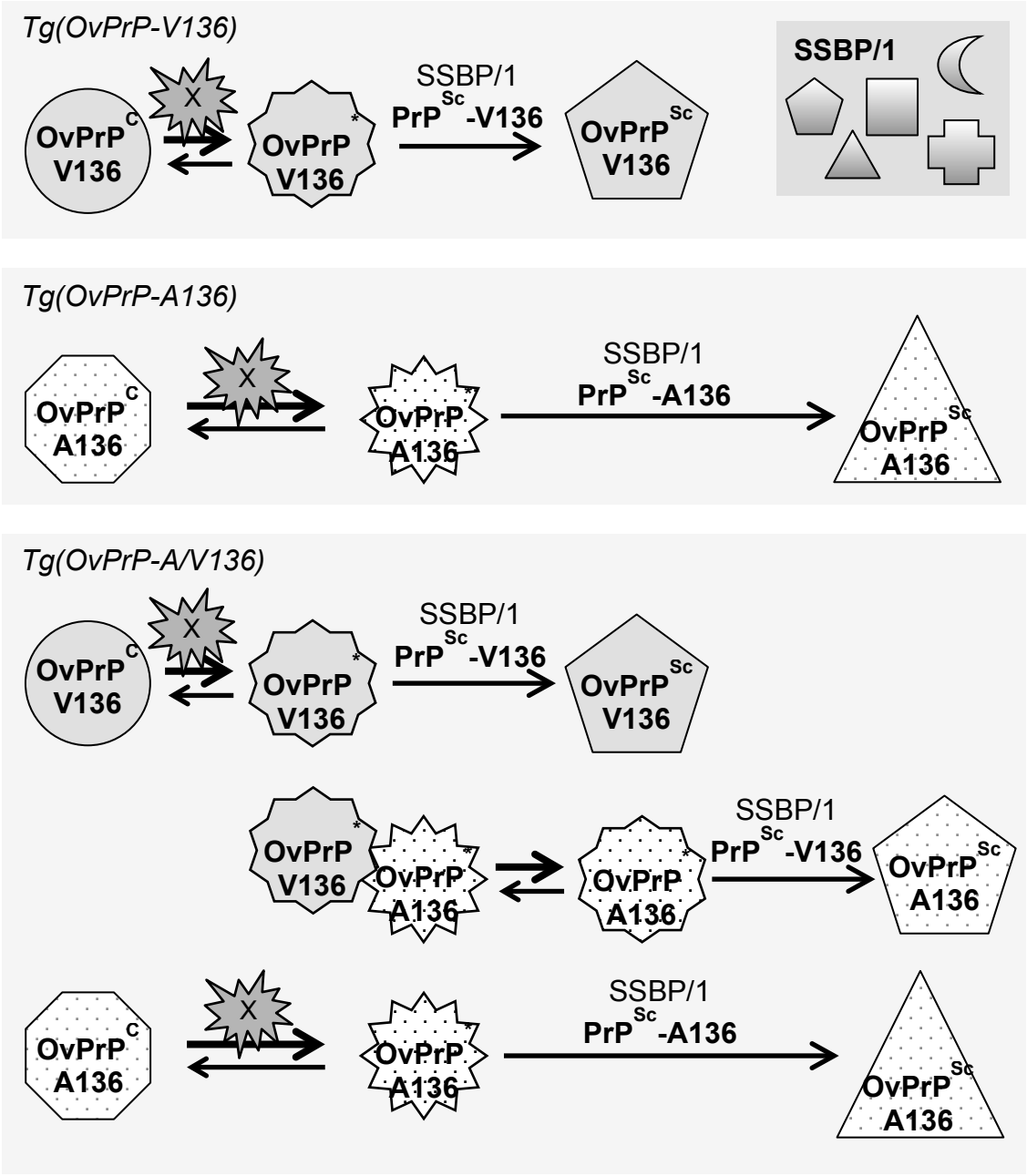
Tg(OvPrP-V136)
OvPrP C V136
X
OvPrP * V136
SSBP/1
PrP Sc -V136
OvPrP Sc V136
SSBP/1
Tg(OvPrP-A136)
OvPrP C A136
X
OvPrP * A136
SSBP/1
PrP Sc -A136
OvPrP Sc A136
Tg(OvPrP-A/V136)
OvPrP C V136
X
OvPrP * V136
SSBP/1
PrP Sc -V136
OvPrP Sc V136
OvPrP * V136
OvPrP * A136
OvPrP * A136
SSBP/1
PrP Sc -V136
OvPrP Sc A136
OvPrP C A136
X
OvPrP * A136
SSBP/1
PrP Sc -A136
OvPrP Sc A136

Figure 4.13. PrP^{Sc} conversion models of SSBP/1 in Tg(OvPrP) expressing both A and V 136 polymorphism: a dominant $OvPrP^{Sc}$-V136 conformation leading to forced templating of $OvPrP^{C}$-A136. The above-proposed models are based on the heterodimer template-associated model. In the models, PrP^{C} is in equilibrium with an intermediate form of PrP*, and the formation of PrP* is thought to be facilitated by a hypothetical protein X. The conversion of PrP* to PrP^{Sc} is a catalytic step, and the operative catalyst might be protein X or other molecules. It is important to note that natural sheep scrapie isolate SSBP/1 consists of mainly a VRQ genotype, however, it is a pool of multiple combinations of genotypes, suggesting that different conformations of PrP^{Sc} are available in the isolate (a box on the top right corner). The first model indicates that the conversion of $OvPrP^{Sc}$-V136 is efficient with the genotype matched SSBP/1-V136, therefore, the survival time of SSBP/1-inoculated Tg(OvPrP-V136) mice is relatively shorter than Tg(OvPrP-A136) mice. The second model describes that the propagation of SSBP/1-A136 with $OvPrP^{C}$-A136 is not as efficient a process as the propagation of SSBP/1-V136 with $OvPrP^{C}$-V136 even though the genotypes between PrP^{Sc} and PrP^{C} are identical. Therefore, the survival time of SSBP/1-inoculated Tg(OvPrP-A136) mice is much longer due to the slow conversion rate of $OvPrP^{Sc}$-A136. In those proposed models, the conformations of PrP^{Sc} are different between $OvPrP^{Sc}$-V136 (pentagon) and $OvPrP^{Sc}$-A136 (triangle), inasmuch as the histoblotting data showed diffused vs. punctate deposition patterns of PrP^{Sc} in SSBP/1-inoculated Tg(OvPrP-V136)$4166^{+/-}$ and Tg(OvPrP-A136)$3533^{+/-}$ mice, respectively (Figure 4.9.). The last model explains when $OvPrP^{C}$-A136 and $OvPrP^{C}$-V136 are co-expressed, the conversion of $OvPrP^{Sc}$-V136 occurs followed by the conversion of $OvPrP^{Sc}$-A136. The intermediate forms of OvPrP*-V136 and OvPrP*-A136 interact together to transform the conformation of OvPrP*-A136 into the conformation of OvPrP*-V136, and the adaptation of OvPrP*-V136 conformation in PrP*-A136 allows SSBP/1-V136 to become a template for the conversion to PrP^{Sc}. Therefore, the conformation of $OvPrP^{Sc}$-A136 is identical to $OvPrP^{Sc}$-V136. In the last proposed model, the conversion of $OvPrP^{Sc}$-A136 is promoted by the presence of other allele V136, and the conversion of both alleles can promote quicker development of disease in SSBP/1-inoculated Tg(OvPrP-A/V136) mice as compared to Tg(OvPrP-V136) mice.

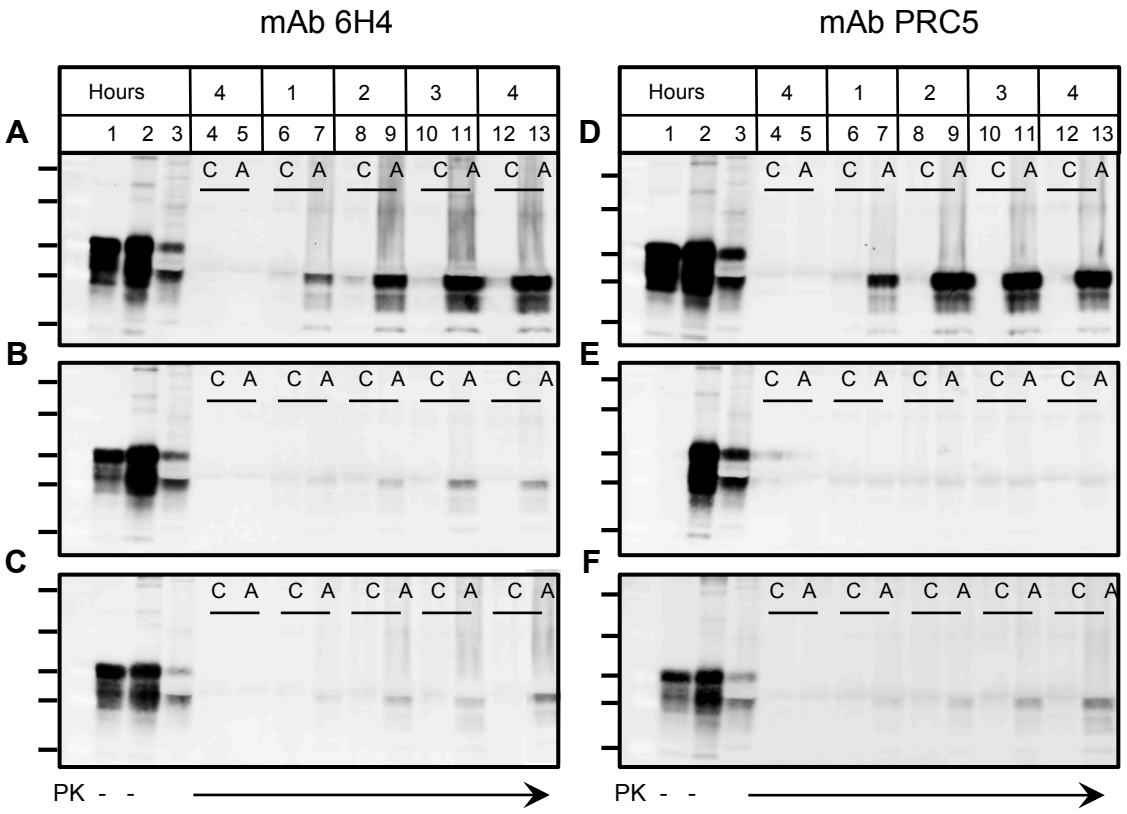

Figure 4.14. Presence of OvPrP^{C}-V136 inhibits the amplification of OvPrP^{Sc}-A136 in PMCA with CH1641-A136 seed. PMCA of CH1641-A136 seed with OvPrP-A136, OvPrP-V136 and the mixture of both was performed. Brain homogenates from CH1641-inoculated Tg(OvPrP-A136)3533$^{+/-}$ mice was used as CH1641-A136 seed and mixed with brain homogenates from healthy Tg(OvPrP-A136)3533$^{+/-}$ (A, D) and Tg(OvPrP-V136)4166$^{+/-}$ (B, E) mice. A mixture of brain homogenates from Tg(OvPrP-A136)3533$^{+/-}$ and Tg(OvPrP-V136)4166$^{+/-}$ mice at the ratio corresponding to equal PrP expression levels was prepared and amplified with CH1641-A136 (C, F). The amplified samples were collected every 12 hours in a total of 48 hours amplification to study the rate of PrP^{Sc} conversion. The genotyped matched reaction of CH1641-A136 seed and OvPrP^{C}-A136 substrate produced OvPrP^{Sc}-A136 efficiently (A and D). However, inefficient amplification of OvPrP^{Sc}-V136 was observed with PMCA of CH1641-A136 (B). When two substrates were mixed, reduced amplification of OvPrP^{Sc} in PMCA of CH1641-A136 was observed (C and F). The western blot with mAb PRC5 showing only OvPrP^{Sc}-A136 allele displayed that the efficiency of OvPrP^{Sc}-A136 conversion was reduced remarkably (F). Samples incubated at 37°C without sonication was used as control (C), and letter A indicates PMCA amplified samples at 37°C with sonication. Lane 1, PK undigested (-) substrate OvPrP-A136 (A, D), OvPrP-V136 (B, E) and mixture of OvPrP-A136 and OvPrP-V136 at 1:2 dilution (C, F); lane 2 and 3, PK (-) and digested (+) CH1641-A136 seed, respectively; lane 4 and 5, digested PMCA reaction sample without seed (No seed); lane 6-13, PK(-) and PK(+) PMCA samples. Molecular marker indicates 53, 36, 28 and 19 KDa from top to bottom.

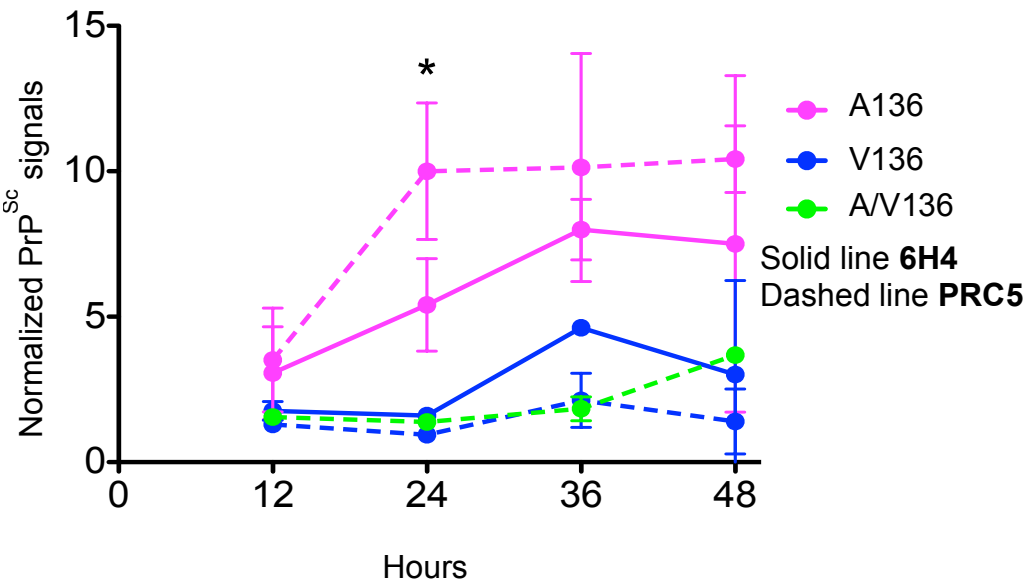

Figure 4.15. The OvPrP^{C}-V136 allele suppressed the conversion of PrP^{Sc}-A136 in the presence of the both alleles in PMCA with CH1641 seed. PMCA of CH1641-A136 seed with OvPrP-A136, OvPrP-V136 and the mixture of both was performed independently, twice, to examine the compatibility of the seed and substrates for the conversion of PrP^{Sc}. Two independent experiments were plotted in the graph. The signals of amplified PrP^{Sc} was normalized to the signals of 37°C incubated control in the same time points. The X-axis indicated a duration of PMCA cycles in a total of 48 hours. Samples were collected every 12 hours. The Y-axis indicates the value of normalized PrP^{Sc} signals. Solid lines are normalized PrP^{Sc} signals from western blots with mAb 6H4 showing a total signal of PrP^{Sc}. Dashed lines are normalized PrP^{Sc} signals from western blots with mAb PRC5 showing only OvPrP^{Sc}-A136. The efficient amplification of OvPrP^{Sc}-A136 (pink solid and dashed lines) and inefficient amplification of OvPrP^{Sc}-V136 (blue solid line) were observed. The green dashed line shows inefficient amplification of PrP^{Sc}-A136 in the presence of OvPrP-V136. Statistical analyses were performed at fixed time points (12, 24, 36 or 48 hours separately) using a one-way ANOVA and showed significant difference indicating with an asterisk at 24 hours (*p<0.013). A Newman-Keuls multiple comparison post-hoc test showed the following groups are statistically significant at 24 hours: A/V136-PRC5 vs. A136-PRC5 and A/V136-6H4 vs. A136-PRC5.

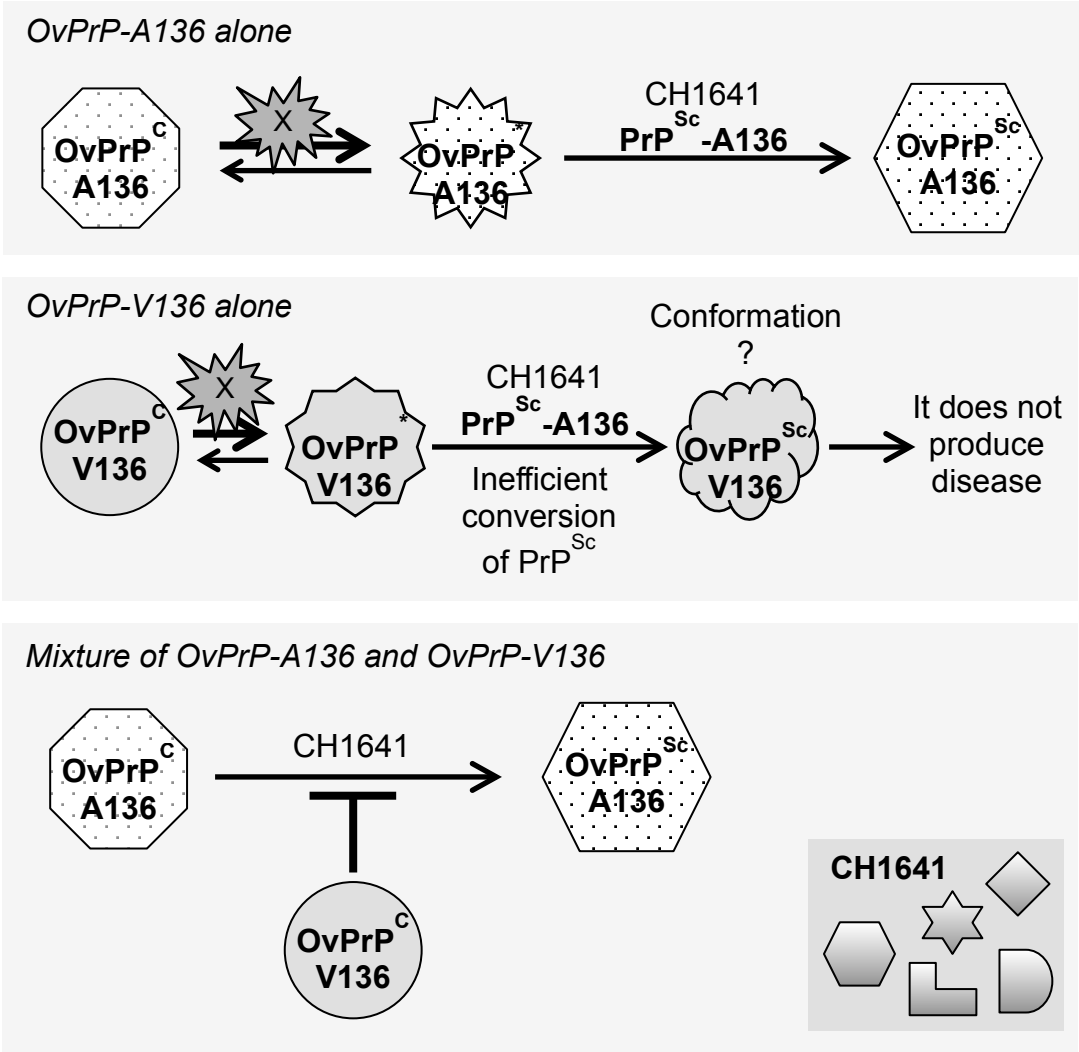
OvPrP-A136 alone
OvPrP C A136
X
OvPrP * A136
CH1641
PrP Sc -A136
OvPrP Sc A136
OvPrP-V136 alone
OvPrP C V136
X
OvPrP * V136
CH1641
PrP Sc -A136
Inefficient conversion of PrP Sc
Conformation ?
OvPrP Sc V136
It does not produce disease
Mixture of OvPrP-A136 and OvPrP-V136
OvPrP C A136
CH1641
OvPrP Sc A136
OvPrP C V136
CH1641

Figure 4.16. PrP^{Sc} conversion models of CH1641 in Tg(OvPrP) expressing A136V polymorphism: an inhibitory effect of $OvPrP^{C}$-V136 on the propagation of $OvPrP^{Sc}$-A136. The above-proposed models are based on the heterodimer template-associated model. In the models, PrP^{C} is in equilibrium with an intermediate form of PrP*, and the formation of PrP* is thought to be facilitated by a hypothetical protein X. The conversion of PrP* to PrP^{Sc} is a catalytic step, and the operative catalyst might be protein X or other molecules. It is important to note that natural sheep scrapie isolate CH1641 consists of mainly a A136 genotype, however, it is a pool of multiple combinations of genotypes, suggesting that different conformations of PrP^{Sc} are available in the isolate (a box on the right bottom corner). The first model describes that CH1641-A136 is able to propagate $OvPrP^{Sc}$-A136 from OvPrP*-A136. The second model shows that the conversion of $OvPrP^{Sc}$-V136 can happen but the process is inefficient. $OvPrP^{Sc}$-V136 might be cleared by a cellular mechanism as soon as PrP^{Sc} is produced. In addition, the rate of PrP^{Sc} conversion is slow enough that the cellular mechanism is able to remove PrP^{Sc} before produce more PrP^{Sc} or aggregates. Thus, CH1641-inoculated Tg(OvPrP-V136) mice did not develop disease, and the accumulation of PK-resistant $OvPrP^{Sc}$ was not observed in their brains. The conformation of $OvPrP^{Sc}$ is unknown. The last model explains the propagation of CH1641-A136 under co-expressions of $OvPrP^{C}$-A136 and $OvPrP^{C}$-V136. The presence of $OvPrP^{C}$-V136 prevents the conversion of $OvPrP^{Sc}$-A136; however, what isoforms of OvPrP-V136 among PrP^{C}, PrP* or PrP^{Sc} play a role in an inhibitory effect on the conversion of PrP^{Sc} is not clear.

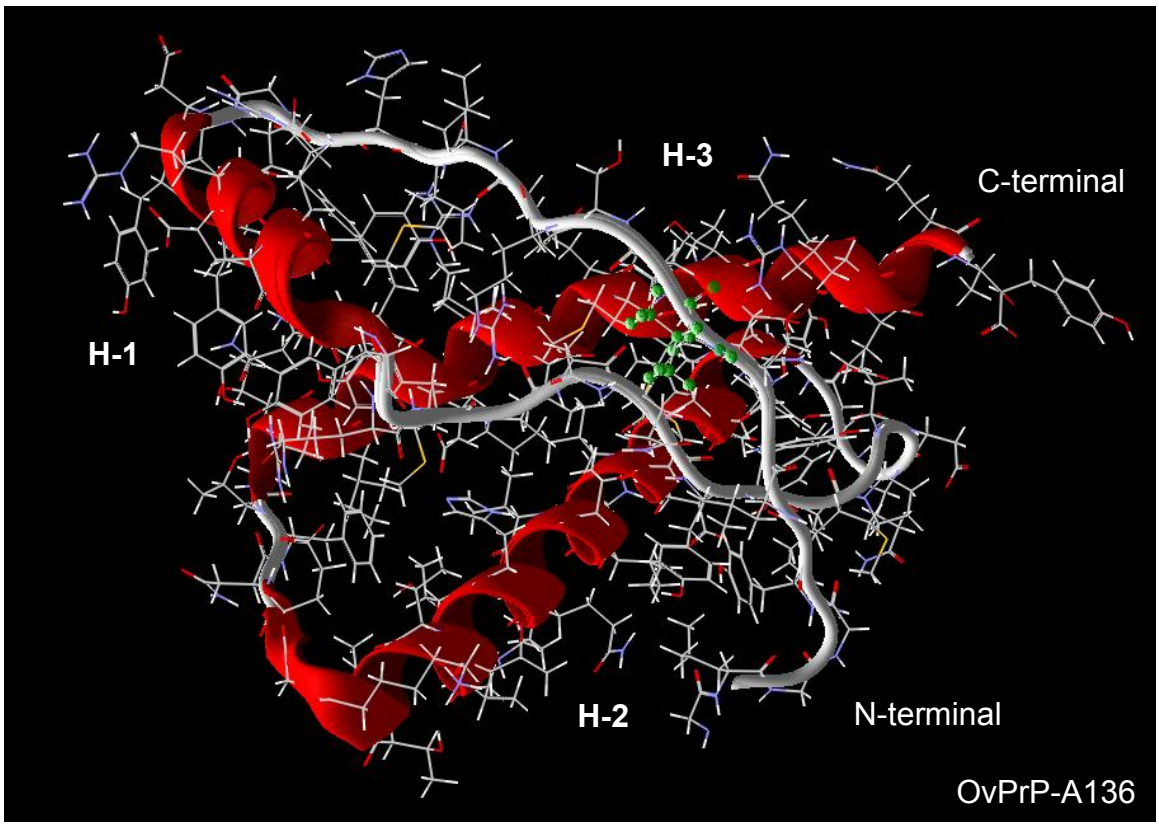
H-3
C-terminal
H-1
H-2
N-terminal
OvPrP-A136

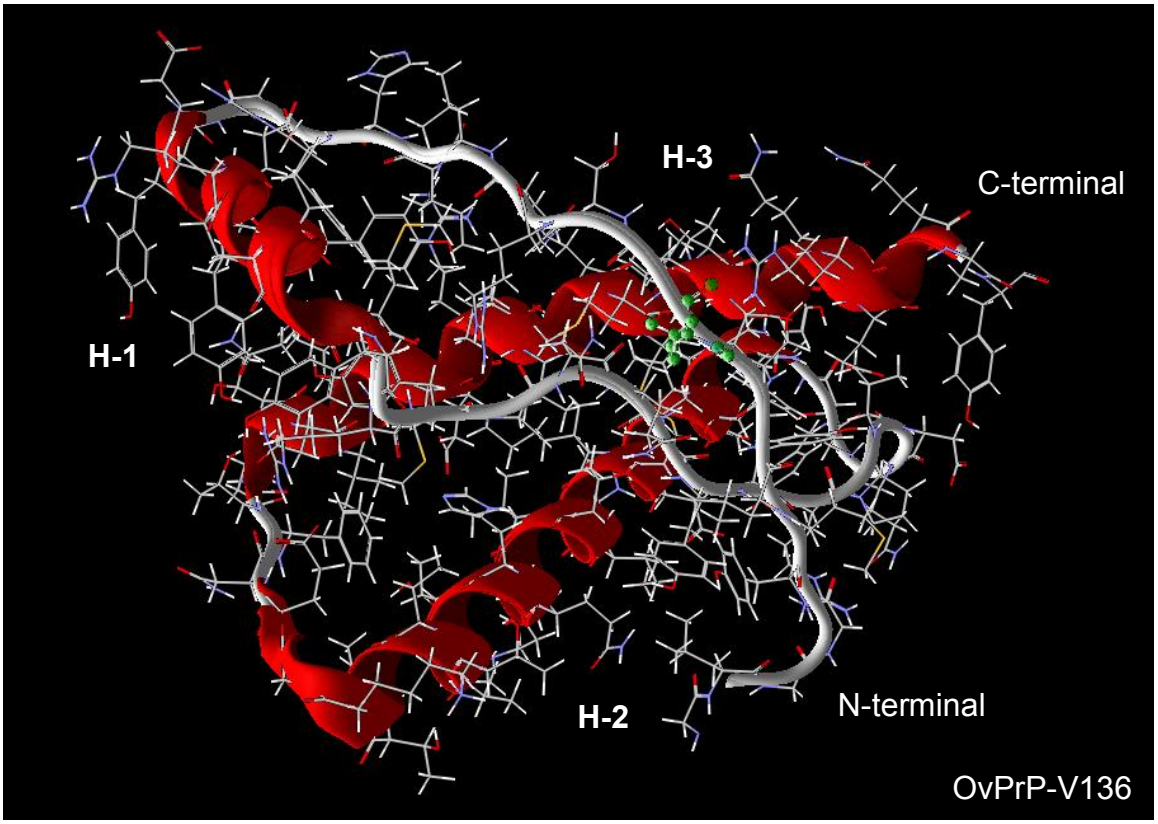
H-3
C-terminal
H-1
H-2
N-terminal
OvPrP-V136

Figure 4.17. 3D structures of ovine PrP expressing either A or V 136 polymorphism. The structures of OvPrPA-136 and OvPrP-V136 **corresponding to amino acid residues 114-228** were visualized in VMD. Each of the structures includes **the disordered N-terminal structure and three α-helices (H1-3) shown in red ribbons**. The top molecule is ovine PrP (residues 114-228) expressing alanine at codon 136. The bottom molecule is ovine PrP (residues 114-228) expressing valine at codon 136. OvPrP 136 polymorphism either alanine (top) or valine (bottom) are shown in green.

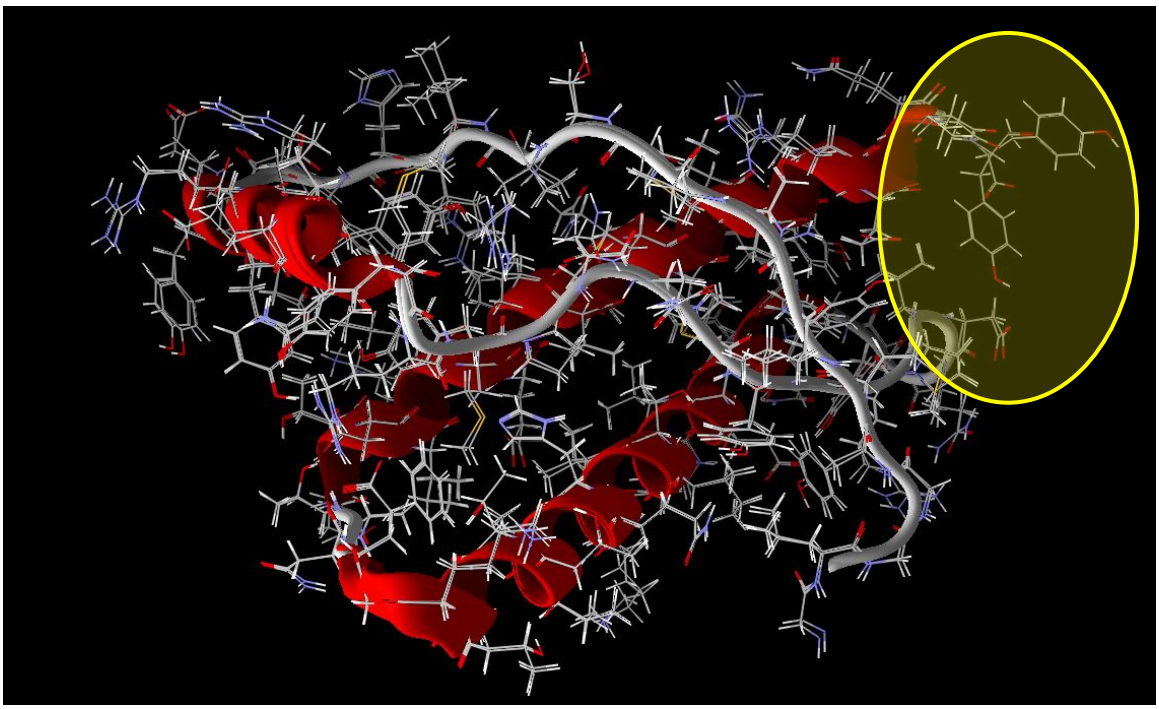

Figure 4.18. Composed 3D structures of ovine PrP expressing 136 polymorphism either alanine or valine. When the structures of OvPrPA-136 and OvPrP-V136 (residues 114-228) were superimposed, the composed image showed that the two structures were not aligned exactly the same. The most apparent difference between two OvPrP structures was the orientation of Y at codon 228 in the C-terminal region (indicated in a yellow circle). Tyrosine at codon 228 in the C-terminal region is facing down to locate in close proximity to the β2-α2 loop in OvPrP-V136 but not OvPrP-A136. In OvPrP-V136, the ring structure of Y228 at the C-terminal region faced down and was positioned in close proximity to the loop between the β2-sheet and α2-helix, suggesting the long-range interaction of the Y at codon 228 and β2-α2 loop. On the other hand, the ring structure of Y228 flipped away from the β2-α2 loop in OvPrP-A136.

A

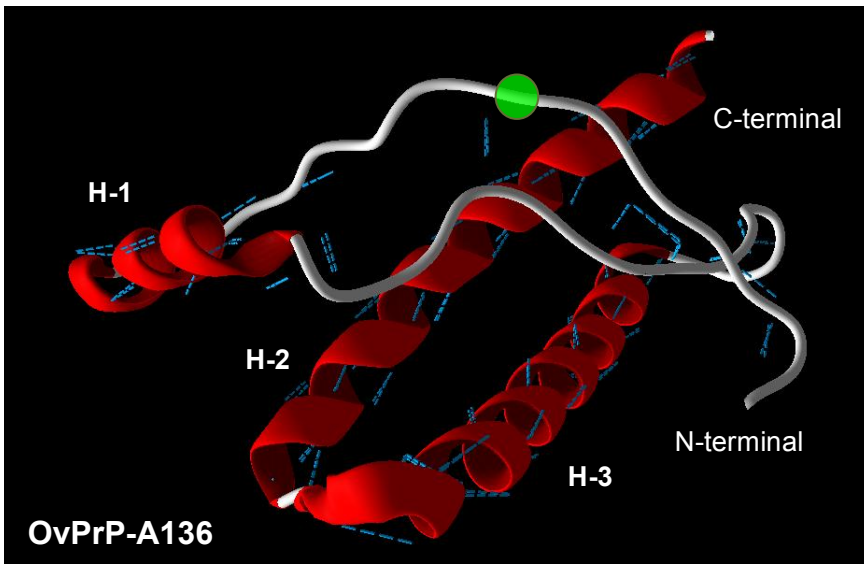
C-terminal
H-1
H-2
N-terminal
H-3
OvPrP-A136

B

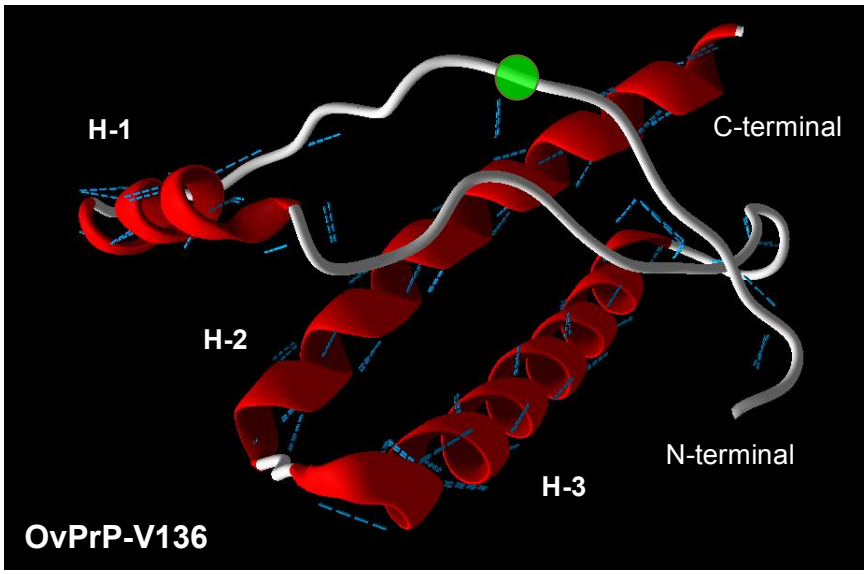
H-1
C-terminal
H-2
N-terminal
H-3
OvPrP-V136

C

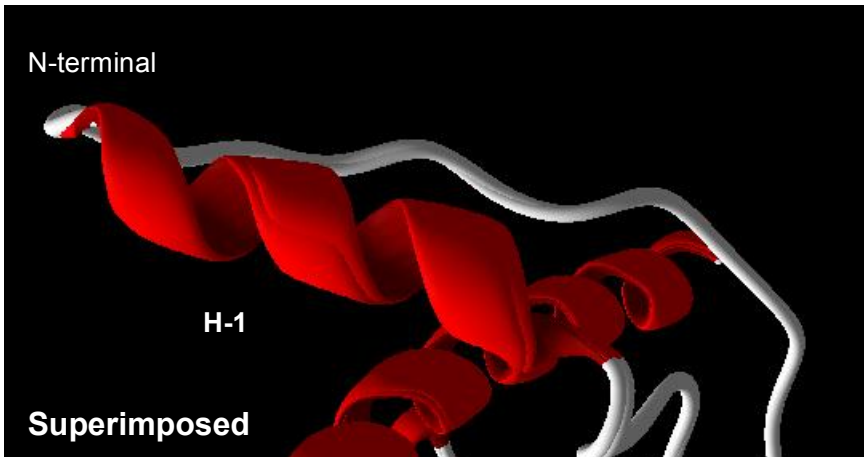
N-terminal
H-1
Superimposed

Figure 4.19. Ribbon diagrams of the C-terminal domain of OvPrP (residues 114-228). A green circle indicates the location of codon 136. Blue dashed lines indicate intramolecular hydrogen bonds. A. OvPrP-A136. B. OvPrP-V136. C. Superimposed images of OvPrP-A136 and OvPrP-V136 are enlarged at the α-helix 1 (H-1). The subtle differences between OvPrP-A136 and OvPrP-V136 were found in the structures of three α-helices (H-1, H-2 and H-3), and most conformational changes were concentrated in H-1. The N-terminal of H-1 was relaxed and C-terminal of H-1 opened up in OvPrP-A136; therefore, the diameter of H-1 in OvPrP-V136 was relatively smaller than OvPrP-A136. In addition, the N-terminal of H-1 had less twist in OvPrP-A136. The difference in H-2 was that the C-terminus had an additional twist in OvPrP-V136 but not OvPrP-A136 (Figure 4.19.A and B.). In more detail, the conformational differences were found in the orientation of the following amino acid residues: asparagine at codon 147 and glutamic acid at codon 155 in H-1, asparagine at codon 176 and lysine at codon 188 in H-2, glutamic acid at codon 203 in H-3 and Y at codon 228.

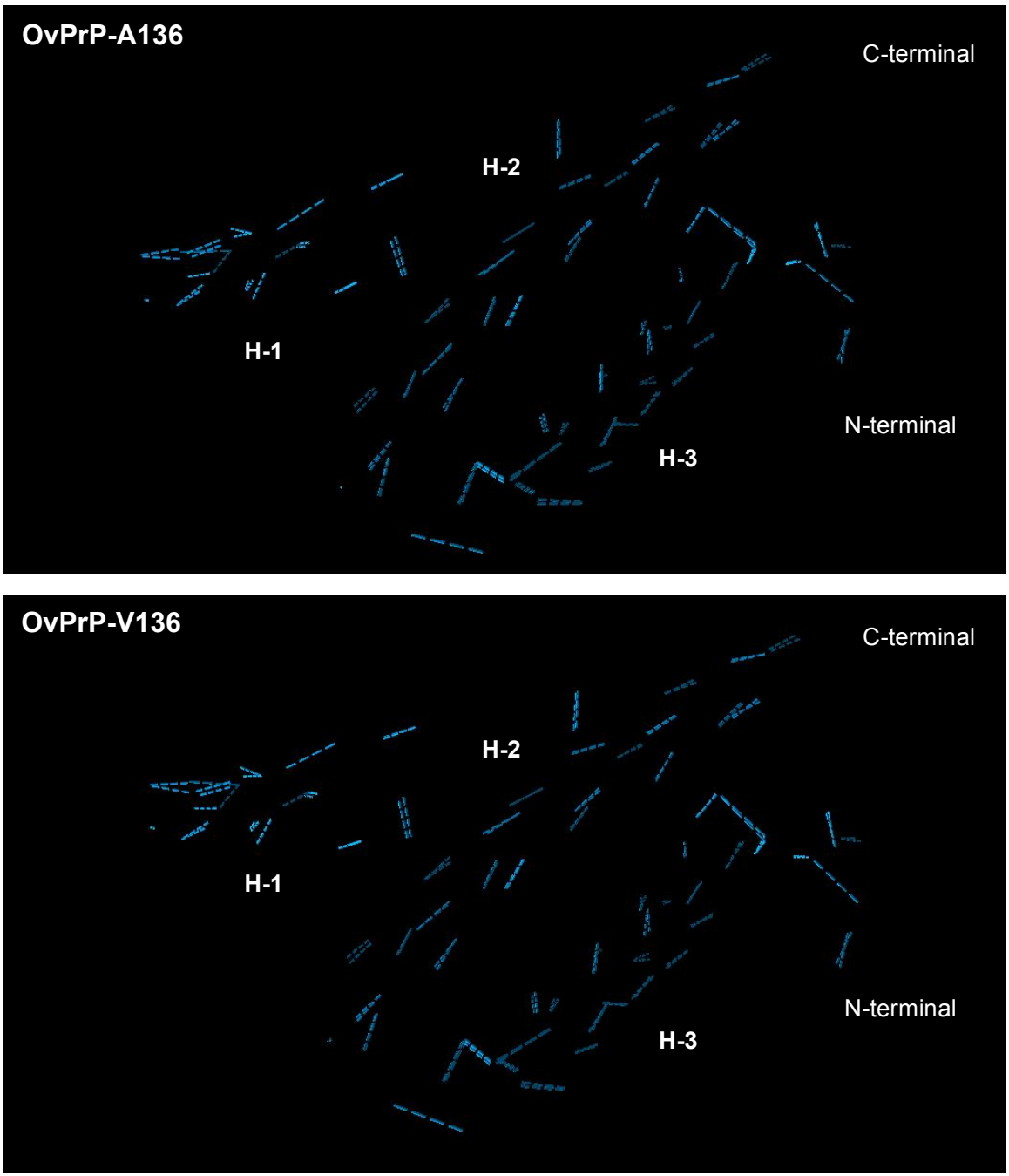

Figure 4.20. Comparison of intramolecular hydrogen bonding in ovine PrP (residues 114-228) with 136 polymorphism either alanine or valine. Blue dashed lines indicate intramolecular hydrogen bonding. A. OvPrP-A136. B. OvPrP-V136. Differences are found especially in the N- or C-terminal of three α-helices. The diagram was generated using VMD.

Chapter 5

Unaltered prion protein expression in Alzheimer disease patients

Published in Prion, 5:2, 109-116; April/May/June 2011

Introduction

For many years, the overlapping clinical, pathological and biochemical characteristics of Alzheimer's and prion diseases suggested a shared pathogenic mechanism. The prion protein (PrP) and the amyloid β (Aβ) peptide, derived from the amyloid precursor protein (APP), both undergo structural transitions associated with a gain of toxic function leading to neurodegeneration (Prusiner, 1998). APP and PrP are directly or indirectly associated on the cell surface (Schmitt-Ulms *et al.*, 2004), and there are similarities in the post-translational processing of both proteins. Analogous to the α-secretase cleavage of APP, PrP^C undergoes proteolytic cleavage at amino acids 110/111 to produce a 17-kDa carboxyl-terminal fragment referred to as C1 (Chen *et al.*, 1995) by the possible action of TNFα-converting enzyme (TACE) or members of the ADAM (α disintegrin and metalloprotease) family. PrP cleavage following residue 89 results in the formation of an approximately 21 kDa carboxy-terminal C2 fragment, which, in infected brains, is resistant to protease digestion and appears to be facilitated by calpain (Yadavalli *et al.*, 2004). These two cleavage sites flank the amino acid charge cluster in the central domain where oligomeric Aβ has been proposed to bind PrP^C (Lauren *et al.*, 2009). Both proteins contain conserved histidine metal-binding domains, GxxxG transmembrane recognition motifs and

histidine-based high-affinity metal-binding sites, which favor the binding of transition metals. Related to this, oxidative stress has been implicated in AD (Martins *et al.*, 1986) and prion disease (Brazier *et al.*, 2006).

There is now convincing evidence that amplification of Aβ aggregates occurs by a prion-like mechanism (Eisele *et al.*, 2010; Eisele *et al.*, 2009; Meyer-Luehmann *et al.*, 2006). Moreover, prion infection is associated and formic acid-extractable Aβ1-42 peptide levels are higher, in transgenic mice expressing mutant APP (Tg2576 mice) compared to non-transgenic controls (Baier *et al.*, 2008), suggesting that cross-seeding of the two abnormally conformed proteins may occur. In line which this observation, the brains of diseased scrapie-infected wild-type mice also contain increase levels of the Aβ1-41 peptide (Parkin *et al.*, 2007). Conformational templating also appears to occur in other protein misfolding diseases (Brundin *et al.*, 2010) involving tau (Frost *et al.*, 2009), α-synuclein (Desplats *et al.*, 2009) and polyglutamine proteins (Ren *et al.*, 2009).

Although soluble oligomeric forms of the Aβ peptide, derived from APP, are proposed as key mediators of synaptic and cognitive dysfunction in AD, the mechanisms by which these events occur remain unclear. Several recent studies suggest a direct mechanistic link between PrP and the Aβ peptide in AD pathogenesis. The studies of Strittmatter and co-workers implicated PrP^C as a major receptor for synthetic soluble Aβ1-42 oligomers, and indicated that PrP^C mediates the deleterious effects of oligomeric Aβ1-42 on synaptic function (Lauren *et al.*, 2009). Soluble Aβ1-42 oligomer binding was shown to occur at amino-acid residues 95–110 of PrP, a region close to the *PRNP*

methionine/valine codon 129 polymorphism, which has numerous important influences on human prion diseases, and is also implicated as a risk factor for early-onset AD (Del Bo *et al.*, 2006; Riemenschneider *et al.*, 2004). In subsequent studies, this group demonstrated a requirement for PrP expression for axonal degeneration, loss of synaptic markers, early death, and learning and memory deficits in AD transgenic mice (Gimbel *et al.*, 2010).

While the foregoing findings implicate PrP as a potential therapeutic target in AD, other studies have been less supportive of this concept. In independent transgenic mouse studies, ablation or overexpression of PrP^C had no effect on impairment of hippocampal synaptic plasticity (Calella *et al.*, 2010). Moreover, while the interaction of Aβ1–42 oligomers with PrP^C was confirmed in separate studies, both PrP-expressing and PrP knockout mice were equally impaired in hippocampal dependent behavioral tests following intracerebroventricular injections of synthetic Aβ1–42 oligomers (Balducci *et al.*). Finally, other studies in which overexpression of PrP *in vitro* was shown to negatively regulate β-secretase (Parkin *et al.*, 2007) would appear to be consistent with a model in which high levels of PrP result in low levels of Aβ1-42 oligomers.

Here we performed an extensive analysis of PrP levels in AD and pre-AD patients to address the hypothesis that variable PrP^C expression is involved in AD pathogenesis.

Materials and Methods

Patients. Frozen samples of hippocampus, superior frontal cortex (BA9) and superior-middle temporal cortex (BA21-22) were obtained from the University of Kentucky Rapid Autopsy Program of the Alzheimer's Disease Clinical Center (UKADC). Tissue was examined from 37 individuals with a mean age of 86.7 ± 7.6 years (Table 5.1.) were examined. These individuals were part of a longitudinal clinical-pathologic study of aging and AD at the UKADC (Davis *et al.*, 1999; Schmitt *et al.*, 2000). The Human Investigations Committee at the University of Kentucky College of Medicine approved the studies. Individuals included in these studies agreed to annual clinical evaluation and brain donation at the time of death. For all subjects, cognitive test scores were available within the last year of life; the average interval from last evaluation to time of death was 7.0 ±3.6 months, with no differences among the three diagnostic groups ($p < 0.1$). Subjects were categorized as no cognitive impairment (NCI; n = 13), amnestic mild cognitive impairment (aMCI; n = 7), mild Alzheimer disease (mAD; n=6), or AD (n = 11) (Petersen, 2004), based on cognitive testing prior to death. The NCI subjects were without a history of dementia or other neurological disorders. Standard criteria for exclusion were the presence of (1) significant cerebral stroke regardless of antemortem date, (2) large cortical infarcts identified in the postmortem neuropathologic evaluation, (3) significant trauma within 12 months before autopsy, (4) individuals on a respirator longer than 12 hours before death, (5) individuals in coma longer than 12 hours immediately

before death, (6) individuals currently undergoing radiation therapy for CNS tumor, or (7) individuals with Lewy bodies.

Details of the UKADC have been published elsewhere in reference (Schmitt *et al.*, 2000). All subjects have detailed mental status testing annually, and have neurologic and physical examinations annually. Subjects had been followed for 1-14 years (median 8.2 years). Once a subject transitioned to having aMCI or mAD, they received the mental status test battery and neurologic evaluation every 6-9 months. The 7 subjects with aMCI, 6 with mAD, and 11 with AD were initially normal on enrollment into the longitudinal study and later developed aMCI and AD during follow-up. All aMCI subjects were amnestic without multi domain involvement. The diagnosis of aMCI, mAD, AD and NCI were defined by consensus conference. Histological examination of NCI subjects showed only age-related changes and Braak stage score of 0-II, meeting the NIA-RI low-likelihood criteria for the histopathologic diagnosis of AD. The clinical criteria for diagnosis of aMCI included (1) memory complaints, (2) intact activities of daily living, (3) objective memory impairment for age and education, (4) failure to meet criteria for dementia, and (5) a clinical dementia rating (CDR) scale score of 0.5. The Braak stage scores had a range of I-V. Clinical progression to AD was diagnostically characterized by (1) a decline in cognitive functions from a previous higher level, (2) decline in one or more areas of cognition in addition to memory, (3) impaired activities of daily living, (4) a CDR score between 0.5-1, and (5) a clinical evaluation that excludes other causes of dementia. The criteria for mAD subjects included the above clinical progression plus a histopathologic

diagnosis that included a Braak stage score of II-VI. For an AD categorization, subjects demonstrated a more progressive intellectual decline as described above, a MMSE less than that of the mAD cohort, and Braak scores of II-VI. None of the mAD subjects were considered to be at the end-stage of the disease progression.

Transgenic mice. Tg(HuPrP-M129)6812$^{+/-}$ mice and Tg(HuPrP-V129)7823$^{+/-}$ mice express human PrP encoding either M or V at codon 129, referred as HuPrP-M129 and HuPrP-V129, respectively (Kurt *et al.*, 2009). Transgenic lines were maintained by breeding with *Prnp*$^{0/0}$ mice maintained on an FVB background (*FVB/Prnp*$^{0/0}$) and transgenic offspring were identified by tail biopsy and extraction of genomic DNA using a Beckman Biomek FX robotic station followed by PCR screening for the presence of the transgene. Approximately, 1 cm of tail tissue was digested overnight at 55°C with proteinase K (0.5 mg/ml final concentration) in 50 mM Tris pH 8.0, 100 mM EDTA, 0.5% SDS, the DNA extracted with phenol and chloroform and concentrated by ethanol precipitation.

Analysis of the *PRNP* codon 129 polymorphism. Genomic DNA was extracted from brain homogenates of the 37 individuals. The sense primer (5'-ATGGCGAACCTTGGCTGCTGGATGC-3') and antisense primer (5'-GTGGTTGTGGTGACCGTGTGCTGCTTGAT-3') were used to amplify the *PRNP* cording sequence using PCR. The *PRNP* codon 129 polymorphism was assessed by digestion of the amplicons with endonucleases NspI (New England

Biolabs. Inc.) and MaeII (HpyCH4IV, New England Biolabs. Inc.), and the digested products were analyzed on 1.2% agarose gels.

Western Blotting. 10% brain homogenates were prepared in sterile phosphate buffered saline (PBS) lacking Ca^{2+} and Mg^{2+} ions. The concentration of a total protein in each sample was determined by bicinchoninic acid assay and standardized for each lane (5 µg per lane). Proteins were resolved by sodium dodecyl sulfate–polyacrylamide gel electrophoresis and transferred to polyvinylidene difluoride Immobilon-FL membranes (Millipore). The transferred membrane was blocked with 5% non-fat milk in 0.5% Tween-20 in Tris-buffered saline (TBST) and immunoprobed with mouse monoclonal antibody anti-PrP 6H4 (Prionics) and 3F4 (Covance) followed by horseradish peroxidase–conjugated anti-mouse secondary antibody. Proteins were visualized using ECL Plus (GE Healthcare) in an FLA-5000 scanner (Fujifilm Life Science). Anti-actin (Pan) Ab-5 monoclonal antibody (NeoMarkers) was used as an internal control.

Statistical analysis. Statistical analysis of western blot data from the frontal and temporal cortices and hippocampus of NCI, aMCI, mAD and AD was performed using a one-way ANOVA for each region separately. When appropriate, differences between groups were probed using a Newman-Keuls post hoc test. Each histogram of PrP^C in western blots was read by MultiGauge (Fujifilm Life Science) and the values were standardized against the histogram value of actin. All data were analyzed with GraphPad Prism 4 and values were expressed as

mean standard deviation. Differences with $P < 0.05$ was considered to be a significant and indicated with asterisks.

Results and Discussion

Table 5.1. summarizes patient characteristics by diagnostic group. Included in our studies were 13 individuals with NCI, 7 patients with aMCI, 6 with mAD, and 11 with AD. Braak and CERAD scores were determined for all samples (Tables 5.2. and Table 5.3.). Age, post-mortem interval (PMI), and brain weight were similar among the various groups (Table 5.1.). Differences in mini-mental state examination (MMSE) scores were highly significant between groups [$F(3,33) = 88.853$, $p < 0.0001$]. Post hoc comparisons using the student Newman-Keuls test showed statistically significant differences between NCI and aMCI ($p < 0.05$), between aMCI and mAD ($p < 0.05$), and between mAD and AD groups ($p < 0.05$). All dementia groups showed lower MMSE scores than NCI. Both AD groups showed lower scores than aMCI patients, while the AD group showed lower scores than mAD (Table 5.1.).

In addition to its important influence on human prion diseases (Wadsworth *et al.*, 2004), the methionine (M)/valine (V) polymorphism at codon 129 of the human PrP gene (*PRNP*) has also been implicated as a risk factor for early-onset AD (Del Bo *et al.*, 2006; Riemenschneider *et al.*, 2004), although its influence as a risk factor for AD has been challenged (Li *et al.*, 2005). Analysis of this polymorphism is also important given its close proximity to the proposed region of Aβ1-42 oligomer binding (Lauren *et al.*, 2009). We analyzed codon 129

genotypes by treating PCR amplified patient genomic DNA samples with NspI or MaeII restriction endonucleases (Figure 5.1.A and B) to distinguish *PRNP* coding sequence restriction fragment length polymorphisms (RFLPs) produced by the M and V codons. The *PRNP* M129 and V129 allele frequencies were approximately 77% and 23% respectively in the NCI group compared to 71% and 29% in the cognitively impaired groups. Valine homozygosity was not observed in the NCI group (Table 5.4.). A previous association of 129V homozygosity and increased risk of early-onset AD was reported in a Dutch population (Dermaut *et al.*, 2003). The mean age in each AD group in the current study is over 80 (Table 5.1.). The period of follow up for patients was up to 14 years with a mean of 8 years approximately, raising the possibility that some case may have been younger onset. Nonetheless, patient numbers in our study are too small to draw definitive conclusions.

To examine a possible relationship between cognitive decline and PrP^C expression, brain homogenates were prepared from frozen samples of hippocampus, superior frontal cortex (BA9) and superior-middle temporal cortex (BA21-22) of NCI, aMCI, mAD and AD patients, and immunoblots of samples containing equivalent total protein levels were probed with either anti-PrP monoclonal antibodies (mAb) 6H4 or 3F4. Levels of PrP in these preparations were determined by densitometric analysis of western blots using actin levels as an internal control in each sample. While we observed a tendency of diminished PrP levels in rostral compared to caudal areas when immunoblots were probed with mAb 6H4, regional differences were not significant, and rostrocaudal

decreases in PrP^C were not confirmed when the experiment was repeated using mAb 3F4 (Figure 5. 2.).

Western blot analysis using both mAb 6H4 and 3F4 showed that expression of PrP^C was not significantly altered among NCI compared to aMCI, mAD or AD in either the frontal and temporal cortices or hippocampus (Figure 5. 3.). Levels of unglycosylated PrP were not higher in AD compared to control cases, although there was a tendency for higher levels of aglycosyl PrP^C levels in the temporal cortex of aMCI patients compared to other study groups, and when measured with mAb 3F4 levels were significantly higher in temporal cortex of aMCI compared to NCI and AD patients (Figure 5.4.). PrP^C expression levels were also independent of *PRNP* codon 129 genotype (Figure 5.5.).

Our results appeared to be in general disagreement with the central topic of recently published studies by Velayos and coworkers (Velayos *et al.*, 2009) which indicated a tendency for lower steady state PrP^C levels in the brains of AD patents compared to controls (Velayos *et al.*, 2009), especially in the hippocampus, an outcome apparently inconsistent with previous reports of increased PrP^C immunereactivity in the temporal cortex, hippocampus (CA2) and subiculum in AD patients compared to controls (Voigtlander *et al.*, 2001). Although not discussed in the context of their data, the report of Valayos and coworkers was significant in light of recent studies implicating PrP^C as a major receptor that mediates the deleterious effects of oligomeric Aβ1-42 on synaptic function (Lauren *et al.*, 2009). Here we observed no differences in total PrP^C levels in AD compared to NCI controls, nor did we observe a graded decrease in

PrP levels with increasing cognitive impairment. The minor observed differences between PrP^C levels probed with mAb 6H4 and mAb 3F4 could be related to the site of the binding of these mAbs to PrP. The epitope mAb 6H4 has been mapped to the sequence DYEDRYYRE, corresponding to PrP residues 144-152 (Korth *et al.*, 1997), while the epitope for 3F4 is located in the KTNMKHM, corresponding to residues 106-112 (Lund *et al.*, 2007; Rubenstein *et al.*, 1999; Zou *et al.*, 2010a). Thus, while mAb 6H4 can detect the proteolytically processed sub-fragment of PrP^C, referred to as C1 (Chen *et al.*, 1995), mAb 3F4 cannot. Because diglycosylated C1 fragments overlap with mono- and non-glycosylated forms of full-length PrP^C, this could potentially affect quantification of PrP^C levels and explain the discrepancy between the two mAbs.

What could explain the discrepancies between our studies and previous report? Velayos and coworkers studied three patients with AD. No clinical information was provided, except that one AD patients also had Down syndrome. Western blotting of PrP^C was recorded in three control human cases and two AD patients. In the present study, we analyzed PrP^C expression in a larger cohort comprised of 37 individuals including 11 AD cases, 6 mAD, 7 aMCI patients and 13 non-demented controls. All patients were well characterized by diagnostic group, and all samples had short post-mortem intervals (Table 5.1-3.). Our analysis also included actin as an internal loading control for all samples. In addition to mAb 6H4, which was also used in the previous study, we used a second thoroughly characterized mAb (3F4) with reactivity against human PrP^C. The high numbers of well-characterized patients, and the rigorous analysis of

regional PrP^C expression allows for meaningful associations (or lack of association in this case) to be made between levels of PrP and the presence of AD.

Velayos and coworkers also reported a shift in the profile of PrP glycosylation, with the unglycosylated form predominating in AD patients compared to controls. While we were also unable to confirm the finding of increased levels of aglycosyl PrPC in AD or mAD patients, we did observe significantly higher levels of unglycosylated PrP in the temporal cortex of aMCI patients compared to NCI and AD (but not mAD) patients. Whether this change corresponding to a specific role for PrP expressing cells in this critical brain region at early stages of the development of AD, prior to the onset of significant neurodegeneration and neuronal loss, remains to be determined.

In summary, we conclude that, if PrP^C is involved in mediating the toxic effects of oligomeric Aβ, then this occurs by a mechanism that does not involve modulation of steady state levels of PrP. This would appear to be an important insight given recent associations of PrP in AD pathogenesis that implicate PrP as a potential therapeutic target.

Table 5.1. General demographics of subjects. [a]*p < 0.05* compared to NCI. [b]*p < 0.05* compared to aMCI. [c]*p <0.05* compared to mAD. Published in Prion, 5:2, 109-116; April/May/June 2011.

	NCI	MCI	eAD	AD	ANOVA
Age (years)					
Group size	13	7	6	11	
Mean ± SD	87.4 ± 7.6	91.1 ± 5.0	85.5 ± 7.2	83.9 ± 8.7	F = 1.416
Range	70 -101	84 – 99	77 - 94	68 - 99	*P > 0.1*
Gender					
Male	3	4	3	5	
Female	10	3	3	6	
PMI (hours)					
Mean ± SD	3.0 ± 0.8	2.9 ± 0.7	3.2 ± 0.9	3.5 ± 0.9	F = 0.988
Range	2.3 – 5	2 – 3.5	2 – 4.5	2 - 5	*P > 0.1*
Brain weight (g)					F = 0.232
Mean ± SD	1177 ± 166	1181 ± 155	1170 ± 57	1137 ± 110	*P > 0.1*
MMSE					
Mean ± SD	28.7 ± 1.7	24.7 ± 2.4[a]	22.2 ± 1.7[ab]	13.4 ± 3.4[abc]	F = 88.853
Range	26 – 30	20 – 27	20 -25	7 - 19	*P < 0.0001*

Table 5.2. Braak scores by clinical diagnosis.
Published in Prion, 5:2, 109-116; April/May/June 2011.

Group (N)	0-II	III-IV	V-VI
NCI (13)	7	5	1
aMCI (7)	2	3	2
mAD (6)	1	2	2
AD (11)	1	0	10

Table 5.3. CERAD classification by clinical diagnosis.
Published in Prion, 5:2, 109-116; April/May/June 2011.

Group (N)	None	Possible	Probable	Definite
NCI (13)	9	0	3	1
aMCI (7)	0	2	3	2
mAD (6)	1	0	1	4
AD (11)	0	0	2	9

Table 5.4. Codon 129 *PRNP* allele frequency and genotype of subjects.
Published in Prion, 5:2, 109-116; April/May/June 2011.

	NCI		MCI		eAD		AD	
	N	%	N	%	N	%	N	%
Allele								
M	20	77	10	71	8	67	16	73
V	6	23	4	29	4	33	6	27
Total	26		14		12		22	
Genotype								
MM	7	54	4	57	3	50	6	55
VV	0	0	1	14	1	17	1	9
MV	6	46	2	29	2	33	4	36
Total	13		7		6		11	

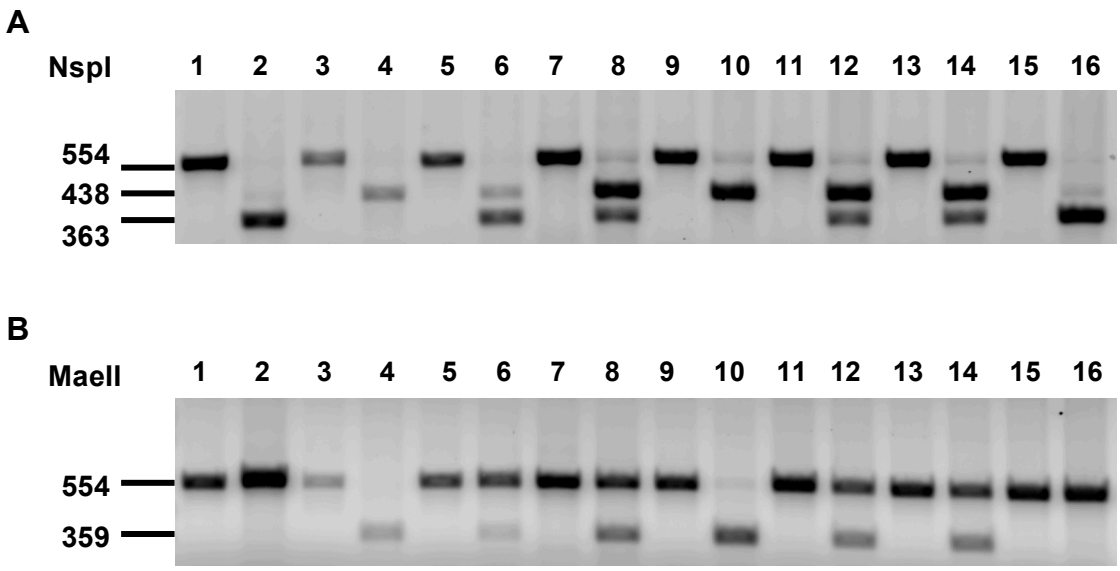

Figure 5.1. Representative restriction fragment length polymorphism (RFLP) analyses. Lanes 1 and 2, brain extracts from Tg(HuPrP-M129)6816$^{+/-}$ mice expressing human PrP-M129; lanes 3 and 4, brain extracts from Tg(HuPrP-V129)7826$^{+/-}$ mice expressing human PrP-V129; lanes 5 and 6, equal mixture of brain extracts from transgenic mice expressing human PrP-M129 and transgenic mice expressing human PrP-V129; lanes 7 – 16, five representative human samples. Odd numbers, undigested PCR samples; even numbers, digested PCR samples. (A) PCR amplified samples treated with restriction enzyme NspI, which cleaves *PRNP* encoding methionine at codon 129. Methionine carriers produce a 363 bp fragment; valine carriers produce a 438 bp fragment. (B) PCR samples treated with MaeII, which cleaves *PRNP* encoding valine at codon 129. Valine carriers produce a 359 bp fragment. Published in Prion, 5:2, 109-116; April/May/June 2011.

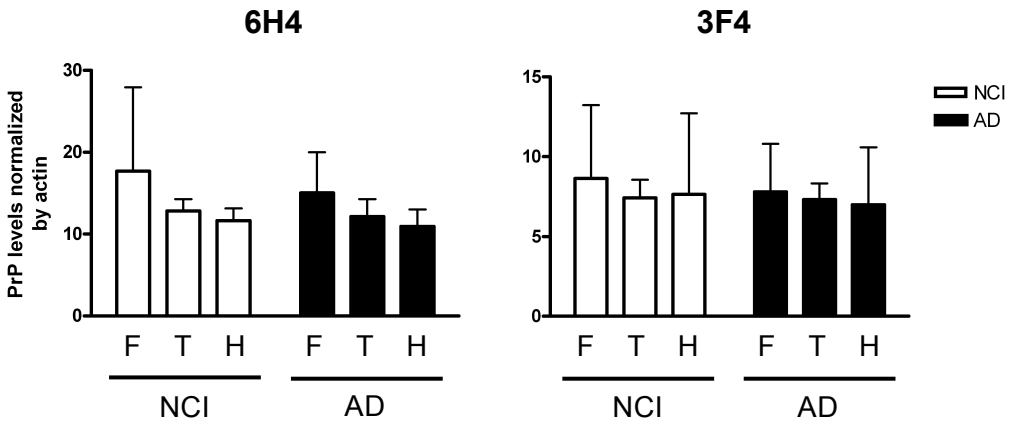

Figure 5.2. Rostrocaudal analysis of PrP^C levels in NCI and AD patients. For all sample, levels of total PrP^C and actin were measured by densitometric scanning of western blots. Each PrP value was normalized to its actin value. Normalized PrP values were compared among the frontal (F) and temporal (T) cortices and hippocampus (H) in NCI and AD groups. Error bars represent standard deviations from the mean. Published in Prion, 5:2, 109-116; April/May/June 2011.

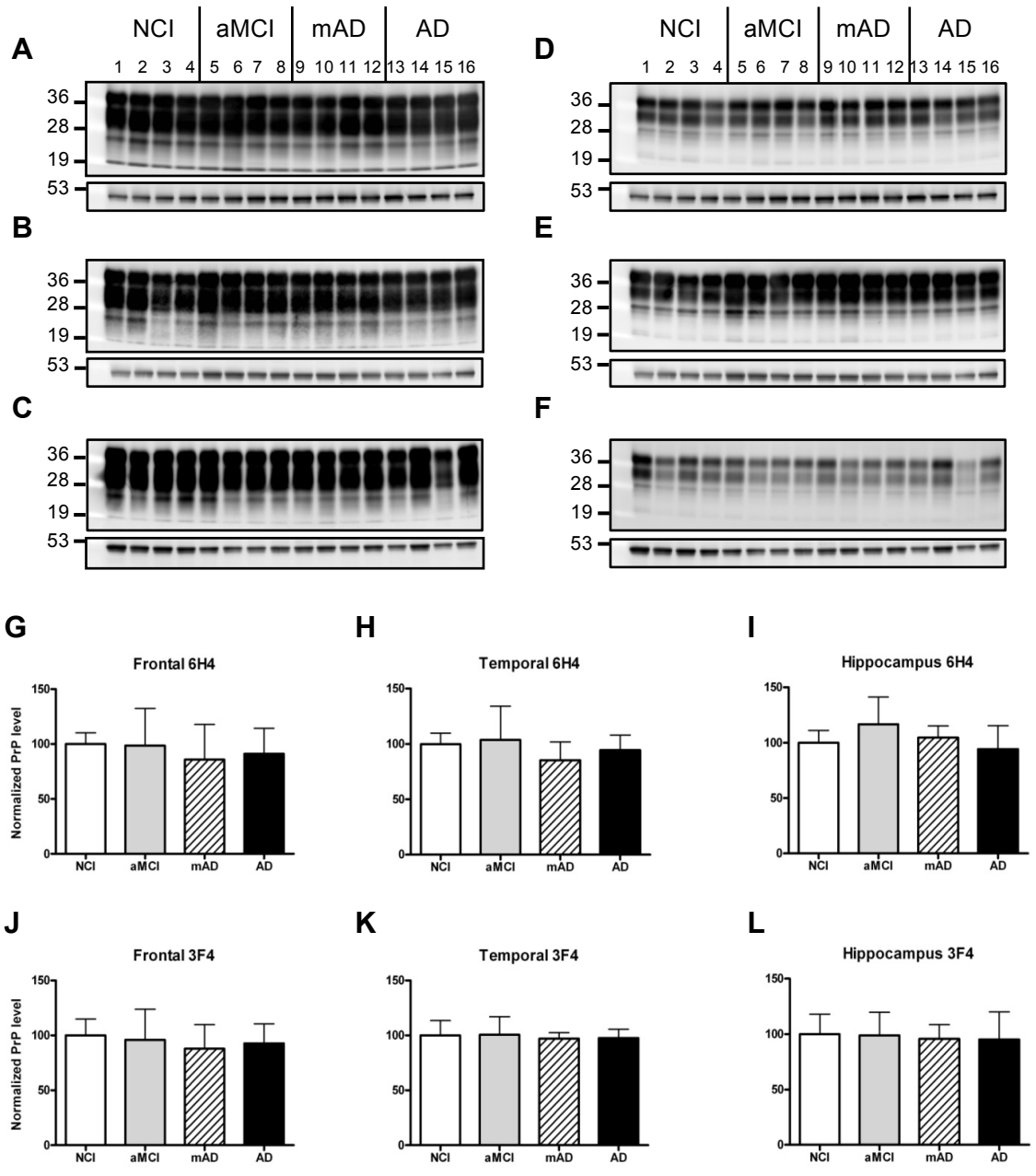
A
B
C
D
E
F
NCI
aMCI
mAD
AD
1 2 3 4 5 6 7 8 9 10 11 12 13 14 15 16
36
28
19
53
G
H
I
J
K
L
Frontal 6H4
Temporal 6H4
Hippocampus 6H4
Frontal 3F4
Temporal 3F4
Hippocampus 3F4
Normalized PrP level
150
100
50
0
NCI
aMCI
mAD
AD

Figure 5.3. Levels of PrP^C in different brain regions of patients with differing levels of cognitive impairment. Representative western blot analyses of brain homogenates from NCI, aMCI, mAD and AD patients are shown. Anti-PrP 6H4 (A-C) and 3F4 (D-F) antibodies were used to compare the levels of PrP^C among the groups. Actin controls are shown below the 6H4 or 3F4 immunoblots. NCI: lanes 1-4. aMCI: 5-8. mAD: 9-12. AD: 13-16. Three brain regions including the frontal (A, D, G and J), temporal (B, E, H and K) cortices and hippocampus (C, F, I and L) were analyzed. Molecular markers indicated are 53, 36, 28 and 19 kDa. Graphs in (G – L) include analyses of all samples from each group. For each sample, levels of total PrP^C were measured by densitometry. For each sample, levels of actin were also assessed. Each PrP value was normalized to its actin value. Means and standard deviations were calculated for each patient group and expressed as the percent value relative to the NCI group. Published in Prion, 5:2, 109-116; April/May/June 2011.

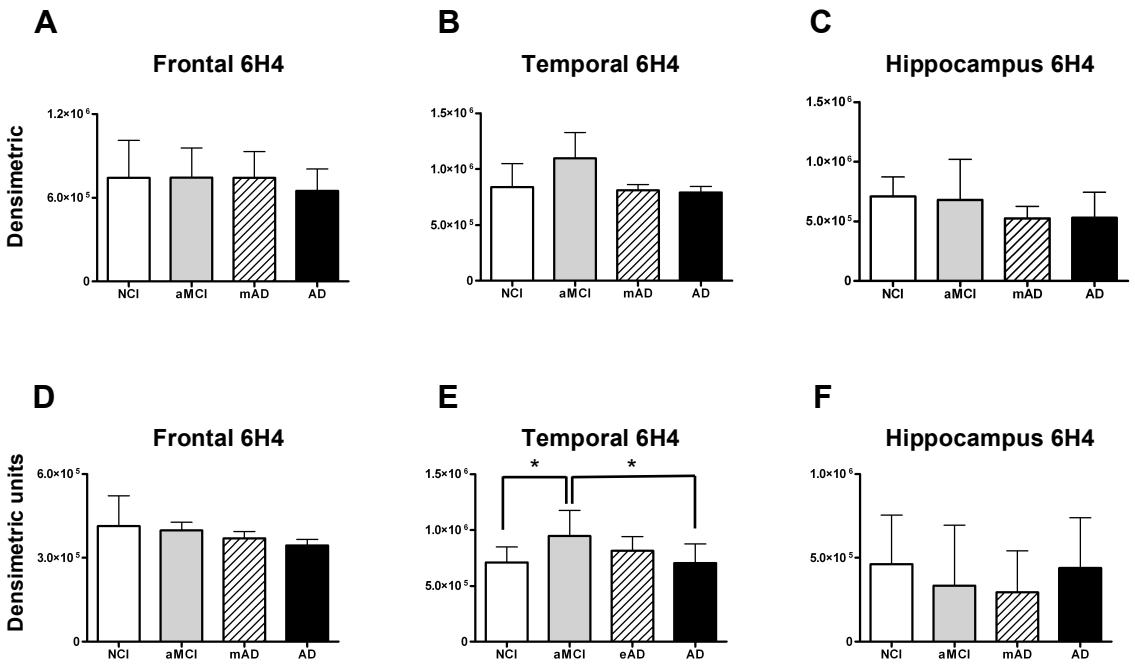

Figure 5.4. Unaltered levels of unglycosylated PrP^C in AD patients compared to NCI individuals. Levels of unglycosylated PrP^C (~ molecular weight 25-30 kDa) were measured by densitometric analysis of western blots. Means and standard deviations were calculated for samples from each patient group. y-axis values are arbitrary densitometric units. * indicates $p< 0.05$. Published in Prion, 5:2, 109-116; April/May/June 2011.

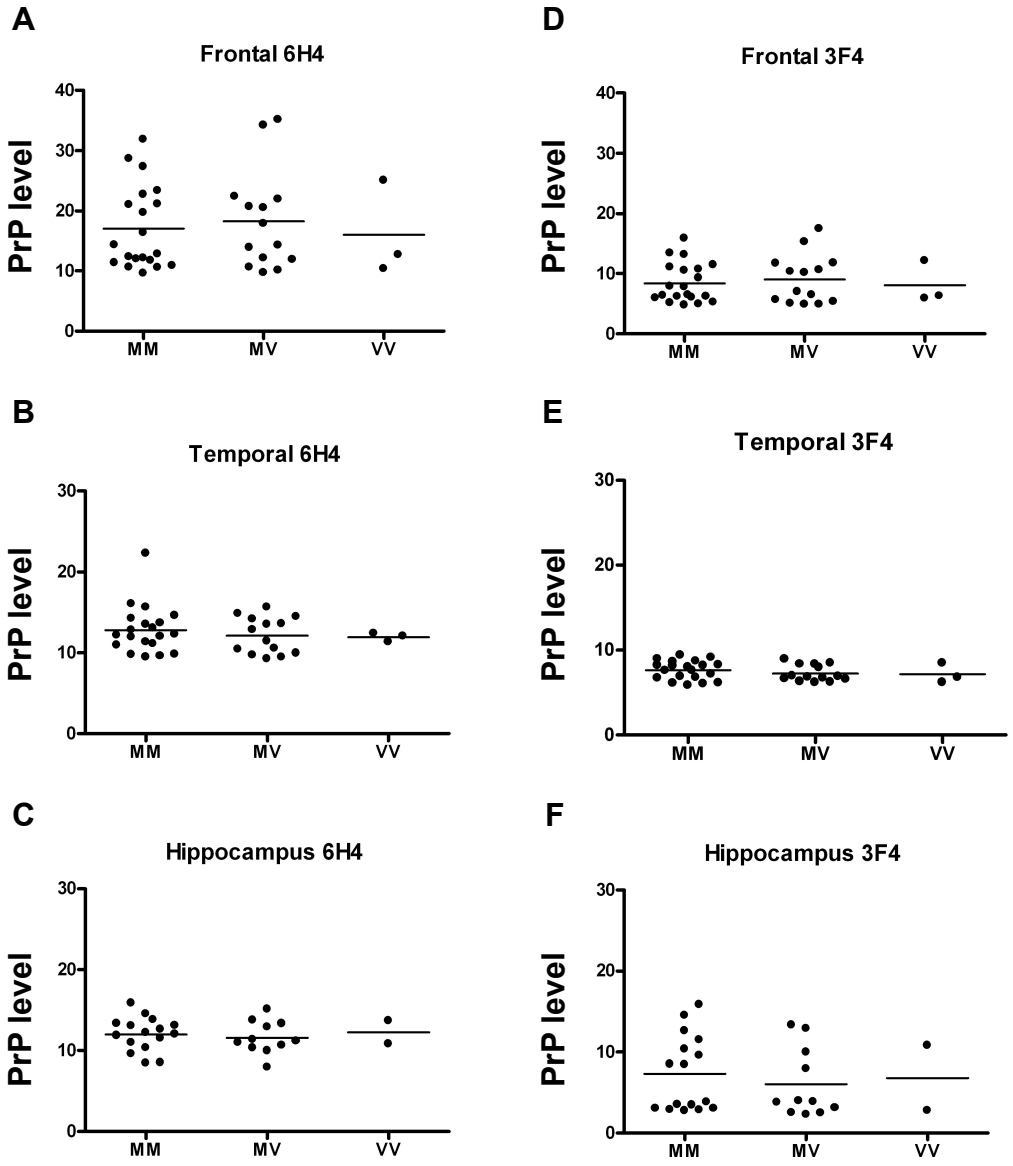

Figure 5.5. Levels of PrP^C do not correlate with human PrP 129 polymorphism in AD patients. Levels of PrP^C were measured by densitometry. For each sample, levels of actin were also assessed. Each PrP value was normalized to its actin value. These values were compared among individuals with various *PRNP* genotypes (M/M, M/V, V/V). (A – C) represent the data analyzed with 6H4; (D – F) represent the data analyzed with 3F4. Three brain regions including the frontal (A and D) and temporal (B and E) cortices and hippocampus (C and F) were analyzed. Published in Prion, 5:2, 109-116; April/May/June 2011.

Chapter 6

Discussion and future directions

Prion diseases are caused by misfolding of a normal PrP^{C} isoform into a pathogenic PrP^{Sc} isoform, and PrP^{Sc} is believed to serve as a template for PrP^{C} to undergo a profound conformational structural change to become a pathogenic PrP^{Sc} isoform (Prusiner, 1998). Moreover, numerous studies show that the conversion of PrP^{C} to PrP^{Sc} is constrained by transmission or species barriers between host PrP^{C} and donor PrP^{Sc}. In Chapter 2, the species barrier between CWD (cervid PrP^{Sc}) and human PrP^{C} was directly determined by inoculating CWD prions into Tg mice expressing human PrP encoding either M or V at codon 129. The results showed that the species barrier between human and cervid was considerably high in CWD prions. To understand the species barrier of prion disease, the conformational selection model has been hypothesized to explain how the species barrier in prion disease restricts transmission of prions (Collinge, 1999, 2010). For example, CWD1, CWD2 and CWD mix prions used in Chapter 2, according to the conformational selection model, contain multiple PrP^{Sc} conformations, and each CWD prion includes the same PrP^{Sc} conformation as well as completely different PrP^{Sc} conformations (Figure 6.1.). Those different PrP^{Sc} conformations, which are unique to each CWD prion, reflect to different properties of CWD prions, referred to as ‘strains’. In the conformation selection model, host PrP^{C} interact donor PrP^{Sc} in preference to selected sets of PrP^{Sc} conformations, and each species prefers different sets of PrP^{Sc} conformations.

For instance, HuPrP^{C}-M129, HuPrP^{C}-V129 and cervid PrP^{C} prefer completely different sets of PrP^{Sc} conformations to facilitate conversion of PrP^{C} to PrP^{Sc} (Figure 6.1.). CWD contains the PrP^{Sc} conformations, which are preferred by cervid PrP^{C}, therefore, donor CWD PrP^{Sc} could convert cervid PrP^{C} into PrP^{Sc} resulting in accumulation of proteinase-resistant PrP^{Sc} and development of disease. On the other hand, CWD prions do not contain the PrP^{Sc} conformations, which are preferred by HuPrP-M129 or HuPrP-V129 (Figure 6.1.). Thus, no accumulation of proteinase-resistant PrP^{Sc} is detected, and no disease development is confirmed. If HuPrP^{C} preferred PrP^{Sc} conformations present in CWD prions, concentrations of the preferred PrP^{Sc} were too low to facilitate PrP^{Sc} conversion to reach a detectable level. Thus, the rate of PrP^{Sc} conversion by CWD in Tg(HuPrP-M129)6816$^{+/-}$ and Tg(HuPrP-V129)7826$^{+/-}$ mice was not be efficient to accumulate proteinase-resistant PrP^{Sc} in the brain. Since some of CWD-inoculated Tg(HuPrP-M129)6816$^{+/-}$ and Tg(HuPrP-V129)7826$^{+/-}$ mice presented clinical signs without accumulation of proteinase-resistant PrP^{Sc} in their brains, this suggest the great possibility of presence of PrP^{Sc} conformations preferred by HuPrP-M129 and HuPrP-V129 in CWD. This question would be possible to test by inoculating the brain materials from CWD-inoculated Tg(HuPrP-M129)6816$^{+/-}$ and Tg(HuPrP-V129)7826$^{+/-}$ mice with clinical signs into genotype matched Tg(HuPrP) mice. If any animals develop disease during the secondary passage of CWD, it suggests the presence of human PrP^{C} preferred PrP^{Sc} conformations in CWD.

The conformational selection model proposes that PrP^{C} preferentially interacts with preferred PrP^{Sc} conformations to convert itself into PrP^{Sc}, suggesting that interactions between host PrP^{C} and donor PrP^{Sc} at the level of the tertiary structures play important roles in PrP^{Sc} conversion. The tertiary structure of proteins is, in general, predominantly assessed by the primary structure of proteins. The series of cell culture studies in Chapter 3 tested whether modifying the primary structure of mouse PrP^{C} led to alter susceptibility to mouse-adapted RML scrapie prion. I particularly asked that introducing substitutions of amino acids in specific regions of PrP where majority of differences among mammalian PrPs were clustered, involve in the transmission barrier of RML and CWD prions by identifying accumulation of proteinase-resistant PrP^{Sc} post infection. The present *in vitro* data suggest that the primary structure of PrP encodes crucial information to fold itself into a defined tertiary structure to facilitate conversion of PrP^{Sc}.

Most cellular proteins need to be folded into correct conformations to gain own functions, and numerous studies have reported that molecular chaperones play an important role in maintaining functional protein conformations (Hartl & Hayer-Hartl, 2009). There has been increasing numbers of molecular chaperones reported to serve different functions in protein folding (Hartl & Hayer-Hartl, 2009). Nonetheless, an essential function of molecular chaperones is to catalyze or mediate a proper folding process of proteins or to recognize misfolded proteins for degradation. Moreover, chaperons could provide an adequate space for proteins to be able to unfold and refold into a proper

conformation in a dynamic and busy cellular environment. It is important to note that molecular chaperones are defined by any molecules that interact with any proteins to assist and/or stabilize functional protein folding, and structures of molecular chaperones are not clearly defined all the time (Hartl, 1996; Hartl & Hayer-Hartl, 2009).

Protein misfolding in neurodegenerative diseases has been associated with molecular chaperones, and elevated levels of molecular chaperones, such as, heat shock proteins (HSPs) have been reported in Alzheimer's disease, Parkinson's disease and prion disease (reviewed in (Brownell *et al.*, 2012)). For example, increased levels of small heat shock proteins (sHSPs) were reported in scrapie-affected sheep (Vidal *et al.*, 2009), BSE-inoculated Tg mice (Tortosa *et al.*, 2008), and CJD-diseased human brains, especially in neurons and glial cells (Renkawek *et al.*, 1992). sHSPs are distinguished from large heat shock proteins by molecular weights. sHSPs bind misfolded proteins to prevent from forming aggregations until large heat shock proteins come to accommodate refolding process. Increased levels of HSPs in those neurodegenerative diseased brains suggest cells attempt to clear misfolded proteins or aggregates; however, the cellular clearance mechanism mediated by HSPs might slowly compromised over a long period of time, resulting in accumulation of aggregated proteins.

On the contrary, other group of molecular chaperones might mediate a misfolding process of proteins, such as PrP^{Sc}. Unidentified molecular chaperons, we denote 'protein X', might play a role in conversion of PrP^{Sc} from PrP^{C} in neurons. In PrP^{Sc} conversion models including the heterodimer template-

associated and nucleated-polymerization models (Figure 1.2.), PrP^{Sc} is thermodynamically stable compared to PrP^{C}. Thus, it will be necessary to overcome the energy barrier for PrP^{Sc} conversion to take place (Figure 6.2.). Moreover, protein X might assist in unfolding, refolding and/or stabilizing proper conformation of PrP^{Sc} (Figure 6.2.). In addition to overcoming the energy barrier using a catalyst, the spontaneous conversion of PrP^{C} to PrP^{Sc} could be induced by increasing concentration of PrP^{Sc}.

The conformational selection model was introduced earlier to explain the species barrier, which is determined by compatible conformations between host PrP^{C} and donor PrP^{Sc}. In addition to the conformational selection model, an unidentified catalyst or molecular chaperone, we denote hypothetical 'protein X' might paly an important role in the species barrier of prion diseases. 'Protein X' could be a species-specific molecular chaperone to facilitate PrP^{Sc} conversion. As a matter of fact, the Tg mouse study using a human-mouse chimera PrP demonstrated that Tg mice expressing human-mouse chimera PrP were susceptible to human prions, whereas Tg mice expressing human PrP were resistant to the same human prions (Telling *et al.*, 1995). Both host PrP^{C} and donor PrP^{Sc} are from humans; however, cellular factors are from mice. This Tg mouse study suggests that a species-specific molecular interaction is required to facilitate PrP^{Sc} conversion, which might be mediated by 'protein X'. Therefore, the susceptibility or resistance to prions might also be determined by 'protein X'.

Further, 'protein X' could be a group of chaperones to mediate in unfolding, refolding and stabilizing newly synthesized PrP^{Sc}. Another possibilities

are that ‘protein X’ could be co-chaperone to assist a chaperone or could be one subunit in a functional chaperone. This one piece of subunits in chaperone might alter a normal function of existing chaperones to facilitate PrP^{Sc} conversion. If a group of molecular chaperones involves in PrP^{Sc} conversion, not all molecular chaperones determine the species barrier of prion diseases. Some of subunits in molecular chaperones might be well conserved among mammalian species, whereas other subunits are unique to species. Those species-specific molecular chaperones might play a key role in the species barrier of prion diseases.

The PrP^{Sc} conversion models in Figure 6.3. explain how a species-specific protein X determines transmission of CWD and RML prions in cervid and CWD and CJD prions in humans. According to the conformation selection model, host PrP^{C} selects preferred PrP^{Sc} conformations to facilitate substantial conformational change using donor PrP^{Sc} as a template. Even though host PrP^{C} finds preferred PrP^{Sc} conformation, the conversion of PrP^{C} into PrP^{Sc} does not occur spontaneously without any catalysts because of the high energy barrier (Figure 6.2.). In order for PrP^{C} to become PrP^{Sc} resulting in disease development within a host lifespan or within a certain period of time, a catalyst or molecular chaperone becomes essential to facilitate PrP^{Sc} conversion by lowering the energy barrier. An unidentified catalyst or molecular chaperone ‘protein X’ is a species-specific in the proposed conversion models (Figure 6.3.). For example, cervid carries a cervid-specific chaperone, and the cervid-specific chaperone might be completely different from a chaperone found in humans. A cervid-specific chaperone could facilitate the conversion of cervid PrP^{C} with cervid

preferred PrP^{Sc} and stabilize newly synthesized PrP^{Sc} (Figure 6.3.A). On the other hand, mouse adapted RML scrapie prion dose not contain cervid PrP^{C} preferred PrP^{Sc} conformations, and the cervid-specific chaperone could not mediate PrP^{Sc} conversion (Figure 6.3.B). As a result, RML prion could not produce PrP^{Sc} and disease in cervid. CWD prions do not contain human PrP^{C} ($HuPrP^{C}$) preferred PrP^{Sc} conformations, further, a human-specific protein X could not facilitate PrP^{Sc} conversion (Figure 6.3.C). Thus, CWD prions failed to develop disease in humans. When $HuPrP^{C}$ find preferred PrP^{Sc} conformations, such as, CJD prions, $HuPrP^{Sc}$ conversion occurs (Figure 6.3.D). A human-specific protein X could facilitate PrP^{Sc} conversion, as a result, humans develop CJD.

The rabbit epithelial kidney (RK13) cell culture system was used to test whether altering amino acids in specific regions of mouse PrP altered susceptibility to species matched prion (mouse adapted RML scrapie prion) in Chapter 3. RK13 cells expressing a wild-type mouse PrP^{C} (RKM cells) are highly susceptible to mouse adapted scrapie RML prion (Figure 6.4.A). However, RKM cells are not susceptible to CWD because PrP^{Sc} conformations in CWD are not mouse PrP^{C} preferred PrP^{Sc} conformations (Figure 6.4.B). The series of cell culture studies in Chapter 3 suggest that altering even one amino acid in specific regions of mouse PrP, where majority of differences among mammalian species are clustered, could result in loss of susceptibility to RML prion (Figure 6.4.C). Since wild-type and variant mouse PrP are expressed in rabbit epithelial kidney (RK13) cells, ‘protein X’ is a rabbit-specific. Therefore, the present *in vitro* data

shows the primary structure of host PrP^C primarily determines susceptibility to RML prion. These results also suggest that properties of mouse-specific and rabbit-specific chaperones might be functionally identical. To test whether a rabbit-specific and mouse-specific 'protein X' is functionally identical in RML transmission, Tg mice expressing the same variant mouse PrP used in the cell culture studies could be inoculated with RML to see whether develop disease. If results turn out to be consistent with the *in vitro* data, mice and rabbits have functionally identical molecular chaperones to facilitate PrP^{Sc} conversion. If those Tg mice expressing variant mouse PrP develop disease with RML, a mouse-specific chaperone has more capacity to facilitate PrP^{Sc} conversion of variant mouse PrP^C with RML prion. Thus, molecular chaperones in mouse and rabbit are functionally different in respect to PrP^{Sc} conversion.

The intraspecies transmission barrier of prion disease could be explained by the conformational selection model. In sheep, susceptibility and resistance to sheep scrapie prions are strongly controlled by ovine PrP polymorphisms especially at codon 136 encoding either A or V (Goldmann *et al.*, 1991; Goldmann *et al.*, 1994). According to the conformational selection model, SSBP/1 sheep scrapie prion include multiple PrP^{Sc} conformations, which can be classified into at least two groups based on the results in Chapter 4 (Figure 6.5.). One group contains PrP^{Sc} conformations with the $OvPrP^{Sc}$-V136 properties (a blue box in SSBP/1 in Figure 6.5.), while another group consists of completely different sets of PrP^{Sc} conformations, which have the identical properties to $OvPrP^{Sc}$-A136 (a pink box in SSBBP/1 in Figure 6.5.). CH1641 sheep scrapie

prion also has multiple PrP^{Sc} conformations; however, a further classification of PrP^{Sc} conformations is unclear (Figure 6.5.). $OvPrP^{C}$-V136 prefers a specific set of PrP^{Sc} conformations (blue boxes in Figure 6.5.), on the other hand, $OvPrP^{C}$-A136 prefers a different sets of PrP^{Sc} conformations (pink boxes in Figure 6.6.). SSBP/1 prion contains $OvPrP^{C}$-V136 preferred PrP^{Sc} conformations, and CH1641 does not. Thus, OvPrP-V136 is only susceptible to SSBP/1. Both SSBP/1 and CH1641 prions include $OvPrP^{C}$-A136 preferred PrP^{Sc} conformations, therefore, OvPrP-A136 is susceptible to both SSBP/1 and CH1641. However, $OvPrP^{C}$-A136 preferred PrP^{Sc} conformations are not the major conformations in SSBP/1. Lower concentration of $OvPrP^{C}$-A136 preferred PrP^{Sc} conformations in SSBP/1 prion are available for $OvPrP^{Sc}$-A136 conversion. The probability of $OvPrP^{Sc}$-A136 conversion is considerably low, therefore, $OvPrP^{C}$-A136 requires a longer period of time to accumulate $OvPrP^{Sc}$-A136 and to develop disease with SSBP/1.

A hypothetical chaperone ‘protein X’ might involve in the conversion of $OvPrP^{Sc}$-A136 and $OvPrP^{Sc}$-V136 (Figure 6.6.). In the following $OvPrP^{Sc}$-V136 and $OvPrP^{Sc}$-A136 conversion models, an unidentified molecular chaperone ‘protein X’ might be linked to an ovine PrP 136 polymorphism. An OvPrP-V136-specific protein X facilitates the conversion of $OvPrP^{C}$-V136 into PrP^{Sc} using $OvPrP^{Sc}$-V136 in SSBP/1 as a template and stabilizes newly synthesized $OvPrP^{Sc}$-V136 (Figure 6.6.A-1). However, the OvPrP-V136-specific protein X is not most efficient chaperone for $OvPrP^{Sc}$-V136 conversion with $OvPrP^{Sc}$-A136 in SSBP/1 prion (Figure 6.6.A-2). Therefore, $OvPrP^{Sc}$-V136 conversion requires a

longer time with SSBP/1-A136 prion. In addition, newly synthesized $OvPrP^{Sc}$-V136 might never accumulate in cells because a cellular clearance mechanism could promptly remove $OvPrP^{Sc}$-V136 as slowly synthesized.

Although an OvPrP-A136-specific protein X might facilitate the conversion of $OvPrP^{C}$-A136 into PrP^{Sc} with SSBP/1-V136 prion, the OvPrP-A136-specific protein X might not be most efficient chaperone to facilitate $OvPrP^{Sc}$-A136 conversion with SSBP/1-V136 prion (Figure 6.6.B-1). Thus, the rate of PrP^{Sc} conversion will not be fast enough to accumulate PrP^{Sc} in the brain and to develop disease. On the other hand, the OvPrP-A136-specific protein X could facilitate the conversion of $OvPrP^{C}$-A136 into PrP^{Sc} using $OvPrP^{Sc}$-A136 in SSBP/1 as a template (Figure 6.6.B-2). Newly synthesized $OvPrP^{Sc}$-A136 could be stabilized by the OvPrP-A136-specific protein X.

There is also another possibility that 'protein X' might not be linked to the ovine PrP polymorphism at codon 136, rather universal in ovine, referred to as ovine-specific 'protein X'. An ovine-specific protein X facilitates PrP^{Sc} conversion in both OvPrP-A136 and OvPrP-V136 sheep (Figure 6.6. C and D).

In a heterozygous state, an unidentified molecular chaperone 'protein X' could be an ovine-specific or OvPrP-A136-specific and OvPrP-V136-specific. If 'protein X' is linked to the ovine PrP polymorphism at codon 136, both OvPrP-A136-specific and OvPrP-V136-specific 'protein X' will be available to facilitate PrP^{Sc} conversion in heterozygous for A/V 136. Conversions of both $OvPrP^{C}$-V136 and $OvPrP^{C}$-A136 into PrP^{Sc} are taken place in the heterozygous state, even though rates of PrP^{Sc} conversion differ between $OvPrP^{Sc}$-V136 and

$OvPrP^{Sc}$-A136 (Figure 6.7.). Either ovine-specific or OvPrP-V136-specific 'protein X' could facilitate $OvPrP^{Sc}$-V136 conversion and stabilize newly synthesized $OvPrP^{Sc}$-V136 (Figure 6.7.A.). The conversion rate of $OvPrP^{Sc}$-V136 is higher than $OvPrP^{Sc}$-A136. The conversion of $OvPrP^{C}$-A136 into PrP^{Sc} will be facilitated by either ovine-specific or OvPrP-A136-specific 'protein X', and the ovine-specific or OvPrP-A136-specific 'protein X' could stabilize newly synthesized $OvPrP^{Sc}$-A136 (Figure 6.7.C). In addition to the above conversion mechanisms of $OvPrP^{Sc}$-V136 (Figure 6.7.B) or $OvPrP^{Sc}$-A136 (Figure 6.7.C), a 'dominant' templating mechanism of $OvPrP^{Sc}$-V136 conformation, which leads to forced templating of $OvPrP^{C}$-A136, is also occurring in the heterozygous state. In the 'dominant' templating mechanism, $OvPrP^{Sc}$-V136 helps to convert $OvPrP^{C}$-A136 to PrP^{Sc} using an ovine-specific or OvPrP-V136-specific protein X. Therefore, this newly synthesized $OvPrP^{Sc}$-A136 obtains the identical properties with a template $OvPrP^{Sc}$-V136.

CH1641 sheep scrapie prion is most susceptible to OvPrP-A136 and most resistant to OvPrP-V136 (Goldmann *et al.*, 1994). CH1641 sheep scrapie prion does not include $OvPrP^{C}$-V136 preferred PrP^{Sc} conformations based on the conformational selection model (Figure 6.5.). OvPrP-V136-specific or ovine-specific 'protein X' is available to facilitate PrP^{Sc} conversion. Either ovine-specific or OvPrP-V136-specific 'protein X' could not accommodate the $OvPrP^{C}$-V136-CH1641 PrP^{Sc} complex to facilitate PrP^{Sc} conversion (Figure 6.8.A-(1).). If 'protein X' is linked to OvPrP-V136, PrP^{Sc} conversion does not take place due to the OvPrP-V136-specific protein X. Even though those 'protein X' could

accommodate the OvPrP^{C}-V136-CH1641 PrP^{Sc} complex, inefficient 'protein X' could not mediate PrP^{Sc} conversion fast enough to accumulate PrP^{Sc} in the brain (Figure 6.8.A-(2)). A cellular clearance mechanism might remove newly synthesized PrP^{Sc} as slowly synthesized. CH1641 sheep scrapie prion includes OvPrP^{C}-A136 preferred PrP^{Sc} conformations (Figure 6.5.B). Either OvPrP-A136-specific protein X or ovine-specific protein X facilitates OvPrP^{Sc}-A136 conversion and stabilizes newly synthesized OvPrP^{Sc}-A136.

In the heterozygous state, OvPrP^{Sc}-A136 conversion is inhibited by the presence of OvPrP^{C}-V136 or OvPrP-V136-specific protein X. OvPrP^{C}-V136 inhibits the conversion of OvPrP^{C}-A136 by preventing interactions among OvPrP-A136, CH1641-PrP^{Sc} and/or 'protein X' (Figure 6.8.C-1). Even though an appropriate 'protein X' is available, 'protein X' could not mediate OvPrP^{Sc}-A136 conversion. The OvPrP-V136-specific 'protein X' could not facilitate OvPrP^{Sc}-A136 conversion (Figure 6.8.C-2). In the heterozygous state, the OvPrP-V136-specific 'protein X' is available and becomes an inhibitor or antagonist by interacting with the OvPrP^{C}-A136-CH1641 PrP^{Sc} complex before an appropriate OvPrP-A136-specific protein X interact with the PrP^{C}-PrP^{Sc} complex.

Up to this point, I have explained the PrP^{Sc} conversion models based on the conformational selection model using 'hypothetical protein X'. In order to identify 'protein X', it would be helpful to think where the conversion of PrP^{C} into PrP^{Sc} happens in cells. Cell culture studies reported that PrP^{C} was able to convert to PrP^{Sc} at the cholesterol-rich, detergent-soluble microdomains of the plasma membrane (Goold *et al.*, 2011; Taraboulos *et al.*, 1995) followed by

trimming the amino terminus of PrP^{Sc} in an acidic environment such as lysosome (Caughey *et al.*, 1991). These studies suggest that PrP^{Sc} conversion happens at the intercellular and intracellular environments (Figure 6.9.). in order to involve in PrP^{Sc} conversion, catalysts or molecular chaperones, 'protein X', which could mediate PrP^{Sc} conversion, might be membrane-bound molecules and closely located to PrP^{C} at the cholesterol-rich microdomains of the plasma membrane. Molecules in lysosome might mediate PrP^{Sc} conversion in vesicles. Therefore, 'protein X' should be intracellular molecules usually available in neurons.

During prion infection, infectious, abnormal PrP^{Sc} isoform is taken into lysosomes by fusing phagocytic vesicles with lysosomes or by translocating with chaperones and transporting through chaperones into lysosomes. Recent studies in tauopathy in Alzheimer's disease revealed that unfolded tau is translocated by a heat-shock chaperone to lysosome and transported into lysosome through a transporter (reviewed in (Kaushik & Cuervo, 2012)). The chaperon-mediated autophagy, which degrades proteins in lysosomes, can only degrade unfolded tau, and aggregated tau could malfunction the transporters on lysosomes (reviewed in (Kaushik & Cuervo, 2012)). In prion disease, PrP^{Sc} could enter the intracellular space by phagocytosis for degradation or PrP^{Sc} in the cytosol could be transported into lysosomes using a similar mechanism to tau transportation in lysosome. However, degradation of PrP^{Sc} might turn into multiplying truncated PrP^{Sc} templates in lysosomes. Some studies reported that truncated PrP^{Sc} could convert host PrP^{C} into PrP^{Sc} and a full-length of PrP^{Sc} is not necessary for PrP^{Sc} conversion (Fischer *et al.*, 1996; Rogers *et al.*, 1993).

Taken together, ‘protein X’ could be present on the microdomains of the plasma membrane, lysosomes as well as cytosol. Thus, there are increasing possibilities that ‘protein X’ could be multiple intracellular molecules. Moreover, the intracellular molecules could be diverged among mammalian species since the transmission/species barrier is an important factor in developing prion disease.

‘Protein X’ hypothesis is not necessarily widely accepted in prion field, and so far ‘protein X’ is still hypothetical possibly molecular chaperone. However, through the course of the dissertation work, I started thinking more about true existence of ‘protein X’ and actual functions in prion pathogenesis. Although the identity of ‘protein X’ and how it involves in prion pathogenesis might be overlooked, the results of this dissertation work strongly implies the presence of ‘protein X’ to understand the underlying mechanisms of PrP^{Sc} conversion, transmission/species barrier, and propagating new prion strains within the same species.

In order to support the proposed models of PrP^{Sc} conversion with ‘protein X’, more questions need to be addressed. First, what is conformational compatibility? Is it only the conformations between PrP^{C} and PrP^{Sc}? Or does the conformation of the PrP^{C}-PrP^{Sc}-chaperone ‘protein X’ complex determine the transmission barrier? How many chaperones involve in PrP^{Sc} conversion? Does ‘protein X’ become available only when PrP^{Sc} in neurons or all the time? It would be helpful to further understand the transmission/species barrier of prion disease if more precise conformations of PrP^{Sc} in each prion strain could be available. It

might be possible to study the interactions between PrP^C and molecular chaperone 'protein X' by blocking the potential epitope where is the loop between β2-sheet and α2-helix in PrP^C using antibodies against the epitope. Additionally, it would be helpful to identify whether known molecular chaperones are up or down regulated upon infection. Understanding the transmission/species barrier in prion disease is crucial to develop early detection assays and strain specific treatments for prion disease.

The potential functions of PrP were suggested by the studies in the pathogenesis of AD (Gimbel *et al.*, 2010; Lauren *et al.*, 2009), therefore, further understanding roles of PrP^C in the pathogenesis of AD will greatly help to identify the function of PrP^C. In order to study a relationship between expression levels of PrP^C and its functions in AD patient brains, the expression levels of PrP were determined in the brains of individuals with AD at three different stages of cognitive impairments. The three brain regions including the frontal and temporal cortices and hippocampus were examined; however, unaltered expression levels of PrP^C in those brain regions from different stages of AD did not help to identify the function of PrP^C in the present study. It suggests that increased or decreased levels of PrP^C are not associated with PrP^C mediated functions in the pathogenesis of AD. Unaltered expression levels of PrP^C and increased level of Aβ in the brains of AD patients suggest that the interaction between PrP^C and Aβ induces neurotoxic effects, as proposed by Strittmatter (Gimbel *et al.*, 2010; Lauren *et al.*, 2009). Therefore, the increased level of Aβ is could be driving force

to bind PrP^C to form more Aβ+PrP^C complex with neuronal toxicity causing cell death and ultimately developing AD.

In future studies, it will be useful to determine the affinity of the complex formation between PrP^C and Aβ. In addition, it will be interesting to quantify the amount of the Aβ+PrP^C complexes in the time course of cell death and also to identify the threshold levels of the Aβ+PrP^C complexes or Aβ alone that cells can manage before inducing neuronal toxicity.

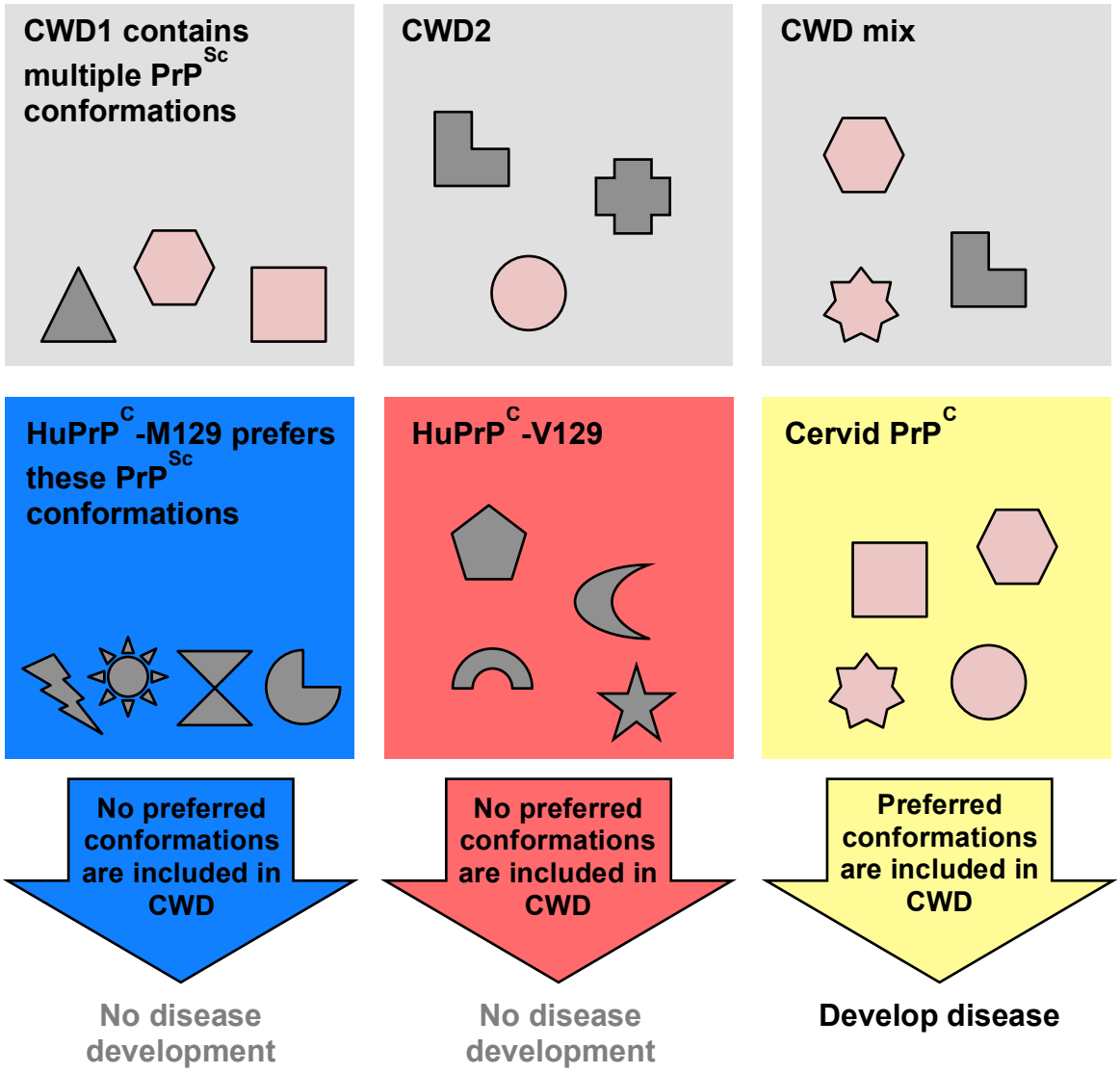
CWD1 contains multiple PrP^Sc conformations
CWD2
CWD mix
HuPrP^C-M129 prefers these PrP^Sc conformations
HuPrP^C-V129
Cervid PrP^C
No preferred conformations are included in CWD
No preferred conformations are included in CWD
Preferred conformations are included in CWD
No disease development
No disease development
Develop disease

Figure 6.1. The species barrier between cervid and human in interspecies transmission of CWD. This diagram is based on the conformational selection model, which explains PrP^{C} preferentially interacts with preferred PrP^{Sc} conformations to facilitate PrP^{Sc} conversion. Three gray boxes on the top show that multiple PrP^{Sc} conformations include in CWD1, CWD2 and CWD mix. Different shapes and colors represent different conformations. The bottom three boxes indicate potential host species including $HuPrP^{C}$-M129 (blue box), $HuPrP^{C}$-V129 (red box) and cervid PrP^{C} (yellow box). Each host PrP^{C} selectively interacts with preferred PrP^{Sc} conformations. Since any CWD prions do not include $HuPrP^{C}$-M129 and $HuPrP^{C}$-V129 preferred PrP^{Sc} conformations, PrP^{Sc} in CWD prions could not become a template to convert these $HuPrP^{C}$ into PrP^{Sc}. Therefore, $HuPrP^{C}$-M129 and $HuPrP^{C}$-V129 do not develop disease. On the other hand, CWD prions contain cervid PrP^{C} preferred PrP^{Sc} conformations, showing in different shapes in red color. Thus, PrP^{Sc} in CWD converts cervid PrP^{C} into PrP^{Sc}, resulting in the development of disease.

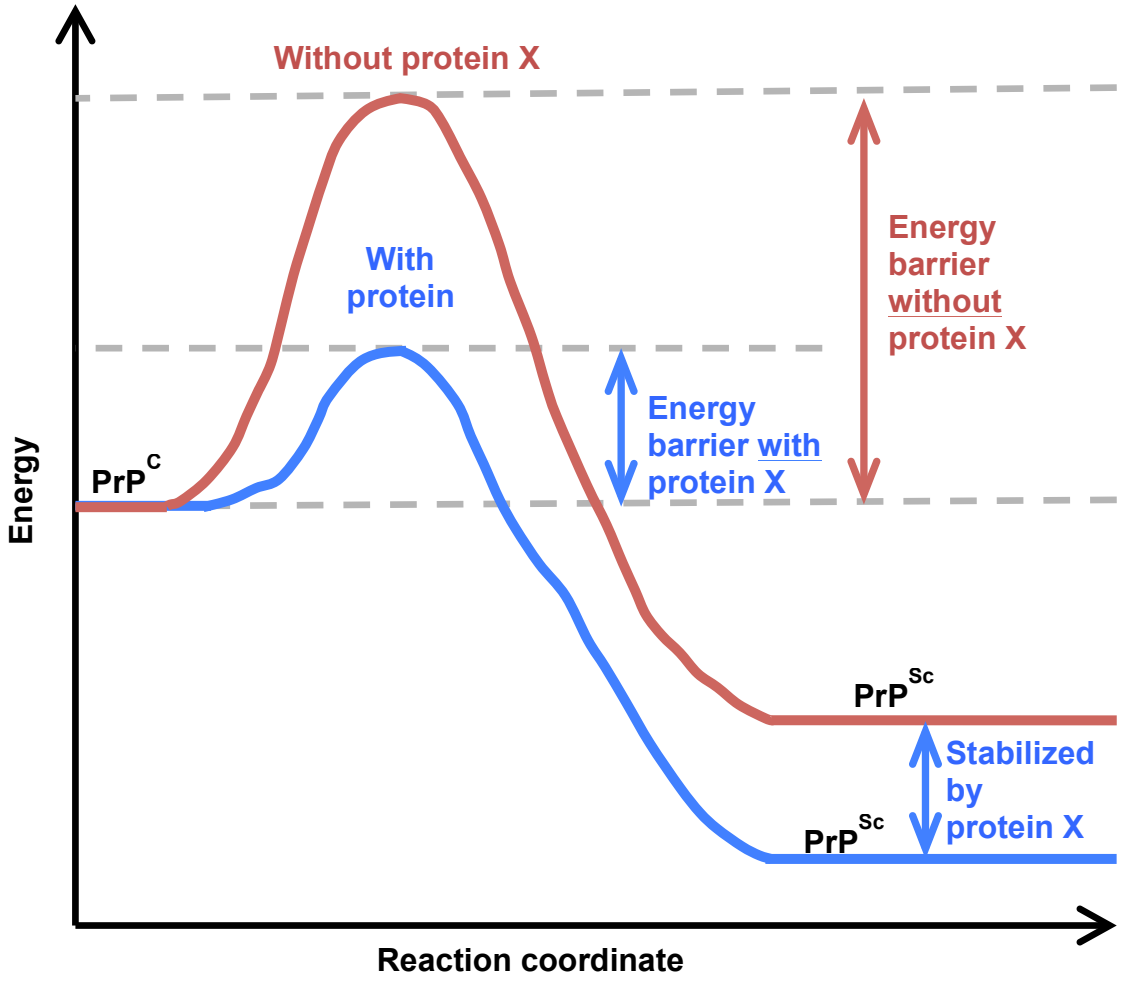

Figure 6.2. Hypothetical chaperone 'protein X' lowers the energy barrier of the conversion of PrP^{C} into PrP^{Sc} and stabilizes newly synthesized PrP^{Sc}. In this model, PrP^{Sc} is thermodynamically stable compared to PrP^{C}; furthermore, the conversion of PrP^{Sc} from PrP^{C} does not happen spontaneously without a catalyst or chaperon, such as, hypothetical 'protein X'. The conversion of PrP^{C} into PrP^{Sc} without 'protein X' (red arrow) requires overcoming the high energy barrier than the reaction with 'protein X' (blue arrow). 'Protein X' could reduce the energy barrier to facilitate the conversion of PrP^{C} into PrP^{Sc}. Moreover, newly synthesized PrP^{Sc} is stabilized by 'protein X'.

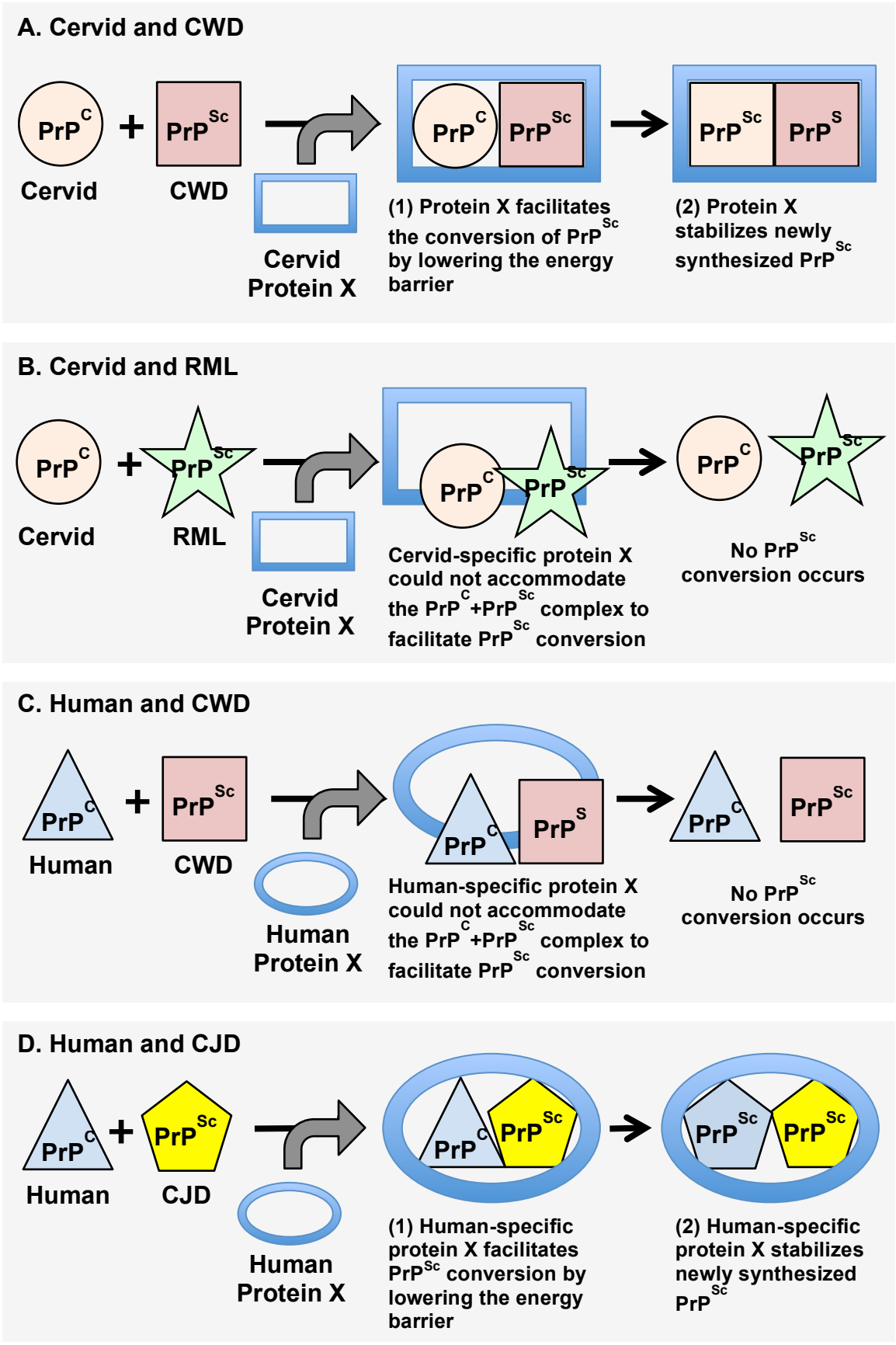
A. Cervid and CWD
PrP C
PrP Sc
Cervid
CWD
Cervid Protein X
(1) Protein X facilitates the conversion of PrP Sc by lowering the energy barrier
PrP Sc
PrP S
(2) Protein X stabilizes newly synthesized PrP Sc
B. Cervid and RML
PrP C
PrP Sc
Cervid
RML
Cervid Protein X
Cervid-specific protein X could not accommodate the PrP C +PrP Sc complex to facilitate PrP Sc conversion
No PrP Sc conversion occurs
C. Human and CWD
PrP C
PrP Sc
Human
CWD
Human Protein X
Human-specific protein X could not accommodate the PrP C +PrP Sc complex to facilitate PrP Sc conversion
PrP S
No PrP Sc conversion occurs
D. Human and CJD
PrP C
PrP Sc
Human
CJD
Human Protein X
(1) Human-specific protein X facilitates PrP Sc conversion by lowering the energy barrier
(2) Human-specific protein X stabilizes newly synthesized PrP Sc

Figure 6.3. Proposed models explain 'protein X' plays a key role in determining the species barrier of prion diseases in addition to the conformational selection model. According to the conformation selection model, host PrP^{C} preferentially interacts with preferred PrP^{Sc} conformations and undergoes substantial conformational change using donor PrP^{Sc} as a template. As shown in Figure 6.2., the conversion of PrP^{C} into PrP^{Sc} does not occur spontaneously without any catalysts because of the high energy barrier. In order for PrP^{C} to convert into PrP^{Sc} and accumulate to cause disease within a host lifespan or within a certain period of time, a catalyst or molecular chaperone plays an important role in PrP^{Sc} conversion. An unidentified catalyst or molecular chaperon, we denote hypothetical 'protein X'. In this model, 'protein X' is a species-specific. For example, cervid carries a cervid-specific chaperon, and the cervid-specific chaperon might be completely different from a chaperon found in humans. A. Cervid PrP^{C} and cervid preferred PrP^{Sc} could interact with a cervid-specific chaperon to mediate PrP^{Sc} conversion, and the cervid-specific 'protein X' stabilizes newly synthesized PrP^{Sc}. B. PrP conformations between cervid (host) and RML mouse prion (donor) are not compatible. Moreover, the cervid-specific chaperone could not accommodate the cervid PrP^{C}-mouse PrP^{Sc} complex to facilitate PrP^{Sc} conversion, resulting in no disease development. C. PrP^{Sc} conformations in CWD prion are not human PrP^{C} ($HuPrP^{C}$) preferred PrP^{Sc} conformations, and a human-specific protein X could not facilitate PrP^{Sc} conversion. Thus, no disease is developed. D. When $HuPrP^{C}$ finds preferred PrP^{Sc} conformations, such as, in CJD prions, $HuPrP^{Sc}$ conversion occurs. In addition, a human-specific 'protein X' could facilitate PrP^{Sc} conversion. As a result, humans develop CJD.

Wild-type and variant mouse PrP are expressed in rabbit epithelial kidney (RK13) cells, and each RK13 cells are infected with RML.

A. Wild-type mouse and RML

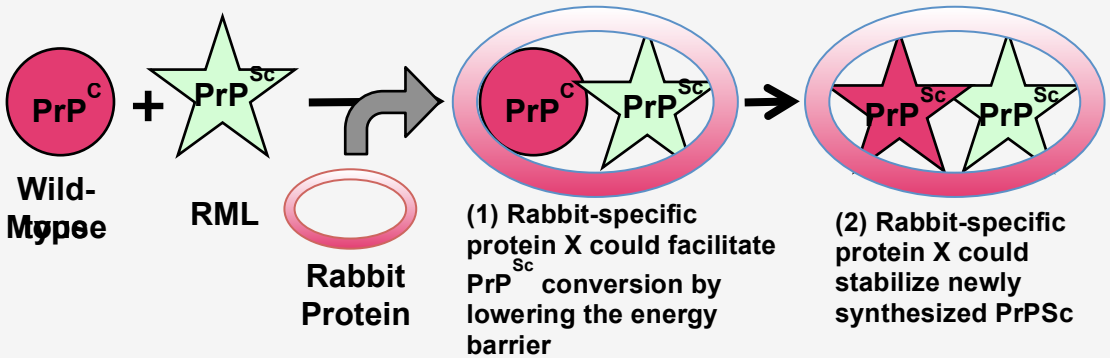

B. Wild-type mouse and CWD

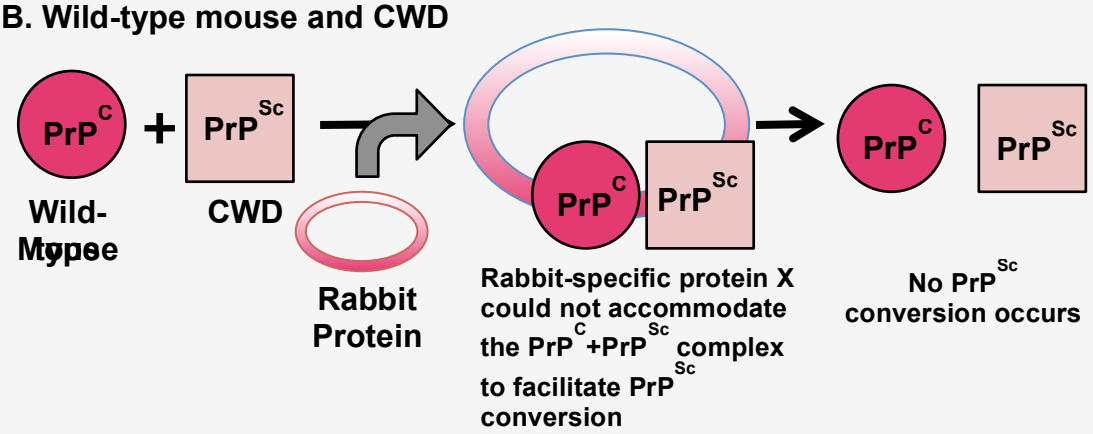

C. Variant mouse and RML

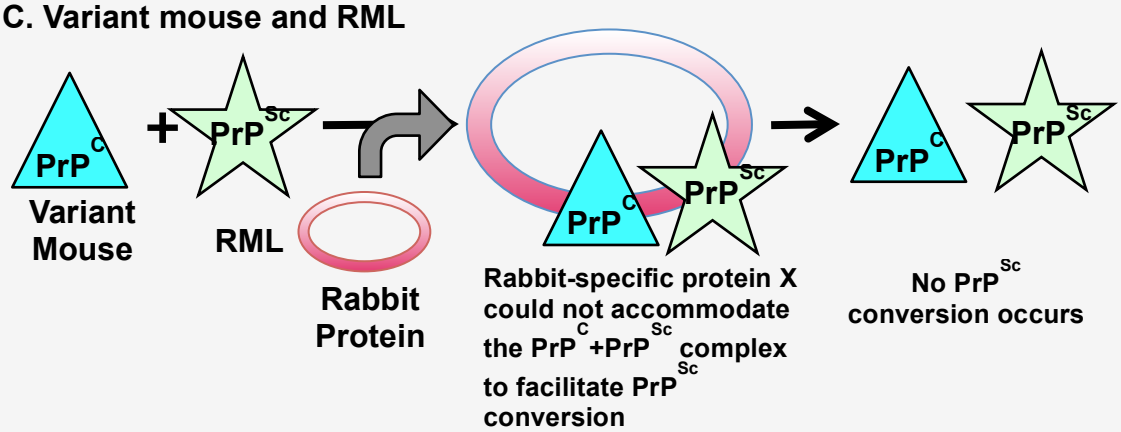

Figure 6.4. Conformational selection model is used to explain how RML mouse prion could not convert variant mouse PrP in RK13 cell culture systems. The rabbit epithelial kidney (RK13) cell culture system was used to test whether changing amino acids in specific regions of mouse PrP altered susceptibility to species matched prion (mouse adapted RML scrapie prion) in Chapter 3. A. RK13 cells expressing a wild-type mouse PrP^{C} (RKM cells) is highly susceptible to mouse adapted scrapie RML prion. B. However, RKM cells are not susceptible to CWD because PrP^{Sc} conformations in CWD are not mouse PrP^{C} preferred PrP^{Sc} conformations. C. The series of cell culture studies in Chapter 3 suggest that substituting even one amino acid in the specific regions of mouse PrP, where majority of differences among mammalian species are clustered, could result in loss of susceptibility to RML prion. Since wild-type and variant mouse PrP are expressed in rabbit epithelial kidney (RK13) cells, 'protein X' is a rabbit-specific. Therefore, the present *in vitro* data shows the primary structure of host PrP^{C} is a predominant determinant in susceptibility to RML prion. These results also suggest that properties of mouse-specific and rabbit-specific chaperones might be functionally identical.

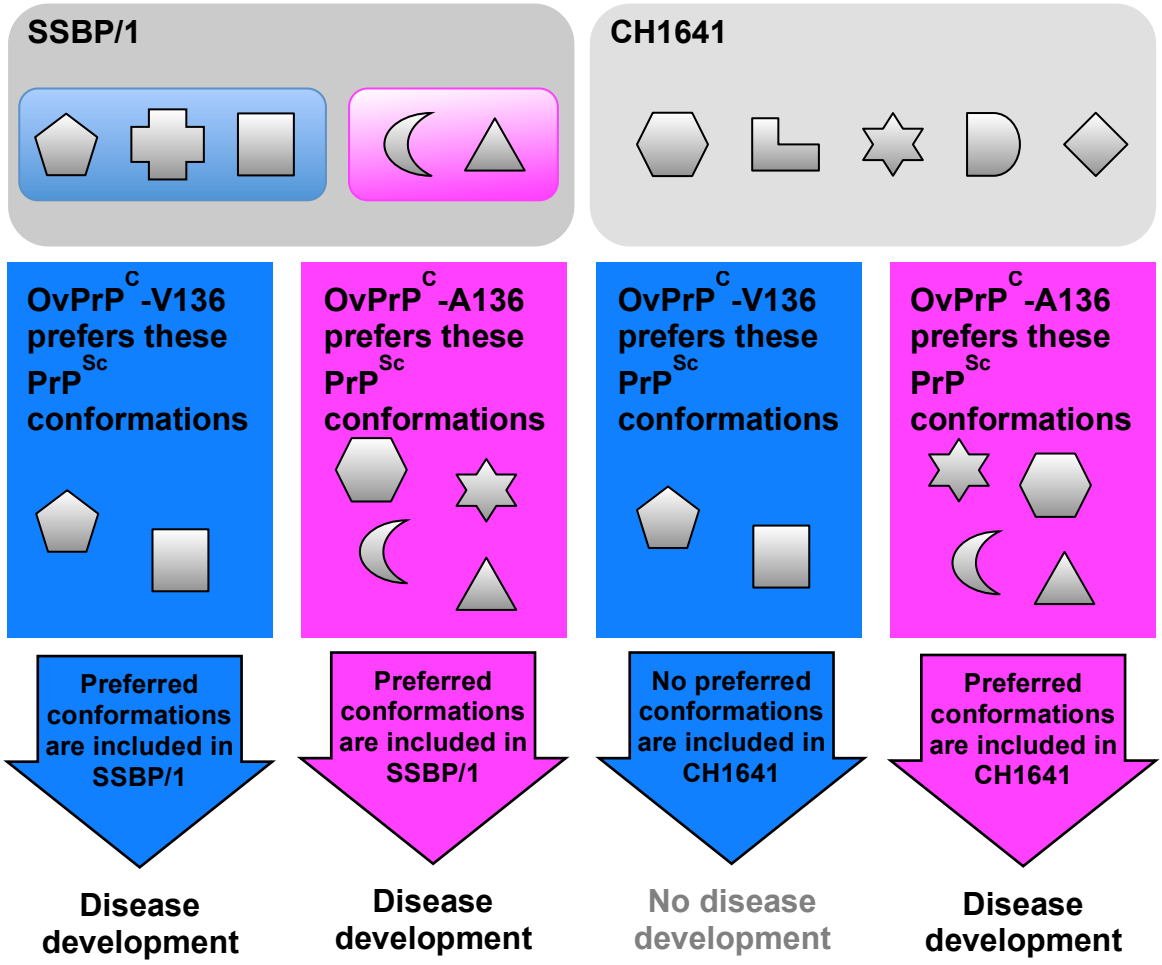

Figure 6.5. Conformational selection model to explain the intraspecies transmission barrier of SSBP/1 and CH1641 prions in sheep. The conformational selection model explains PrP^{C} preferentially interacts with preferred PrP^{Sc} conformations to facilitate PrP^{Sc} conversion. The top gray box on left presents multiple PrP^{Sc} conformations include in SSBP/1 sheep scrapie prion, and the blue and pink boxes in SSBP/1 (left gray box) indicate different PrP^{Sc} conformations in SSBP/1 could be classified into at least two groups based on the findings in histoblot data in Chapter 4. The right gray box on the top presents different sets of multiple PrP^{Sc} conformations are contained in CH1641 sheep scrapie prion. Different shapes represent different conformations. The bottom four boxes indicate potential host species including $OvPrP^{C}$-V136 (blue boxes) and $OvPrP^{C}$-A136 (pink boxes). Each host $OvPrP^{C}$ selectively interacts with different sets of preferred PrP^{Sc} conformations. SSBP/1 prion contains $OvPrP^{C}$-V136 preferred PrP^{Sc} conformations, and CH1641 does not. $OvPrP^{C}$-V136 is only susceptible to SSBP/1. Both SSBP/1 and CH1641 prions include $OvPrP^{C}$-A136 preferred PrP^{Sc} conformations, therefore, $OvPrP^{C}$-A136 is susceptible to both SSBP/1 and CH1641. However, $OvPrP^{C}$-A136 preferred PrP^{Sc} conformations are not major PrP^{Sc} conformations in SSBP/1. Lower

amount of OvPrP^{C}-A136 preferred PrP^{Sc} conformations are available for OvPrP^{C}-A136 to interact and utilize for PrP^{Sc} conversion. Therefore, OvPrP^{C}-A136 requires a longer period of time to develop disease with SSBP/1.

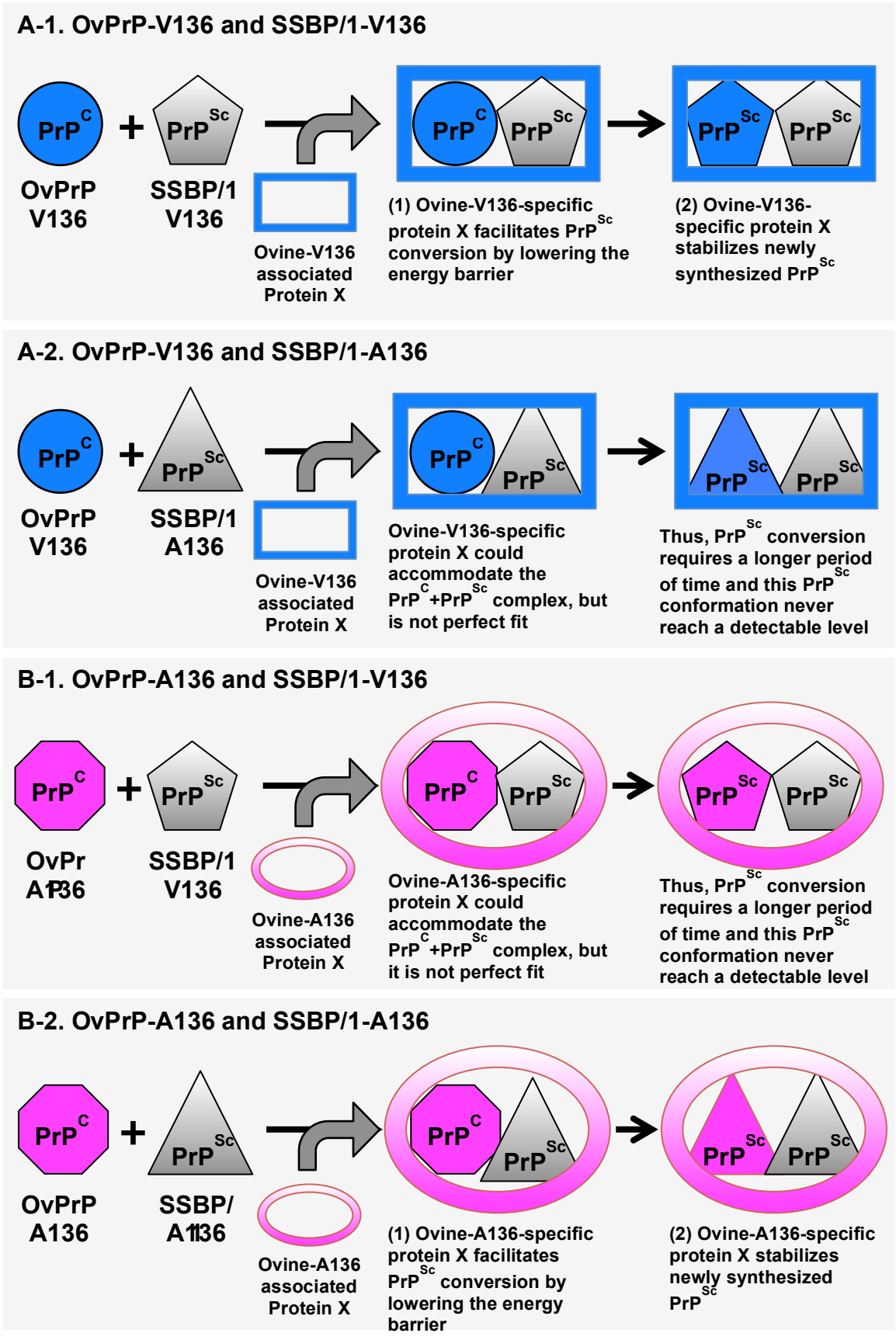
A-1. OvPrP-V136 and SSBP/1-V136
PrP C
PrP Sc
OvPrP V136
SSBP/1 V136
Ovine-V136 associated Protein X
(1) Ovine-V136-specific protein X facilitates PrP Sc conversion by lowering the energy barrier
(2) Ovine-V136-specific protein X stabilizes newly synthesized PrP Sc
A-2. OvPrP-V136 and SSBP/1-A136
OvPrP V136
SSBP/1 A136
Ovine-V136 associated Protein X
Ovine-V136-specific protein X could accommodate the PrP C +PrP Sc complex, but is not perfect fit
Thus, PrP Sc conversion requires a longer period of time and this PrP Sc conformation never reach a detectable level
B-1. OvPrP-A136 and SSBP/1-V136
SSBP/1 V136
Ovine-A136 associated Protein X
Ovine-A136-specific protein X could accommodate the PrP C +PrP Sc complex, but it is not perfect fit
Thus, PrP Sc conversion requires a longer period of time and this PrP Sc conformation never reach a detectable level
B-2. OvPrP-A136 and SSBP/1-A136
OvPrP A136
Ovine-A136 associated Protein X
(1) Ovine-A136-specific protein X facilitates PrP Sc conversion by lowering the energy barrier
(2) Ovine-A136-specific protein X stabilizes newly synthesized PrP Sc

C-1. OvPrP-V136 and SSBP/1-V136

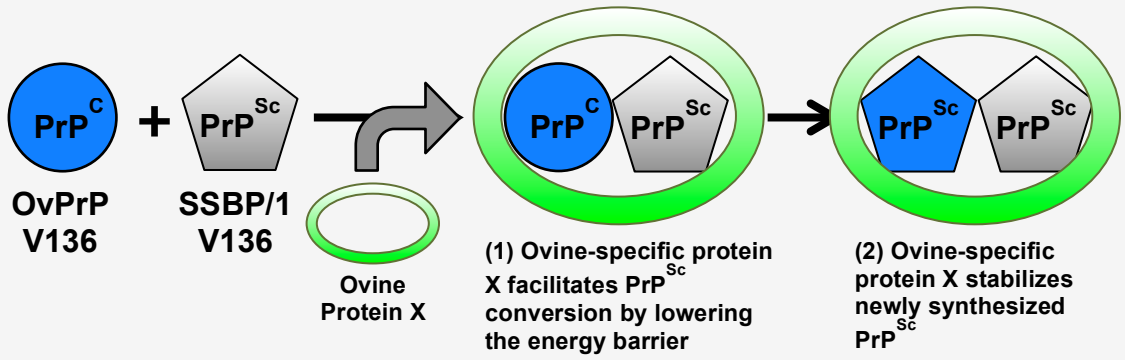

C-2. OvPrP-V136 and SSBP/1-A136

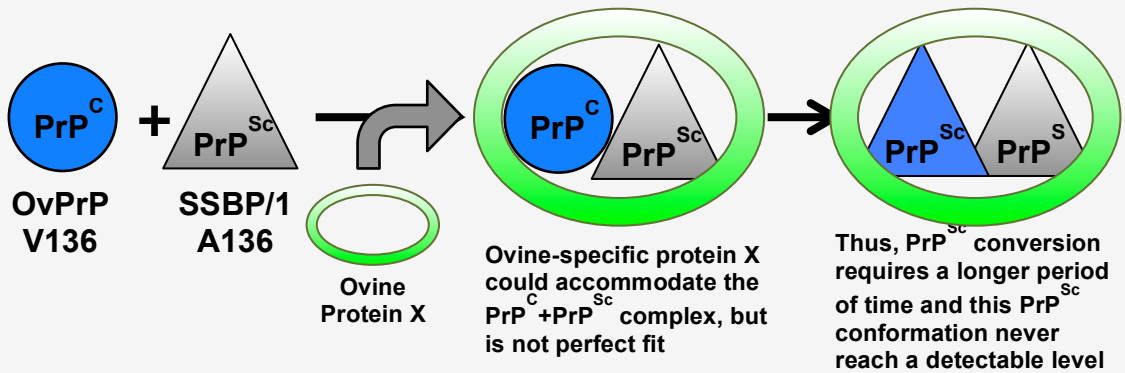

D-1. OvPrP-A136 and SSBP/1-V136

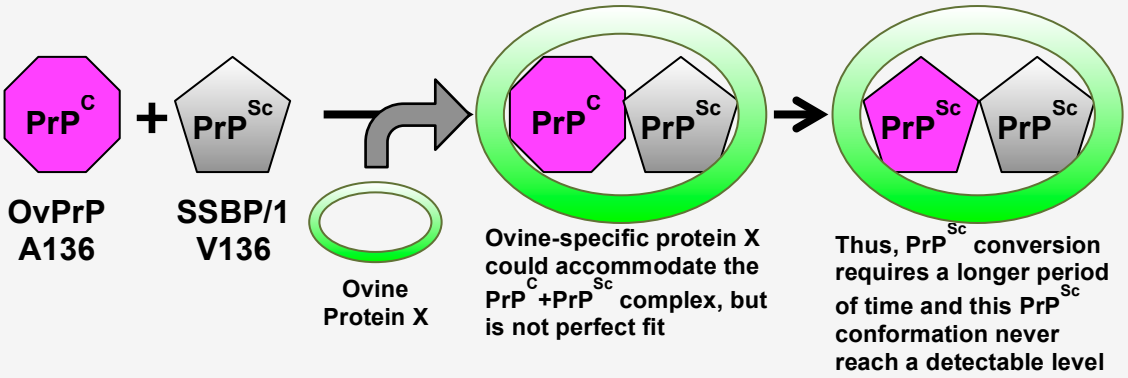

D-2. OvPrP-A136 and SSBP/1-A136

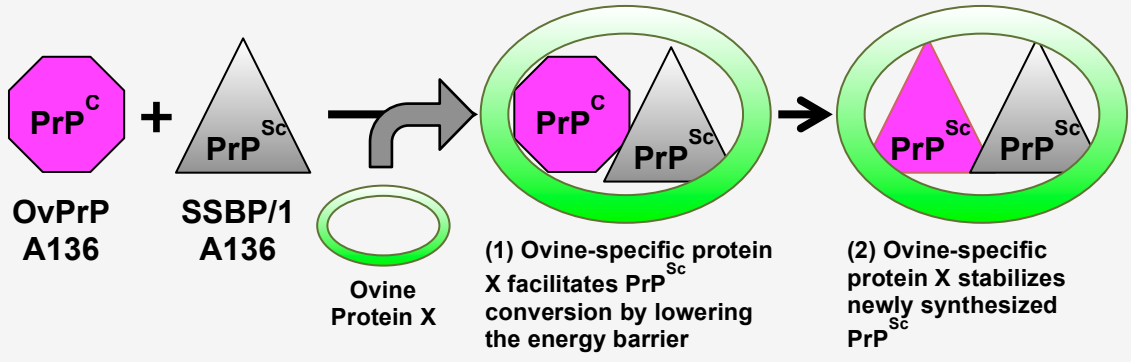

Figure 6.6. SSBP/1 conversion models of OvPrP^{Sc}-A136 and OvPrP^{Sc}-V136: ovine-specific 'protein X' catalyzes PrP^{Sc} conversion and stabilizes newly synthesized PrP^{Sc}. In the A and B models, an unidentified molecular chaperone 'protein X' is link to the ovine PrP 136 polymorphism. A-1. An OvPrP-V136-specific 'protein X' facilitates the conversion of OvPrP^{C}-V136 into PrP^{Sc} using OvPrPSc-V163 in SSBP/1. Newly synthesized OvPrP^{Sc}-V136 is also stabilized by the OvPrP-V136-specific 'protein X'. A-2. The OvPrP-V136-specific 'protein X' could accommodate the OvPrP^{C}-V136-SSBP/1-A136 PrP^{Sc} complex to facilitate the conversion of OvPrP^{Sc}-V136 using OvPrP^{Sc}-A136 in SSBP/1; however, the OvPrP-V136-specific 'protein X' is not most efficient chaperone for the OvPrP^{C}-V136-SSBP/1-A136 PrP^{Sc} complex. Therefore, OvPrPSc-V136 conversion requires a longer time with OvPrP^{Sc}-A136 as a template. Newly synthesized OvPrP^{Sc}-V136 might never accumulate in neurons because a cellular clearance mechanism could promptly remove PrP^{Sc} as slowly synthesized. B-1. An OvPrP-A136-specific 'protein X' might be able to accommodate the OvPrP^{C}-A136-SSBP/1-V136 PrP^{Sc} complex to facilitate the conversion of OvPrP^{Sc}-A136; however, the OvPrP-A136-specific 'protein X' is not most efficient chaperone for the conversion of OvPrP^{C}-A136 into PrP^{Sc} using OvPrP^{Sc}-V136 in SSBP/1. Thus, OvPrP^{Sc}-V136 conversion will take a longer time. In addition, a cellular clearance mechanism could remove newly synthesized OvPrP^{Sc}-A136 as slowly synthesized. B-2. The OvPrP-A136-specific 'protein X' facilitates the conversion of OvPrP^{C}-A136 into PrP^{Sc} using OvPrP^{Sc}-A136 in SSBP/1a1. Newly synthesized OvPrP^{Sc}-A136 is also stabilized by the OvPrP-A136-specific 'protein X'. In the C and D models, an unidentified molecular chaperone 'protein X' is universal among ovine. An ovine-specific 'protein X' facilitates PrP^{Sc} conversion in both OvPrP-A136 and OvPrP-V136 sheep.

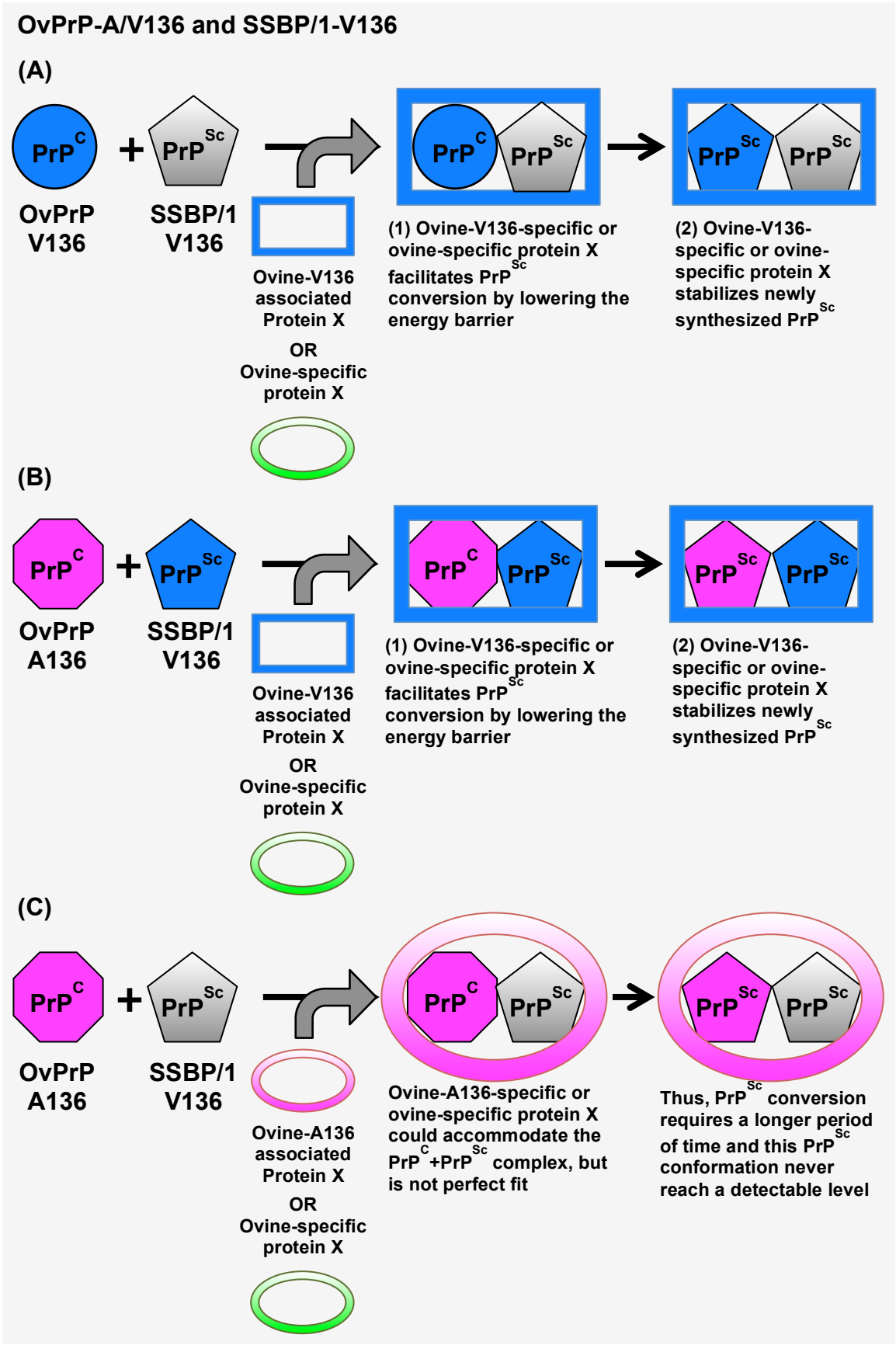
OvPrP-A/V136 and SSBP/1-V136
(A)
PrP C
PrP Sc
OvPrP V136
SSBP/1 V136
Ovine-V136 associated Protein X
OR
Ovine-specific protein X
(1) Ovine-V136-specific or ovine-specific protein X facilitates PrP Sc conversion by lowering the energy barrier
(2) Ovine-V136-specific or ovine-specific protein X stabilizes newly synthesized PrP Sc
(B)
OvPrP A136
SSBP/1 V136
Ovine-V136 associated Protein X
OR
Ovine-specific protein X
(1) Ovine-V136-specific or ovine-specific protein X facilitates PrP Sc conversion by lowering the energy barrier
(2) Ovine-V136-specific or ovine-specific protein X stabilizes newly synthesized PrP Sc
(C)
OvPrP A136
SSBP/1 V136
Ovine-A136 associated Protein X
OR
Ovine-specific protein X
Ovine-A136-specific or ovine-specific protein X could accommodate the PrP C +PrP Sc complex, but is not perfect fit
Thus, PrP Sc conversion requires a longer period of time and this PrP Sc conformation never reach a detectable level

Figure 6.7. SSBP/1 conversion models of $OvPrP^{Sc}$-V136 and $OvPrP^{Sc}$-A136 in the OvPrP 136 A/V heterozygous: OvPrP-V136-specific 'protein X' facilitates a dominant 'templating' of $OvPrP^{Sc}$-V136 to convert $OvPrP^{C}$-A136 conversion. In a heterozygous state, an identified molecular chaperone 'protein X' could be an ovine-specific universal protein X or OvPrP-A136-specific and OvPrP-V136-specific protein X. If 'protein X' is linked to the ovine 136 polymorphism, both OvPrP-A136-specific and OvPrP-V136-specific 'protein X' will be available to facilitate PrP^{Sc} conversion. In the heterozygous state, conversions of both $OvPrP^{C}$-V136 and $OvPrP^{C}$-A136 into PrP^{Sc} are taken place even though rates of PrP^{Sc} conversion differ between $OvPrP^{Sc}$-V136 and $OvPrP^{Sc}$-A136. (A). The conversion of $OvPrP^{C}$-V136 into PrP^{Sc} will be facilitated by either universal ovine-specific or OvPrP-V136-specific 'protein X', and newly synthesized $OvPrP^{Sc}$-V136 will be stabilized by 'protein X'. (C). The conversion rate of $OvPrP^{Sc}$-V136 is higher than $OvPrP^{Sc}$-A136. The conversion of $OvPrP^{C}$-A136 into PrP^{Sc} will be facilitated by either ovine-specific universal 'protein X' or OvPrP-A136-specific 'protein X', and the ovine-specific or OvPrP-A136-specific 'protein X' could stabilize newly synthesized $OvPrP^{Sc}$-A136. (B). In addition to the above conversion mechanisms of $OvPrP^{Sc}$-V136 or $OvPrP^{Sc}$-A136, a 'dominant' templating mechanism of $OvPrP^{Sc}$-V136 conformation, which leads to forced templating of $OvPrP^{C}$-A136, is also occurring in the heterozygous state. In the 'dominant' templating mechanism, $OvPrP^{Sc}$-V136 helps to convert $OvPrP^{C}$-A136 to PrP^{Sc} using an ovine-specific or OvPrP-V136-specific 'protein X'. Therefore, this newly synthesized $OvPrP^{Sc}$-A136 obtains the same properties as a template $OvPrP^{Sc}$-V136.

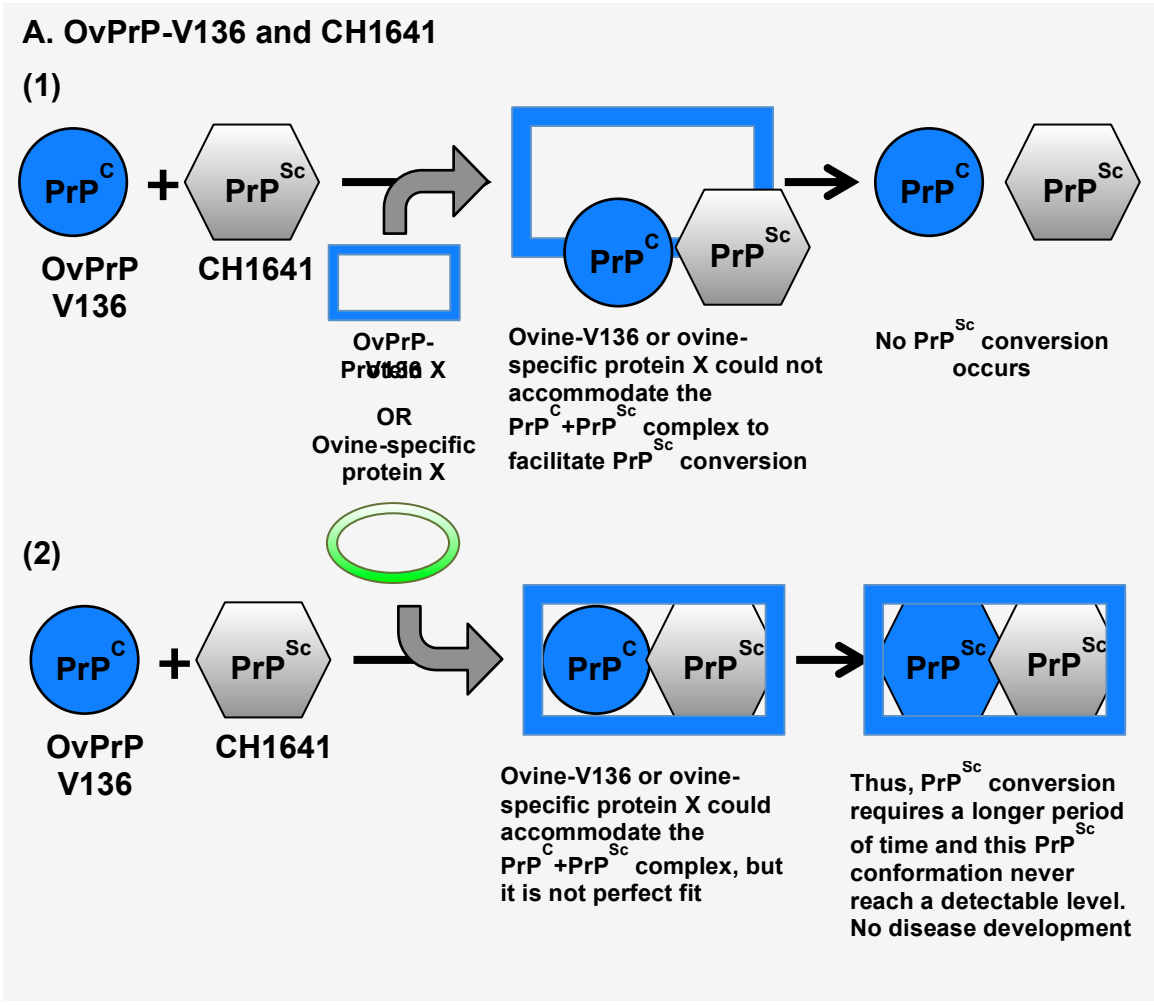
A. OvPrP-V136 and CH1641
(1)
PrP C
PrP Sc
OvPrP V136
CH1641
OvPrP-
OR
Ovine-specific protein X
Ovine-V136 or ovine-specific protein X could not accommodate the PrP C +PrP Sc complex to facilitate PrP Sc conversion
No PrP Sc conversion occurs
(2)
Ovine-V136 or ovine-specific protein X could accommodate the PrP C +PrP Sc complex, but it is not perfect fit
Thus, PrP Sc conversion requires a longer period of time and this PrP Sc conformation never reach a detectable level. No disease development

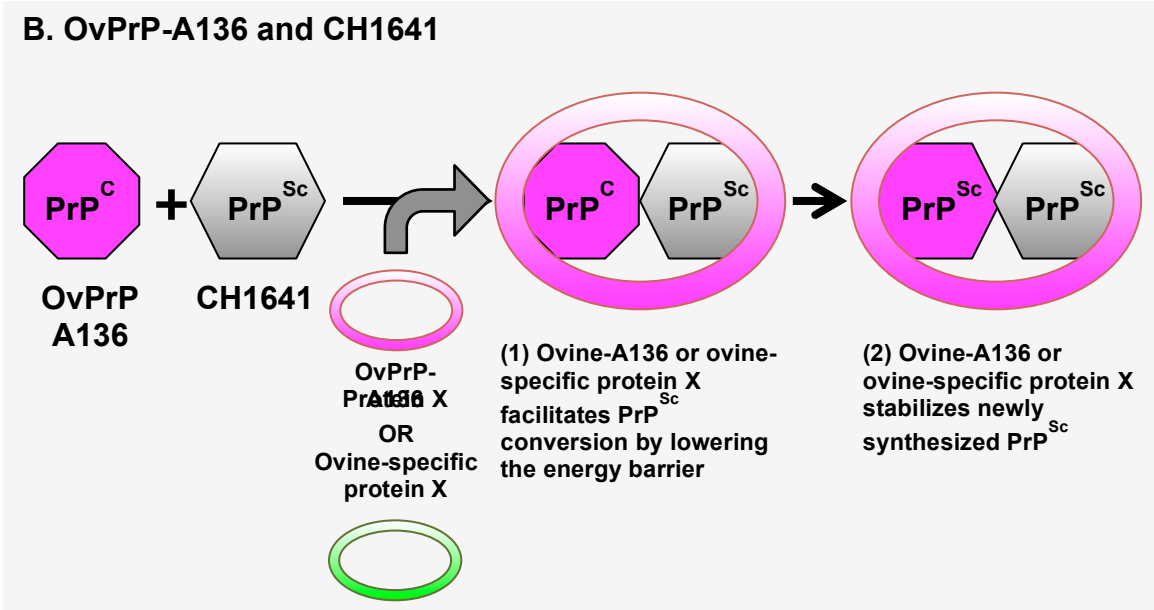
B. OvPrP-A136 and CH1641
PrP C
PrP Sc
OvPrP A136
CH1641
OvPrP-
OR
Ovine-specific protein X
(1) Ovine-A136 or ovine-specific protein X facilitates PrP Sc conversion by lowering the energy barrier
(2) Ovine-A136 or ovine-specific protein X stabilizes newly synthesized PrP Sc

C. OvPrP-A/V136 and CH1641

(1)

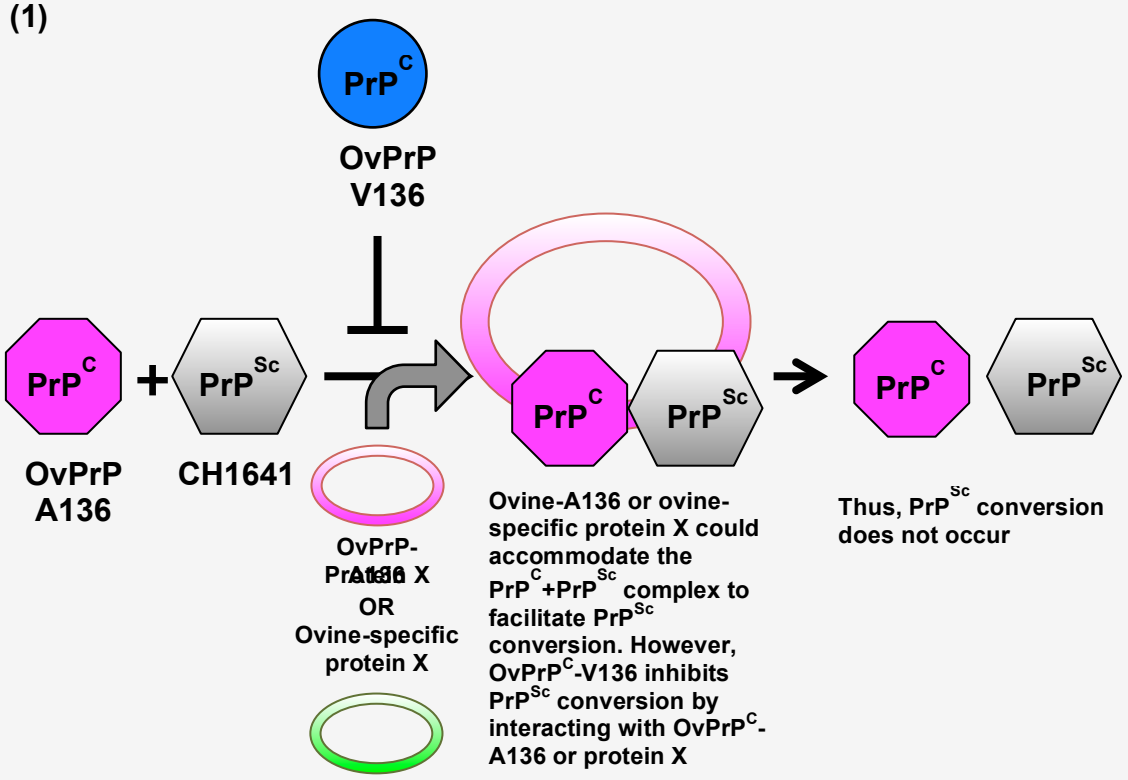

(2)

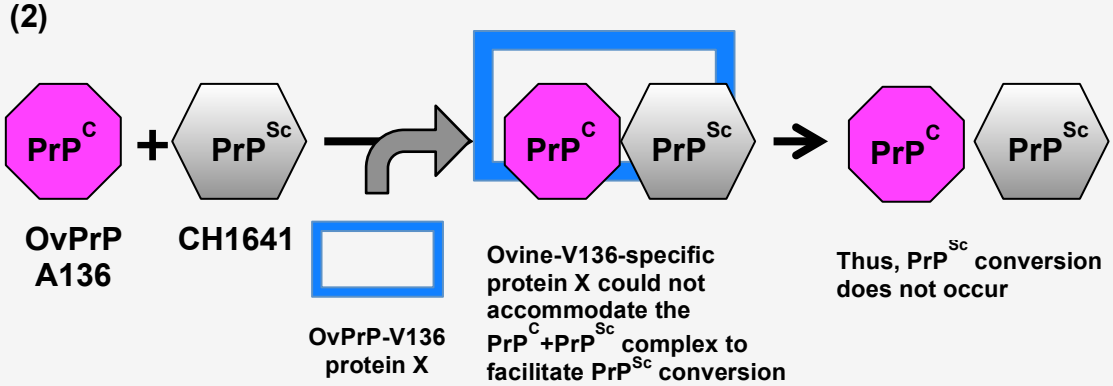

Figure 6.8. CH1641 conversion models of $OvPrP^{Sc}$-V136 and $OvPrP^{Sc}$-A136: Conversion of $OvPrP^{Sc}$-A136 is inhibited by the presence of $OvPrP^{C}$-V136 and/or OvPrP-V136-specific 'protein X' in the OvPrP 136 A/V heterozygous state. CH1641 sheep scrapie prion is most susceptible to OvPrP-A136 and most resistant to OvPrP-V136. A. CH1641 sheep scrapie prion does not include $OvPrP^{C}$-V136 preferred PrP^{Sc} conformations based on the conformational selection model (Figure 6.5.). OvPrP-V136-specific or ovine-specific universal 'protein X' is available to facilitate PrP^{Sc} conversion. A-(1) Neither ovine-specific nor OvPrP-V136-specific 'protein X' could accommodate the $OvPrP^{C}$-V136-CH1641 PrP^{Sc} complex to facilitate PrP^{Sc} conversion. If 'protein X' is linked to OvPrP-V136, PrP^{Sc} conversion does not take place due to the OvPrP-V136-specific 'protein X'. A-(2) Even though those 'protein X' could accommodate the $OvPrP^{C}$-V136-CH1641 PrP^{Sc} complex, inefficient 'protein X' could not mediate PrP^{Sc} conversion fast enough to accumulate PrP^{Sc} in the brain. A cellular clearance mechanism could promptly remove newly synthesized PrP^{Sc} as slowly synthesized. B. $OvPrP^{C}$-A136 preferred PrP^{Sc} conformations are included in CH1641 sheep scrapie prion (Figure 6.5.). Either OvPrP-A136-specific 'protein X' or ovine-specific 'protein X', could facilitate PrP^{Sc} conversion and stabilize newly synthesized $OvPrP^{Sc}$-A136. C. In the heterozygous state, $OvPrP^{Sc}$-A136 conversion is inhibited by the presence of $OvPrP^{C}$-V136 or OvPrP-V136-specific 'protein X'. C-(1). $OvPrP^{C}$-V136 inhibits the conversion of $OvPrP^{C}$-A136 by interacting with OvPrP-A136, CH1641-PrP^{Sc}, or protein X to prevent from forming an $OvPrP^{C}$-A136-CH1641 PrP^{Sc} complex. Even though most efficient 'protein X' is available, 'protein X' could not mediate PrP^{Sc} conversion. C-(2). The OvPrP-V136-specific 'protein X' could not facilitate $OvPrP^{Sc}$-A136 conversion. In the heterozygous state, the OvPrP-V-specific 'protein X' is available and becomes an inhibitor or antagonist by interacting with the $OvPrP^{C}$-A136-CH1641 PrP^{Sc} complex before most efficient OvPrP-A136-specific 'protein X' interact with the PrP^{C}-PrP^{Sc} complex.

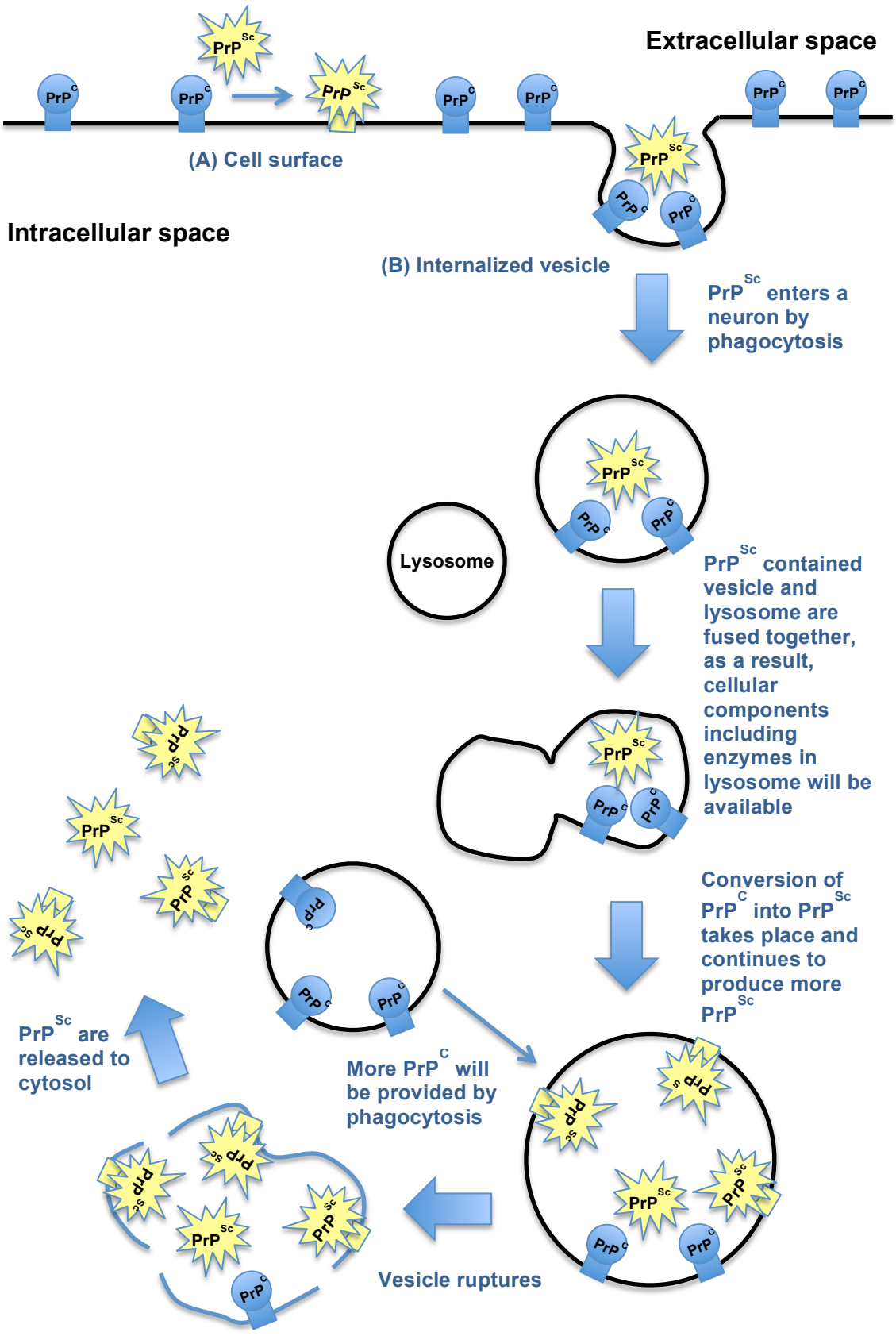
Extracellular space
Intracellular space
(A) Cell surface
(B) Internalized vesicle
PrP^Sc enters a neuron by phagocytosis
Lysosome
PrP^Sc contained vesicle and lysosome are fused together, as a result, cellular components including enzymes in lysosome will be available
Conversion of PrP^C into PrP^Sc takes place and continues to produce more PrP^Sc
More PrP^C will be provided by phagocytosis
PrP^Sc are released to cytosol
Vesicle ruptures

Figure 6.9. PrP^{Sc} conversion sites in neuron. A. PrP^{Sc} conversion occurs at the cholesterol-rich microdomains in the plasma membrane. B. PrP^{Sc} can enter neurons by phagocytosis. A phagocytic vesicle can fuse to lysosomes. Proteolytic enzymes and other molecules become available in the fused vesicles. PrP^{Sc} conversion occurs in lysosomes possibly utilizing molecules from lysosomes. New PrP^{C} could be provided by phagocytosis to continue converting PrP^{Sc} in lysosomes. The vesicles eventually rupture and newly synthesized PrP^{Sc} will be released to the cytosol. Some PrP^{Sc} will be captured by molecular chaperones to translocate into lysosomes for degradation.

References

Adrover, M., Pauwels, K., Prigent, S., de Chiara, C., Xu, Z., Chapuis, C., Pastore, A. & Rezaei, H. (2010). Prion fibrillization is mediated by a native structural element that comprises helices H2 and H3. *The Journal of biological chemistry* **285**, 21004-21012.

Alper, T., Cramp, W. A., Haig, D. A. & Clarke, M. C. (1967). Does the agent of scrapie replicate without nucleic acid? *Nature* **214**, 764-766.

Alvarez, I., Royo, L. J., Gutierrez, J. P., Fernandez, I., Arranz, J. J. & Goyache, F. (2007). Genetic diversity loss due to selection for scrapie resistance in the rare Spanish Xalda sheep breed. *Livestock Science* **111**, 204-212.

Angers, R. C., Browning, S. R., Seward, T. S., Sigurdson, C. J., Miller, M. W., Hoover, E. A. & Telling, G. C. (2006). Prions in skeletal muscles of deer with chronic wasting disease. *Science* **311**, 1117.

Angers, R. C., Seward, T. S., Napier, D., Green, M., Hoover, E., Spraker, T., O'Rourke, K., Balachandran, A. & Telling, G. C. (2009). Chronic wasting disease prions in elk antler velvet. *Emerging infectious diseases* **15**, 696-703.

Angers, R. C., Kang, H. E., Napier, D., Browning, S., Seward, T., Mathiason, C., Balachandran, A., McKenzie, D., Castilla, J. & other authors (2010). Prion strain mutation determined by prion protein conformational compatibility and primary structure. *Science* **328**, 1154-1158.

Asante, E. A., Linehan, J. M., Desbruslais, M., Joiner, S., Gowland, I., Wood, A. L., Welch, J., Hill, A. F., Lloyd, S. E. & other authors (2002). BSE prions propagate as either variant CJD-like or sporadic CJD-like prion strains in transgenic mice expressing human prion protein. *The EMBO journal* **21**, 6358-6366.

Asante, E. A., Gowland, I., Grimshaw, A., Linehan, J. M., Smidak, M., Houghton, R., Osiguwa, O., Tomlinson, A., Joiner, S. & other authors (2009). Absence of spontaneous disease and comparative prion susceptibility of transgenic mice expressing mutant human prion proteins. *The Journal of general virology* **90**, 546-558.

Avbelj, M., Hafner-Bratkovic, I. & Jerala, R. (2011). Introduction of glutamines into the B2-H2 loop promotes prion protein conversion. *Biochemical and biophysical research communications* **413**, 521-526.

Baeten, L. A., Powers, B. E., Jewell, J. E., Spraker, T. R. & Miller, M. W. (2007). A natural case of chronic wasting disease in a free-ranging moose (Alces alces shirasi). *Journal of wildlife diseases* **43**, 309-314.

Baier, M., Apelt, J., Riemer, C., Gultner, S., Schwarz, A., Bamme, T., Burwinkel, M. & Schliebs, R. (2008). Prion infection of mice transgenic for human APPSwe: increased accumulation of cortical formic acid extractable Abeta(1-42) and rapid scrapie disease development. *International journal of developmental neuroscience : the official journal of the International Society for Developmental Neuroscience* **26**, 821-824.

Balducci, C., Beeg, M., Stravalaci, M., Bastone, A., Sclip, A., Biasini, E., Tapella, L., Colombo, L., Manzoni, C. & other authors (2010). Synthetic amyloid-beta oligomers impair long-term memory independently of cellular prion protein. *Proceedings of the National Academy of Sciences of the United States of America* **107**, 2295-2300.

Baron, T., Crozet, C., Biacabe, A. G., Philippe, S., Verchere, J., Bencsik, A., Madec, J. Y., Calavas, D. & Samarut, J. (2004). Molecular analysis of the protease-resistant prion protein in scrapie and bovine spongiform encephalopathy transmitted to ovine transgenic and wild-type mice. *Journal of virology* **78**, 6243-6251.

Barria, M. A., Telling, G. C., Gambetti, P., Mastrianni, J. A. & Soto, C. (2011). Generation of a new form of human PrP(Sc) in vitro by interspecies transmission from cervid prions. *The Journal of biological chemistry* **286**, 7490-7495.

Bartz, J. C., Marsh, R. F., McKenzie, D. I. & Aiken, J. M. (1998). The host range of chronic wasting disease is altered on passage in ferrets. *Virology* **251**, 297-301.

Basler, K., Oesch, B., Scott, M., Westaway, D., Walchli, M., Groth, D. F., McKinley, M. P., Prusiner, S. B. & Weissmann, C. (1986). Scrapie and cellular PrP isoforms are encoded by the same chromosomal gene. *Cell* **46**, 417-428.

Baylis, M. & Goldmann, W. (2004). The genetics of scrapie in sheep and goats. *Current molecular medicine* **4**, 385-396.

Baylis, M., Chihota, C., Stevenson, E., Goldmann, W., Smith, A., Sivam, K., Tongue, S. & Gravenor, M. B. (2004). Risk of scrapie in British sheep of different prion protein genotype. *The Journal of general virology* **85**, 2735-2740.

Beck, K. E., Sallis, R. E., Lockey, R., Simmons, M. M. & Spiropoulos, J. (2010). Ovine PrP genotype is linked with lesion profile and immunohistochemistry patterns after primary transmission of classical scrapie to wild-type mice. *Journal of neuropathology and experimental neurology* **69**, 483-497.

Begara-McGorum, I., Gonzalez, L., Simmons, M., Hunter, N., Houston, F. & Jeffrey, M. (2002). Vacuolar lesion profile in sheep scrapie: factors influencing its variation and relationship to disease-specific PrP accumulation. *Journal of comparative pathology* **127**, 59-68.

Belay, E. D., Maddox, R. A., Williams, E. S., Miller, M. W., Gambetti, P. & Schonberger, L. B. (2004). Chronic wasting disease and potential transmission to humans. *Emerging infectious diseases* **10**, 977-984.

Belt, P. B., Muileman, I. H., Schreuder, B. E., Bos-de Ruijter, J., Gielkens, A. L. & Smits, M. A. (1995). Identification of five allelic variants of the sheep PrP gene and their association with natural scrapie. *The Journal of general virology* **76 (Pt 3)**, 509-517.

Bessen, R. A. & Marsh, R. F. (1992a). Biochemical and physical properties of the prion protein from two strains of the transmissible mink encephalopathy agent. *Journal of virology* **66**, 2096-2101.

Bessen, R. A. & Marsh, R. F. (1992b). Identification of two biologically distinct strains of transmissible mink encephalopathy in hamsters. *The Journal of general virology* **73 (Pt 2)**, 329-334.

Bett, C., Fernandez-Borges, N., Kurt, T. D., Lucero, M., Nilsson, K. P., Castilla, J. & Sigurdson, C. J. (2012). Structure of the beta2-alpha2 loop and interspecies prion transmission. *The FASEB journal : official publication of the Federation of American Societies for Experimental Biology*.

Bilheude, J. M., Brun, A., Morel, N., Diaz San Segundo, F., Lecroix, S., Espinosa, J. C., Gonzalez, L., Steele, P., Grassi, J. & other authors (2007). Discrimination of sheep susceptible and resistant to transmissible spongiform encephalopathies by an haplotype specific monoclonal antibody. *Journal of virological methods* **145**, 169-172.

Billeter, M., Riek, R., Wider, G., Hornemann, S., Glockshuber, R. & Wuthrich, K. (1997). Prion protein NMR structure and species barrier for prion diseases. *Proceedings of the National Academy of Sciences of the United States of America* **94**, 7281-7285.

Bolton, D. C., McKinley, M. P. & Prusiner, S. B. (1982). Identification of a protein that purifies with the scrapie prion. *Science* **218**, 1309-1311.

Borchelt, D. R., Scott, M., Taraboulos, A., Stahl, N. & Prusiner, S. B. (1990). Scrapie and cellular prion proteins differ in their kinetics of synthesis and topology in cultured cells. *The Journal of cell biology* **110**, 743-752.

Brazier, M. W., Lewis, V., Ciccotosto, G. D., Klug, G. M., Lawson, V. A., Cappai, R., Ironside, J. W., Masters, C. L., Hill, A. F. & other authors (2006). Correlative studies support lipid peroxidation is linked to PrP(res) propagation as an early primary pathogenic event in prion disease. *Brain research bulletin* **68**, 346-354.

Brownell, S. E., Becker, R. A. & Steinman, L. (2012). The protective and therapeutic function of small heat shock proteins in neurological diseases. *Frontiers in immunology* **3**, 74.

Bruce, M. E., Will, R. G., Ironside, J. W., McConnell, I., Drummond, D., Suttie, A., McCardle, L., Chree, A., Hope, J. & other authors (1997). Transmissions to mice indicate that 'new variant' CJD is caused by the BSE agent. *Nature* **389**, 498-501.

Brundin, P., Melki, R. & Kopito, R. (2010). Prion-like transmission of protein aggregates in neurodegenerative diseases. *Nature reviews Molecular cell biology* **11**, 301-307.

Bueler, H., Aguzzi, A., Sailer, A., Greiner, R. A., Autenried, P., Aguet, M. & Weissmann, C. (1993). Mice devoid of PrP are resistant to scrapie. *Cell* **73**, 1339-1347.

Bueler, H., Fischer, M., Lang, Y., Bluethmann, H., Lipp, H. P., DeArmond, S. J., Prusiner, S. B., Aguet, M. & Weissmann, C. (1992). Normal development and behaviour of mice lacking the neuronal cell-surface PrP protein. *Nature* **356**, 577-582.

Calella, A. M., Farinelli, M., Nuvolone, M., Mirante, O., Moos, R., Falsig, J., Mansuy, I. M. & Aguzzi, A. (2010). Prion protein and Abeta-related synaptic toxicity impairment. *EMBO molecular medicine* **2**, 306-314.

Callahan, M. A., Xiong, L. & Caughey, B. (2001). Reversibility of scrapie-associated prion protein aggregation. *The Journal of biological chemistry* **276**, 28022-28028.

Carlson, G. A., Kingsbury, D. T., Goodman, P. A., Coleman, S., Marshall, S. T., DeArmond, S., Westaway, D. & Prusiner, S. B. (1986). Linkage of prion protein and scrapie incubation time genes. *Cell* **46**, 503-511.

Carlson, G. A., Ebeling, C., Yang, S. L., Telling, G., Torchia, M., Groth, D., Westaway, D., DeArmond, S. J. & Prusiner, S. B. (1994). Prion isolate specified allotypic interactions between the cellular and scrapie prion proteins in congenic and transgenic mice. *Proceedings of the National Academy of Sciences of the United States of America* **91**, 5690-5694.

Caughey, B., Raymond, G. J., Ernst, D. & Race, R. E. (1991). N-terminal truncation of the scrapie-associated form of PrP by lysosomal protease(s): implications regarding the site of conversion of PrP to the protease-resistant state. *Journal of virology* **65**, 6597-6603.

Caughey, B., Kocisko, D. A., Raymond, G. J. & Lansbury, P. T., Jr. (1995). Aggregates of scrapie-associated prion protein induce the cell-free conversion of protease-sensitive prion protein to the protease-resistant state. *Chemistry & biology* **2**, 807-817.

Caughey, B., Race, R. E., Ernst, D., Buchmeier, M. J. & Chesebro, B. (1989). Prion protein biosynthesis in scrapie-infected and uninfected neuroblastoma cells. *Journal of virology* **63**, 175-181.

Chen, K. C., Xu, M., Wedemeyer, W. J. & Roder, H. (2011). Microsecond unfolding kinetics of sheep prion protein reveals an intermediate that correlates with susceptibility to classical scrapie. *Biophysical journal* **101**, 1221-1230.

Chen, S. G., Teplow, D. B., Parchi, P., Teller, J. K., Gambetti, P. & Autilio-Gambetti, L. (1995). Truncated forms of the human prion protein in normal brain and in prion diseases. *The Journal of biological chemistry* **270**, 19173-19180.

Christen, B., Perez, D. R., Hornemann, S. & Wuthrich, K. (2008). NMR structure of the bank vole prion protein at 20 degrees C contains a structured loop of residues 165-171. *Journal of molecular biology* **383**, 306-312.

Christen, B., Hornemann, S., Damberger, F. F. & Wuthrich, K. (2009). Prion protein NMR structure from tammar wallaby (Macropus eugenii) shows that the beta2-alpha2 loop is modulated by long-range sequence effects. *Journal of molecular biology* **389**, 833-845.

Chronic Wasting Disease Alliance (2012). CHRONOLOGY OF SIGNIFICANT EVENTS IN THE HISTORY OF CHRONIC WASTING DISEASE. http://www.cwd-info.org/index.php/fuseaction/about.timeline.

Cobb, N. J., Sonnichsen, F. D., McHaourab, H. & Surewicz, W. K. (2007). Molecular architecture of human prion protein amyloid: a parallel, in-register beta-structure. *Proceedings of the National Academy of Sciences of the United States of America* **104**, 18946-18951.

Cohen, F. E., Pan, K. M., Huang, Z., Baldwin, M., Fletterick, R. J. & Prusiner, S. B. (1994). Structural clues to prion replication. *Science* **264**, 530-531.

Coitinho, A. S., Lopes, M. H., Hajj, G. N., Rossato, J. I., Freitas, A. R., Castro, C. C., Cammarota, M., Brentani, R. R., Izquierdo, I. & other authors (2007). Short-term memory formation and long-term memory consolidation are enhanced by cellular prion association to stress-inducible protein 1. *Neurobiology of disease* **26**, 282-290.

Coitinho, A. S., Freitas, A. R., Lopes, M. H., Hajj, G. N., Roesler, R., Walz, R., Rossato, J. I., Cammarota, M., Izquierdo, I. & other authors (2006). The interaction between prion protein and laminin modulates memory consolidation. *The European journal of neuroscience* **24**, 3255-3264.

Colby, D. W. & Prusiner, S. B. (2011). Prions. *Cold Spring Harbor perspectives in biology* **3**, a006833.

Collinge, J. (1999). Variant Creutzfeldt-Jakob disease. *Lancet* **354**, 317-323.

Collinge, J. (2010). Medicine. Prion strain mutation and selection. *Science* **328**, 1111-1112.

Collinge, J., Sidle, K. C., Meads, J., Ironside, J. & Hill, A. F. (1996). Molecular analysis of prion strain variation and the aetiology of 'new variant' CJD. *Nature* **383**, 685-690.

Collinge, J., Whittington, M. A., Sidle, K. C., Smith, C. J., Palmer, M. S., Clarke, A. R. & Jefferys, J. G. (1994). Prion protein is necessary for normal synaptic function. *Nature* **370**, 295-297.

Collinge, J., Whitfield, J., McKintosh, E., Beck, J., Mead, S., Thomas, D. J. & Alpers, M. P. (2006). Kuru in the 21st century--an acquired human prion disease with very long incubation periods. *Lancet* **367**, 2068-2074.

Collinge, J., Whitfield, J., McKintosh, E., Frosh, A., Mead, S., Hill, A. F., Brandner, S., Thomas, D. & Alpers, M. P. (2008). A clinical study of kuru patients with long incubation periods at the end of the epidemic in Papua New Guinea. *Philosophical transactions of the Royal Society of London Series B, Biological sciences* **363**, 3725-3739.

Colucci, M., Moleres, F. J., Xie, Z. L., Ray-Chaudhury, A., Gutti, S., Butefisch, C. M., Cervenakova, L., Wang, W., Goldfarb, L. G. & other authors (2006). Gerstmann-Straussler-Scheinker: a new phenotype with 'curly' PrP deposits. *Journal of neuropathology and experimental neurology* **65**, 642-651.

Commission, E. (2003). 100/EC Commission decision laying down minimum requirements for the establishment of breeding programs for resistance to transmissible spongiform encephalopathies in sheep. *Off J L* **41**, 41-45.

Cordier, C., Bencsik, A., Philippe, S., Betemps, D., Ronzon, F., Calavas, D., Crozet, C. & Baron, T. (2006). Transmission and characterization of bovine spongiform encephalopathy sources in two ovine transgenic

mouse lines (TgOvPrP4 and TgOvPrP59). *The Journal of general virology* **87**, 3763-3771.

Courageot, M. P., Daude, N., Nonno, R., Paquet, S., Di Bari, M. A., Le Dur, A., Chapuis, J., Hill, A. F., Agrimi, U. & other authors (2008). A cell line infectible by prion strains from different species. *The Journal of general virology* **89**, 341-347.

Cuillé, J. & Chelle, P. L. (1936). La maladie dite tremblante du mouton est-elle inoculable. *CR Acad Sci* **203**, 1552-1554.

Cuillé, J. & Chelle, P. L. (1938). La tremblante du mouton est bien inoculable. *Comptes rendus de l'Académie des Sciences de Paris* **206**, 78-79.

Danilov, E., Bukina, N. & Akulova, B. (1974). Encephalopathy in mink. *Krolikokovod Zverovod* **17**, 34.

Davanipour, Z., Goodman, L., Alter, M., Sobel, E., Asher, D. & Gajdusek, D. C. (1984). Possible modes of transmission of Creutzfeldt-Jakob disease. *The New England journal of medicine* **311**, 1582-1583.

Davis, D. G., Schmitt, F. A., Wekstein, D. R. & Markesbery, W. R. (1999). Alzheimer neuropathologic alterations in aged cognitively normal subjects. *Journal of neuropathology and experimental neurology* **58**, 376-388.

Debatin, L., Streffer, J., Geissen, M., Matschke, J., Aguzzi, A. & Glatzel, M. (2008). Association between deposition of beta-amyloid and pathological prion protein in sporadic Creutzfeldt-Jakob disease. *Neuro-degenerative diseases* **5**, 347-354.

DebBurman, S. K., Raymond, G. J., Caughey, B. & Lindquist, S. (1997). Chaperone-supervised conversion of prion protein to its protease-resistant form. *Proceedings of the National Academy of Sciences of the United States of America* **94**, 13938-13943.

Del Bo, R., Scarlato, M., Ghezzi, S., Martinelli-Boneschi, F., Fenoglio, C., Galimberti, G., Galbiati, S., Virgilio, R., Galimberti, D. & other authors (2006). Is M129V of PRNP gene associated with Alzheimer's disease? A case-control study and a meta-analysis. *Neurobiology of aging* **27**, 770 e771-770 e775.

Deleault, N. R., Lucassen, R. W. & Supattapone, S. (2003). RNA molecules stimulate prion protein conversion. *Nature* **425**, 717-720.

Dermaut, B., Croes, E. A., Rademakers, R., Van den Broeck, M., Cruts, M., Hofman, A., van Duijn, C. M. & Van Broeckhoven, C. (2003). PRNP Val129 homozygosity increases risk for early-onset Alzheimer's disease. *Annals of neurology* **53**, 409-412.

Desplats, P., Lee, H. J., Bae, E. J., Patrick, C., Rockenstein, E., Crews, L., Spencer, B., Masliah, E. & Lee, S. J. (2009). Inclusion formation and neuronal cell death through neuron-to-neuron transmission of alpha-synuclein. *Proceedings of the National Academy of Sciences of the United States of America* **106**, 13010-13015.

Dickinson, A. G. (1976). Scrapie in sheep and goats. *Frontiers of biology* **44**, 209-241.

Dickinson, A. G. & Outram, G. W. (1988). Genetic aspects of unconventional virus infections: the basis of the virino hypothesis. *Ciba Foundation symposium* **135**, 63-83.

Dickinson, A. G., Meikle, V. M. & Fraser, H. (1968). Identification of a gene which controls the incubation period of some strains of scrapie agent in mice. *Journal of comparative pathology* **78**, 293-299.

Drisaldi, B., Stewart, R. S., Adles, C., Stewart, L. R., Quaglio, E., Biasini, E., Fioriti, L., Chiesa, R. & Harris, D. A. (2003). Mutant PrP is delayed in its exit from the endoplasmic reticulum, but neither wild-type nor mutant PrP undergoes retrotranslocation prior to proteasomal degradation. *The Journal of biological chemistry* **278**, 21732-21743.

Duffy, P., Wolf, J., Collins, G., DeVoe, A. G., Streeten, B. & Cowen, D. (1974). Letter: Possible person-to-person transmission of Creutzfeldt-Jakob disease. *The New England journal of medicine* **290**, 692-693.

Dukur, Il, Geller, V. I., Chizhov, V. A., Roikhel, V. M. & Pogodina, V. V. (1986). [Clinico-morphological study of transmissible encephalopathy of mink]. *Voprosy virusologii* **31**, 220-225.

Eghiaian, F., Grosclaude, J., Lesceu, S., Debey, P., Doublet, B., Treguer, E., Rezaei, H. & Knossow, M. (2004). Insight into the PrPC-->PrPSc conversion from the structures of antibody-bound ovine prion scrapie-susceptibility variants. *Proceedings of the National Academy of Sciences of the United States of America* **101**, 10254-10259.

Eghiaian, F., Daubenfeld, T., Quenet, Y., van Audenhaege, M., Bouin, A. P., van der Rest, G., Grosclaude, J. & Rezaei, H. (2007). Diversity in prion protein oligomerization pathways results from domain expansion as revealed by hydrogen/deuterium exchange and disulfide linkage. *Proceedings of the National Academy of Sciences of the United States of America* **104**, 7414-7419.

Eiden, M., Hoffmann, C., Balkema-Buschmann, A., Muller, M., Baumgartner, K. & Groschup, M. H. (2010). Biochemical and immunohistochemical characterization of feline spongiform encephalopathy in a German captive cheetah. *The Journal of general virology* **91**, 2874-2883.

Eisele, Y. S., Obermuller, U., Heilbronner, G., Baumann, F., Kaeser, S. A., Wolburg, H., Walker, L. C., Staufenbiel, M., Heikenwalder, M. & other authors (2010). Peripherally applied Abeta-containing inoculates induce cerebral beta-amyloidosis. *Science* **330**, 980-982.

Eisele, Y. S., Bolmont, T., Heikenwalder, M., Langer, F., Jacobson, L. H., Yan, Z. X., Roth, K., Aguzzi, A., Staufenbiel, M. & other authors (2009). Induction of cerebral beta-amyloidosis: intracerebral versus systemic Abeta inoculation. *Proceedings of the National Academy of Sciences of the United States of America* **106**, 12926-12931.

Endo, T., Groth, D., Prusiner, S. B. & Kobata, A. (1989). Diversity of oligosaccharide structures linked to asparagines of the scrapie prion protein. *Biochemistry* **28**, 8380-8388.

Fernandez-Funez, P., Zhang, Y., Sanchez-Garcia, J., Jensen, K., Zou, W. Q. & Rincon-Limas, D. E. (2011). Pulling rabbits to reveal the secrets of the prion protein. *Communicative & integrative biology* **4**, 262-266.

Ferrer, I., Blanco, R., Carmona, M., Puig, B., Ribera, R., Rey, M. J. & Ribalta, T. (2001). Prion protein expression in senile plaques in Alzheimer's disease. *Acta Neuropathol* **101**, 49-56.

Fischer, M., Rulicke, T., Raeber, A., Sailer, A., Moser, M., Oesch, B., Brandner, S., Aguzzi, A. & Weissmann, C. (1996). Prion protein (PrP) with amino-proximal deletions restoring susceptibility of PrP knockout mice to scrapie. *The EMBO journal* **15**, 1255-1264.

Foster, J. D. & Dickinson, A. G. (1988a). THE UNUSUAL PROPERTIES OF CH1641, A SHEEP-PASSAGED ISOLATE OF SCRAPIE. *Vet Rec* **123**, 5-8.

Foster, J. D. & Dickinson, A. G. (1988b). The unusual properties of CH1641, a sheep-passaged isolate of scrapie. *The Veterinary record* **123**, 5-8.

Foster, J. D. & Hunter, N. (1991). Partial dominance of the sA allele of the Sip gene for controlling experimental scrapie. *The Veterinary record* **128**, 548-549.

Foster, J. D., Hope, J. & Fraser, H. (1993). Transmission of bovine spongiform encephalopathy to sheep and goats. *The Veterinary record* **133**, 339-341.

Fraser, H. & Dickinson, A. G. (1973). Scrapie in mice. Agent-strain differences in the distribution and intensity of grey matter vacuolation. *Journal of comparative pathology* **83**, 29-40.

Frost, B., Jacks, R. L. & Diamond, M. I. (2009). Propagation of tau misfolding from the outside to the inside of a cell. *The Journal of biological chemistry* **284**, 12845-12852.

Gajdusek, D. C. (1994a). Spontaneous generation of infectious nucleating amyloids in the transmissible and nontransmissible cerebral amyloidoses. *Molecular neurobiology* **8**, 1-13.

Gajdusek, D. C. (1994b). Nucleation of amyloidogenesis in infectious and noninfectious amyloidoses of brain. *Annals of the New York Academy of Sciences* **724**, 173-190.

Gambetti, P., Puoti, G. & Zou, W. Q. (2011). Variably protease-sensitive prionopathy: a novel disease of the prion protein. *Journal of molecular neuroscience : MN* **45**, 422-424.

Gambetti, P., Dong, Z., Yuan, J., Xiao, X., Zheng, M., Alshekhlee, A., Castellani, R., Cohen, M., Barria, M. A. & other authors (2008). A novel human disease with abnormal prion protein sensitive to protease. *Annals of neurology* **63**, 697-708.

Garcao, P., Oliveira, C. R. & Agostinho, P. (2006). Comparative study of microglia activation induced by amyloid-beta and prion peptides: role in neurodegeneration. *J Neurosci Res* **84**, 182-193.

Gimbel, D. A., Nygaard, H. B., Coffey, E. E., Gunther, E. C., Lauren, J., Gimbel, Z. A. & Strittmatter, S. M. (2010). Memory impairment in transgenic Alzheimer mice requires cellular prion protein. *The Journal of*

neuroscience : the official journal of the Society for Neuroscience **30**, 6367-6374.

Goldmann, W., Hunter, N., Benson, G., Foster, J. D. & Hope, J. (1991). Different scrapie-associated fibril proteins (PrP) are encoded by lines of sheep selected for different alleles of the Sip gene. *The Journal of general virology* **72 (Pt 10)**, 2411-2417.

Goldmann, W., Hunter, N., Smith, G., Foster, J. & Hope, J. (1994). PrP genotype and agent effects in scrapie: change in allelic interaction with different isolates of agent in sheep, a natural host of scrapie. *The Journal of general virology* **75 (Pt 5)**, 989-995.

Goold, R., Rabbanian, S., Sutton, L., Andre, R., Arora, P., Moonga, J., Clarke, A. R., Schiavo, G., Jat, P. & other authors (2011). Rapid cell-surface prion protein conversion revealed using a novel cell system. *Nature communications* **2**, 281.

Gordon, W. S. (1946). Advances in veterinary research. *The Veterinary record* **58**, 516-525.

Gorfe, A. A. & Caflisch, A. (2007). Ser170 controls the conformational multiplicity of the loop 166-175 in prion proteins: implication for conversion and species barrier. *The FASEB journal : official publication of the Federation of American Societies for Experimental Biology* **21**, 3279-3287.

Gossert, A. D., Bonjour, S., Lysek, D. A., Fiorito, F. & Wuthrich, K. (2005). Prion protein NMR structures of elk and of mouse/elk hybrids.

Proceedings of the National Academy of Sciences of the United States of America **102**, 646-650.

Green, K. M. (2007). *Mechanistic studies of interspecies prion transmission*. Ph.D. thesis, University of Kentucky.

Green, K. M., Browning, S. R., Seward, T. S., Jewell, J. E., Ross, D. L., Green, M. A., Williams, E. S., Hoover, E. A. & Telling, G. C. (2008). The elk PRNP codon 132 polymorphism controls cervid and scrapie prion propagation. *The Journal of general virology* **89**, 598-608.

Hadlow, W. J. & Karstad, L. (1968). Transmissible encephalopathy of mink in Ontario. *The Canadian veterinary journal La revue veterinaire canadienne* **9**, 193-196.

Haley, N. J., Seelig, D. M., Zabel, M. D., Telling, G. C. & Hoover, E. A. (2009). Detection of CWD prions in urine and saliva of deer by transgenic mouse bioassay. *PloS one* **4**, e4848.

Haraguchi, T., Fisher, S., Olofsson, S., Endo, T., Groth, D., Tarentino, A., Borchelt, D. R., Teplow, D., Hood, L. & other authors (1989). Asparagine-linked glycosylation of the scrapie and cellular prion proteins. *Archives of biochemistry and biophysics* **274**, 1-13.

Hardy, J. & Gwinn-Hardy, K. (1998). Genetic classification of primary neurodegenerative disease. *Science* **282**, 1075-1079.

Harper, J. D. & Lansbury, P. T., Jr. (1997). Models of amyloid seeding in Alzheimer's disease and scrapie: mechanistic truths and physiological

consequences of the time-dependent solubility of amyloid proteins. *Annual review of biochemistry* **66**, 385-407.

Hartl, F. U. (1996). Molecular chaperones in cellular protein folding. *Nature* **381**, 571-579.

Hartl, F. U. & Hayer-Hartl, M. (2009). Converging concepts of protein folding in vitro and in vivo. *Nature structural & molecular biology* **16**, 574-581.

Hartsough, G. R. & Burger, D. (1965). Encephalopathy of Mink: I. Epizootiologic and Clinical Observations. *The Journal of infectious diseases* **115**, 387-392.

Hartung, J., Zimmermann, H. & Johannsen, U. (1970). [Infectious encephalopathy in the mink. 1. Clinical-epizootiological and experimental studies]. *Monatshefte fur Veterinarmedizin* **25**, 385-388.

Hayasaka, K., Gojobori, T. & Horai, S. (1988). Molecular phylogeny and evolution of primate mitochondrial DNA. *Mol Biol Evol* **5**, 626-644.

Herms, J. W., Kretzchmar, H. A., Titz, S. & Keller, B. U. (1995). Patch-clamp analysis of synaptic transmission to cerebellar purkinje cells of prion protein knockout mice. *The European journal of neuroscience* **7**, 2508-2512.

Heske, J., Heller, U., Winklhofer, K. F. & Tatzelt, J. (2004). The C-terminal globular domain of the prion protein is necessary and sufficient for import into the endoplasmic reticulum. *The Journal of biological chemistry* **279**, 5435-5443.

Holscher, C., Bach, U. C. & Dobberstein, B. (2001). Prion protein contains a second endoplasmic reticulum targeting signal sequence located at its C terminus. *The Journal of biological chemistry* **276**, 13388-13394.

Hope, J., Morton, L. J., Farquhar, C. F., Multhaup, G., Beyreuther, K. & Kimberlin, R. H. (1986). The major polypeptide of scrapie-associated fibrils (SAF) has the same size, charge distribution and N-terminal protein sequence as predicted for the normal brain protein (PrP). *The EMBO journal* **5**, 2591-2597.

Horiuchi, M. & Caughey, B. (1999). Specific binding of normal prion protein to the scrapie form via a localized domain initiates its conversion to the protease-resistant state. *The EMBO journal* **18**, 3193-3203.

Houston, E. F., Halliday, S. I., Jeffrey, M., Goldmann, W. & Hunter, N. (2002). New Zealand sheep with scrapie-susceptible PrP genotypes succumb to experimental challenge with a sheep-passaged scrapie isolate (SSBP/1). *The Journal of general virology* **83**, 1247-1250.

Hunter, N. (2007). Scrapie: uncertainties, biology and molecular approaches. *Biochimica et biophysica acta* **1772**, 619-628.

Hunter, N. & Cairns, D. (1998). Scrapie-free Merino and Poll Dorset sheep from Australia and New Zealand have normal frequencies of scrapie-susceptible PrP genotypes. *The Journal of general virology* **79 (Pt 8)**, 2079-2082.

Hunter, N., Foster, J. D., Goldmann, W., Stear, M. J., Hope, J. & Bostock, C. (1996). Natural scrapie in a closed flock of Cheviot sheep occurs only in specific PrP genotypes. *Archives of virology* **141**, 809-824.

Ikeda, T., Horiuchi, M., Ishiguro, N., Muramatsu, Y., Kai-Uwe, G. D. & Shinagawa, M. (1995). Amino acid polymorphisms of PrP with reference to onset of scrapie in Suffolk and Corriedale sheep in Japan. *The Journal of general virology* **76 (Pt 10)**, 2577-2581.

Isaacs, J. D., Jackson, G. S. & Altmann, D. M. (2006). The role of the cellular prion protein in the immune system. *Clinical and experimental immunology* **146**, 1-8.

Jackson, W. S., Borkowski, A. W., Faas, H., Steele, A. D., King, O. D., Watson, N., Jasanoff, A. & Lindquist, S. (2009). Spontaneous generation of prion infectivity in fatal familial insomnia knockin mice. *Neuron* **63**, 438-450.

Jacobs, J. G., Bossers, A., Rezaei, H., van Keulen, L. J., McCutcheon, S., Sklaviadis, T., Lantier, I., Berthon, P., Lantier, F. & other authors (2011). Proteinase K-resistant material in ARR/VRQ sheep brain affected with classical scrapie is composed mainly of VRQ prion protein. *Journal of virology* **85**, 12537-12546.

Jeffrey, M. & Gonzalez, L. (2007). Classical sheep transmissible spongiform encephalopathies: pathogenesis, pathological phenotypes and clinical disease. *Neuropathology and applied neurobiology* **33**, 373-394.

Jewell, J. E., Conner, M. M., Wolfe, L. L., Miller, M. W. & Williams, E. S. (2005). Low frequency of PrP genotype 225SF among free-ranging mule deer (Odocoileus hemionus) with chronic wasting disease. *The Journal of general virology* **86**, 2127-2134.

Johannsen, U. & Hartung, J. (1970). [Infectious encephalopathy in the mink. 2. Pathological-morphological studies]. *Monatshefte fur Veterinarmedizin* **25**, 389-395.

Johnson, C., Johnson, J., Vanderloo, J. P., Keane, D., Aiken, J. M. & McKenzie, D. (2006). Prion protein polymorphisms in white-tailed deer influence susceptibility to chronic wasting disease. *The Journal of general virology* **87**, 2109-2114.

Kaneko, K., Zulianello, L., Scott, M., Cooper, C. M., Wallace, A. C., James, T. L., Cohen, F. E. & Prusiner, S. B. (1997). Evidence for protein X binding to a discontinuous epitope on the cellular prion protein during scrapie prion propagation. *Proceedings of the National Academy of Sciences of the United States of America* **94**, 10069-10074.

Kang, H., Chu Chun Weng, Eri Saijo, Vicki Saylor, Jifeng Bian,, Sehun Kim, L. R., Rachel Angers, Jason Bartz, Nora Hunter, and & Telling, G. (2012). Characterization of conformation-dependent prion protein epitopes. *Journal of Biochemistry-Submitted*.

Kaushik, S. & Cuervo, A. M. (2012). Chaperone-mediated autophagy: a unique way to enter the lysosome world. *Trends in cell biology* **22**, 407-417.

Kim, B. H., Lee, H. G., Choi, J. K., Kim, J. I., Choi, E. K., Carp, R. I. & Kim, Y. S. (2004). The cellular prion protein (PrPC) prevents apoptotic neuronal cell death and mitochondrial dysfunction induced by serum deprivation. *Brain research Molecular brain research* **124**, 40-50.

Kim, T. Y., Shon, H. J., Joo, Y. S., Mun, U. K., Kang, K. S. & Lee, Y. S. (2005). Additional cases of Chronic Wasting Disease in imported deer in Korea. *The Journal of veterinary medical science / the Japanese Society of Veterinary Science* **67**, 753-759.

Kirkwood, J. K. & Cunningham, A. A. (1994). Epidemiological observations on spongiform encephalopathies in captive wild animals in the British Isles. *The Veterinary record* **135**, 296-303.

Klitzman, R. L., Alpers, M. P. & Gajdusek, D. C. (1984). The Natural Incubation Period of Kuru and the Episodes of Transmission in Three Clusters of Patients. *Neuroepidemiology* **3**, 3-20.

Koch, T. K., Berg, B. O., De Armond, S. J. & Gravina, R. F. (1985). Creutzfeldt-Jakob disease in a young adult with idiopathic hypopituitarism. Possible relation to the administration of cadaveric human growth hormone. *The New England journal of medicine* **313**, 731-733.

Kocisko, D. A., Priola, S. A., Raymond, G. J., Chesebro, B., Lansbury, P. T., Jr. & Caughey, B. (1995). Species specificity in the cell-free conversion of prion protein to protease-resistant forms: a model for the scrapie species barrier. *Proceedings of the National Academy of Sciences of the United States of America* **92**, 3923-3927.

Kocisko, D. A., Come, J. H., Priola, S. A., Chesebro, B., Raymond, G. J., Lansbury, P. T. & Caughey, B. (1994). Cell-free formation of protease-resistant prion protein. *Nature* **370**, 471-474.

Kondo, K. & Kuroiwa, Y. (1982). A case control study of Creutzfeldt-Jakob disease: association with physical injuries. *Annals of neurology* **11**, 377-381.

Kong, Q., Huang, S., Zou, W., Vanegas, D., Wang, M., Wu, D., Yuan, J., Zheng, M., Bai, H. & other authors (2005). Chronic wasting disease of elk: transmissibility to humans examined by transgenic mouse models. *The Journal of neuroscience : the official journal of the Society for Neuroscience* **25**, 7944-7949.

Korth, C., Stierli, B., Streit, P., Moser, M., Schaller, O., Fischer, R., Schulz-Schaeffer, W., Kretzschmar, H., Raeber, A. & other authors (1997). Prion (PrPSc)-specific epitope defined by a monoclonal antibody. *Nature* **390**, 74-77.

Kupfer, L., Eiden, M., Buschmann, A. & Groschup, M. H. (2007). Amino acid sequence and prion strain specific effects on the in vitro and in vivo convertibility of ovine/murine and bovine/murine prion protein chimeras. *Biochimica et biophysica acta* **1772**, 704-713.

Kurt, T. D., Telling, G. C., Zabel, M. D. & Hoover, E. A. (2009). Trans-species amplification of PrP(CWD) and correlation with rigid loop 170N. *Virology* **387**, 235-243.

Kutzer, T., Pfeiffer, I. & Brenig, B. (2002). Identification of new allelic variants in the ovine prion protein (PrP) gene. *Journal of Animal Breeding and Genetics* **119**, 201-208.

Kuwahara, C., Takeuchi, A. M., Nishimura, T., Haraguchi, K., Kubosaki, A., Matsumoto, Y., Saeki, K., Matsumoto, Y., Yokoyama, T. & other authors (1999). Prions prevent neuronal cell-line death. *Nature* **400**, 225-226.

Laplanche, J. L., Chatelain, J., Westaway, D., Thomas, S., Dussaucy, M., Brugere-Picoux, J. & Launay, J. M. (1993). PrP polymorphisms associated with natural scrapie discovered by denaturing gradient gel electrophoresis. *Genomics* **15**, 30-37.

Lauren, J., Gimbel, D. A., Nygaard, H. B., Gilbert, J. W. & Strittmatter, S. M. (2009). Cellular prion protein mediates impairment of synaptic plasticity by amyloid-beta oligomers. *Nature* **457**, 1128-1132.

Le Dur, A., Beringue, V., Andreoletti, O., Reine, F., Lai, T. L., Baron, T., Bratberg, B., Vilotte, J. L., Sarradin, P. & other authors (2005). A newly identified type of scrapie agent can naturally infect sheep with resistant PrP genotypes. *Proceedings of the National Academy of Sciences of the United States of America* **102**, 16031-16036.

Leggett, M. M., Dukes, J. & Pirie, H. M. (1990). A spongiform encephalopathy in a cat. *The Veterinary record* **127**, 586-588.

Lezmi, S., Bencsik, A., Monks, E., Petit, T. & Baron, T. (2003). First case of feline spongiform encephalopathy in a captive cheetah born in France:

PrP(sc) analysis in various tissues revealed unexpected targeting of kidney and adrenal gland. *Histochemistry and cell biology* **119**, 415-422.

Li, J., Browning, S., Mahal, S. P., Oelschlegel, A. M. & Weissmann, C. (2010). Darwinian evolution of prions in cell culture. *Science* **327**, 869-872.

Li, X., Rowland, L. P., Mitsumoto, H., Przedborski, S., Bird, T. D., Schellenberg, G. D., Peskind, E., Johnson, N., Siddique, T. & other authors (2005). Prion protein codon 129 genotype prevalence is altered in primary progressive aphasia. *Annals of neurology* **58**, 858-864.

Liberski, P. P., Sikorska, B., Guiroy, D. & Bessen, R. A. (2009). Transmissible mink encephalopathy - review of the etiology of a rare prion disease. *Folia neuropathologica / Association of Polish Neuropathologists and Medical Research Centre, Polish Academy of Sciences* **47**, 195-204.

Lledo, P. M., Tremblay, P., DeArmond, S. J., Prusiner, S. B. & Nicoll, R. A. (1996). Mice deficient for prion protein exhibit normal neuronal excitability and synaptic transmission in the hippocampus. *Proceedings of the National Academy of Sciences of the United States of America* **93**, 2403-2407.

Lloyd, S. E., Linehan, J. M., Desbruslais, M., Joiner, S., Buckell, J., Brandner, S., Wadsworth, J. D. & Collinge, J. (2004). Characterization of two distinct prion strains derived from bovine spongiform encephalopathy transmissions to inbred mice. *The Journal of general virology* **85**, 2471-2478.

Lu, X., Wintrode, P. L. & Surewicz, W. K. (2007). Beta-sheet core of human prion protein amyloid fibrils as determined by hydrogen/deuterium exchange. *Proceedings of the National Academy of Sciences of the United States of America* **104**, 1510-1515.

Lund, C., Olsen, C. M., Tveit, H. & Tranulis, M. A. (2007). Characterization of the prion protein 3F4 epitope and its use as a molecular tag. *Journal of neuroscience methods* **165**, 183-190.

Lysek, D. A., Schorn, C., Nivon, L. G., Esteve-Moya, V., Christen, B., Calzolai, L., von Schroetter, C., Fiorito, F., Herrmann, T. & other authors (2005). Prion protein NMR structures of cats, dogs, pigs, and sheep. *Proceedings of the National Academy of Sciences of the United States of America* **102**, 640-645.

Maciulis, A., Hunter, N., Wang, S., Goldmann, W., Hope, J. & Foote, W. C. (1992). Polymorphisms of a scrapie-associated fibril protein (PrP) gene and their association with susceptibility to experimentally induced scrapie in Cheviot sheep in the United States. *American journal of veterinary research* **53**, 1957-1960.

Marsh, R. F. & Bessen, R. A. (1993). Epidemiologic and experimental studies on transmissible mink encephalopathy. *Developments in biological standardization* **80**, 111-118.

Marsh, R. F., Kincaid, A. E., Bessen, R. A. & Bartz, J. C. (2005). Interspecies transmission of chronic wasting disease prions to squirrel monkeys (Saimiri sciureus). *Journal of virology* **79**, 13794-13796.

Martins, R. N., Harper, C. G., Stokes, G. B. & Masters, C. L. (1986). Increased cerebral glucose-6-phosphate dehydrogenase activity in Alzheimer's disease may reflect oxidative stress. *Journal of neurochemistry* **46**, 1042-1045.

Masel, J., Jansen, V. A. & Nowak, M. A. (1999). Quantifying the kinetic parameters of prion replication. *Biophysical chemistry* **77**, 139-152.

Masters, C. L. & Richardson, E. P., Jr. (1978). Subacute spongiform encephalopathy (Creutzfeldt-Jakob disease). The nature and progression of spongiform change. *Brain : a journal of neurology* **101**, 333-344.

Mathiason, C. K., Hays, S. A., Powers, J., Hayes-Klug, J., Langenberg, J., Dahmes, S. J., Osborn, D. A., Miller, K. V., Warren, R. J. & other authors (2009). Infectious prions in pre-clinical deer and transmission of chronic wasting disease solely by environmental exposure. *PloS one* **4**, e5916.

Mathiason, C. K., Powers, J. G., Dahmes, S. J., Osborn, D. A., Miller, K. V., Warren, R. J., Mason, G. L., Hays, S. A., Hayes-Klug, J. & other authors (2006). Infectious prions in the saliva and blood of deer with chronic wasting disease. *Science* **314**, 133-136.

Mawhinney, S., Pape, W. J., Forster, J. E., Anderson, C. A., Bosque, P. & Miller, M. W. (2006). Human prion disease and relative risk associated with chronic wasting disease. *Emerging infectious diseases* **12**, 1527-1535.

Mead, S., Poulter, M., Uphill, J., Beck, J., Whitfield, J., Webb, T. E., Campbell, T., Adamson, G., Deriziotis, P. & other authors (2009). Genetic risk factors for variant Creutzfeldt-Jakob disease: a genome-wide association study. *Lancet neurology* **8**, 57-66.

Medori, R., Tritschler, H. J., LeBlanc, A., Villare, F., Manetto, V., Chen, H. Y., Xue, R., Leal, S., Montagna, P. & other authors (1992). Fatal familial insomnia, a prion disease with a mutation at codon 178 of the prion protein gene. *The New England journal of medicine* **326**, 444-449.

Meyer-Luehmann, M., Coomaraswamy, J., Bolmont, T., Kaeser, S., Schaefer, C., Kilger, E., Neuenschwander, A., Abramowski, D., Frey, P. & other authors (2006). Exogenous induction of cerebral beta-amyloidogenesis is governed by agent and host. *Science* **313**, 1781-1784.

Miller, M. W., Williams, E. S., Hobbs, N. T. & Wolfe, L. L. (2004). Environmental sources of prion transmission in mule deer. *Emerging infectious diseases* **10**, 1003-1006.

Miller, M. W., Williams, E. S., McCarty, C. W., Spraker, T. R., Kreeger, T. J., Larsen, C. T. & Thorne, E. T. (2000). Epizootiology of chronic wasting disease in free-ranging cervids in Colorado and Wyoming. *Journal of wildlife diseases* **36**, 676-690.

Millhauser, G. L. (2007). Copper and the prion protein: methods, structures, function, and disease. *Annual review of physical chemistry* **58**, 299-320.

Mobley, W. C., Neve, R. L., Prusiner, S. B. & McKinley, M. P. (1988). Nerve growth factor increases mRNA levels for the prion protein and the beta-

amyloid protein precursor in developing hamster brain. *Proceedings of the National Academy of Sciences of the United States of America* **85**, 9811-9815.

Moudjou, M., Treguer, E., Rezaei, H., Sabuncu, E., Neuendorf, E., Groschup, M. H., Grosclaude, J. & Laude, H. (2004). Glycan-controlled epitopes of prion protein include a major determinant of susceptibility to sheep scrapie. *Journal of virology* **78**, 9270-9276.

Nico, P. B., de-Paris, F., Vinade, E. R., Amaral, O. B., Rockenbach, I., Soares, B. L., Guarnieri, R., Wichert-Ana, L., Calvo, F. & other authors (2005). Altered behavioural response to acute stress in mice lacking cellular prion protein. *Behavioural brain research* **162**, 173-181.

Nishida, N., Tremblay, P., Sugimoto, T., Shigematsu, K., Shirabe, S., Petromilli, C., Erpel, S. P., Nakaoke, R., Atarashi, R. & other authors (1999). A mouse prion protein transgene rescues mice deficient for the prion protein gene from purkinje cell degeneration and demyelination. *Laboratory investigation; a journal of technical methods and pathology* **79**, 689-697.

Oesch, B., Westaway, D., Walchli, M., McKinley, M. P., Kent, S. B., Aebersold, R., Barry, R. A., Tempst, P., Teplow, D. B. & other authors (1985). A cellular gene encodes scrapie PrP 27-30 protein. *Cell* **40**, 735-746.

Oosawa, F. & Asakura, S. (1975). *Thermodynamics of the Polymerization of Protein*, vol. 20. Academic Press London.

Pan, K. M., Baldwin, M., Nguyen, J., Gasset, M., Serban, A., Groth, D., Mehlhorn, I., Huang, Z., Fletterick, R. J. & other authors (1993). Conversion of alpha-helices into beta-sheets features in the formation of the scrapie prion proteins. *Proceedings of the National Academy of Sciences of the United States of America* **90**, 10962-10966.

Parkin, E. T., Watt, N. T., Hussain, I., Eckman, E. A., Eckman, C. B., Manson, J. C., Baybutt, H. N., Turner, A. J. & Hooper, N. M. (2007). Cellular prion protein regulates beta-secretase cleavage of the Alzheimer's amyloid precursor protein. *Proceedings of the National Academy of Sciences of the United States of America* **104**, 11062-11067.

Parry, H. B. (1962). Scrapie: a transmissible and hereditary disease of sheep. *Heredity (Edinb)* **17**, 75-105.

Pattison, I. H. & Millson, G. C. (1961). Scrapie produced experimentally in goats with special reference to the clinical syndrome. *Journal of comparative pathology* **71**, 101-109.

Perez, D. R., Damberger, F. F. & Wuthrich, K. (2010). Horse prion protein NMR structure and comparisons with related variants of the mouse prion protein. *Journal of molecular biology* **400**, 121-128.

Pergami, P., Jaffe, H. & Safar, J. (1996). Semipreparative chromatographic method to purify the normal cellular isoform of the prion protein in nondenatured form. *Analytical biochemistry* **236**, 63-73.

Petersen, R. C. (2004). Mild cognitive impairment as a diagnostic entity. *Journal of internal medicine* **256**, 183-194.

Prigent, S. & Rezaei, H. (2011). PrP assemblies: spotting the responsible regions in prion propagation. *Prion* **5**, 69-75.

Prusiner, S. B. (1982). Novel proteinaceous infectious particles cause scrapie. *Science* **216**, 136-144.

Prusiner, S. B. (1998). Prions. *Proceedings of the National Academy of Sciences of the United States of America* **95**, 13363-13383.

Prusiner, S. B. (2004). *Prion biology and diseases*. CSHL Press.

Prusiner, S. B., Cochran, S. P. & Alpers, M. P. (1985). Transmission of scrapie in hamsters. *The Journal of infectious diseases* **152**, 971-978.

Prusiner, S. B., Bolton, D. C., Groth, D. F., Bowman, K. A., Cochran, S. P. & McKinley, M. P. (1982). Further purification and characterization of scrapie prions. *Biochemistry* **21**, 6942-6950.

Prusiner, S. B., Scott, M., Foster, D., Pan, K. M., Groth, D., Mirenda, C., Torchia, M., Yang, S. L., Serban, D. & other authors (1990). Transgenetic studies implicate interactions between homologous PrP isoforms in scrapie prion replication. *Cell* **63**, 673-686.

Race, B., Meade-White, K., Race, R. & Chesebro, B. (2009a). Prion infectivity in fat of deer with chronic wasting disease. *Journal of virology* **83**, 9608-9610.

Race, B., Meade-White, K. D., Miller, M. W., Barbian, K. D., Rubenstein, R., LaFauci, G., Cervenakova, L., Favara, C., Gardner, D. & other authors (2009b). Susceptibilities of nonhuman primates to chronic wasting disease. *Emerging infectious diseases* **15**, 1366-1376.

Race, R., Meade-White, K., Raines, A., Raymond, G. J., Caughey, B. & Chesebro, B. (2002). Subclinical scrapie infection in a resistant species: persistence, replication, and adaptation of infectivity during four passages. *The Journal of infectious diseases* **186 Suppl 2**, S166-170.

Raymond, G. J., Bossers, A., Raymond, L. D., O'Rourke, K. I., McHolland, L. E., Bryant, P. K., 3rd, Miller, M. W., Williams, E. S., Smits, M. & other authors (2000). Evidence of a molecular barrier limiting susceptibility of humans, cattle and sheep to chronic wasting disease. *The EMBO journal* **19**, 4425-4430.

Reitz, C., Conrad, C., Roszkowski, K., Rogers, R. S. & Mayeux, R. (2012). Effect of Genetic Variation in LRRTM3 on Risk of Alzheimer Disease. *Archives of neurology*.

Ren, P. H., Lauckner, J. E., Kachirskaia, I., Heuser, J. E., Melki, R. & Kopito, R. R. (2009). Cytoplasmic penetration and persistent infection of mammalian cells by polyglutamine aggregates. *Nature cell biology* **11**, 219-225.

Renkawek, K., de Jong, W. W., Merck, K. B., Frenken, C. W., van Workum, F. P. & Bosman, G. J. (1992). alpha B-crystallin is present in reactive glia in Creutzfeldt-Jakob disease. *Acta neuropathologica* **83**, 324-327.

Riek, R., Hornemann, S., Wider, G., Billeter, M., Glockshuber, R. & Wuthrich, K. (1996). NMR structure of the mouse prion protein domain PrP(121-231). *Nature* **382**, 180-182.

Riemenschneider, M., Klopp, N., Xiang, W., Wagenpfeil, S., Vollmert, C., Muller, U., Forstl, H., Illig, T., Kretzschmar, H. & other authors (2004). Prion protein codon 129 polymorphism and risk of Alzheimer disease. *Neurology* **63**, 364-366.

Rigter, A. & Bossers, A. (2005). Sheep scrapie susceptibility-linked polymorphisms do not modulate the initial binding of cellular to disease-associated prion protein prior to conversion. *The Journal of general virology* **86**, 2627-2634.

Roder, H. & Colon, W. (1997). Kinetic role of early intermediates in protein folding. *Current opinion in structural biology* **7**, 15-28.

Rogers, M., Yehiely, F., Scott, M. & Prusiner, S. B. (1993). Conversion of truncated and elongated prion proteins into the scrapie isoform in cultured cells. *Proceedings of the National Academy of Sciences of the United States of America* **90**, 3182-3186.

Roucou, X. & LeBlanc, A. C. (2005). Cellular prion protein neuroprotective function: implications in prion diseases. *J Mol Med (Berl)* **83**, 3-11.

Roucou, X., Gains, M. & LeBlanc, A. C. (2004). Neuroprotective functions of prion protein. *Journal of neuroscience research* **75**, 153-161.

Rubenstein, R., Kascsak, R. J., Papini, M., Kascsak, R., Carp, R. I., LaFauci, G., Meloen, R. & Langeveld, J. (1999). Immune surveillance and antigen conformation determines humoral immune response to the prion protein immunogen. *Journal of neurovirology* **5**, 401-413.

Saborio, G. P., Permanne, B. & Soto, C. (2001). Sensitive detection of pathological prion protein by cyclic amplification of protein misfolding. *Nature* **411**, 810-813.

Sakaguchi, S., Katamine, S., Nishida, N., Moriuchi, R., Shigematsu, K., Sugimoto, T., Nakatani, A., Kataoka, Y., Houtani, T. & other authors (1996). Loss of cerebellar Purkinje cells in aged mice homozygous for a disrupted PrP gene. *Nature* **380**, 528-531.

Sandberg, M. K., Al-Doujaily, H., Sigurdson, C. J., Glatzel, M., O'Malley, C., Powell, C., Asante, E. A., Linehan, J. M., Brandner, S. & other authors (2010). Chronic wasting disease prions are not transmissible to transgenic mice overexpressing human prion protein. *The Journal of general virology* **91**, 2651-2657.

Schatzl, H. M., Da Costa, M., Taylor, L., Cohen, F. E. & Prusiner, S. B. (1995). Prion protein gene variation among primates. *Journal of molecular biology* **245**, 362-374.

Schmitt, F. A., Davis, D. G., Wekstein, D. R., Smith, C. D., Ashford, J. W. & Markesbery, W. R. (2000). "Preclinical" AD revisited: neuropathology of cognitively normal older adults. *Neurology* **55**, 370-376.

Schmitt-Ulms, G., Hansen, K., Liu, J., Cowdrey, C., Yang, J., DeArmond, S. J., Cohen, F. E., Prusiner, S. B. & Baldwin, M. A. (2004). Time-controlled transcardiac perfusion cross-linking for the study of protein interactions in complex tissues. *Nature biotechnology* **22**, 724-731.

Scott, M., Groth, D., Foster, D., Torchia, M., Yang, S. L., DeArmond, S. J. & Prusiner, S. B. (1993). Propagation of prions with artificial properties in transgenic mice expressing chimeric PrP genes. *Cell* **73**, 979-988.

Scott, M. R., Kohler, R., Foster, D. & Prusiner, S. B. (1992). Chimeric prion protein expression in cultured cells and transgenic mice. *Protein science : a publication of the Protein Society* **1**, 986-997.

Scott, M. R., Will, R., Ironside, J., Nguyen, H. O., Tremblay, P., DeArmond, S. J. & Prusiner, S. B. (1999). Compelling transgenetic evidence for transmission of bovine spongiform encephalopathy prions to humans. *Proceedings of the National Academy of Sciences of the United States of America* **96**, 15137-15142.

Seidel, B., Thomzig, A., Buschmann, A., Groschup, M. H., Peters, R., Beekes, M. & Terytze, K. (2007). Scrapie Agent (Strain 263K) can transmit disease via the oral route after persistence in soil over years. *PloS one* **2**, e435.

Sigurdson, C. J., Nilsson, K. P., Hornemann, S., Manco, G., Fernandez-Borges, N., Schwarz, P., Castilla, J., Wuthrich, K. & Aguzzi, A. (2010). A molecular switch controls interspecies prion disease transmission in mice. *The Journal of clinical investigation* **120**, 2590-2599.

Sigurdson, C. J., Nilsson, K. P., Hornemann, S., Heikenwalder, M., Manco, G., Schwarz, P., Ott, D., Rulicke, T., Liberski, P. P. & other authors (2009). De novo generation of a transmissible spongiform encephalopathy

by mouse transgenesis. *Proceedings of the National Academy of Sciences of the United States of America* **106**, 304-309.

Sigurdson, C. J., Joshi-Barr, S., Bett, C., Winson, O., Manco, G., Schwarz, P., Rulicke, T., Nilsson, K. P., Margalith, I. & other authors (2011). Spongiform encephalopathy in transgenic mice expressing a point mutation in the beta2-alpha2 loop of the prion protein. *The Journal of neuroscience : the official journal of the Society for Neuroscience* **31**, 13840-13847.

Sohn, H.-j. (2011). Chronic Wasting Disease (CWD) outbreaks and surveillance program in the Republic of Korea. In *PRION2011 Pre-Conferance Workshop TSEs in animals and their environment*. Montreal, Canada.

Spiropoulos, J., Casalone, C., Caramelli, M. & Simmons, M. M. (2007). Immunohistochemistry for PrPSc in natural scrapie reveals patterns which are associated with the PrP genotype. *Neuropathology and applied neurobiology* **33**, 398-409.

Stahl, N., Borchelt, D. R. & Prusiner, S. B. (1990). Differential release of cellular and scrapie prion proteins from cellular membranes by phosphatidylinositol-specific phospholipase C. *Biochemistry* **29**, 5405-5412.

Stahl, N., Borchelt, D. R., Hsiao, K. & Prusiner, S. B. (1987). Scrapie prion protein contains a phosphatidylinositol glycolipid. *Cell* **51**, 229-240.

Stahl, N., Baldwin, M. A., Teplow, D. B., Hood, L., Gibson, B. W., Burlingame, A. L. & Prusiner, S. B. (1993). Structural studies of the

scrapie prion protein using mass spectrometry and amino acid sequencing. *Biochemistry* **32**, 1991-2002.

Tamguney, G., Miller, M. W., Giles, K., Lemus, A., Glidden, D. V., DeArmond, S. J. & Prusiner, S. B. (2009a). Transmission of scrapie and sheep-passaged bovine spongiform encephalopathy prions to transgenic mice expressing elk prion protein. *The Journal of general virology* **90**, 1035-1047.

Tamguney, G., Giles, K., Bouzamondo-Bernstein, E., Bosque, P. J., Miller, M. W., Safar, J., DeArmond, S. J. & Prusiner, S. B. (2006). Transmission of elk and deer prions to transgenic mice. *Journal of virology* **80**, 9104-9114.

Tamguney, G., Miller, M. W., Wolfe, L. L., Sirochman, T. M., Glidden, D. V., Palmer, C., Lemus, A., DeArmond, S. J. & Prusiner, S. B. (2009b). Asymptomatic deer excrete infectious prions in faeces. *Nature* **461**, 529-532.

Taraboulos, A., Jendroska, K., Serban, D., Yang, S. L., DeArmond, S. J. & Prusiner, S. B. (1992). Regional mapping of prion proteins in brain. *Proceedings of the National Academy of Sciences of the United States of America* **89**, 7620-7624.

Taraboulos, A., Scott, M., Semenov, A., Avrahami, D., Laszlo, L. & Prusiner, S. B. (1995). Cholesterol depletion and modification of COOH-terminal targeting sequence of the prion protein inhibit formation of the scrapie isoform. *The Journal of cell biology* **129**, 121-132.

Taylor, D. M. (1989). Scrapie agent decontamination: implications for bovine spongiform encephalopathy. *The Veterinary record* **124**, 291-292.

Taylor, D. M. (1996). Exposure to, and Inactivation of, the Unconventional Agents that Cause Transmissible Degenerative Encephalopathies #. In *T Prion Diseases* (Methods in Molecular Medicine), vol. 3, pp. 105-118.

Taylor, D. R. & Hooper, N. M. (2006). The prion protein and lipid rafts. *Molecular membrane biology* **23**, 89-99.

Telling, G. C., Scott, M., Mastrianni, J., Gabizon, R., Torchia, M., Cohen, F. E., DeArmond, S. J. & Prusiner, S. B. (1995). Prion propagation in mice expressing human and chimeric PrP transgenes implicates the interaction of cellular PrP with another protein. *Cell* **83**, 79-90.

Telling, G. C., Scott, M., Hsiao, K. K., Foster, D., Yang, S. L., Torchia, M., Sidle, K. C., Collinge, J., DeArmond, S. J. & other authors (1994). Transmission of Creutzfeldt-Jakob disease from humans to transgenic mice expressing chimeric human-mouse prion protein. *Proceedings of the National Academy of Sciences of the United States of America* **91**, 9936-9940.

Telling, G. C., Parchi, P., DeArmond, S. J., Cortelli, P., Montagna, P., Gabizon, R., Mastrianni, J., Lugaresi, E., Gambetti, P. & other authors (1996). Evidence for the conformation of the pathologic isoform of the prion protein enciphering and propagating prion diversity. *Science* **274**, 2079-2082.

Thackray, A. M., Hopkins, L. & Bujdoso, R. (2007). Proteinase K-sensitive disease-associated ovine prion protein revealed by conformation-dependent immunoassay. *The Biochemical journal* **401**, 475-483.

Thorgeirsdottir, S., Sigurdarson, S., Thorisson, H. M., Georgsson, G. & Palsdottir, A. (1999). PrP gene polymorphism and natural scrapie in Icelandic sheep. *The Journal of general virology* **80 (Pt 9)**, 2527-2534.

Tortosa, R., Vidal, E., Costa, C., Alamillo, E., Torres, J. M., Ferrer, I. & Pumarola, M. (2008). Stress response in the central nervous system of a transgenic mouse model of bovine spongiform encephalopathy. *Veterinary journal (London, England : 1997)* **178**, 126-129.

Tsui-Pierchala, B. A., Encinas, M., Milbrandt, J. & Johnson, E. M., Jr. (2002). Lipid rafts in neuronal signaling and function. *Trends in neurosciences* **25**, 412-417.

Turk, E., Teplow, D. B., Hood, L. E. & Prusiner, S. B. (1988). Purification and properties of the cellular and scrapie hamster prion proteins. *European journal of biochemistry / FEBS* **176**, 21-30.

Tzaban, S., Friedlander, G., Schonberger, O., Horonchik, L., Yedidia, Y., Shaked, G., Gabizon, R. & Taraboulos, A. (2002). Protease-sensitive scrapie prion protein in aggregates of heterogeneous sizes. *Biochemistry* **41**, 12868-12875.

U.S. Department of Agriculture, A. a. P. H. (2012). National Scrapie Eradication Program.

Vassallo, N. & Herms, J. (2003). Cellular prion protein function in copper homeostasis and redox signalling at the synapse. *Journal of neurochemistry* **86**, 538-544.

Velayos, J. L., Irujo, A., Cuadrado-Tejedor, M., Paternain, B., Moleres, F. J. & Ferrer, V. (2009). The cellular prion protein and its role in Alzheimer disease. *Prion* **3**, 110-117.

Vidal, E., Acín, C., Foradada, L., Monzón, M., Márquez, M., Monleón, E., Pumarola, M., Badiola, J. J. & Bolea, R. (2009). Immunohistochemical Characterisation of Classical Scrapie Neuropathology in Sheep. *Journal of comparative pathology* **141**, 135-146.

Vilette, D., Andreoletti, O., Archer, F., Madelaine, M. F., Vilotte, J. L., Lehmann, S. & Laude, H. (2001). Ex vivo propagation of infectious sheep scrapie agent in heterologous epithelial cells expressing ovine prion protein. *Proceedings of the National Academy of Sciences of the United States of America* **98**, 4055-4059.

Vilotte, J. L., Soulier, S., Essalmani, R., Stinnakre, M. G., Vaiman, D., Lepourry, L., Da Silva, J. C., Besnard, N., Dawson, M. & other authors (2001). Markedly increased susceptibility to natural sheep scrapie of transgenic mice expressing ovine prp. *Journal of virology* **75**, 5977-5984.

Voigtlander, T., Kloppel, S., Birner, P., Jarius, C., Flicker, H., Verghese-Nikolakaki, S., Sklaviadis, T., Guentchev, M. & Budka, H. (2001). Marked increase of neuronal prion protein immunoreactivity in Alzheimer's disease and human prion diseases. *Acta neuropathologica* **101**, 417-423.

Wadsworth, J. D., Asante, E. A., Desbruslais, M., Linehan, J. M., Joiner, S., Gowland, I., Welch, J., Stone, L., Lloyd, S. E. & other authors (2004). Human prion protein with valine 129 prevents expression of variant CJD phenotype. *Science* **306**, 1793-1796.

Wang, F., Wang, X., Yuan, C. G. & Ma, J. (2010). Generating a prion with bacterially expressed recombinant prion protein. *Science* **327**, 1132-1135.

Wells, G. A., Scott, A. C., Johnson, C. T., Gunning, R. F., Hancock, R. D., Jeffrey, M., Dawson, M. & Bradley, R. (1987). A novel progressive spongiform encephalopathy in cattle. *The Veterinary record* **121**, 419-420.

Westaway, D., Goodman, P. A., Mirenda, C. A., McKinley, M. P., Carlson, G. A. & Prusiner, S. B. (1987). Distinct prion proteins in short and long scrapie incubation period mice. *Cell* **51**, 651-662.

Westaway, D., Zuliani, V., Cooper, C. M., Da Costa, M., Neuman, S., Jenny, A. L., Detwiler, L. & Prusiner, S. B. (1994a). Homozygosity for prion protein alleles encoding glutamine-171 renders sheep susceptible to natural scrapie. *Genes & development* **8**, 959-969.

Westaway, D., DeArmond, S. J., Cayetano-Canlas, J., Groth, D., Foster, D., Yang, S. L., Torchia, M., Carlson, G. A. & Prusiner, S. B. (1994b). Degeneration of skeletal muscle, peripheral nerves, and the central nervous system in transgenic mice overexpressing wild-type prion proteins. *Cell* **76**, 117-129.

Whittington, M. A., Sidle, K. C., Gowland, I., Meads, J., Hill, A. F., Palmer, M. S., Jefferys, J. G. & Collinge, J. (1995). Rescue of neurophysiological

phenotype seen in PrP null mice by transgene encoding human prion protein. *Nature genetics* **9**, 197-201.

Wickner, R. B., Edskes, H. K., Shewmaker, F., Kryndushkin, D. & Nemecek, J. (2009). Prion variants, species barriers, generation and propagation. *Journal of biology* **8**, 47.

Wilesmith, J. W., Ryan, J. B. & Atkinson, M. J. (1991). Bovine spongiform encephalopathy: epidemiological studies on the origin. *The Veterinary record* **128**, 199-203.

Wilesmith, J. W., Wells, G. A., Cranwell, M. P. & Ryan, J. B. (1988). Bovine spongiform encephalopathy: epidemiological studies. *The Veterinary record* **123**, 638-644.

Will, R. G. & Matthews, W. B. (1982). Evidence for case-to-case transmission of Creutzfeldt-Jakob disease. *Journal of neurology, neurosurgery, and psychiatry* **45**, 235-238.

Will, R. G., Ironside, J. W., Zeidler, M., Cousens, S. N., Estibeiro, K., Alperovitch, A., Poser, S., Pocchiari, M., Hofman, A. & other authors (1996). A new variant of Creutzfeldt-Jakob disease in the UK. *Lancet* **347**, 921-925.

Williams, E. S. (2005). Chronic wasting disease. *Veterinary pathology* **42**, 530-549.

Williams, E. S. & Young, S. (1980). Chronic wasting disease of captive mule deer: a spongiform encephalopathy. *Journal of wildlife diseases* **16**, 89-98.

Williams, E. S. & Young, S. (1982). Spongiform encephalopathy of Rocky Mountain elk. *Journal of wildlife diseases* **18**, 465-471.

Williams, E. S. & Young, S. (1992). Spongiform encephalopathies in Cervidae. *Rev Sci Tech* **11**, 551-567.

Wilson, R., Plinston, C., Hunter, N., Casalone, C., Corona, C., Tagliavini, F., Suardi, S., Ruggerone, M., Moda, F. & other authors (2012). Chronic Wasting Disease and Atypical forms of BSE and scrapie are not transmissible to mice expressing wild-type levels of human PrP. *The Journal of general virology*.

Windig, J. J., Meuleman, H. & Kaal, L. (2007). Selection for scrapie resistance and simultaneous restriction of inbreeding in the rare sheep breed "Mergellander". *Preventive veterinary medicine* **78**, 161-171.

Windig, J. J., Eding, H., Moll, L. & Kaal, L. (2004). Effects on inbreeding of different strategies aimed at eliminating scrapie sensitivity alleles in rare sheep breeds in The Netherlands. *Anim Sci* **79**, 11-20.

Winklhofer, K. F., Tatzelt, J. & Haass, C. (2008). The two faces of protein misfolding: gain- and loss-of-function in neurodegenerative diseases. *EMBO J* **27**, 336-349.

Wood, J. L., Lund, L. J. & Done, S. H. (1992). The natural occurrence of scrapie in moufflon. *The Veterinary record* **130**, 25-27.

World Health Organization (2012). Variant Creutzfeldt-Jakob disease. Fact sheet N°180. http://www.who.int/mediacentre/factsheets/fs180/en/index.html.

Wyatt, J. M., Pearson, G. R., Smerdon, T. N., Gruffydd-Jones, T. J., Wells, G. A. & Wilesmith, J. W. (1991). Naturally occurring scrapie-like spongiform encephalopathy in five domestic cats. *The Veterinary record* **129**, 233-236.

Yadavalli, R., Guttmann, R. P., Seward, T., Centers, A. P., Williamson, R. A. & Telling, G. C. (2004). Calpain-dependent endoproteolytic cleavage of PrPSc modulates scrapie prion propagation. *The Journal of biological chemistry* **279**, 21948-21956.

Zahn, R., Liu, A., Luhrs, T., Riek, R., von Schroetter, C., Lopez Garcia, F., Billeter, M., Calzolai, L., Wider, G. & other authors (2000). NMR solution structure of the human prion protein. *Proceedings of the National Academy of Sciences of the United States of America* **97**, 145-150.

Zhang, J. (2011). Comparison studies of the structural stability of rabbit prion protein with human and mouse prion proteins. *Journal of theoretical biology* **269**, 88-95.

Zou, W. Q., Langeveld, J., Xiao, X., Chen, S., McGeer, P. L., Yuan, J., Payne, M. C., Kang, H. E., McGeehan, J. & other authors (2010a). PrP conformational transitions alter species preference of a PrP-specific antibody. *The Journal of biological chemistry* **285**, 13874-13884.

Zou, W. Q., Puoti, G., Xiao, X., Yuan, J., Qing, L., Cali, I., Shimoji, M., Langeveld, J. P., Castellani, R. & other authors (2010b). Variably protease-sensitive prionopathy: a new sporadic disease of the prion protein. *Annals of neurology* **68**, 162-172.

ERI SAIJO, B.S., M.S.

Curriculum Vita

Born: Tokyo, Japan

Education:

2007 – Present
Doctor of Philosophy Candidate
Department of Microbiology, Immunology and Molecular Genetics
University of Kentucky, Lexington KY

2007
Master of Science in Biology
Thesis: Neurogenesis and gliogenesis in adult bullfrog brains
Arizona State University, Tempe AZ

2003
Bachelor of Science in Molecular Biosciences and Biotechnologies
Arizona State University, Tempe AZ

Laboratory experience:

2011 – Present
Research Assistant
Dr. Glenn Telling
Prion Research Program
Department of Microbiology, Immunology and Pathology
Colorado State University, Fort Collins CO

2007 – Present
Ph.D. Candidate
Dr. Glenn Telling
Department of Microbiology, Immunology and Molecular Genetics
University of Kentucky, Lexington KY

2004 – 2007
Graduate Research Assistant
Dr. Miles Orchinik
Department of Biology
Arizona State University, Tempe AZ

2003 – 2004
Research Associate

Ribomed Biotechnologies, Inc. Phoenix AZ

2002 – 2003 Undergraduate Research Assistant
Biology Research Experience for Undergraduate (BREU)
Dr. Miles Orchinik
Department of Biology
Arizona State University, Tempe AZ

Publications:

- Saijo, E., Green, K, Browning, S., Hunter, N., Bartz, J. & Telling, G. "**A 'dominant' OvPrP^{Sc}-V136 conformation leads to forced templating of OvPrP^{C}-ARQ,"** (In preparation for publication)
- Saijo, E., Scheff, S. & Telling, G. **"Unaltered Prion Protein Expression in Alzheimer's Disease Patients,"** Prion, 5:2, 109-116; April/May/June 2011

Oral presentations:

May 2011 "A 'dominant' OvPrP^{Sc}-V136 conformation leads to forced templating of OvPrP^{C}-ARQ," TSE's in animals and their environment satellite workshop in PRION, Montreal, QC, Canada

November 2010 "Prion protein structural compatibility and prion pathogenesis," Microbiology, Immunology and Molecular Genetics Department seminar, University of Kentucky, Lexington, KY

April 2010 "Prion protein and Alzheimer's disease," Microbiology, Immunology and Molecular Genetics Department seminar, University of Kentucky, Lexington, KY

March 2009 "Generation and characterization of novel anti-PrP monoclonal antibodies," Prion mini-symposium, University of Kentucky, Lexington, KY

September 2008 "CCR2 deficiency impairs microglial accumulation and accelerates Alzheimer's disease pathology" Microbiology, Immunology and Molecular Genetics Department seminar, University of Kentucky, Lexington, KY

Poster presentations:

May 2012 "Transgenetic modeling of the CWD species barrier to human," PRION, Amsterdam, Netherlands

May 2011	"Immunologic and transgenetic tools for studying mechanisms of conformational templating across PrP primary structure differences," PRION, Montreal, QC, Canada
July 2010	"Prion protein expression and M/V 129 polymorphism in Alzheimer's disease patients," Asia-Oceania Symposium on Prion Diseases, Sapporo, Japan
October 2008	"The role of prion protein in Alzheimer's disease," Microbiology, Immunology and Molecular Genetics Department retreat, University of Kentucky, Lexington, KY

Travel grants:

May 2012	The Graduate School, University of Kentucky, Lexington KY
July 2010	The Graduate School, University of Kentucky, Lexington KY